Spring 2018

Hydrodynamics study of the bubble columns with intense vertical heat-exchanging tubes using gamma-ray computed tomography and radioactive particle tracking techniques

Abbas Jawad Sultan

Department: Chemical and Biochemical Engineering

HYDRODYNAMICS STUDY OF THE BUBBLE COLUMNS WITH INTENSE VERTICAL HEAT-EXCHANGING TUBES USING GAMMA-RAY COMPUTED TOMOGRAPHY AND RADIOACTIVE PARTICLE TRACKING TECHNIQUES

by

ABBAS JAWAD SULTAN

A DISSERTATION

Presented to the Faculty of the Graduate School of the

MISSOURI UNIVERSITY OF SCIENCE AND TECHNOLOGY

In Partial Fulfillment of the Requirements for the Degree

DOCTOR OF PHILOSOPHY

in

CHEMICAL ENGINEERING

2018

Approved by

Dr. Muthanna Al-Dahhan, Advisor
Dr. Hyoung K. Lee
Dr. Shoaib Usman
Dr. Joontaek Park
Dr. Fateme Rezaei

PUBLICATION DISSERTATION OPTION

The introduction section of this dissertation gives information about Fischer-Tropsch synthesis, bubble and slurry bubble columns, critical review of the previous studies for the bubble columns with and without vertical internals, motivation and objectives of this study. The body of this dissertation consists of the following four articles:

Paper I, pages 31-90, Overcoming the gamma-ray computed tomography data processing pitfalls for bubble column equipped with vertical internal tubes has been submitted to the Canadian Journal of Chemical Engineering (under review).

Paper II, pages 91-159, Influence of the size of heat-exchanging internals on the gas holdup distribution in a bubble column using gamma-ray computed tomography has been submitted to the Chemical Engineering Science Journal (under review).

Paper III, pages 160-215, Impact of heat-exchanging tube configurations on the gas holdup distribution in bubble columns using gamma-ray computed tomography has been submitted to the International Journal of Multiphase Flow (under review).

Paper IV, pages 216-264, Investigating the influence of the configuration of the bundle of heat exchanging tubes and column size on the gas holdup distributions in bubble columns via gamma-ray computed tomography has been submitted to the Experimental Thermal and Fluid Science Journal (under review).

Finally, recommendations for the future studies in the field of bubble and slurry bubble columns with heat-exchanging tubes are listed in the last section of this dissertation.

ABSTRACT

Understanding the hydrodynamics of bubble columns with and without vertical heat-exchanging tubes is a necessity for the proper design, scale-up, and operation of these reactors. To achieve this goal, systematic experiments were performed to visualize and quantify the influence of the presence of vertical internal tubes on the gas holdup distributions and their profiles, axial liquid velocity, and turbulent parameters (i.e., normal and shear stresses; turbulent kinetic energy) by using advanced gamma-ray computed tomography (CT) and radioactive particle tracking (RPT). In this study, the experiments were conducted in 6- and 18-inch bubble columns with an air-water system as the working fluid, under a wide range of superficial gas velocities (5-45 cm/s). Three configurations of vertical internals (i.e., hexagonal, circular without a central tube, and circular with a central tube plus vertical internals), as well as the vertical internals sizes, were examined in this study. These three configurations were designed to cover 25% of the column's cross-sectional area (CSA) to represent the percentage of the covered area utilized in the Fischer-Tropsch process. Reconstructed CT images reveal that the configurations of the vertical internal tubes significantly impacted the gas holdup distribution over the CSA of the column. Additionally, the bubble column equipped with 1-inch vertical internals exhibited a more uniform gas holdup distribution than the column with 0.5-inch internals. Moreover, a remarkable increase in the gas holdup values at the wall region was achieved in the churn turbulent flow regime due to the insertion of vertical internals inside the column. Furthermore, pronounced peaks of the gas holdup and axial liquid velocity were observed in the inner gaps between the vertical internals.

ACKNOWLEDGMENTS

After a journey of research effort and diligence culminated in the completion of this work, my praises and thanks are to Allah Almighty for his grace and blessing to me. I wish to express my sincerest thanks and gratitude to my advisor Prof. Muthanna Al-Dahhan for his considerable efforts, advice, guidance, encouragement, and support throughout my Ph.D. study, which helped me to overcome many obstacles, and his critical review of my papers significantly enhanced my skills. I am also extending my sincere thanks to all members of my committee, Dr. Hyoung Lee, Dr. Shoaib Usman, Dr. Joontaek Park, and Dr. Fateme Rezaei, for examining my dissertation and enriching it with valuable tips and guidance that help to make it the best. I want to express my gratitude to my sponsor, The Higher Committee for Education Development in Iraq, for awarding me a fully funded scholarship and for their friendly assistance throughout my Ph.D. study. I would like to gratefully thank my lab-mate, and my lifetime friend, Laith Sabri, for his valuable assistance and insightful discussions and suggestions. I appreciatively would like to thank my research group members. My special thanks and appreciation also goes to Dr. Fadha Al Falahi, Dean Lenz, Marlene Albrecht, Krista Welschmeyer, Emily Seals, Emily Kost, and Dawn Schacht for providing all the assistance that the students need. My sincere thanks go to my professors and colleagues at University of Technology, Baghdad, Iraq for their help and support. I wish to thank all my relatives and friends in Iraq and the United States who have encouraged and supported me during my Ph.D. journey. I would like to give special thanks to my dear parents and siblings for their encouragement and support. Finally, great thanks to my lovely wife (Majida) and kids (Mohammed, Muthadher, Ameer, Ali, Zahraa) for their patience and persistent support during my doctoral program.

TABLE OF CONTENTS

LIST OF ILLUSTRATIONS

PAPER I

PAPER III

LIST OF TABLES

1. INTRODUCTION

As a result of growing world population, growing urbanization, and growing middle class, the world energy consumption rate will increase by 48% between 2012 and 2040 according to the international energy outlook (Figure 1.1). That means more crude oil will be used to meet the energy shortage, which will impact the environment due to more fossil fuel emissions. Therefore, there is much more need to improve sustainability by seeking clean alternative energy sources to provide more environmentally friendly products.

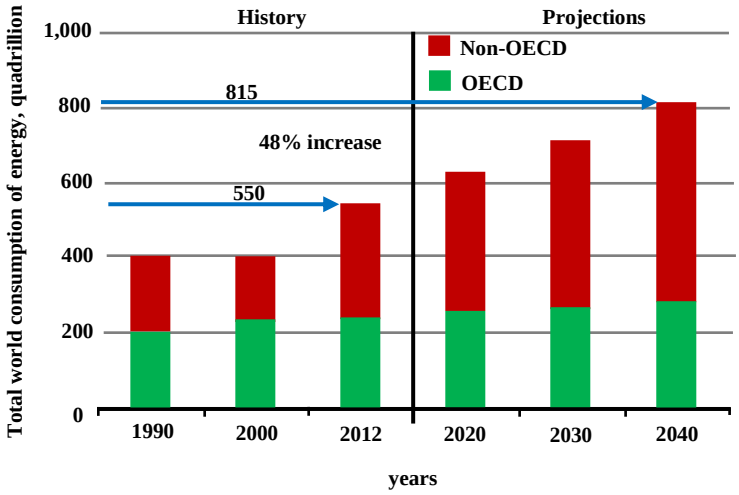

Figure 1.1: World energy consumption between 1990 and 2040 [1]

Among the alternative energy sources, the clean liquid fuels and chemical products obtained via Fischer-Tropsch (FT) synthesis have stimulated strong interest of researchers in both industry and academia. This interest in FT synthesis has grown because this process can use different feedstock such as coal, natural gas, biomass, and biogas through gasifying these feedstocks to syngas (i.e., a mixture of CO and H_2) by gasification process. Additionally, some of these feedstocks such as coal, natural gas, and biomass are abundant.

Furthermore, the products of this process are friendly to the environment, which will satisfy the environmental laws in the future [2].

Processes technology of converting natural gas, coal, and biomass to liquid fuels by FT synthesis are typically termed as gas to liquid (GTL), coal to liquid (CTL), and biomass to liquid (BTL) [3–7]. This technology has appeared as an alternative to the traditional refining of crude oil and offers new investments in natural and clean resources. These are multistep processes (GTL, CTL, BTL) for converting different feedstocks (e.g., natural gas, coal, biomass, and biogas) through their conversion to synthesis gas (i.e., CO and H_2) into higher molecular weight hydrocarbons using the FT process, as shown in Figure 1.2 The FT process was first invented by Franz Fischer and Hans Tropsch in the 1930s at the Kaiser-Wilhelm (currently Max Plank) Institute for Coal Research in Mulheim during World War II to fit the demand for fuel with plenty of coal resources [8].

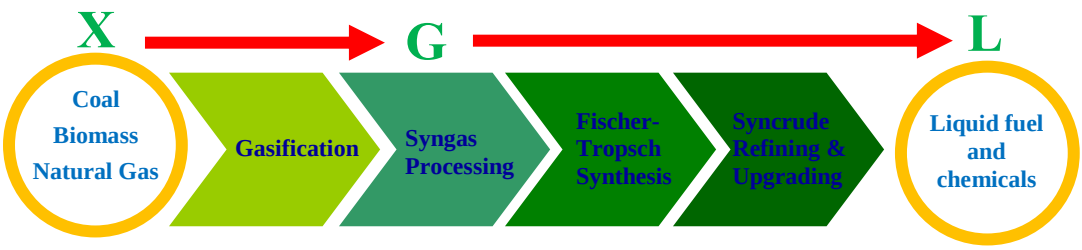

Figure 1.2: Process diagram of producing liquid fuels and chemicals by Fischer-Tropsch synthesis

Different types of multiphase reactors have been used for the FT process (Figure 1.3), such as multi-tubular fixed bed, fluidized bed, circulating fluidized bed, and slurry bubble column reactors. Nevertheless, slurry bubble column reactors have been selected for low-temperature (200-250 C^o) FT synthesis in recent years because they offer many advantages during operation and maintenance processes.

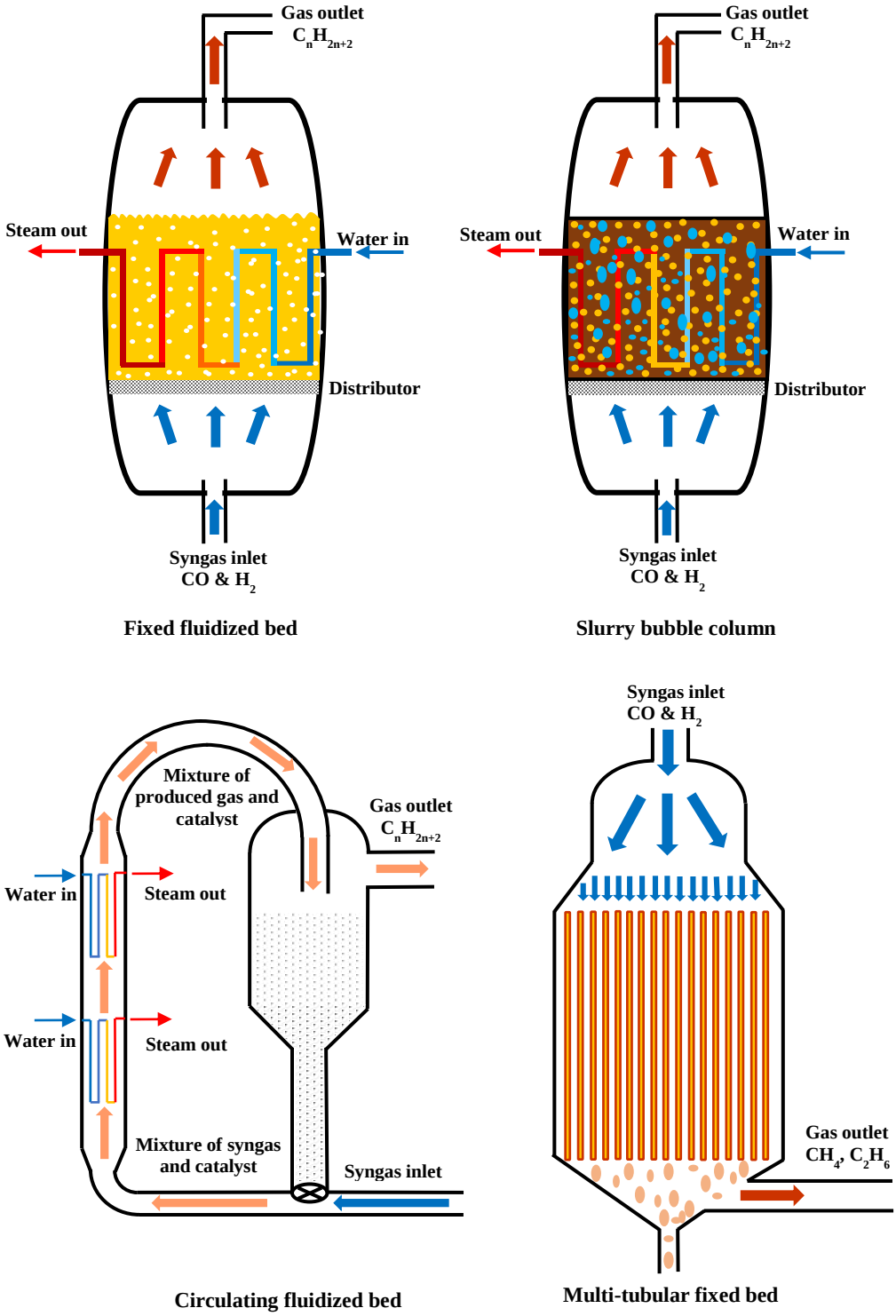

Figure 1.3: Schematic illustration of different types of reactor that used in Fischer-Tropsch synthesis

Bubble and slurry bubble column reactors are typically cylindrical columns where the gas phase is sparged continuously from the bottom of these columns as bubbles through a gas distributor (i.e., gas sparger) into liquid or slurry (liquid-solid) phases. The solid phase in a slurry bubble column reactor consists of fine catalyst particles with a size range of 5-150 μm [9]. The liquid or slurry phase is usually fed to these columns in co-current or counter-current ways and sometimes in batch mode. A schematic diagram of bubble/slurry bubble column is displayed in Figure 1.4.

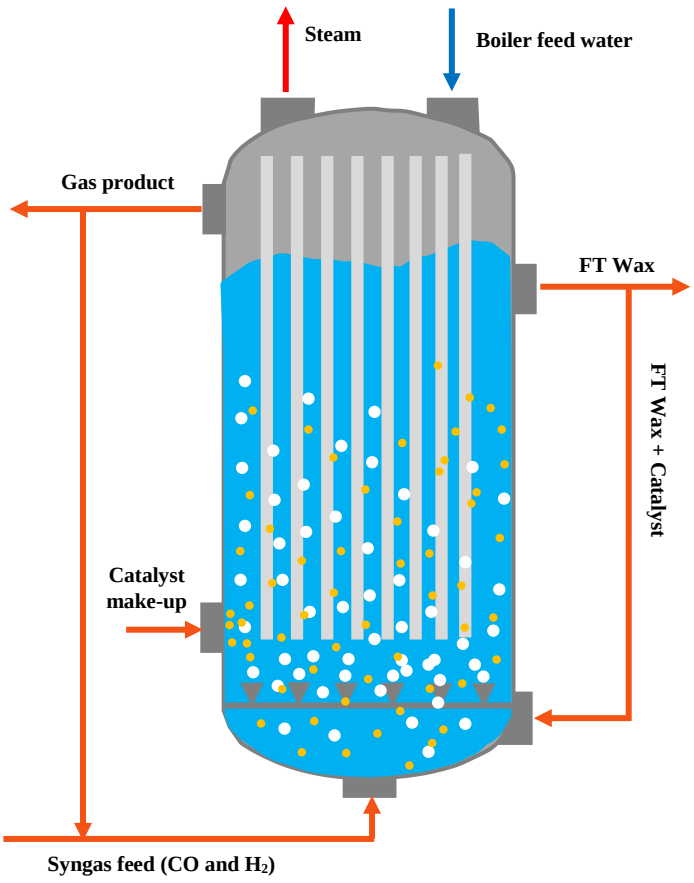

Figure 1.4: Schematic diagram of bubble/slurry bubble column reactor

Depending on the application of these column reactors, the bubble and slurry bubble columns can be operated under bubbly flow regime conditions (i.e., under low superficial gas velocities) such as in the cultivation process for algae [10] or can be run in churn turbulent flow regime (i.e., under high superficial gas velocities) as in the FT process [11].

By comparison to other multiphase reactors such as fluidized bed and trickle bed during the operation and maintenance processes, the bubble and slurry bubble columns have many advantages, including the following:

- Providing high heat and mass transfer rates because of the efficient contact and interaction between the phases (gas-liquid in bubble column or gas-liquid-solid in a slurry bubble column).
- Allowing easy control of the operating temperature.
- Offering sufficient heat recovery by equipping these reactors with a bundle of cooling tubes.
- Maintaining the overall activity of the fine catalyst for these columns during the operation.
- Capability of online catalyst activation through withdrawal of the inactive catalyst and renewing it by adding a fresh one.
- Ability to handle high operating pressure due to the absence of moving pieces.
- Eliminating the severe erosion and plugging problems caused by the catalyst.
- Reducing manufacturing, operation, and maintenance costs for these columns due to their simple construction.

These advantages and features of the bubble and slurry bubble columns make them superior to other multiphase reactors for chemical, petrochemical, biochemical, pharmaceutical, metallurgical, and mineral industrial processes. The FT synthesis [12], liquid phase methanol synthesis (LPMeoH) [13], hydrogenation of maleic acid (MAC) [14], acetic acid production [15], cyclohexanol manufacturing [16], and many others are examples of uses of these reactors in chemical and petrochemical processes. Additionally, they are used widely in biochemical and pharmaceutical industries such as algae and bacteria culturing [17], mold fungi culturing [18], antibiotic fermentation [19], single cell protein production [20], animal cell culturing [21], and sewage and wastewater treatment [22].

Most of the uses of these bubble and slurry bubble column reactors involve exothermic reactions such as Fischer-Tropsch synthesis and many others as displayed in Table 1.1. When these exothermic chemical reactions occur, excess heat releases to mixture materials, causes overheating of the catalyst, and consequently affects the reaction selectivity. This is considered a major problem in the design and safe operation of these reactors.

This issue of excess heat generated from the exothermic chemical reaction in these reactors can be solved by inserting a bundle of vertical cooling tubes, where the heat can be extracted by converting the cooling water to saturated steam which can benefit other process units. However, the presence of dense vertical heat-exchanging tubes impacts the fluid dynamics, mixing intensity, heat and mass transfer rates, reaction rate, and consequently the performance of these reactors. It is well known that the process of scale-up and design of these reactors in the absence of heat-exchanging tubes are still challenging

engineering tasks due to the absence of phenomenological models which can describe the hydrodynamics of these reactors accurately.

Additionally, these tasks are challenging due to the lack of reliable hydrodynamics information over a wide range of industrial operating conditions, especially in the bubble/slurry bubble column reactors with vertical heat-exchanging tubes. This lack comes from the complexity of the interaction among the phases which further increase in the presence of vertical heat exchanging tubes. Therefore, there is a great need for detailed knowledge of hydrodynamics, which is extremely important for proper design, scale-up, and simulation for bubble and slurry bubble column reactors with intense internals.

Table 1.1: Example of applications of bubble and slurry bubble columns for exothermic reactions [23]

Industrial process	Heat of reaction (kJ/mol)
Acetic Acid	-1270
Benzoic Acid	-628
Wet air oxidation of sewage sludge	-435
Cyclohexanol	-294
Acetic Acid	-294
Acetone	-255
Fischer–Tropsch synthesis	-210
1,2–Dichloroethane	-180
Vinyl Acetate	-176
Cumene	-113

1.1. RESEARCH MOTIVATION

Although using these heat-exchanging tubes extensively in the industrial applications of bubble/slurry bubble columns for exothermic reactions, a limited number of studies have addressed the effects of these heat-exchanging tubes on the hydrodynamics and bubble properties of these reactors.

Among these limited studies, Chen et al. [24] performed the first comprehensive study of the hydrodynamics of the bubble column in the presence of the vertical internals by employing computer automatic radioactive particle tracking (CARPT) and computed tomography (CT) techniques. The authors performed their experiments in 18-inch bubble columns with and without vertical internal tubes for two systems including air-water and air-drakeoil system. The vertical internal tubes used in their investigation were arranged in a circular configuration inside the bubble column, as shown in Figure 1.5. These internal tubes were designed to cover 5% of the total cross-sectional area (CSA) of the column, similar to the occupied area by industrial heat-exchanging tubes for methanol synthesis. They applied a limited range of superficial gas velocity of 2-10 cm/s. Their experimental results in terms of gas holdup distributions and their profiles for the bubble columns with and without vertical internals reveal that under a superficial gas velocity of 10 cm/s, axisymmetric gas holdup distribution was obtained in a fully developed flow regime for two studied systems (air-water and air-drakeoil). Additionally, the magnitude of the gas holdup in the presence of vertical internals was slightly higher than in the column without vertical internals. Moreover, they reported that the presence of vertical internals has insignificant effects on the liquid circulation velocity for the studied superficial gas

velocity conditions. Furthermore, they found that the turbulent stresses and eddy diffusivities significantly decrease in the existence of these vertical internal tubes.

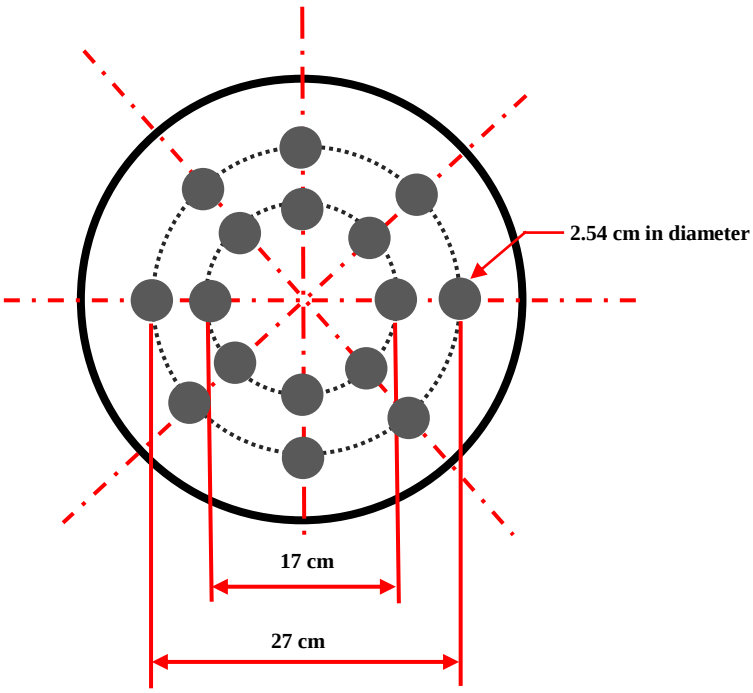

Figure 1.5: Configuration of vertical internals inside an 18-inch bubble column [24]

Forret and co-workers [25] studied the impacts of the presence of a bundle of the vertical internals on axial liquid velocity and liquid mixing in 1 m diameter bubble column with an air-water system and under a superficial gas velocity of 15 cm/s by implementing Pitot tube and standard tracer method. The vertical internals employed in their work have covered 25% of the total cross-sectional area (CSA) of the bubble column and are arranged in a square pitch inside the column. The author noted that the fluctuations of the liquid velocity and radial dispersion decreased while the liquid circulation was increased in the presence of the vertical internals, as shown in Figure 1.6. Also, they found that implementing the standard one-dimensional (1D) axial dispersion model to predict the liquid mixing is still applicable in large-scale bubble columns in the absence of the vertical

internal tubes. However, this model is not appropriate for the bubble column with the presence of vertical internals. Therefore, the author developed a 2D model to account for the effects of the vertical internals on the liquid mixing in radial and axial direction.

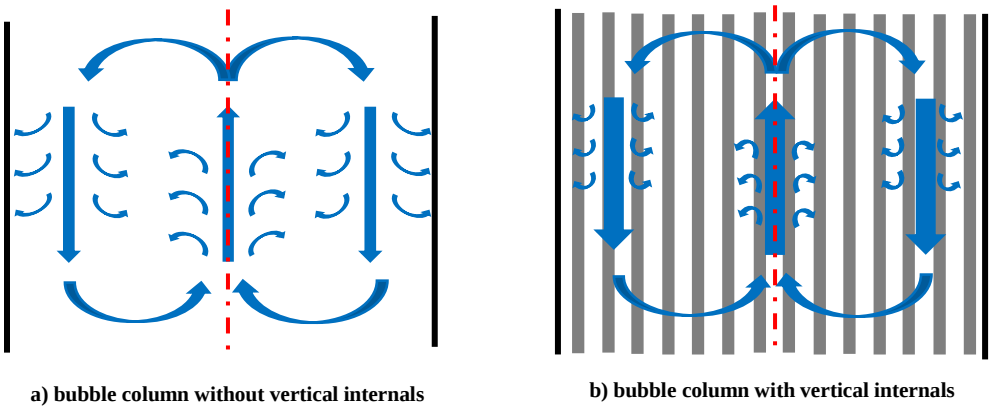

Figure 1.6: Schematic illustration of liquid recirculation in bubble columns without and with vertical internal tubes [25]

Larachi et al. [26] performed the first 3D CFD simulation study for a bubble column equipped with vertical internals. Larachi's group simulated the influence of vertical internals on the liquid circulation in a bubble column by using a two-fluid Euler model. In their study, five pilot and large-scale bubble columns with and without vertical internals operating with an air-water system under a superficial gas velocity of 12 cm/s were simulated to assess the impacts of these vertical internal tubes on the liquid circulation and mixing behavior. In their simulation, the vertical internals were arranged in four different configurations (Figure 1.7) to address the effect of these configurations on the hydrodynamics of these reactors. Their simulation reveals that the gas holdup distribution obtained in the bubble column with vertical internals was entirely different from the one achieved in the column without vertical internals, where the large-scale and coherent

meandering gas twirls that were obtained in the bubble column without vertical internals were replaced by smaller pocket whose size was governed by inter-tube gaps. Also, they reported that the vertical internal arrangements have a significant effect on the flow behavior. Vertical internals arranged uniformly inside the column produce flow behavior similar to bubble column without vertical internals, while internals arranged non-uniformly inside column produce complex flow behavior. Furthermore, they found that the liquid turbulent kinetic energy remarkably reduced when the vertical internal tubes were inserted inside the bubble column.

This work contributes a lot to the field of bubble column with vertical internals; however, their simulations were built on questionable assumptions. For example, they assumed constant bubble diameter (5 and 19 mm) while their simulations had been done on churn turbulent flow regime (12 cm/s), which is characterized by a wide range of bubble sizes (5 mm to 5 cm) [27] due to coalescence and break-up of bubbles. Additionally, the authors applied only drag force as the interfacial force in their simulation and ignored others such as lift force, turbulent dispersion force, and added mass force, even though some studies have reported that incorporating some or all the interfacial forces will improve the prediction of flow pattern [28]. Furthermore, the simulation results for a bubble column with internals were not validated via any benchmark experimental data due to the lack of experimental data of details hydrodynamics for bubble column with vertical internals at that time.

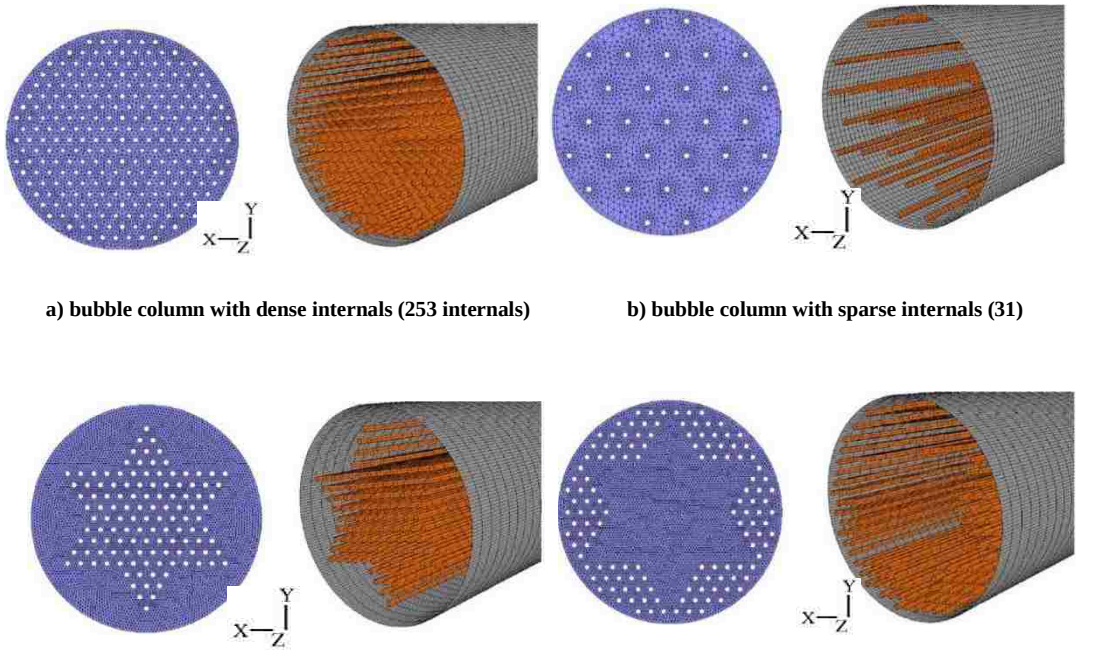

a) bubble column with dense internals (253 internals) **b) bubble column with sparse internals (31)**

c)bubble column with star internals (121) (wall clearance) **d)bubble column with star internals (132) (core clearance)**

Figure 1.7: Different types of vertical internal tube configurations [26]

Youssef and Al-Dahhan [29] conducted the first systematic study of bubble dynamics in the bubble column with vertical internals. In their study, the local gas holdup and bubble properties such as gas-liquid interfacial area, bubble chord length, and bubble velocity distributions were measured in an 8-inch (19 cm) diameter bubble column by implementing the four-point optical fiber probe technique. The local gas holdup and bubble properties were measured in the 8-inch bubble column with and without vertical internals for an air-water system under different superficial gas velocities that ranged from 3-20 cm/s. In their study, they examined the influence of vertical internals, which covered 5% and 22% of the total cross-sectional area (CSA) of the column to represent heat-exchanging tubes used in the LPMeoH synthesis and the FT process, respectively. The vertical internals that covered 5% of the total cross-sectional area were arranged in a circular configuration, while the vertical internals that occupied 25% of the total CSA were organized in a

hexagonal arrangement, as shown in Figure 1.8. Their experimental results and analysis showed that the presence of dense vertical internals (i.e., covering 22% of CSA) caused an increase in the local gas holdup and specific interfacial area. However, insignificant impacts were observed on the local gas holdup and bubble properties when the fewer of the vertical internals (i.e., occupying 5% of CSA) were present inside the column. Also, the authors found that the bubble chord length was decreased in the bubble column equipped densely with vertical internals, which in turn caused a decrease in the bubble rise velocity.

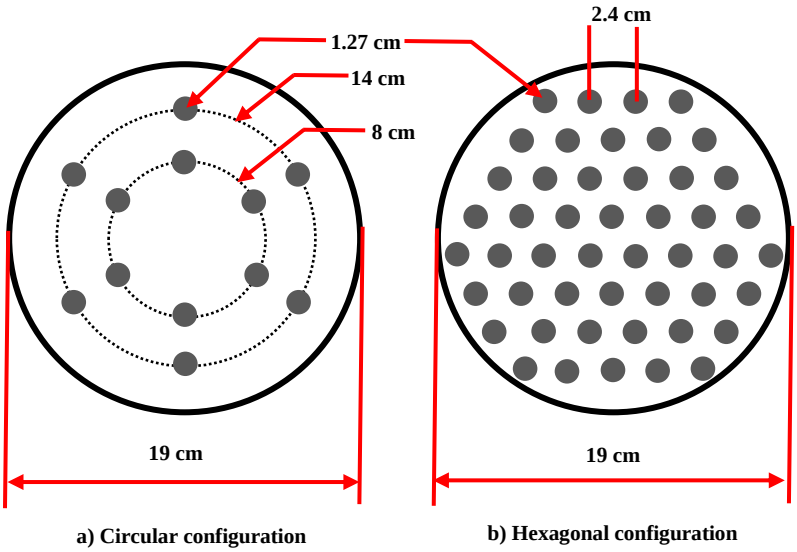

Figure 1.8: Schematic diagram of vertical internal configuration [29]

Boutet et al. [30] utilized computational fluid dynamics (CFD) to simulate the hydrodynamic/thermal coupling in a 15.1 cm diameter bubble column equipped with a bundle of two U-shaped cooling tubes (Figure 1.9) at a superficial gas velocity of 0.343 m/s for air-sylthem XLT (i.e., heat transfer fluid) system. They reported that the gas holdup in the center column with internals was less than that in a column without internals, while higher axial liquid velocity was obtained in the bubble column with internals than the

column without internals. Additionally, they concluded that the local eddy length scale was reduced in the presence of internals. Furthermore, the heat removal was found to be significantly affected by the position of internals.

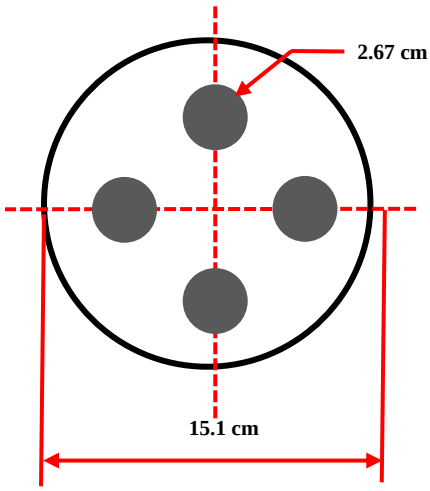

Figure 1.9: Schematic diagram for configuration of vertical internals [30]

Youssef and et al. [31] extended their investigations to an 18-inch pilot-scale bubble column with vertical internals to address and assess the influence of these vertical internal tubes on the local gas holdup and bubble properties of an air-water system by using the same four-point optical fiber probe technique. The author employed the same configurations (i.e., circular and hexagonal arrangements) of vertical internals that was used in their previous work as shown in Figure 1.8. They conducted their experiments under the churn turbulent flow regime meet the industrial conditions in terms of superficial gas velocities (i.e., 20, 30 45 cm/s). The authors noticed that the existence of dense vertical internals (i.e., covering 25% of the total CSA) increases the overall and local gas holdup magnitude for the studied superficial gas velocities. Additionally, they found that the specific interfacial area was remarkably increased in the wall region of the bubble column

equipped densely with vertical internals while the bubble chord lengths were significantly decreased. Moreover, the impact of using different sizes of the bubble columns with vertical internals was found insignificant on the local gas holdup and bubble properties.

Hamed [32] implemented different advanced measurement techniques such as four-point optical fiber probe, gas tracer, and optical oxygen probe to address the influence of vertical internals and column diameters on the bubble properties, axial gas mixing, and overall volumetric mass transfer. In addition to his measurements, he developed and validated a 2D model to predict the gas velocity profile in a bubble column in the absence and the presence of vertical internals. The author conducted his experiments in different sizes of column, including 8 and 18-inch bubble columns with and without vertical internals (i.e., the same columns and vertical internals configurations used in the study of Youssef and et al. [31]) under high superficial gas velocities (particularly at 20, 30, and 45 cm/s). His measurement and analysis disclose that the presence of vertical internals caused an increase in the center-line gas velocity and a significant decrease in the axial gas mixing, while gas-liquid mass transfer coefficient was decreased after inserting these vertical internal tubes. Also, he concluded that the observed enhancement in the gas circulation and the increase in the magnitude of gas mixing were caused by increasing the diameter of the bubble column.

Guan et al. [33] investigated the bubble behavior numerically in terms of the bubble trajectory, bubble shape, bubble rise velocity, and bubble breakup and turbulence by using the volume fluid (VOF) model. In their simulation, they built geometries for vertical internals arranged in a square and triangular pitch with different percentage of covered cross-sectional area (CSA) by vertical internals (mainly 5, 10, 20%). These simulations

were performed for one compartment (i.e., single gap) between vertical internals for square and triangular arrangements, as displayed in Figure 1.10. Their simulation results for single bubble behavior show that the walls of the vertical internals have significant effects on the single bubble behavior in terms of the bubble breakup and turbulent structures. Additionally, they observed that the characteristics of vertical internals such as pitch type (i.e., square and triangular) and the percentage of the occupied area by these internal tubes have an impact on the rocking intensity of the bubble and its frequency. Furthermore, the bubble rise velocity was found to be decreased strongly with the increase of the percentage of occluded cross-sectional area (CSA) by these vertical internal tubes.

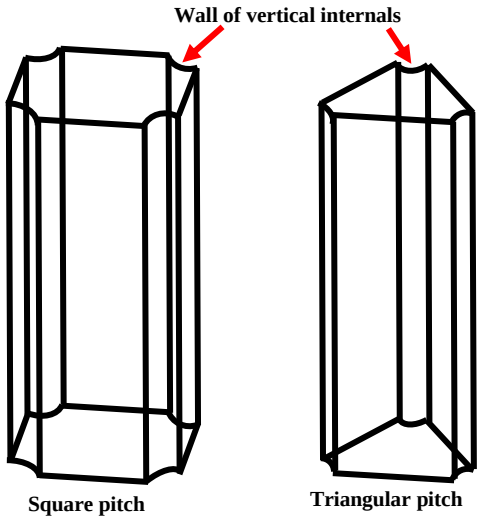

Figure 1.10: Illustration of single compartment for square and triangular pitch [33]

Guan et al. [34] experimentally studied the influence of the presence of pin-fin tubes and their arrangements on the gas holdup and liquid velocity in 0.8 m bubble column for an air-water system by using an electrical resistivity probe and Pavlov tube under a wide range of superficial gas velocities (8-62 cm/s). The pin-fin tubes covered 9.2% of the

total cross-sectional area of the column and were arranged uniformly and non-uniformly over the column cross-sectional area, as displayed in Figure 1.11. The non-uniform arrangement of these pin-fin tubes was created by symmetrically removing two tubes that were close to the wall region, as shown Figure 1.11b. Their experimental data indicated that the gas holdup and liquid velocity were strongly affected by using the pin-fin tubes instead of the plain tubes, where the presence of pin-fin tubes inside the bubble column significantly reduced the height of the distributor region as compared to the bubble column with plain tubes. Also, they found the non-uniform arrangement of pin-fin tubes produce a complicated flow pattern, where this arrangement creates severe gas short-circuiting and even no downflow for liquid in this area. The flow pattern was not changed much when the non-uniform arrangement of plain tubes was used as compared to the bubble column with pin-fin tubes.

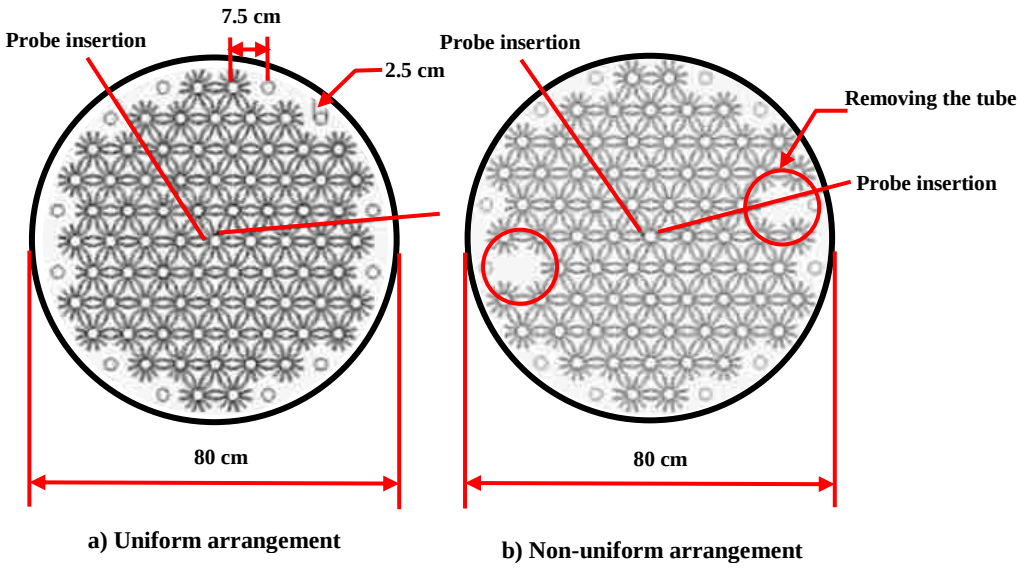

Figure 1.11: Schematic diagram of configuration of pin-fin tubes [34]

Extensive investigations in the Multiphase Reactors Engineering and Applications Laboratory (mReal) at Missouri University of Science and Technology in the field of bubble column reactors have also covered studies on the bubble column with vertical internals. Among these extensive investigations, Kagumba and Al-Dahhan [35] addressed the influence of the presence of vertical internals and their sizes on the local gas holdup, bubble passage frequency, specific interfacial area, bubble chord lengths, and axial bubble velocity in 6-inch bubble columns for an air-water system by employing a four-point optical fiber probe. The vertical internal tubes for both diameters occupied 25% of the total cross-sectional area of the column, representing the heat-exchanging tubes used in the industrial Fischer-Tropsch (FT) synthesis. The 0.5-inch diameter of vertical internal tubes was arranged in a hexagonal configuration, while 1-inch tubes were organized in a circular arrangement over the column's cross-sectional area, as shown in Figure 1.12. The author also assessed the impact of using total and the free cross-sectional area for calculating operating superficial gas velocity for the bubble column with the vertical internals on the local gas holdup and bubble properties. They reported that under a high superficial gas velocity condition (i.e., under a churn turbulent flow regime), the effect of using smaller vertical internals (i.e., 0.5-inch diameter) was insignificant on the overall and local gas holdup magnitudes if the superficial gas velocity remain same based on the free cross-sectional area for the flow. However, an enhancement in the bubble passage frequency, an increase in the specific interfacial area, and a decrease in the magnitude of bubble rise velocity were observed based on using 0.5-inch vertical internals. Additionally, they concluded that considering the total cross-sectional area to calculate the operating gas velocity in the bubble column with vertical internals caused misleading results.

Interestingly, they found that the overall and local gas holdups achieved in the bubble column with vertical internals can be obtained in the bubble column with vertical internals when these columns with vertical internals operate under a high superficial gas velocity and these gas velocities calculated based on the free-cross-sectional area for the flow. This investigation has enhanced the fundamental understanding and has enriched data of the bubble dynamics for the bubble column equipped densely with vertical internals, which is entirely missing in the open literature as highlighted by Guan et al. [33]. However, this study does not maintain the similarity of the configurations for both diameters of vertical internals where the 0.5-inch vertical internal tubes were arranged in a hexagonal shape, while the 1-inch vertical internals were arranged in a circular arrangement over the cross-sectional area of the column. Thus, the variation in the gas holdup and bubble properties could be because of the vertical internal configurations, not their sizes. Therefore, there is much need to address and assess the effect of the size of vertical internals when they are arranged in a similar configuration.

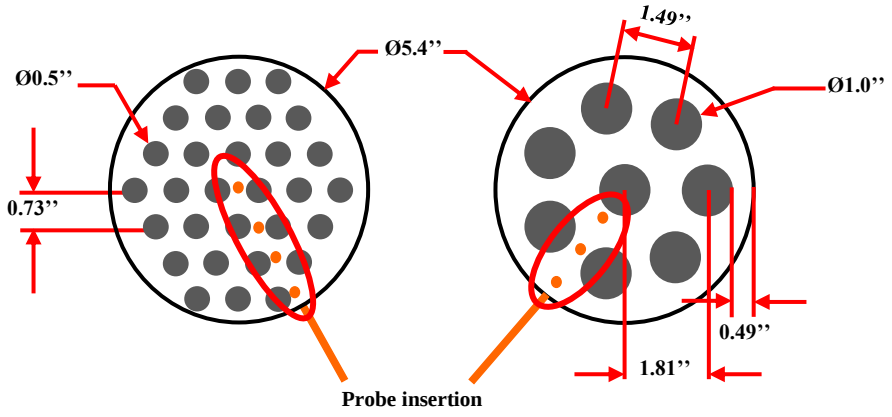

Figure 1.12: Schematic diagram for 0.5 and 1-inch of vertical internals arrangements [35]

Jasim [36] addressed the issue of maintaining the similar configurations when he studied the effects of the presence of vertical internals, their diameters, and their arrangements on the local gas holdup, gas-liquid interfacial area, bubble passage frequency, bubble chord length, and bubble rise velocity by utilizing the four-point optical fiber probe technique. His experiments were carried out in a 6-inch bubble column for an air-water system under a wide range of superficial gas velocity that covered the bubbly, transition, and churn turbulent flow regimes (2-45 cm/s calculated based on free CSA for the columns with vertical internals). The vertical internal tubes in this investigation were selected for blocking 25% of the total cross-sectional area (CSA) of the column to represent the same occupied space by industrial heat-exchanging tubes for the Fischer-Tropsch (FT) process. In this study, both sizes of the vertical internals were arranged in a circular configuration (Figure 1.13) over the cross-sectional area of the column to accurately assess and quantify the effect of the presence of the vertical internals and their size on the bubble dynamics.

In his study, Jasim found that the local gas holdup and specific interfacial area were enhanced in the wall region of the bubble column with 1-inch vertical internals compared to the bubble column without and with 0.5-inch vertical internals. Also, he reported that vertical internal configurations strongly impact the bubble dynamics as compared to the bubble column in the absence of vertical internals. Moreover, Jasim concluded that the 0.5-inch internals with a circular configuration gave symmetric gas holdup profiles along the diameter of the column, while the 0.5-inch internals with the hexagonal arrangement led to a distinct asymmetric gas holdup diameter profile.

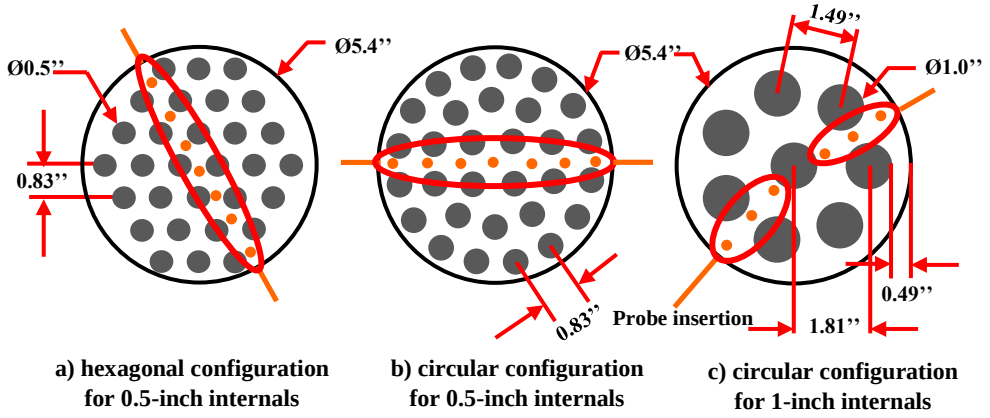

Figure 1.13: Schematic diagram of hexagonal and circular configurations for 0.5 and 1-inch vertical internal tubes [36]

Al-Dahhan and co-authors [37,38] were among one of the first research groups that visualized and quantified the presence of dense heat-exchanging tubes on the cross-sectional gas holdup distribution and their profiles, 3D liquid velocity field, Reynolds stresses, turbulent kinetic energy, and turbulent eddy diffusivities in a non-invasive way by using advanced gamma-ray computed tomography (CT) and radioactive particle tracking (RPT) techniques. This detailed hydrodynamics study was conducted in 6-inch bubble columns in the absence and presence of vertical internals for air-water-system under a wide range of superficial gas velocities, which were covered homogenous (bubbly flow regime) and heterogeneous (churn flow regime) flow regimes (i.e., 5-45 cm/s). A bundle of 30 vertical tubes arranged in a hexagonal configuration (Figure 1.14) and blocking 25% of the total cross-sectional area of the bubble column was chosen by the investigators to match the percentage of occupied area for the industrial FT synthesis. Their tomography images revealed that the gas holdup distributions for the columns with and without vertical internals were almost symmetric for all studied superficial gas velocities except for high superficial gas velocities in the bubble column with the presence of vertical internals. Their

results also indicated that the presence of vertical internals significantly increased the centerline and negative axial liquid velocity under any studied superficial gas velocity. Furthermore, they found that the normal and shear stresses, turbulent kinetic energy, and eddy diffusivity of liquid phase sharply decreased when the column was equipped with vertical internals.

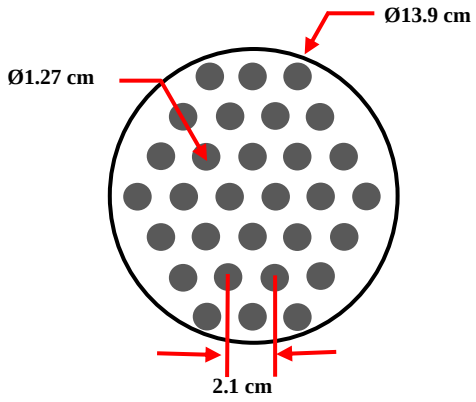

Figure 1.14: Schematic diagram of hexagonal configuration for 0.5-inch internals [37]

Guan and Yang [39] numerical analyzed the influence of involving more than interfacial forces such as lift force, turbulent dispersion force and wall force beside to the drag force on the prediction the hydrodynamics in a pilot-scale bubble column with and without internals for the air-water system under operating superficial gas velocities of 12 and 31 cm/s. The researchers performed their simulation for 48-cm bubble columns without and with vertical internal tubes that were arranged in a triangular pitch and blocked 5% of the total cross-sectional area of the column, as displayed in Figure 1.15. Based on their simulation results, they concluded that incorporating lateral forces such as lift force, turbulent dispersion force and wall force with the drag force is optional for simulation bubble column without vertical internals while the lateral forces are required for the bubble

column with the vertical internals to predict the hydrodynamics of these columns accurately.

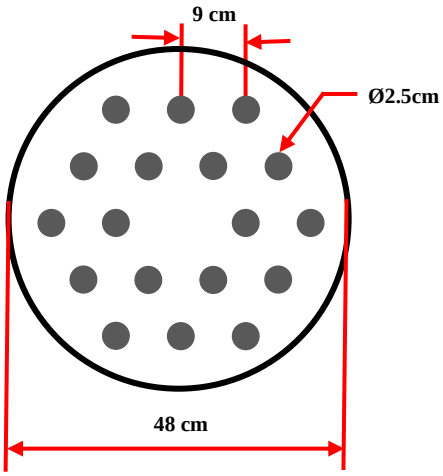

Figure 1.15: Schematic diagram for vertical internals arrangements [39]

Recently, an investigation of the liquid phase hydrodynamic and mixing behavior in bubble columns equipped with vertical internals was performed by Kalaga et al. [40,41]. The primary goal of their investigation was to examine the influence of vertical internal tubes, superficial gas and liquid velocity on the gas holdup distribution, axial liquid velocity, liquid mixing behavior in the bubble columns with different configurations of vertical internals by using radioactive particle tracking (RPT) and residence time distribution (RTD) techniques. Their study was carried out in a 12-cm inner diameter bubble column in which both air and water were fed concurrently. Six different vertical internals configurations which were covered a wide range of occupied cross-sectional area of the column (i.e., 0-63% of the total CSA of the column) was examined in this study, as shown in Figure 1.16. However, due to the practical limitations of RPT technique, RPT experiments were conducted in batch mode bubble columns without and with 1 and 5 vertical internals while the RTD experiments were performed for continuous bubble

column without and with vertical internals (all configurations of internals). The obtained experimental results in terms of gas holdup distribution, axial liquid velocity, and the liquid phase dispersion coefficient were found to be strongly impacted by superficial gas velocity, liquid velocity, and vertical internals configuration.

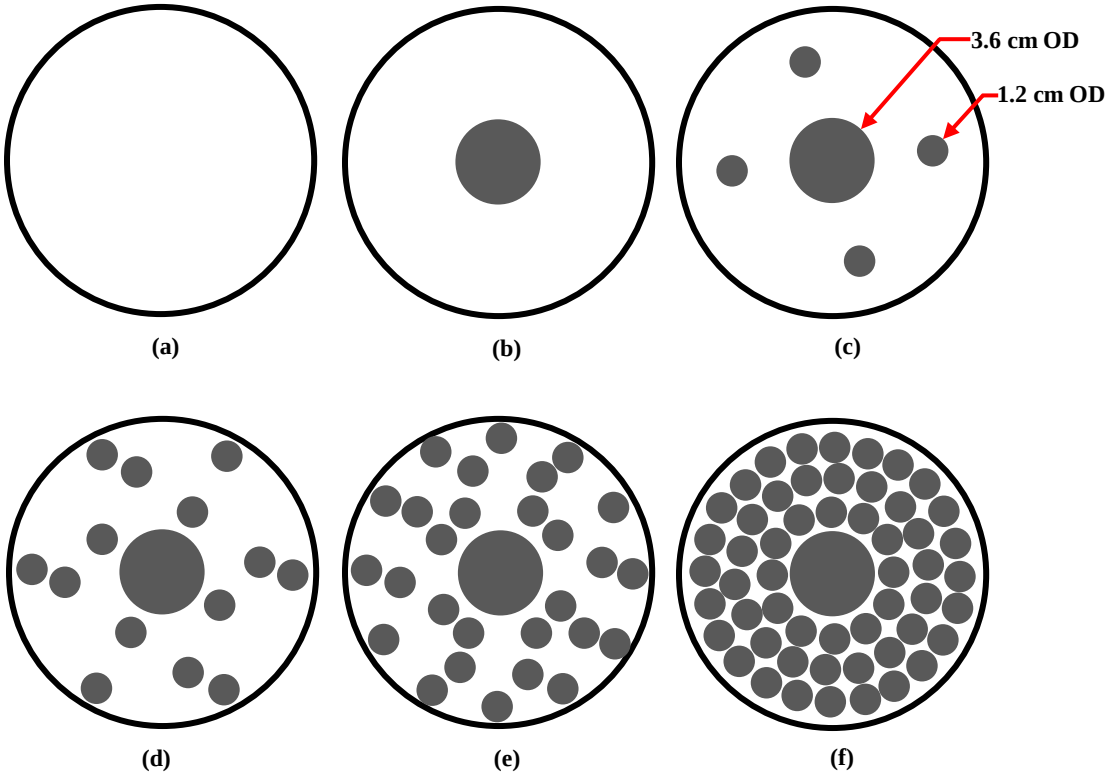

Figure 1.16: Schematic diagram of vertical internals configurations employed in RPT experiments (a-c) and RTD (a-f) experiments [40]

According to the preceding investigations and discussion, the majority of these studies was conducted by using a probe-based technique. The probes are invasive, and even they are small sizes still providing a point measurement (i.e., local points) that requires extensive experimental work to assess the effect of the operating and design parameters. Other reported studies did not focus on the dense of vertical internals and limit for a fewer number of vertical internals due to the limitation of measurement technique. Among other

hydrodynamic studies for the bubble column with dense vertical internals, only Al Mesfer et al. investigated the effect of these vertical internal tubes on the details of hydrodynamics by using non-invasive techniques such as CT and RPT. However, it was limited to one geometry configuration (hexagonal arrangement), one size of tubes (0.5-inch) and one size of the column (6-inch).

Accordingly, the reported studies on the bubble column with vertical internals have some limitations as mentioned earlier and hence they are insufficient for adequately understanding the impact of the vertical internals on the hydrodynamics of these reactors. Therefore, the primary goal of this investigation is to improve the fundamental understanding of the impacts of these vertical internal tubes on the hydrodynamics of the bubble column. To achieve this goal, a close investigation of the influence of vertical internals, their diameters, their configurations on the cross-sectional gas holdup distributions and their profiles, axial liquid velocity, and turbulent parameters, is much needed.

The knowledge and findings acquired from this work along with the previous investigations in terms of the hydrodynamics and bubble properties will significantly enrich and improve the understanding of the influence of heat-exchanging tubes on the performance of the bubble and slurry bubble columns. Additionally, it will provide valuable hydrodynamics information, which can be used for developing, designing, and scaling up these kinds of reactors. Moreover, these unique experimental results can be used as benchmarking data to evaluate and validate CFD simulations and mechanistic phenomenological models, which in turn will facilitate the processes of the design, scale-up, and operation of these reactors. Furthermore, the obtained results and findings can be

applied to boiling water reactors which are used for generating electrical power, where these reactors are equipped with a bundle of intense fuel rods that evaporate the water and turns it into steam which powers the turbine.

1.2. RESEARCH OBJECTIVES

The main goal of this study is to improve and advance the fundamental understanding and knowledge of the influence of vertical internal tubes on the hydrodynamics of the bubble column. To accomplish this goal, extensive benchmarking experimental investigations and analysis will be conducted to visualize and quantify for the first time the impacts of the presence of dense vertical internal tubes, their diameters, their configurations on the cross-sectional gas holdup distributions and their profiles, liquid velocity field, and turbulent parameters by using advanced gamma-ray computed tomography (CT) and radioactive particle tracking (RPT) techniques. Therefore, the following objectives are set for this study:

1. Overcoming the gamma-ray computed tomography data processing pitfalls for bubble column equipped with vertical internal tubes.
2. Visualizing and quantifying the influence of the size of heat-exchanging tubes (internals) on the gas holdup distribution in a bubble column.
3. Assessing the impact of the heat exchanging tube configurations on gas holdup distribution in bubble column.
4. Investigating the influence of a bundle of heat-exchanging tubes, their configuration, and column size on the gas holdup distributions in a bubble column.
5. Studying the influence of vertical internal diameters on the liquid velocity field and turbulent parameters.

REFERENCES

[1] U.S. Energy Information Administration, International Energy Outlook 2016, 2016. doi:www.eia.gov/forecasts/ieo/pdf/0484(2016).pdf.

[2] J. Hu, F. Yu, Y. Lu, Application of Fischer–Tropsch Synthesis in Biomass to Liquid Conversion, Catalysts. 2 (2012) 303–326.

[3] R. Guettel, U. Kunz, T. Turek, Reactors for Fischer-Tropsch synthesis, Chem. Eng. Technol. 31 (2008) 746–754.

[4] H. Jung, J.-I. Yang, J.H. Yang, H.-T. Lee, D.H. Chun, H.-J. Kim, Investigation of Fischer–Tropsch synthesis performance and its intrinsic reaction behavior in a bench scale slurry bubble column reactor, Fuel Process. Technol. 91 (2010) 1839–1844.

[5] D.A. Wood, C. Nwaoha, B.F. Towler, Gas-to-liquids (GTL): A review of an industry offering several routes for monetizing natural gas, J. Nat. Gas Sci. Eng. 9 (2012) 196–208.

[6] S. Saeidi, M.K. Nikoo, A. Mirvakili, S. Bahrani, N.A. Saidina Amin, M.R. Rahimpour, Recent advances in reactors for low-temperature Fischer-Tropsch synthesis: process intensification perspective, Rev. Chem. Eng. 31 (2015) 19–21.

[7] O.M. Basha, L. Sehabiague, A. Abdel-Wahab, B.I. Morsi, Fischer-Tropsch Synthesis in Slurry Bubble Column Reactors: Experimental Investigations and Modeling - A Review, Int. J. Chem. React. Eng. 13 (2015) 201–288.

[8] L. Sehabiague, Modeling, scaleup and optimization of slurry bubble column reactors for Fischer-Tropsch synthesis, 2012.

[9] R. Krishna, J.W. a. De Swart, J. Ellenberger, G.B. Martina, C. Maretto, Gas holdup in slurry bubble columns: Effect of column diameter and slurry concentrations, AIChE J. 43 (1997) 311–316.

[10] H.-P. Luo, Analyzing and Modeling of Airlift Photobioreactors for Microalgal and Cyanobacteria Cultures by, Washington, 2005.

[11] A. Shaikh, M.H. Al-Dahhan, A Review on Flow Regime Transition in Bubble Columns, Int. J. Chem. React. Eng. 5 (2007). doi:10.2202/1542-6580.1368.

[12] N. Rados, A. Shaikh, M.H. Al-Dahhan, Solids flow mapping in a high pressure slurry bubble column, Chem. Eng. Sci. 60 (2005) 6067–6072.

[13] P. Chen, P. Gupta, M.P. Dudukovic, B.A. Toseland, Hydrodynamics of slurry bubble column during dimethyl ether (DME) synthesis: Gas-liquid recirculation model and radioactive tracer studies, Chem. Eng. Sci. 61 (2006) 6553–6570.

[14] A. Shaikh, M. Al-Dahhan, A new method for online flow regime monitoring in bubble column reactors via nuclear gauge densitometry, Chem. Eng. Sci. 89 (2013) 120–132.

[15] L.T. Angenent, K. Karim, M.H. Al-Dahhan, B.A. Wrenn, R. Domíguez-Espinosa, Production of bioenergy and biochemicals from industrial and agricultural wastewater, Trends Biotechnol. 22 (2004) 477–485.

[16] P.M.W. S. Schlfiter , A. Steiff, Heat transfer in two- and three-phase bubble column reactors with internals, Chem. Eng. Process. 34 (1995) 157–172.

[17] H.P. Luo, A. Kemoun, M.H. Al-Dahhan, J.M.F. Sevilla, J.L.G. Sánchez, F.G. Camacho, E.M. Grima, Analysis of photobioreactors for culturing high-value microalgae and cyanobacteria via an advanced diagnostic technique: CARPT, Chem. Eng. Sci. 58 (2003) 2519–2527.

[18] B.W. Lee, Optical Probes in Multiphase Reactors, Washington University in St. Louis, 2016.

[19] B. Ong, Experimental Investigation of Bubble Column Hydrodynamics - Effect of Elevated Pressure and Superficial Gas Velocity -, Washington University, 2003.

[20] P. Chen, J. Sanyal, M.P.P. Duduković, Numerical simulation of bubble columns flows: Effect of different breakup and coalescence closures, Chem. Eng. Sci. 60 (2005) 1085–1101.

[21] G. Salierno, M. Maestri, S. Piovano, M. Cassanello, M.A. Cardona, D. Hojman, H. Somacal, Calcium alginate beads motion in a foaming three-phase bubble column, Chem. Eng. J. 324 (2017) 358–369.

[22] A. Prakash, A. Margaritis, H. Li, M.A. Bergougnou, Hydrodynamics and local heat transfer measurements in a bubble column with suspension of yeast, Biochem. Eng. J. 9 (2001) 155–163.

[23] A.A. Youssef, M.H. Al-Dahhan, M.P. Dudukovic, Bubble columns with internals: A review, Int. J. Chem. React. Eng. 11 (2013) 169–223.

[24] J. Chen, F. Li, S. Degaleesan, P. Gupta, M.H. Al-Dahhan, M.P. Dudukovic, B.A. Toseland, Fluid dynamic parameters in bubble columns with internals, Chem. Eng. Sci. 54 (1999) 2187–2197.

[25] A. Forret, J.M. Schweitzer, T. Gauthier, R. Krishna, D. Schweich, Liquid dispersion in large diameter bubble columns, with and without internals, Can. J. Chem. Eng. 81 (2003) 360–366.

[26] F. Larachi, D. Desvigne, L. Donnat, D. Schweich, Simulating the effects of liquid circulation in bubble columns with internals, Chem. Eng. Sci. 61 (2006) 4195–4206.

[27] A. Gupta, S. Roy, Euler-Euler simulation of bubbly flow in a rectangular bubble column: Experimental validation with Radioactive Particle Tracking, Chem. Eng. J. 225 (2013) 818–836.

[28] M. V. Tabib, S.A. Roy, J.B. Joshi, CFD simulation of bubble column-An analysis of interphase forces and turbulence models, Chem. Eng. J. 139 (2008) 589–614.

[29] A.A. Youssef, M.H. Al-Dahhan, Impact of internals on the gas holdup and bubble properties of a bubble column, Ind. Eng. Chem. Res. 48 (2009) 8007–8013.

[30] F. Laborde-Boutet, Cédric and Larachi, CFD Simulations of Hydrodynamic/Thermal Coupling Phenomena in a Bubble Column with Internals, AIChE J. 56 (2010) 2397–2411.

[31] A.A. Youssef, M.E. Hamed, J.T. Grimes, M.H. Al-Dahhan, M.P. Duduković, Hydrodynamics of pilot-scale bubble columns: Effect of internals, Ind. Eng. Chem. Res. 52 (2013) 43–55.

[32] M. Hamed, Hydrodynamics, mixing, and mass transfer in bubble columns with internals, Washington University in St. Louis, 2012.

[33] X. Guan, Z. Li, L. Wang, Y. Cheng, X. Li, CFD simulation of bubble dynamics in bubble columns with internals, Ind. Eng. Chem. Res. 53 (2014) 16529–16538.

[34] X. Guan, Y. Gao, Z. Tian, L. Wang, Y. Cheng, X. Li, Hydrodynamics in bubble columns with pin-fin tube internals, Chem. Eng. Res. Des. 102 (2015) 196–206.

[35] M. Kagumba, M.H. Al-Dahhan, Impact of internals size and configuration on bubble dynamics in bubble columns for alternative clean fuels production, Ind. Eng. Chem. Res. 54 (2015) 1359–1372.

[36] A. Jasim, The impact of heat exchanging internals on hydrodynamics of bubble column reactor, Missouri University of Science and Technology, 2016.

[37] M. Al Mesfer, A. Sultan, M. Al-Dahhan, Impacts of dense heat exchanging internals on gas holdup cross-sectional distributions and profiles of bubble column using gamma ray Computed Tomography (CT) for FT synthesis, Chem. Eng. J. 300 (2016) 317–333.

[38] M.K. Al Mesfer, A.J. Sultan, M.H. Al-Dahhan, Study the effect of dense internals on the liquid velocity field and turbulent parameters in bubble column for Fischer–Tropsch (FT) synthesis by using Radioactive Particle Tracking (RPT) technique, Chem. Eng. Sci. 161 (2017) 228–248.

[39] X. Guan, N. Yang, CFD simulation of pilot-scale bubble columns with internals: Influence of interfacial forces, Chem. Eng. Res. Des. 126 (2017) 109–122.

[40] D. V. Kalaga, A. Yadav, S. Goswami, V. Bhusare, H.J. Pant, S. V. Dalvi, J.B. Joshi, S. Roy, Comparative analysis of liquid hydrodynamics in a co-current flow-through bubble column with densely packed internals via radiotracing and Radioactive Particle Tracking (RPT), Chem. Eng. Sci. 170 (2017) 332–346.

[41] D. V. Kalaga, H.J. Pant, S. V. Dalvi, J.B. Joshi, S. Roy, Investigation of hydrodynamics in bubble column with internals using radioactive particle tracking (RPT), AIChE J. 63 (2017) 4881–4894.

PAPER

I. OVERCOMING THE GAMMA-RAY COMPUTED TOMOGRAPHY DATA PROCESSING PITFALLS FOR BUBBLE COLUMN EQUIPPED WITH VERTICAL INTERNAL TUBES

Abbas J. Sultan, Laith S. Sabri, Jianbin Shao, Muthanna H. Al-Dahhan †

Multiphase Reactors Engineering and Applications Laboratory (mReal), *Department of Chemical and Biochemical Engineering, Missouri University of Science and Technology, Rolla, MO 65409-1230. USA*

ABSTRACT

This study identifies and addresses some major pitfalls that are involved in the visualization and quantification of the gas-liquid distributions and their profiles in the bubble column with internals using the gamma-ray computed tomography (CT) technique. Some of these pitfalls encountered in the scanning of bubble columns with internals are using an improper reference scan, applying the same experimental scanning procedure and mathematical relationships for estimating the gas holdup in the column without internals to the column with internals. The experimental results revealed that the selection of the inappropriate reference scan for CT experiments would significantly affect the reconstructed linear attenuation coefficient values and consequently the gas holdup results. Additionally, the reconstructed linear attenuation values showed good agreement with theoretical values when considering air as reference scans. However, disagreement is observed when using the empty column with internals as a reference scan. Moreover, it was found that using the proper reference scan eliminated the errors not only for the reconstructed linear attenuation coefficients but also for the gas holdup values near the wall region. Furthermore, the CT technique was capable of capturing the small thickness (5 mm) of the wall for phantom and bubble columns as well as the internals when the air was used

as the reference scan. Finally, a new methodology has been implemented to exclude the internals from the cross-sectional images, and the azimuthally averaged gas holdup profiles to provide accurate and reliable results for comparison and validation purposes for the bubble column with internals.

Keywords: Bubble column with internals, cross-sectional gas holdup, CT technique.

†Correspondence author at Chemical & Biochemical Engineering Department, Missouri University of Science and Technology, Rolla, MO, 65409. Tel.: +1 573-578-8973. E-mail: aldahhanm@mst.edu

1. INTRODUCTION

Bubble and slurry bubble column reactors have been extensively used in industrial processes, particularly in chemical and biochemical, petroleum and petrochemical, metallurgical and waste treatment processes.[1–4] Most industrial utilizations of the bubble/slurry bubble columns include exothermic reactions such as methanol synthesis (LPMeOH), Fischer-Tropsch (FT) synthesis and many others.[5] The removal of heat generated to maintain the process isothermally is an important consideration for design, scale-up, and safe operation of these types of the reactors.[6,7]

Bubble/slurry bubble column reactors equipped with a bundle of the heat-exchanging tubes are considered favorable for conducting highly exothermic reactions due to their capability of removing the generated heat efficiently, and they can be operated isothermally in the absence of axial and radial gradient temperature.[8,9] However, the presence of the heat-exchanging tubes alters the hydrodynamics of the bubble/slurry bubble columns and consequently, significantly affects the performance, yield, and selectivity of these reactors.[10–15]

Gas holdup distribution is among the most important hydrodynamic parameters governing the liquid/slurry circulation in bubble/slurry bubble columns, and hence governing the rate of mixing, mass, and heat transfer, which in turn controls the performance of these reactors.[16–23] Quantification of the gas holdup distributions and their profiles in these columns equipped with a bundle of the heat exchanging tubes is necessary to advance understanding the hydrodynamics of these multiphase flow systems and to validate and evaluate computational fluid dynamics (CFD) simulations and hydrodynamic models.

Various measurement devices can be used to measure gas holdup in bubble/slurry bubble columns, such as fiber optical probes, conductivity probes, differential pressure probes, ultrasonic techniques, electrical capacitance tomography, X-ray tomography, gamma-ray densitometry, and gamma-ray computed tomography (CT).[24–30] However, gamma-ray computed tomography is superior to other techniques due to its capability to visualize and measure gas holdup over the entire cross-sectional area of the column in dense and opaque flows that are not visible to other measurement devices due to their limitation to measure in single points (such as probe-based measurement) or their a low penetration capability to pass through the high attenuating material (such as X-ray tomography).[31–35]

In the past three decades, the CT technique has been successfully used to visualize and quantify gas-liquid distributions and their profiles in the bubble column without vertical internal tubes. However, the path of scanning a bubble column equipped densely with vertical internal tubes is floored with some pitfalls. These pitfalls of the scanning bubble column with vertical internal tubes are listed here as follows:

- Choosing an improper reference scan.
- Using an inappropriate experimental procedure for scanning a bubble column with vertical internal tubes.
- Implementing an inappropriate relationship for the estimation local gas holdup based on the reconstructed linear attenuation coefficient (μ, cm^{-1}).
- Failure to properly quantify the azimuthally gas holdup profiles of a bubble column with vertical internal tubes.

Unlike scanning a bubble column in the absence of vertical internal tubes, scanning a column with a presence of vertical tubes is a difficult and challenging task. Therefore, there is a need to carefully avoid and address the above issues and concerns to scan a bubble column with vertical tubes that provide correct and reliable gas holdup distribution and their profiles.

The measurement of gas holdup distribution by the gamma-ray computed tomography (CT) technique requires several independent scans for the bubble columns equipped with a bundle of vertical internals at different operating conditions (empty column, a column filled with water only (not flowing), and a column containing air-water (flowing)). However, proper selection of the reference scan to account for the incident counts ($I_\circ$) at the gamma ray source for the Beer-Lambert model $\left((I/I_\circ) = e^{-\mu L}\right)$ represents the most important step in the data processing to achieve the correct transmission ratio, accurate reconstructed linear attenuation coefficients (μ, cm^{-1}), and consequently reliable estimation of the gas holdup distribution. The $I_\circ$ represents the initial intensity of the gamma ray at the source, which is difficult to measure in the gamma-ray computed

tomography scanner because the detectors are located at a certain distance from the gamma-ray source.

For convenience, CT experiments that scan empty columns placed in the center of the CT technique are often used as reference scans that provides the attenuation of the column wall materials to the gamma ray that is negligible (such as with aluminum) or is considered negligible due to the small thickness of the wall when the material of the column wall attenuates the gamma ray (like with Plexiglas or a stainless-steel column wall). Additionally, the line beams of the gamma ray from the source toward its detectors arranged in an arc (3rd generation of CT) pass different lengths through the column wall since the collimator's source is made to provide fan beams to the arc arrangement of the detectors. If the wall materials of the column attenuate the gamma ray noticeably, then the empty column as a reference scan could affect the quality, accuracy, and the reliability of the results significantly by considering that the attenuation of the wall is negligible due to the small thickness of the wall. Additionally, considering the column with vertical internal tubes as the reference scan, this could be problematic whether the materials of the internals are from low attenuated materials to gamma rays (such as aluminum) or high attenuated materials to gamma rays (such as steel or even Plexiglas). Moreover, using the same experimental scanning procedure and mathematical equations to estimate the local gas holdup for the bubble column without vertical internal tubes to the column with vertical tubes can lead to incorrect values of the gas holdup.

Therefore, there is an urgent need to establish an experimental scanning procedure and mathematical equations to precisely estimate gas holdup in the bubble column equipped with vertical internal tubes. Furthermore, the cross-sectional gas holdup

distribution and the azimuthally averaged gas holdup profile in the presence of the vertical internals tend to produce a significant error and lead to inaccuracies in the estimation of the gas holdup profiles if the same algorithm and programs are used for the column without vertical internals.

These situations and conditions cause pitfalls in the results of gamma ray CT scanner' and need to be addressed and analyzed properly. Owing to the complexity of multiphase flow in the bubble column equipped with vertical internal tubes and limitations of measurement techniques, unfortunately no systematic study has been taken and reported that analyzes such effects. Accordingly, this study tackles these issues systematically to bring the attention to researchers of the proper steps, procedure, and model equations that can be used to produce reliable CT results. In this work, an experimental scanning method, mathematical equations for correctly calculating gas holdup for two (air-water) and three (air-water with internals) phases, and methodology for excluding the internals from gas holdup distributions and their azimuthally averaged profiles have been established and developed to overcome the pitfalls caused by using improper methods and mathematical equations in addition to the pitfalls due to the type of reference scans used.

The major outcome of this study is to provide confidence in CT measuring in general and in calculating the time-averaged cross-sectional gas holdup distributions and their profiles for the bubble columns equipped with or without a bundle of heat-exchanging tubes. Outlining and addressing the pitfalls that are associated with scanning bubble columns with vertical internal tubes will help and guide those scanning these columns to avoid these pitfalls and provide reliable gas holdup distribution and their profiles.

2. EXPERIMENTAL SETUP

In this work, all the measurements of the time-averaged cross-sectional gas holdup distributions and their profiles were performed in a Plexiglas bubble column with an inner diameter of 5.5 in. (0.14 m) and a height of 72 in. (1.83 m), as shown schematically in Figure 1. During the experiments, the bubble column was operated using compressed oil-free dry air for the gas phase and purified water for the liquid phase.

The compressed atmospheric air was supplied by an industrial-scale air compressor (Ingersoll Rand Company), which can provide compressed air at a flow rate of 0.35 m^3/s with a working pressure of 200 psi. The compressed air was filtered, dried, and regulated by using the air filter, dryer, and regulator pressure before entering a set of flowmeters. These flowmeters consist of two calibrated flowmeters (Brooks Instrument Company) connected parallel to cover a wide range of superficial gas velocity (0.05-0.45 m/s). Air was introduced continuously into the bubble column at the bottom through the plenum and gas distributor, while water was in a batch mode during all measurements.

The gas distributor used in this work was a perforated plate located above the plenum. The plate had 121 holes, each 0.132 cm in diameter and arranged in a triangular pitch of 1.016 cm, offering a total open area of 1.09%, as shown in Figure 2. It is important to mention that with these characteristics of this gas distributor, the liquid weeping condition (i.e., weeping some liquid into the plenum chamber of the column) was not encountered in these experiments due to high superficial gas velocity was applied (i.e., 45 cm/s) in this study.

Additionally, the dimensionless capacitance number (N_C) was calculated by Eq. 1 to characterize the flow conditions of the bubbles through the orifices of this gas distributor.[36–38]

$$N_C = \frac{4V_{ch}g\rho_l}{\pi d_o^2 P_h} \quad (1)$$

where V_{ch} represents the volume of the plenum chamber (m^3); g represents gravitational acceleration (m/s^2), ρ_l represents the density of the liquid (kg/m^3), d_o represents the orifice diameter (m), P_h represents the hydrostatic pressure at the orifice plate (MPa). Under a condition of N_C smaller than 1, the flow rate of bubbles through the orifice of the gas distributor is invariant (i.e., constant flow conditions) while for N_C higher than 9 the flow condition is variable (i.e., gas flow rate generates variable pressure).[39,40] However, the calculated N_C for this gas distributor is 1.65 (which lies between 1 and 9), which indicates there no weeping under studied superficial gas velocity. Vertical Plexiglas tubes with 1 in. (2.54 cm) in diameter covering ~25% of the total cross-sectional area of the column were used in this study to represent the same cross-sectional area occluded by industrial heat-exchanging tubes used in Fischer-Tropsch synthesis.[41–43] These internals were arranged in a circular configuration, which consisted of one bundle of seven internals surrounding one vertical internal at the center, as exhibited in Figure 3. It is worth mentioning that these internal tubes were placed and secured vertically inside the bubble column at a distance 3 in. (0.0762 m) above the gas distributor and extended up to the end of the column by using three circular supports (spacers) and the upper plate to omit the vibration and make them more stable during the experiments. The Plexiglas material for the column wall and vertical internals has been selected in this study for promoting eye visualization despite its linear

attenuation coefficient (0.098 cm^{-1}) being higher than water (0.086 cm^{-1}). However, it would be best to overcome the Plexiglas issue by using a material for the column wall and vertical internals or the vertical internals alone that has a low linear attenuation coefficient. This should be considered for future studies. In this study, the averaged dynamic liquid level was kept at constant level 62 in. (1.58 m) (H/D = 10.3) from the gas distributor by tuning the initial static height of liquid loaded on the column. The experiments were conducted at room temperature and atmospheric pressure in churn turbulent flow regime (i.e., under a constant superficial gas velocity of 45 cm/s). The superficial gas velocity was chosen to satisfy industrial interest where usually FT process operates under churn turbulent flow regime condition (i.e., which characterized by heterogeneous bubble's structure) to achieve high volumetric productivity. This superficial gas velocity was calculated based on the total cross-sectional area (TCSA) of the bubble column without vertical internal tubes, while it was computed based on the free cross-sectional area (FCSA) for the flow in the case using a bubble column with vertical internal tubes. The free cross-sectional area (FCSA) for the flow can be defined by the following equation:

$$\begin{aligned} &Free\ cross\text{-}sectional\ area\ (FCSA) \\ &= \Big((total\ cross\text{-}sectional\ area\ of\ the\ bubble\ column\ without\ internals\ \left(\frac{\pi}{4} D_c^2\right)) \\ &- (cross\text{-}sectional\ area\ occupied\ by\ internals\ \left((\frac{\pi}{4} D_t^2) \times N \right)) \Big) \end{aligned}$$

where D_c and D_t represent the column and tube diameters, respectively, while N represents the number of vertical internal tubes. All CT scans were conducted in the fully developed region at the axial level of 0.76 m (H/D = 5.1) where the gas holdup distribution relatively does not change axially beyond this level.[7,21] Experiments were replicated twice to check for data reproducibility.

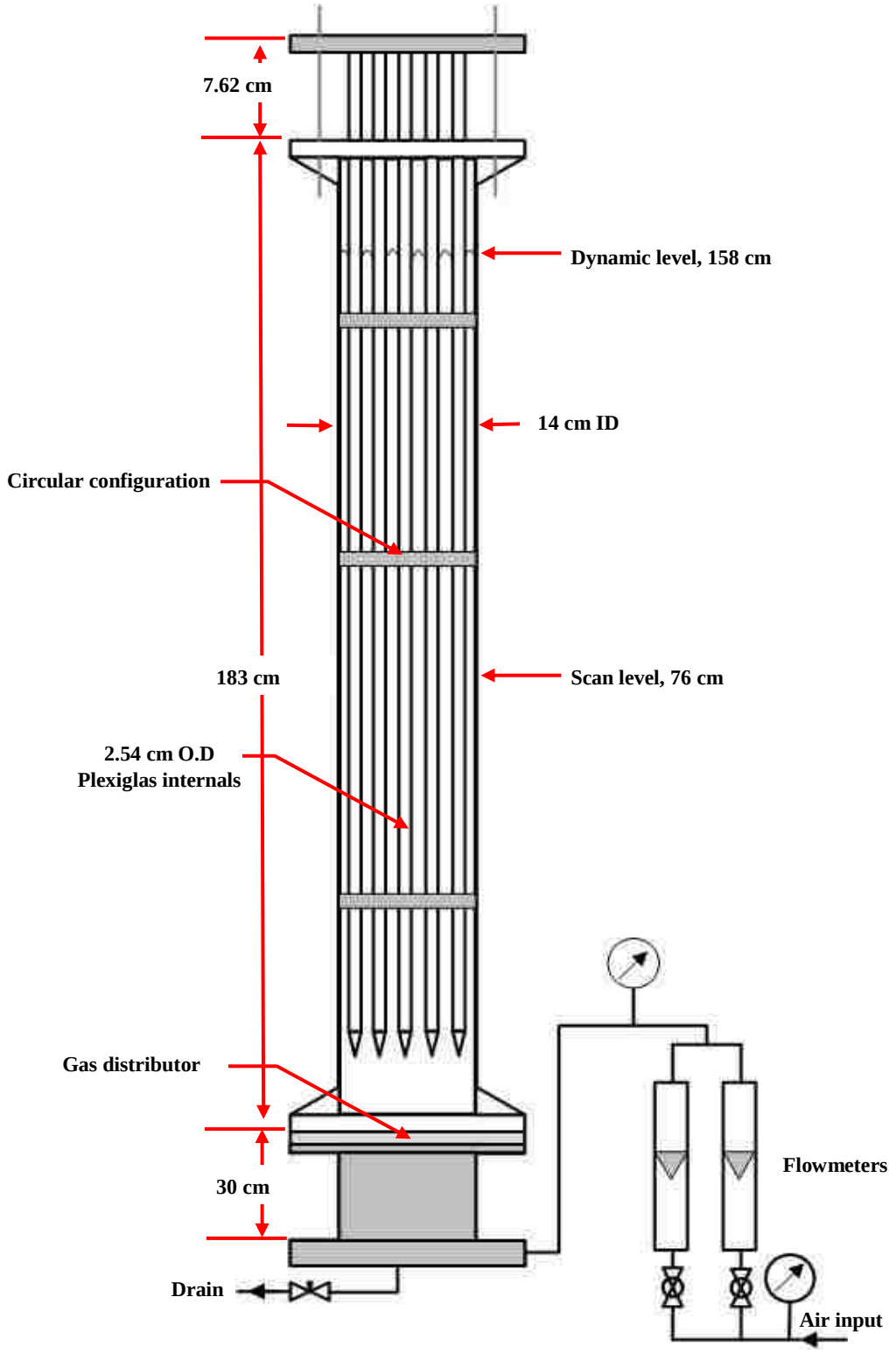

Figure 1: Schematic diagram of the used bubble column with vertical internal tubes

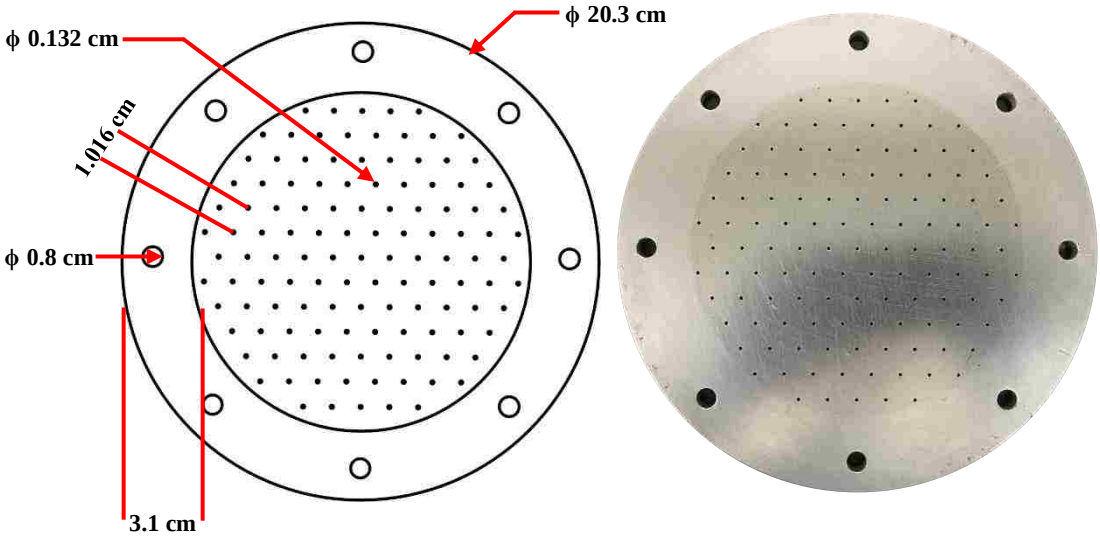

Figure 2: Schematic diagram and photo of the gas distributor (perforated plate)

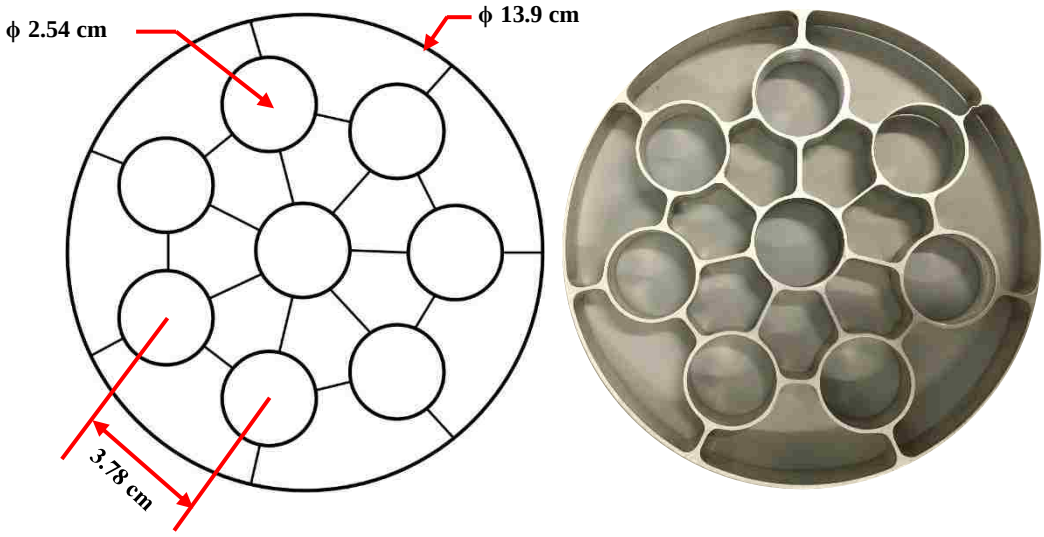

Figure 3: Schematic diagram and photo of the circular configuration of vertical internals

3. GAMMA-RAY COMPUTED TOMOGRAPHY (CT)

Gamma ray computed tomography is a noninvasive technique that provides the cross-sectional images at different axial levels by rotating the gamma source and its detectors around the object. It is a useful tool to visualize, quantify, and diagnose the phase

distributions of the multiphase flow reactors that cannot be measured by other measurement techniques.

During this study, the time-averaged gas holdup distribution measurements were conducted with a single-source gamma-ray computed tomography (CT) technique, which is the part of the current dual-source gamma-ray computed tomography that was designed and advanced in-house by Varma[44] and is presently available in the Multiphase Reactors Engineering and Application Laboratory (mReal) at Missouri University of Science and Technology (Missouri S&T). Figure 4 and Figure 5 exhibit schematically and photographically of the CT technique with bubble column equipped with a bundle of vertical internals.

The CT technique has been successfully applied to measure the phase holdup distribution in different multiphase flow reactors with various scale sizes at mReal such as 12 in. (0.3 m) pebble bed reactor[45,46], 6 in. (0.152 m) bubble column[9,47], 6 in. (0.152 m) and 18 in. (0.46 m) fluidized beds[48–51], and 3 in. (0.076 m) and 6 in. (0.152 m) spouted bed reactors.[52–55] Details on the mechanical design, hardware, software, and operation of the CT technique have been discussed elsewhere by Varma.[44] Therefore, the CT setup is shortly reviewed here.

The available CT scanner consists of a 250 mCi Cs-137 source (662 keV, 37 years half-life) and 50 mCi Co-60 (1173 and 1333 keV, 5.27 years half-life) housed in the lead and tungsten-shielded containers, respectively. Each gamma-ray source is facing a center of the arc, which consists of the 15-sodium iodide (NaI) scintillation detectors. Although the current CT technique is composed of two gamma-ray sources (i.e., Cs-137 and Co-60), only the Cs-137 source was used in this investigation to visualize and quantify the gas-

liquid distributions over the entire cross-section area of the columns with and without vertical internals.

The reason for using only one gamma-ray source in this study is due to the bubble columns with and without vertical internals (i.e., they are stationary) involve only two-phase (i.e., only gas and liquid phases are moving dynamically). However, for three-phases moving dynamically such as a slurry bubble column (gas-liquid-solid phases) require two gamma-ray sources (Cs-137and Co-60) to image and measure gas and solid holdup distributions, which is not the case in this current study.

Both gamma-ray sources and their array detectors are attached to a rotatable circular plate that has a 30 in. (0.76 m) diameter circular open space that is designed for the column to be scanned. This rotatable circular plate is connected to the square plate (base plate) that also has the same size of the circular hole. This base plate is connected to four vertical threaded rods that are joined with the upper and lower end of the aluminum structure of the CT setup to allow all assembly to move up and down to scan any level along the column.

The height of the threaded rods is 120 in. (3 m), and therefore the CT technique can scan objects up to 108 in. (2.75 m) in height and 30 in. (0.76 m) in diameter. Cs-137 and Co-60 sources, as well as their detectors, are arranged and designed in a way to provide gamma-ray beams (fan beams) with 40° in a horizontal plane and 5 mm in height through collimating the sources by a lead collimator device, as shown in Figure 4.

The fan beam with the current CT technique covers columns up to 24 in. (0.6 m) in diameter for scanning. The detectors for both sources are also well collimated with the lead collimator, each of which has a thin slit 2 mm in width and 5 mm in height to obtain

narrow gamma-ray beams and minimize the scattered gamma ray to achieve a better spatial resolution (2 mm).[56–58] During CT scans, the circular plate rotates automatically around the column with an angle of 1.84^{o} degrees for each rotation (view) by using programmed stepping motor. Hence, the circular plate moves 197 times to complete a full CT scan (360^{o}). For each rotation of a circular plate, the array of Cs-137detectors moves 21 times with 0.13^{o} for each movement through the independent programmed stepping motor.

This arrangement for the moving of circular plate and the array of detectors has designed to increase the number of protections that passed through the column to enhance the quality of reconstructed images. Therefore, more than 62,000 projections (i.e.,197 views × 315 projections per view) of the gamma ray that passed through the column and recorded for image reconstruction. The recorded projections were measured with the sampling rate of 60 data samples at 10 Hz. The full scan took 8.25 hours to finish.

The alternating minimization algorithm (AM) was applied in this study to reconstruct the linear attenuation coefficient distribution (μ, cm^{-1}). This algorithm was advanced by O'Sullivan et al.[59] and successfully implemented by Varma et al.[60] in two phase systems to reconstruct the images of cross-sectional phase distributions.

The AM algorithm is an iterative procedure that describes the stochastic nature of gamma-rays which makes this algorithm preferable to others reconstruction algorithms such as Fourier transform (FT)[61] , back projection (BP)[62], expectation-maximization (EM)[60], and filtered back projection (FBP)[63].

In this reconstruction algorithm, the maximum likelihood problem was remodeled as double minimization of I-divergence. The criteria of I-divergence was proposed by Csiszar[64], which represents the variation between the modeled transmission of photons by

the Beer-Lambert's law and the measured transmission of photons through the studied object. This AM algorithm does not encounter any approximation (i.e., exact process) through minimization step as compared to expectation-maximization (EM) algorithm[60] and this makes AM superior to EM algorithm due to the latter involves some approximation.

All presented results in this study in terms of the linear attenuation coefficient and gas holdup distributions are time-averaged where the projections of gamma-ray beam measured and recorded over a sufficiently long time (i.e., 8.25 hours with the sampling rate of 60 projections at 10 Hz) and assembled to reconstruct the linear attenuation coefficient and the subsequently gas holdup.

This long time averaging for gamma-ray projections is inherently accounting for most fluctuations in gas holdup along any gamma-ray projection.

According to the radiation safety rules, the CT setup was shielded from all sides by lead to minimize and eliminate the radiation dose around the CT technique. Moreover, gamma-ray sources of CT were well sealed and shielded to prevent any leaks, and hence the CT setup is safe to be utilized in the experiments if all the operational protocols are followed.

It is noteworthy that there are protocols for operating the gamma-ray computed tomography (CT) technique safely, which were approached by the Environmental Health and Safety Department at Missouri University of Science and Technology (Missouri S&T) for authorized users and radiation workers.

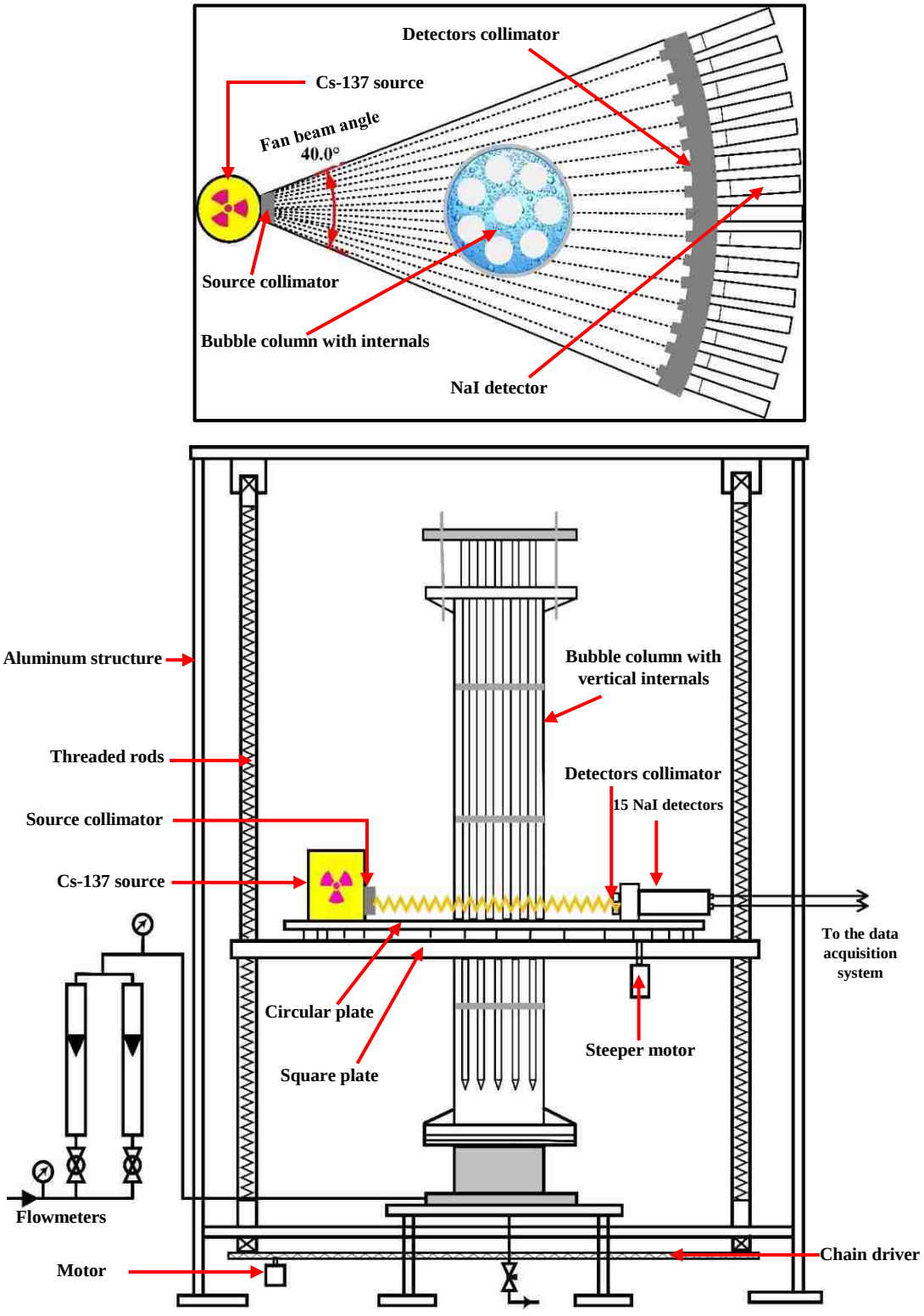

Figure 4: Schematic diagram of the single source gamma ray computed tomography (CT) technique with bubble column

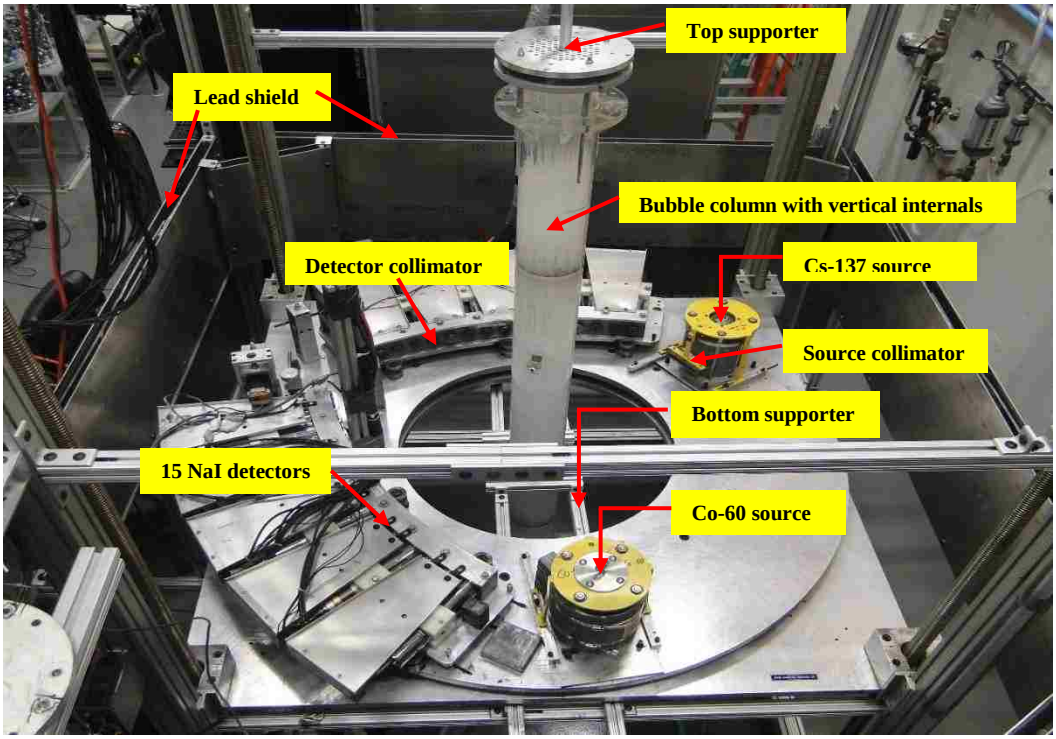

Figure 5: Photo of the dual-source gamma ray computed tomography (CT) technique where single gamma source (Cs-137) was used with bubble column during CT scan

4. PROPER ESTIMATION OF THE GAS HOLDUP DISTRIBUTION AND EXPERIMENTAL PROCEDURES FOR SCANNING BUBBLE COLUMNS WITH AND WITHOUT VERTICAL INTERNALS

4.1. ESTIMATION OF THE LOCAL GAS HOLDUP IN BUBBLE COLUMN WITHOUT INTERNALS

The Beer-Lambert's law can express the intensity of a beam of gamma-ray that is transmitted through a bubble column[16,58,65]:

$$T = \frac{I}{I_\circ} = e^{-\rho\bar{\mu}l} \tag{2}$$

$$A = Ln\left(\frac{I_\circ}{I}\right) = +\rho\bar{\mu}l \tag{3}$$

where T: transmission ratio, $I_\circ$: the initial intensity of gamma ray, I: the intensity of gamma ray transmitted across bubble columns with and without vertical internal tubes, ρ: density

of medium (g/cm^3), $\bar{\mu}$: mass attenuation coefficient (cm^2/g) of a material, l: path length through the medium (cm). The term of $Ln\left(\frac{I_\circ}{I}\right)$ is equal to the integral sum of the measured attenuation that passes through the materials along the beam path (i.e., it is a summation of attenuation values in all pixels along the path of the gamma-ray beam).

In CT scanning, the attenuations are measured along some such beam paths through the bubble columns with and without vertical internal tubes from different angles. To obtain local attenuation measurements by CT technique, the domain of the bubble column first was discretized to a square matrix with a dimension of 80 by 80 pixels.

Hence, for a two-phase bubble column without vertical internal tubes (air-water) operating at any studied superficial gas velocity, the total attenuation in each pixel (i, j) can be written as follows:

$$A_{g\text{-}l,ij} = \left(\rho_g \bar{\mu}_g l_g + \rho_l \bar{\mu}_l l_l \right)_{ij} \tag{4}$$

where ij represents the index of pixels in the square matrix of the studied domain since $l_g = \varepsilon_{g,ij} L_{ij}, l_l = \varepsilon_{l,ij} L_{ij}, L_{ij} = l_g + l_l,$ and $\varepsilon_g + \varepsilon_l = 1.$

Therefore, Eq. (4) becomes as:

$$A_{g\text{-}l,ij} = \rho_{g,ij} \bar{\mu}_{g,ij} \varepsilon_{g,ij} L_{ij} + \rho_{l,ij} \bar{\mu}_{l,ij} L_{ij} - \rho_{l,ij} \bar{\mu}_{l,ij} L_{ij} \varepsilon_{g,ij} \tag{5}$$

where L_{ij} represents the length along which a gamma ray beam passes through this pixel while $\varepsilon_{g,ij}\ and\ \varepsilon_{l,ij}$ represent the local gas and liquid holdups in each pixel (ij). In the case of the scan the column is filled with water only (single phase). Therefore, the attenuation in each pixel can be expressed by:

$$A_{l,ij} = \rho_{l,ij} \bar{\mu}_{l,ij} \varepsilon_{l,ij} L_{ij} = \rho_{l,ij} \bar{\mu}_{l,ij} L_{ij}\ , where\ \varepsilon_{l,ij} = 1 \tag{6}$$

By substituting Eq. (6) into Eq. (5), we obtain

$$A_{g\text{-}l,ij} = \rho_{g,ij}\bar{\mu}_{g,ij}\varepsilon_{g,ij}L_{ij} + A_{l,ij} - A_{l,ij}\varepsilon_{g,ij} \tag{7}$$

Since $\rho_g, \mu_g \ll \rho_l, \mu_l$. Hence, the attenuation caused by only gas phase (air) is negligible $\rho_g\bar{\mu}_g\varepsilon_{g,ij}L_{ij} \cong 0$. Then the local gas holdup can be obtained from the following equation.

$$\varepsilon_{g,ij} = 1 - \frac{A_{g\text{-}l,ij}}{A_{l,ij}} \tag{8}$$

since $$A_{g\text{-}l,ij} = \rho_{g\text{-}l,ij}\bar{\mu}_{g\text{-}l,ij}L_{ij} = \mu_{g\text{-}l,ij}L_{ij}$$

$$A_{l,ij} = \rho_{l,ij}\bar{\mu}_{l,ij}L_{ij} = \mu_{l,ij}L_{ij}$$

$$\varepsilon_{g,ij} = 1 - \frac{A_{g\text{-}l,ij}}{A_{l,ij}} = 1 - \frac{\mu_{g\text{-}l,ij}L_{ij}}{\mu_{l,ij}L_{ij}} = 1 - \frac{\mu_{g\text{-}l,ij}}{\mu_{l,ij}} \tag{9}$$

$$\varepsilon_{l,ij} = 1 - \varepsilon_{g,ij} \tag{10}$$

where $\mu_{l,ij}\ and\ \mu_{g\text{-}l,ij}$ represents the linear attenuation coefficients for liquid and gas-liquid in each pixel (cm^{-1}), respectively.

4.2. EXPERIMENTAL SCANNING PROCEDURE FOR BUBBLE COLUMN WITHOUT INTERNALS

For measuring a gas holdup distribution over the entire cross-sectional of the bubble column without tubes (two phase), the following scanning procedure (Figure 6) was developed as follows:

- Scan without a column (i.e. air only) between a gamma source and its detectors and consider it as reference scan ($I_\circ$).

- Scan a column filled with water only (I_l) and then compute transimssion ratio $(I_l/I_\circ)$ for determing $A_{l,ij}$.
- Scan a column containing air–water operates at any studied superficial gas velocity $(I_{g\text{-}l})$ and then calculate transimssion ratio $(I_{g\text{-}l}/I_\circ)$ for determing $A_{g\text{-}l,ij}$.

By implementing the alternating minimization (AM) algorithm for each transmission ratio $(I_{g\text{-}l}/I_\circ)$, $(I_l/I_\circ)$ independently, one can reconstruct the linear attenuation coefficients (μ, cm^{-1}) for gas-liquid $\mu_{g\text{-}l,ij}$ and liquid $\mu_{l,ij}$, respecitively. Finally, local gas and liquid holdups can be directily calculated by applying Eqs.(9) and (10).

4.3. ESTIMATION OF THE GAS HOLDUP IN A BUBBLE COLUMN WITH INTERNALS (THREE-PHASES)

The use of the available experimental scanning procedure and mathematical expression for estimation of the gas holdup distribution and their profiles in a bubble column with vertical internal tubes can lead to incorrect estimates since they are based on bubble column without vertical tubes. Therefore, in this section, new mathematical equations and experimental scanning procedure for bubble column equipped with vertical internal tubes are established and presented to achieve a reliable estimation of the gas holdup distribution and their profiles.

The bubble column with vertical tubes considers three-phases system (gas-solid-liquid), and since the vertical of tubes are stagnant (not moving) therefore single, the gamma-ray source is enough to distinguish between phase. However, dual gamma-ray sources are required to distinguish between three phases that are dynamically moving as in the slurry bubble column.[66,67]

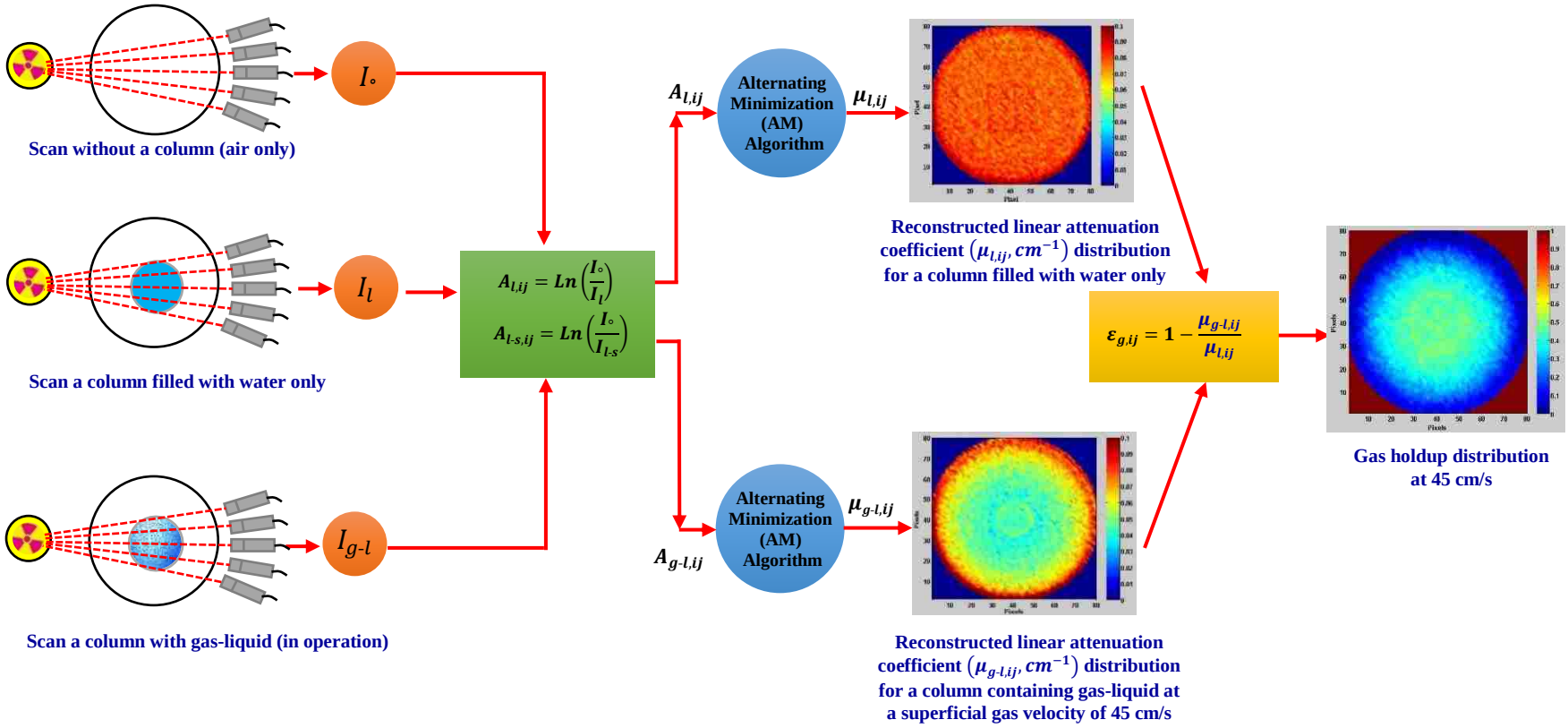

Figure 6: Experimental procedure for scanning a bubble column without vertical internal tubes

For a three-phase bubble column with vertical internal tubes (air-solid-water), the total attenuation in each pixel can be expressed by:

$$A_{g\text{-}l\text{-}s,ij} = \left(\rho_g \bar{\mu}_g l_g + \rho_l \bar{\mu}_l l_l + \rho_s \bar{\mu}_s l_s\right)_{ij} \tag{11}$$

since $l_g = \varepsilon_{g,ij} L_{ij}$, $l_l = \varepsilon_{l,ij} L_{ij}$, $l_s = \varepsilon_{s,ij} L_{ij}$ $where$ $L_{ij} = l_g + l_l + l_s$, hence, Eq. (11) becomes

$$A_{g\text{-}l\text{-}s,ij} = \rho_{g,ij} \bar{\mu}_{g,ij} \varepsilon_{g,ij} L_{ij} + \rho_{l,ij} \bar{\mu}_{l,ij} \varepsilon_{l,ij} L_{ij} + \rho_{s,ij} \bar{\mu}_{s,ij} \varepsilon_{s,ij} L_{ij} \tag{12}$$

since $\varepsilon_g + \varepsilon_l + \varepsilon_s = 1$. Therefore, Eq. (12) can be rewritten as

$$A_{g\text{-}l\text{-}s,ij} = \rho_{g,ij} \bar{\mu}_{g,ij} \varepsilon_{g,ij} L_{ij} + \rho_{l,ij} \bar{\mu}_{l,ij} L_{ij} (1 - \varepsilon_{g,ij} - \varepsilon_{s,ij}) + \rho_{s,ij} \bar{\mu}_{s,ij} \varepsilon_{s,ij} L_{ij} \tag{13}$$

due to $\rho_g, \mu_g \ll \rho_s, \mu_s$ and ρ_l, μ_l . Thus, the attenuation caused by only gas phase (air) is negligible ($\rho_{g,ij} \mu_{g,ij} \varepsilon_{g,ij} L_{ij} \cong 0$). Eq. (13) is simplified to:

$$A_{g\text{-}l\text{-}s,ij} = \rho_{l,ij} \bar{\mu}_{l,ij} L_{ij} (1 - \varepsilon_{g,ij} - \varepsilon_{s,ij}) + \rho_{s,ij} \bar{\mu}_{s,ij} \varepsilon_{s,ij} L_{ij} \tag{14}$$

since $A_{l,ij} = \rho_{l,ij} \mu_{l,ij} \varepsilon_{l,ij} L_{ij} = \rho_{l,ij} \mu_{l,ij} L_{ij}, where\ \varepsilon_{l,ij} = 1$. Thus, Eq. (14) becomes

$$A_{g\text{-}l\text{-}s,ij} = A_{l,ij} - A_{l,ij} \varepsilon_{g,ij} - A_{l,ij} \varepsilon_{s,ij} + \rho_{s,ij} \bar{\mu}_{s,ij} \varepsilon_{s,ij} L_{ij} \tag{15}$$

For scanning empty column with internals (air-solid), the total attenuation in each pixel is given by:

$$A_{g\text{-}s,ij} = \rho_{g,ij} \bar{\mu}_{g,ij} \varepsilon_{g,ij} L_{ij} + \rho_{s,ij} \bar{\mu}_{s,ij} \varepsilon_{s,ij} L_{ij} \tag{16}$$

since $\varepsilon_g + \varepsilon_s = 1$. Therefore, Eq. (16) can be written as:

$$A_{g\text{-}s,ij} = \rho_{g,ij} \bar{\mu}_{g,ij} (1 - \varepsilon_{s,ij}) L_{ij} + \rho_{s,ij} \bar{\mu}_{s,ij} \varepsilon_{s,ij} L_{ij} \tag{17}$$

since $\rho_g, \mu_g \ll \rho_s, \mu_s$. Then the attenuation caused by only the gas phase (air) is negligible ($\rho_{g,ij} \mu_{g,ij} (1 - \varepsilon_{s,ij}) L_{ij} \cong 0$). Eq. (17) is simplified to

$$A_{g\text{-}s,ij} = \rho_{s,ij} \bar{\mu}_{s,ij} \varepsilon_{s,ij} L_{ij} \tag{18}$$

For the scanning column with vertical internals filled with water (liquid-solid), the total attenuation in each pixel can be given by

$$A_{l\text{-}s,ij} = \rho_{l,ij}\bar{\mu}_{l,ij}\varepsilon_{l,ij}L_{ij} + \rho_{s,ij}\bar{\mu}_{s,ij}\varepsilon_{s,ij}L_{ij} \tag{19}$$

Since $\varepsilon_l + \varepsilon_s = 1$. Therefore Eq. (19) can be written as follow

$$A_{l\text{-}s,ij} = \rho_{l,ij}\bar{\mu}_{l,ij}L_{ij}(1 - \varepsilon_{s,ij}) + \rho_{s,ij}\bar{\mu}_{s,ij}\varepsilon_{s,ij}L_{ij} \tag{20}$$

$$since\ A_{l,ij} = \rho_{l,ij}\bar{\mu}_{l,ij}\varepsilon_{l,ij}L_{ij} = \rho_{l,ij}\bar{\mu}_{l,ij}L_{ij}\ , where\ \varepsilon_{l,ij} = 1$$

Hence, Eq. (20) becomes

$$A_{l\text{-}s,ij} = A_{l,ij} - A_{l,ij}\varepsilon_{s,ij} + \rho_{s,ij}\bar{\mu}_{s,ij}\varepsilon_{s,ij}L_{ij} \tag{21}$$

By further simplification, Eq. (21) becomes as follow

$$\rho_{s,ij}\bar{\mu}_{s,ij}\varepsilon_{s,ij}L_{ij} = A_{l\text{-}s,ij} - A_{l,ij} + A_{l,ij}\varepsilon_{s,ij} \tag{21}$$

By substituting Eq. (21) into Eq. (16), we obtain

$$A_{g\text{-}l\text{-}s,ij} = A_{l,ij} - A_{l,ij}\varepsilon_{g,ij} - A_{l,ij}\varepsilon_{s,ij} + A_{l-s,ij} - A_{l,ij} + A_{l,ij}\varepsilon_{s,ij} \tag{22}$$

$$\varepsilon_{g,ij} = \frac{A_{l\text{-}s,ij} - A_{g\text{-}l\text{-}s,ij}}{A_{l,ij}} \tag{23}$$

$$since\ A_{l\text{-}s,ij} = \rho_{l\text{-}s,ij}\bar{\mu}_{l\text{-}s,ij}L_{ij} = \mu_{l\text{-}s,ij}L_{ij}$$

$$A_{g\text{-}l\text{-}s,ij} = \rho_{g\text{-}l\text{-}s,ij}\bar{\mu}_{g\text{-}l\text{-}s,ij}L_{ij} = \mu_{g\text{-}l\text{-}s,ij}L_{ij}$$

$$A_{l,ij} = \rho_{l,ij}\bar{\mu}_{l,ij}L_{ij} = \mu_{l,ij}L_{ij}$$

Therefore, Eq. (23) becomes

$$\varepsilon_{g,ij} = \frac{A_{l\text{-}s,ij} - A_{g\text{-}l\text{-}s,ij}}{A_{l,ij}} = \frac{\rho_{l\text{-}s,ij}\,\bar{\mu}_{l\text{-}s,ij}L_{ij} - \rho_{g\text{-}l\text{-}s,ij}\,\bar{\mu}_{g\text{-}l\text{-}s,ij}\,L_{ij}}{\rho_{l,ij}\bar{\mu}_{l,ij}L_{ij}}$$

$$\varepsilon_{g,ij} = \frac{(\mu_{l\text{-}s,ij} - \mu_{g\text{-}l\text{-}s,ij})L_{ij}}{\mu_{l,ij}\,L_{ij}} = \frac{(\mu_{l\text{-}s,ij} - \mu_{g\text{-}l\text{-}s,ij})}{\mu_{l,ij}} \tag{24}$$

For calculating solid holdup in the bubble column with vertical internals (solid phase is stationary), by recalling Eq. (21) and Eq. (18) and by substituting Eq. (18) into Eq. (21), Eq. (21) becomes

$$A_{l\text{-}s,ij} = A_{l,ij} - A_{l,ij}\varepsilon_{s,ij} + A_{g\text{-}s,ij} \tag{25}$$

$$\varepsilon_{s,ij} = 1 - \left(\frac{A_{l\text{-}s,ij} - A_{g\text{-}s,ij}}{A_{l,ij}}\right) = 1 - \left(\frac{\rho_{l\text{-}s,ij}\bar{\mu}_{l\text{-}s,ij}L_{ij} - \rho_{g\text{-}s,ij}\bar{\mu}_{g\text{-}s,ij}L_{ij}}{\rho_{l,ij}\bar{\mu}_{l,ij}L_{ij}}\right)$$

$$\varepsilon_{s,ij} = 1 - \left(\frac{\mu_{l\text{-}s,ij}L_{ij} - \mu_{g\text{-}s,ij}L_{ij}}{\mu_{l,ij}L_{ij}}\right) = 1 - \left(\frac{(\mu_{l\text{-}s,ij} - \mu_{g\text{-}s,ij})L_{ij}}{\mu_{l,ij}L_{ij}}\right) \tag{26}$$

$$= 1 - \left(\frac{\mu_{l\text{-}s,ij} - \mu_{g\text{-}s,ij}}{\mu_{l,ij}}\right)$$

since $\varepsilon_{g,ij} + \varepsilon_{l,ij} + \varepsilon_{s,ij} = 1$. Therefore

$$\varepsilon_{l,ij} = 1 - \varepsilon_{g,ij} - \varepsilon_{s,ij} \tag{27}$$

4.4. EXPERIMENTAL PROCEDURE FOR SCANNING A BUBBLE COLUMN WITH INTERNALS

To visualize and quantify time-averaged gas holdup distributions over the entire cross-sectional of a bubble column packed with vertical internals tubes, an experimental procedure for scanning bubble column with internals (Figure 7) was established and developed as follows:

- Scan without putting a column (i.e. air only) between gamma source and its detectors and consider it as the reference scan $(I_\circ)$.
- Scan a column containing only water (stagnant) (I_l) to determine $A_{l,ij}$.
- Scan an empty column with internal only $(I_{g\text{-}s})$ to estimate $A_{g\text{-}s,ij}$.

- Scan a column with vertical internals and filled with water ($I_{l\text{-}s}$) to calculate $A_{l\text{-}s,ij}$.
- Scan a column with vertical internals containing air–water operates at any selected superficial gas velocity (flowing) $(I_{g\text{-}l\text{-}s})$ to compute $A_{g\text{-}l\text{-}s,ij}$.

The alternating minimization (AM) algorithm was applied to each scan independently to reconstruct the linear attenuation coefficients (cm^{-1}) for liquid-solid $\mu_{l\text{-}s,ij}$, gas-liquid-solid $\mu_{g\text{-}l\text{-}s,ij}$, liquid $\mu_{l,ij}$, and gas–solid $\mu_{g\text{-}s,ij}$, respectively. Finally, local gas, solid, and liquid holdups can be directly obtained by using Eqs. (24), (26), and (27), respectively.

4.5. VALIDATION OF CT SCANNING

CT validation is always required to check the accuracy and performance of the CT technique before each study can be conducted. In this validation procedure, Plexiglas phantom which consists of two concentric cylinders 3-in. (0.076 m) inner and 6-in (0.152 m) outer cylinders, respectively was designed, fabricated, and scanned as illustrated in Figure 8. Independent scans have been performed for the phantom with different cases as follows:

- Case I: Empty phantom.
- Case II: Inner cylinder of the phantom was filled with water while the outer cylinder was empty (i.e. air only).
- Case III: The outer cylinder the phantom was filled with water while the inner cylinder was empty (i.e. air only).
- Case IV: Both internal and external cylinders were filled with water.

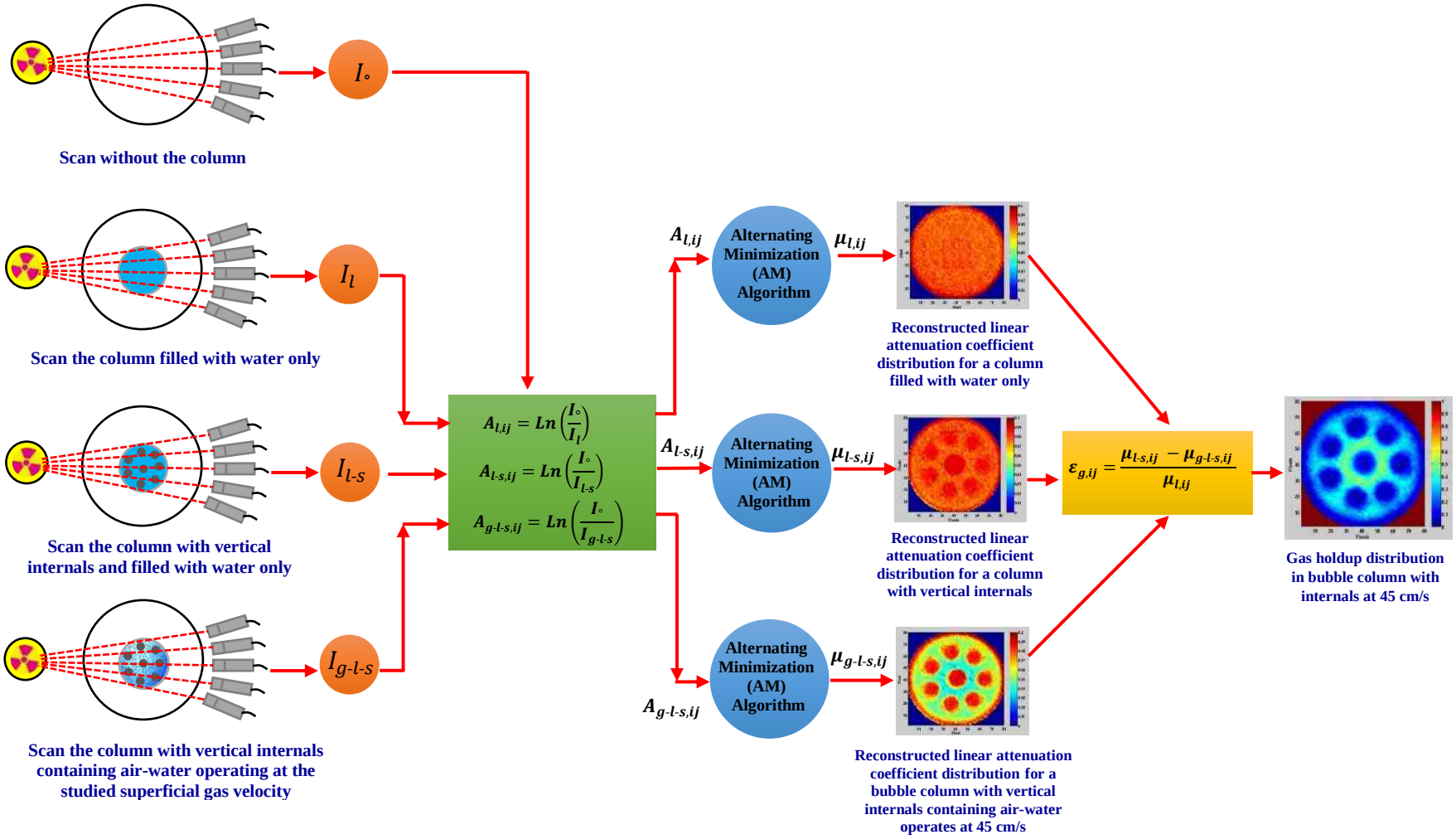

Figure 7: Experimental procedure for scanning bubble column equipped with vertical internal tubes

For each scan (8.25 hours), 62055 projections were detected and recorded by 15 NaI detectors with a sampling rate of 60 data samples at a frequency of 10 Hz to reconstruct cross-sectional images of the linear attenuation coefficient (μ, cm^{-1}) by using the AM algorithm. The resolution of reconstructed images is presented in this study by 80×80 pixels, where each pixel represents an area 1.91 × 1.91 mm of the phantom or bubble columns. The transmission ratio and sinogram figures have been plotted for all CT experiments in the beginning step of data processing (before the reconstruction step) to check the accuracy, and quality of collecting data, and hence they serve as diagnostic tools to discover the detectors defects. The y-axis of transmission ratio figures represents the calculated transmission ratio for all phantom cases while the x-axis represents the angular location of the projection in the fan beam arrangement. All transmission ratio figures which shown in Figure 9 are symmetric and smooth without any detector's artifacts. It is evident from these figures that CT captures the boundaries of inner and outer cylinders of the phantom for all cases.

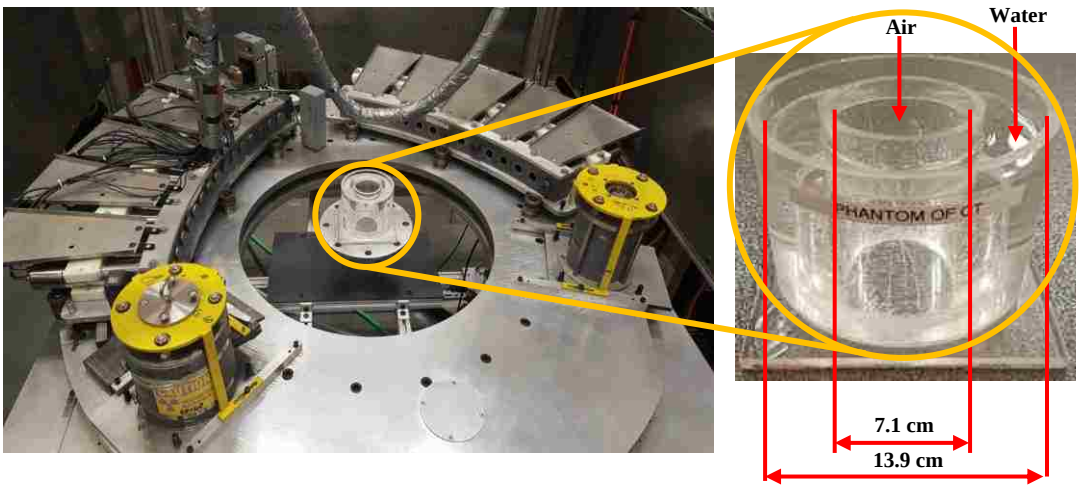

Figure 8: Photo of the dual-source gamma ray computed tomography (CT) technique where single gamma source was used to scan the phantom

The sinogram figures for all phantom cases are displayed in Figure 9, where the y-axis of these figures represents projection number (315), while the x-axis represents the view (source position (197)). The pixels of sinogram figures represent the transmission ratio for corresponding projection number and source positions. As seen from the sinogram figures, the CT was capable of identifying the change in the cases of the phantom, and the absence of artifacts in these figures was evidenced that detectors and their electronics work properly.

It is evident from the reconstructed linear attenuation coefficient (μ, cm^{-1}) images and their diameter profiles, which are presented in Figure 9 and Figure 10 for all cases of the phantom, that the CT technique was capable of retrieving geometry and capturing the wall thickness (5 mm) for inner and outer cylinders of the empty phantom when considering no column (i.e. air only) between gamma-ray source and its detector as the reference scan. Additionally, it was capable of clearly distinguishing between water, air, and Plexiglas. Moreover, the CT technique was able to distinguish between Plexiglas material and water as shown in Figure 9 and Figure 10d for case IV despite the convergence of their linear attenuation coefficients. Furthermore, the reconstructed linear attenuation coefficient values obtained by CT were very close to the theoretical values $\left(\mu_{air} = 0.0001\ cm^{-1}, \mu_{water} = 0.086\ cm^{-1}, and\ \mu_{plexiglas} = 0.098\ cm^{-1}\right)$ with relative percentage difference 1.3, 2.4, and 3.2 cm^{-1} for air, water, and Plexiglas, respectively.[68]

As mentioned earlier, the applied resolution for image reconstruction in this study is 80 × 80 pixels (where each pixel represents 1.91 × 1.91 mm of the studied domain) and cannot use fine pixels due to the detector's collimator size (2 mm in width). Therefore, the

wall thickness of the phantom passes through a fraction of the pixels (i.e., part of the pixel). For example, when reconstructing a linear attenuation coefficient for an empty phantom (i.e., air only), the attenuation at the wall region will be with air while when reconstructing for the phantom with water, the attenuation will be with water, and that affects the results of the final attenuation of that pixel. In other words, in each pixel in wall region, the Plexiglas wall occupies part of a certain area of the pixel, and when conducting an azimuthal average for the linear attenuation in the wall region, it will count peripherally for all these kinds of variation that will provide such differences in the wall region of the phantom (see Figure 9 and Figure 10).

These obtained results in terms of reconstructed linear attenuation coefficient distributions and their diametrical profiles were for the first time achieved this high accuracy as compared to other previous studies[46,48,69] that are scanned the same phantom. Also, in these past studies were unable to reproduce the geometry of the phantom and capture the small thickness of the phantom wall and this was due to using empty phantom as reference scan in their studies.

This difference between current and previous results of the reconstructed linear attenuation coefficient illustrates the importance of selecting a proper reference scan. Therefore, it should always consider air only (no column between the gamma-ray source and its detector) as reference scan to achieve high accuracy of reconstructed linear attenuation coefficient. The obtained results of validation procedures for the CT technique confirm the reliability of CT to visualize and quantify the phase distributions in any multiphase reactors with high accuracy.

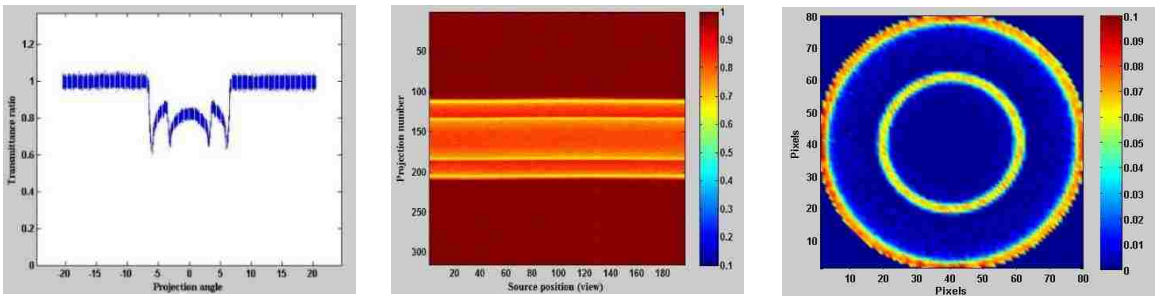

a) Transmission ratio (*I/Io*), b) sinogram, and c) cross-sectional linear attenuation coefficient, cm^{-1} for case I (empty phantom)

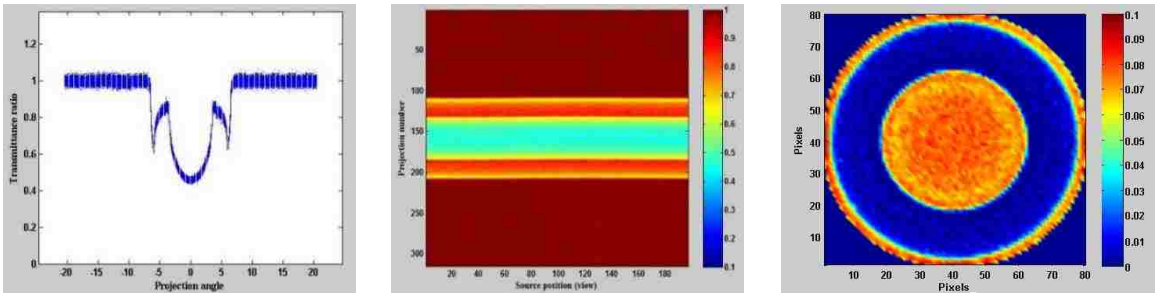

a) Transmission ratio (*I/Io*), b) sinogram, and c) cross-sectional linear attenuation coefficient, $cm^{-1}$for case II (the inner cylinder filled with water)

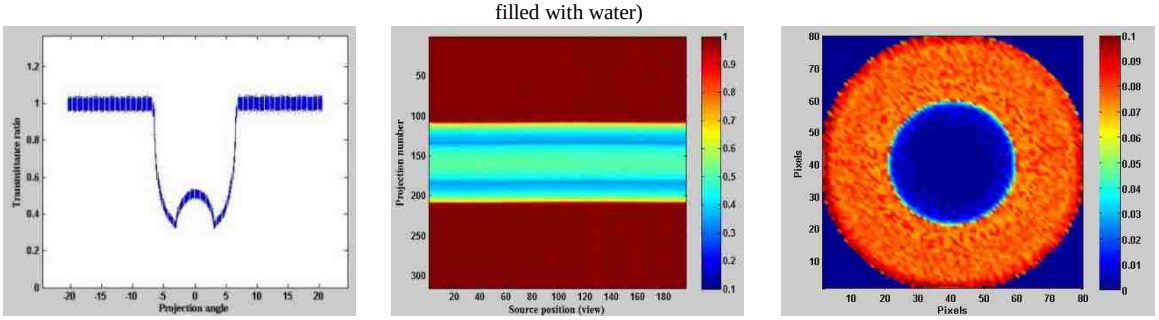

a) Transmission ratio (*I/Io*), b) sinogram, and c) cross-sectional linear attenuation coefficient, $cm^{-1}$for case III (the outer cylinder filled with water)

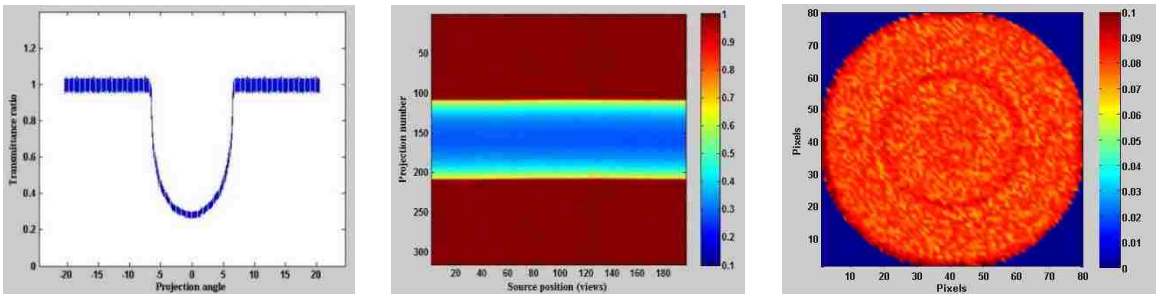

a) Transmission ratio (*I/Io*), b) sinogram, and c) cross-sectional linear attenuation coefficient, $cm^{-1}$for case IV (the inner and outer cylinders filled with water)

Figure 9: Transmission ratio (*I/Io*), sinogram, and cross-sectional linear attenuation coefficients for different cases of the phantom

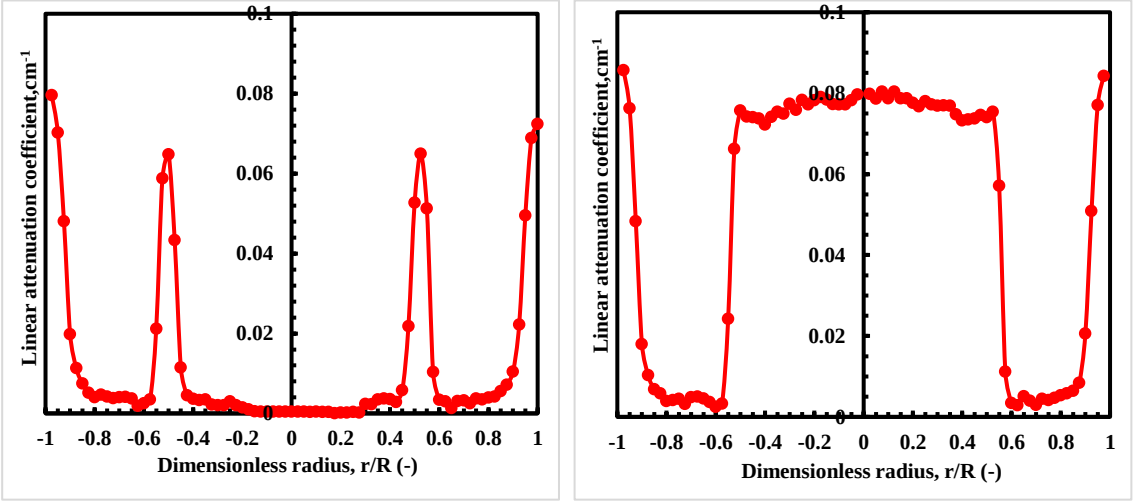

a) Diametrical profile of linear attenuation coefficient for phantom Case I

b) Diametrical profile of linear attenuation coefficient for phantom Case II

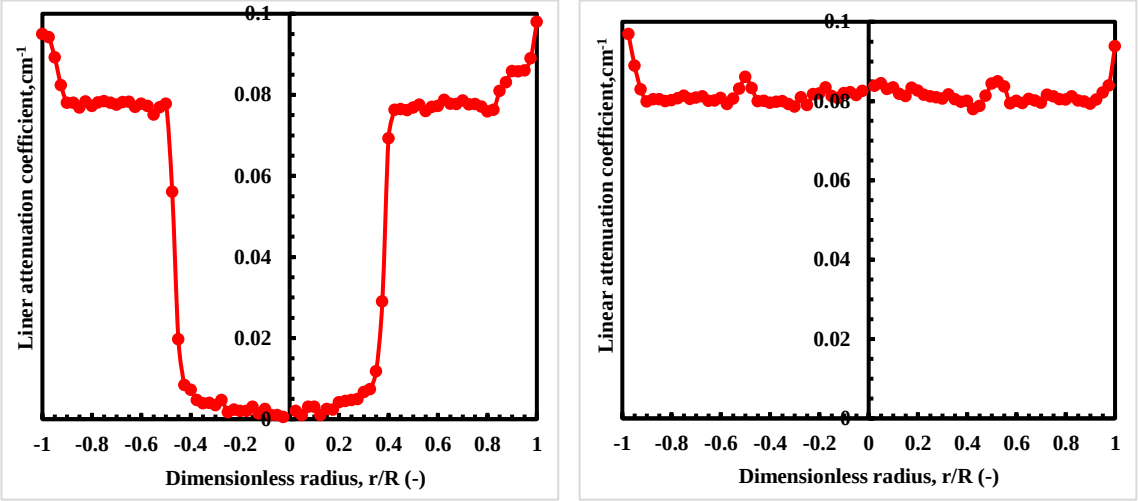

c) Diametrical profile of linear attenuation coefficient for phantom Case III

d) Diametrical profile of linear attenuation coefficient for phantom Case IV

Figure 10: Diametrical profiles of the reconstructed linear attenuation coefficient for various cases of the phantom

5. RESULTS AND DISCUSSION

reliable gas holdup distributions and their profiles in the bubble column with vertical internal tubes can be only achieved through avoiding the pitfalls outlined earlier. Solutions for such pitfalls include using air (i.e., no column between the gamma source and its detector) as reference scan, establishing an experimental procedure for scanning bubble

column with vertical internal tubes, building mathematical expressions for estimating gas holdup properly, and excluding the values of the vertical internals from the gas holdup distribution and their profiles.

In this section, the impact of using improper reference scan on the linear attenuation, gas holdup distributions, and their profiles in the bubble columns with and without vertical internal tubes was demonstrated and addressed. Moreover, a new methodology for excluding the vertical internal tubes from the gas holdup distribution and their azimuthally averaged profiles is also developed and presented in this section.

5.1. EFFECT OF USING DIFFERENT REFERENCE SCANS ON THE RECONSTRUCTED LINEAR ATTENUATION COEFFICIENT DISTRIBUTIONS AND THEIR PROFILES FOR BUBBLE COLUMN WITHOUT INTERNALS

Figure 11 demonstrates the reconstructed linear attenuation coefficient distributions for the column without vertical internal tubes filled with water (no flow) (Figure 11a, b) and the column containing air–water, which operates at a superficial gas velocity of 45 cm/s (Figure 11c, d), using different reference scans [empty column and air (no column)].

It is evident from Figure 11a and c that when the empty column was used as a reference scan, the reconstructed linear attenuation of water and air–water were close to the theoretical values for water and air (0.086, and 0.0001 cm^{-1}), respectively, while the reconstructed linear attenuation for the column wall (Plexiglas) was inconsistent with the theoretical values (0.0988 cm^{-1}). However, Figure 11b and d show a close match between the theoretical values of the linear attenuation coefficient for water, air, and Plexiglas when utilizing air (no column) as the reference scan.

Figure 12 shows the diametrical profiles of the reconstructed linear attenuation coefficient based on using different reference scans [empty column, air (no column)] for the column filled with water (no flow) and the column containing air-water, which operates at a superficial gas velocity of 45 cm/s.

It is evident from Figure 12 that the linear attenuation coefficients for water, air, and Plexiglas reconstructed based on air (no column) are closer to the theoretical values than those calculated based on the empty column as the reference scan. In addition, the obtained results of the linear attenuation coefficient for the wall column (Plexiglas) was too far from the theoretical values (0.0988 cm^{-1}) when it was reconstructed based on the empty column as a reference scan.

For example, at the dimensionless radius (r/R = 0.23), the linear attenuation coefficient of water was 0.0872 cm^{-1} with % relative difference of 1.4% when it was calculated based on air (no column) as the reference scan, while it was 0.081 cm^{-1} with % relative difference of 6% when it was reconstructed based on the empty column. Additionally, in the wall region (r/R = 1), which is important to quantify, the linear attenuation coefficient computed based on air (no column) was 0.093 cm^{-1} with % relative difference of 5.1, while it was 0.01 cm^{-1} with the relative difference of 163% when it was calculated based on the empty column as the reference scan.

From above, one can notice that selecting an improper reference scan leads to propagating errors in the reconstructed linear attenuation coefficient, and consequently, in the gas holdup distributions and their profiles.

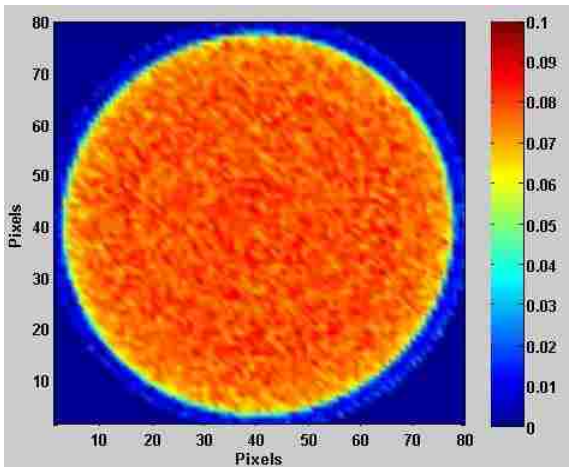

a) Reconstructed linear attenuation coefficient (μ, cm^{-1}) distribution for column filled with water only based on empty column as the reference scan

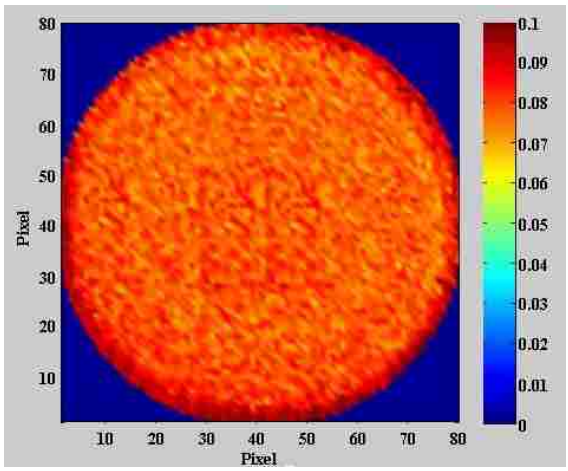

b) Reconstructed linear attenuation coefficient (μ, cm^{-1}) distribution for column filled with water only based on air (no column) as the reference scan

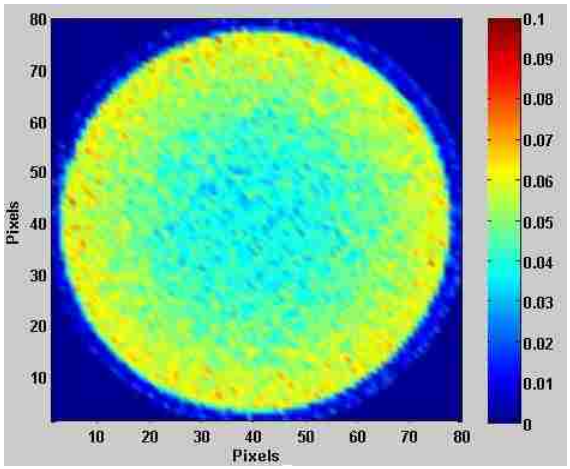

c) Reconstructed linear attenuation coefficient (μ, cm^{-1}) distribution for column containing air-water operates at superficial gas velocity 45 cm/s based on empty column as the reference scan

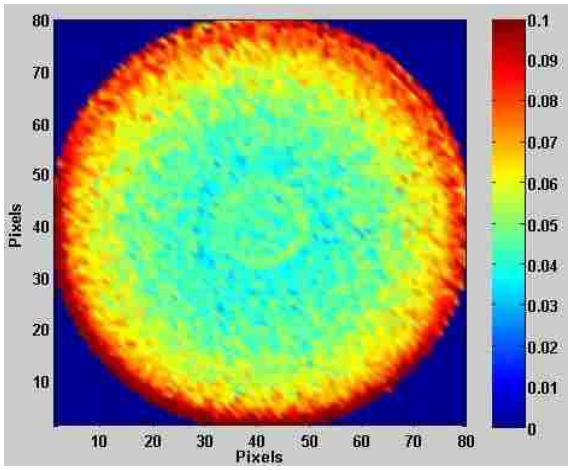

d) Reconstructed linear attenuation coefficient (μ, cm^{-1}) distribution for column containing air-water operates at superficial gas velocity 45 cm/s based on air (no column) as reference scan

Figure 11: Reconstructed linear attenuation coefficient distribution using different reference scans

Selecting an improper reference scan is one of the most significant pitfalls and should be avoided during scanning bubble columns by considering air only as the reference scan (no column between the gamma-ray source and its detectors).

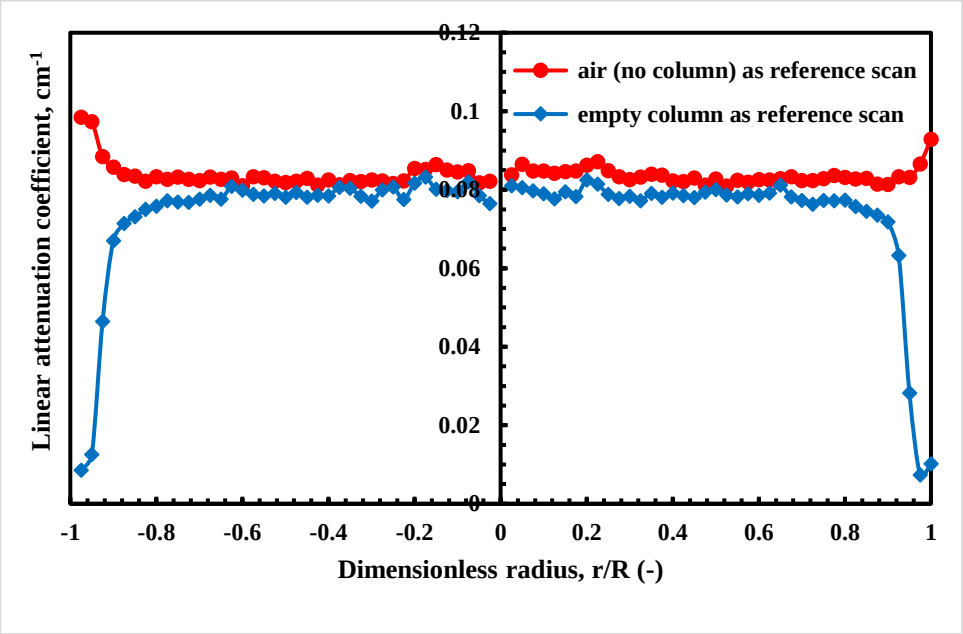

a) Diametrical profile of the reconstructed linear attenuation coefficient (μ, cm^{-1}) for bubble column filled with water only based on different reference scans (empty column, and air (no column))

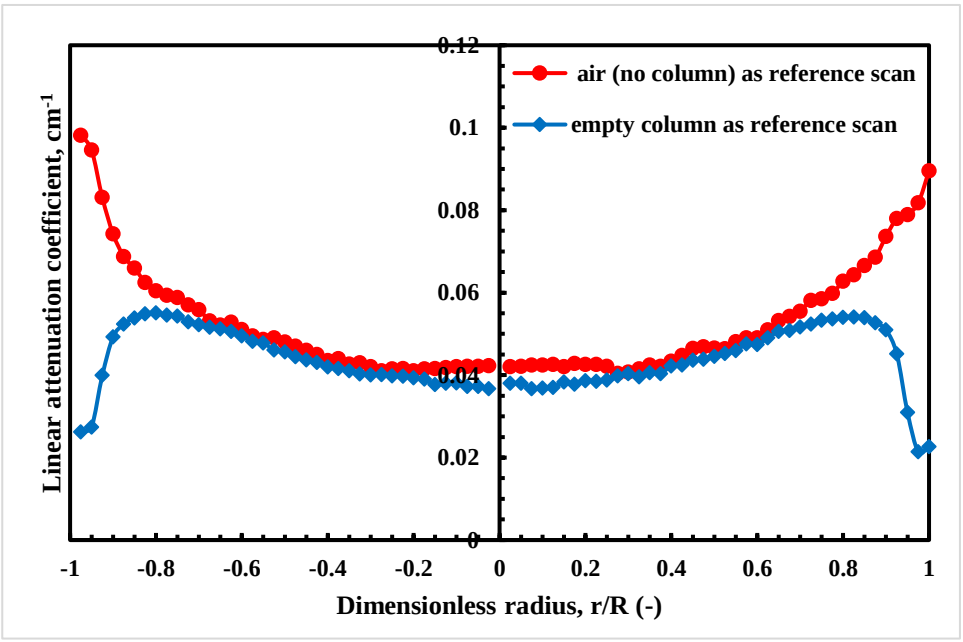

b) Diametrical profile of the reconstructed linear attenuation coefficient (μ, cm^{-1}) for bubble column containing air-water operates at a superficial gas velocity of 45 cm/s based on different reference scans (empty column, and air (no column))

Figure 12: Diametrical profiles of the linear attenuation coefficient reconstructed based on different reference scans (empty column, and air)

5.2. EFFECT OF USING DIFFERENT REFERENCE SCANS ON THE RECONSTRUCTED LINEAR ATTENUATION COEFFICIENT DISTRIBUTIONS AND THEIR PROFILES FOR THE BUBBLE COLUMN WITH INTERNALS

Linear attenuation coefficient distributions for empty column with vertical internals, column with vertical internals filled with water only (no flow), and column with vertical internals containing air–water operating at a superficial gas velocity of 45 cm/s have been reconstructed based on different reference scans [empty column with vertical internals, empty column without vertical internals, air (no column in the path between the source and its detectors)]. The results that demonstrate the impact of using different reference scans are presented in Figure 13. It can be recognized from Figure 13c that the linear attenuation coefficient for the column filled with water only reconstructed based on the empty column with vertical internals as the reference scan is close to the theoretical value of the linear attenuation coefficient of the water. However, the obtained linear attenuation coefficient values for the vertical internals (made of Plexiglas material) and the wall of the Plexiglas column are far away from the theoretical values of Plexiglas (0.0988 cm^{-1}). The possible reason for that is the selection of improper reference scans (empty column with vertical internals), and this has been confirmed when considering empty column without vertical internals as the reference scan, as shown in Figure 13 (a, d, g), where the reconstructed linear attenuation coefficients for water, air-water, and Plexiglas internals were close to the theoretical values except for the wall of the column. However, considering air (no column between the Cs-137 source and its detectors) as the reference scan (incident counts) gives a linear attenuation coefficient for water, air, air-water, and Plexiglas closer to the theoretical values than those mentioned in previous cases, as shown in Figure 13b, e, h. By using air (no column) as a reference scan, CT can capture the wall

and the vertical internals more clearly with linear attenuation coefficient close to the theoretical values.

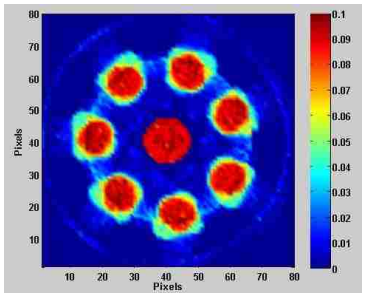

a) Reconstructed linear attenuation coefficient (μ, cm^{-1}) distribution for the empty column with internals based on empty column without internals as the reference scan

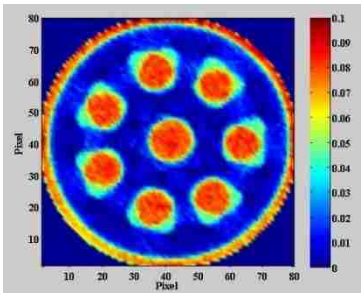

b) Reconstructed linear attenuation coefficient (μ, cm^{-1}) distribution for empty column with internals based on air (no column) as the reference scan

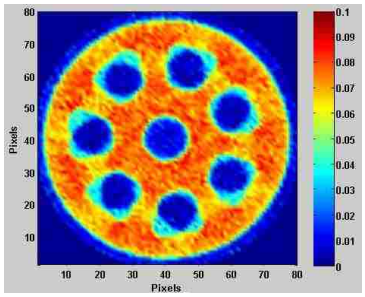

c) Reconstructed linear attenuation coefficient (μ, cm^{-1}) distribution for column with internals filled with water only based on empty column with internals as the reference scan

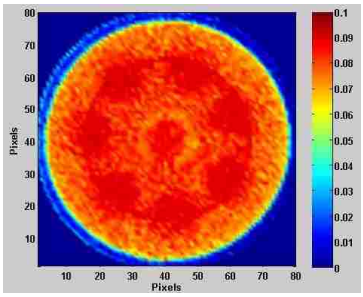

d) Reconstructed linear attenuation coefficient (μ, cm^{-1}) distribution for the column with internals filled with water only based on empty column without internals as the reference scan

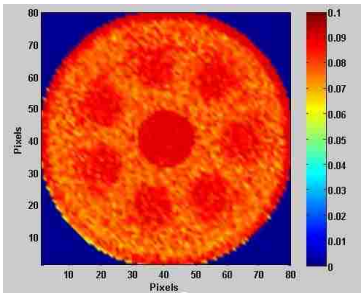

e) Reconstructed linear attenuation coefficient (μ, cm^{-1}) distribution for column with internals filled with water only based on air (no column) as the reference scan

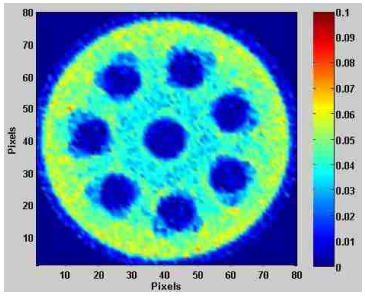

f) Reconstructed linear attenuation coefficient (μ, cm^{-1}) distribution for column with internals containing air-water operates at superficial gas velocity of 45 cm/s based on empty column with internals as the reference scan

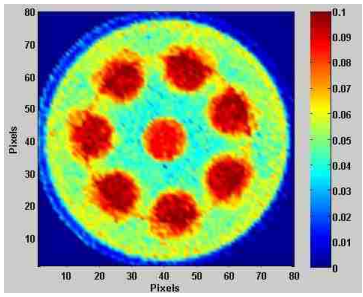

g) Reconstructed linear attenuation coefficient (μ, cm^{-1}) distribution for bubble column with internals containing air-water operates at superficial gas velocity of 45 cm/s based on empty column without internals as the reference scan

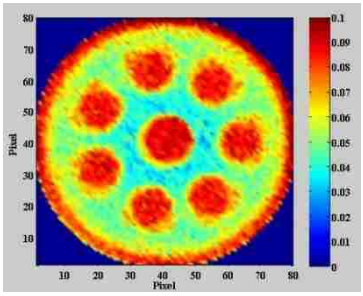

h) Reconstructed linear attenuation coefficient (μ, cm^{-1}) distribution for bubble column with internals containing air-water operates at superficial gas velocity of 45 cm/s based on air (no column) as the reference scan

Figure 13: Reconstructed linear attenuation coefficient distributions using different reference scans (empty column with vertical internals, empty column without vertical internals, air (no column between gamma source and its detectors))

The radial profiles of the reconstructed linear attenuation coefficients (μ, cm^{-1}) computed based on different reference scans [empty column with vertical internals, empty column without vertical internals, air (no column)] for the bubble column with vertical internals operating on the superficial gas velocity of 45 cm/s are shown in Figure 14. These results clearly explain that the linear attenuation coefficients reconstructed based on air (no column) as the reference scan are closer to the theoretical values than the others are. Additionally, the linear attenuation coefficients computed based on the empty column with vertical internals led to inconsistent results with the theoretical values at Plexiglas internals zones and the column wall. For example, at the center of the column, the percentages of the absolute relative differences between the theoretical and experimental linear attenuation coefficient values that are reconstructed based on the empty column with vertical internals, empty column without vertical internals, and air (no column) as reference scans were 92%, 16%, and 5%, respectively. These obtained results confirm that considering an empty column with vertical internals as the reference scan failed to reconstruct the values of the linear attenuation coefficient for solid Plexiglas (vertical internals and the wall of the column), but succeeded to reconstruct them with values close to theoretical values when considering no column (air) as the reference scan. Hence, using air as the reference scan should be considered in the process of scanning bubble columns with and without vertical internal tubes to achieve correct values of the linear attenuation coefficient and subsequently gas holdup values.The scanning the internals only (i.e., without the column wall) could be considered as the reference scan, but this will not affect the outcomes that obtained from using different reference scans because already the column without internals (i.e., empty) have been considered as reference scan.

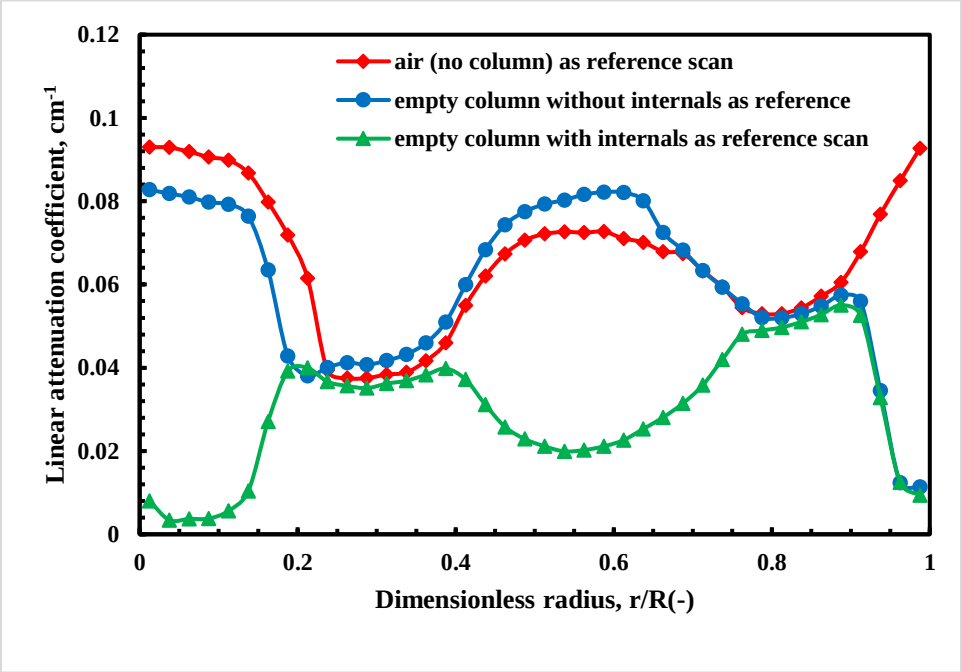

Figure 14: Comparison between reconstructed linear attenuation profiles for bubble column with vertical internals containing air-water and operates at a superficial gas velocity of 45 cm/s based on different reference scans (empty column with internals, empty column without internals, air)

5.3. EFFECT OF THE REFERENCE SCAN, EXPERIMENTAL SCANNING PROCEDURE, AND MATHEMATICAL EXPRESSIONS ON THE CROSS-SECTIONAL GAS HOLDUP DISTRIBUTIONS FOR THE BUBBLE COLUMNS WITH AND WITHOUT INTERNALS

Figure 15 shows the time-averaged cross-sectional gas holdup distribution measured in the fully developed flow region at axial level 0.76 m (H/D = 5.1) for the bubble column without vertical internals operated at a superficial gas velocity of 45 cm/s. Qualitatively, the gas holdup distribution calculated based on the empty column as the reference scan shows more gas in the core of the column and extends more to the wall region than that calculated based on air (no column).

This variation in the local gas holdup distributions is due to using different reference scans, which produced different linear attenuation values and subsequently gas

holdup values because of the estimation of the gas holdup depends mainly on the reconstructed linear attenuation coefficients.

Interestingly, the positions of the vertical internals were clearly distinguished from gas-liquid distribution when the air (no column) was considered as a reference scan, and when the new experimental scanning procedure was applied, and when the new mathematical relationships for the estimation gas holdup in the bubble column with vertical internals were implemented, as shown in Figure 16b.

However, this is not the case in gas holdup distribution calculated based on the empty column with vertical internal tubes as the reference scan, when applying an old experimental scanning procedure, or when implementing old mathematical expressions for the estimation of gas holdup (Figure 16a).

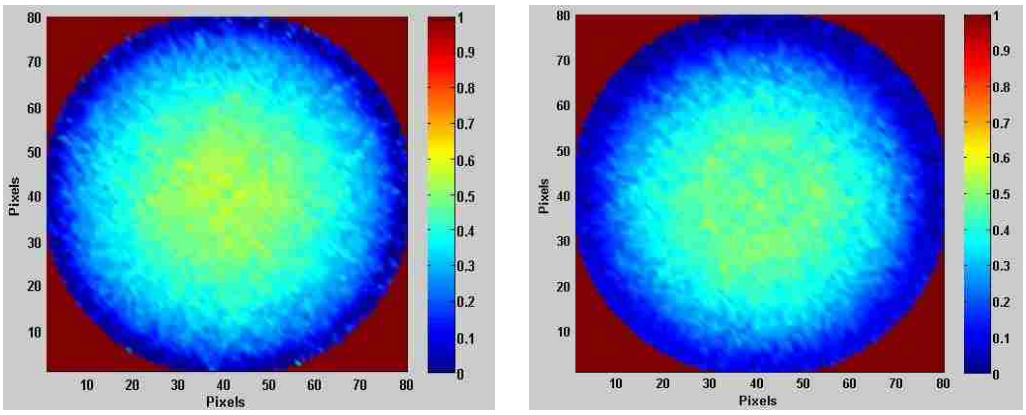

a) Gas holdup distribution estimated based on scanning empty column as the reference scan

b) Gas holdup distribution estimated based on scanning air (no column) as the reference scan

Figure 15: Comparison of the time-averaged cross-sectional gas holdup distribution at a superficial gas velocity of 45 cm/s based on different reference scans

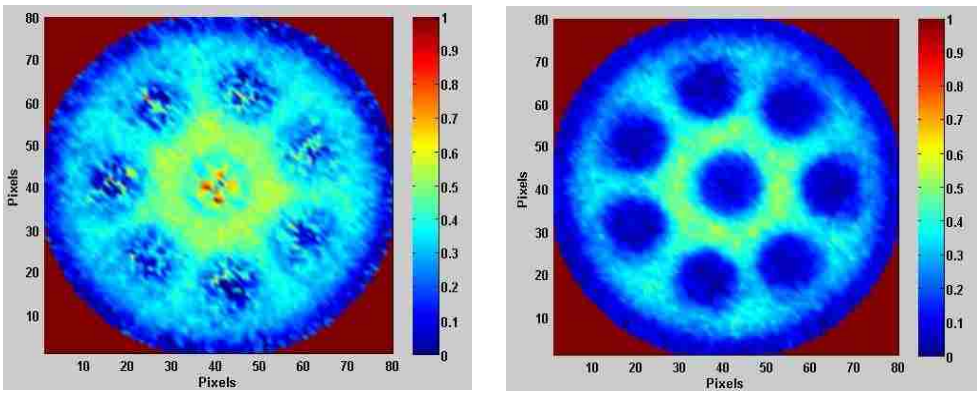

a) Gas holdup distribution estimated based on scanning empty column with internals as the reference scan

b) Gas holdup distribution estimated based on scanning air (no column) as the reference scan

Figure 16: Comparison of the time-averaged cross-sectional gas holdup distribution for bubble column with vertical internals at a superficial gas velocity of 45 cm/s based on different reference scan (empty column with vertical internals, and air (no column))

5.4. EFFECT OF USING DIFFERENT REFERENCE SCANS, NEW EXPERIMENTAL SCANNING PROCEDURE, AND NEW MATHEMATICAL EQUATIONS ON THE GAS HOLDUP PROFILES FOR BUBBLE COLUMNS WITH AND WITHOUT INTERNALS

Figure 17 displays the azimuthally and time-averaged gas holdup profiles in the bubble column without vertical internals operating at a superficial gas velocity of 45 cm/s for different reference scans [empty column without vertical internals, and air (no column)]. It is evident from the profiles that gas holdup calculated based on the empty column is higher than that based on air (no column) as a reference scan at the core and wall regions of the column. For instance, the absolute differences are 5.5% and 6.9% at the center (r/R = 0.038) and wall (r/R = 0.9) regions of the column, respectively. This difference between gas holdup profiles due to using different reconstructed linear attenuation coefficients, which are calculated based on different reference scans. It is important to mention that the measurements of the gas holdup obtained by CT technique in the bubble column without vertical internals operated at a superficial gas velocity of 45

cm/s were validated by using a four-point optical fiber probe as an independent technique to check the accuracy and the reproducibility of the CT data. This optical probe technique is currently available in our laboratory (mReal) and has been successfully used to measure the local gas holdup and bubble properties (bubble passage frequency, bubble chord lengths, specific interfacial area, and bubble rise velocity) in different types of multiphase reactors. More details about the four-point optical fiber probe technique can be found elsewhere.[8,24,43] The verification process included repeating the operation of the bubble column without vertical internals under the same operating conditions (i.e., maintaining the same dynamic level and superficial gas velocity, 45 cm/s) with CT scan and measuring the local gas holdup at the same axial level of CT scan. Figure 18 illustrates the comparison between local gas holdup profiles obtained by CT and optical probe under the same operating condition (i.e., under a superficial gas velocity of 45 cm/s). The analysis of comparison for the local gas holdup values obtained by CT and optical probe techniques reveals that both techniques produce convergent gas holdup values. For example, the average absolute relative difference between the profiles is 7.3%, which confirms the accuracy and reproducibility of CT data. The radial profiles of azimuthally and time-averaged gas holdup for the bubble column with vertical internals operating at a superficial gas velocity of 45 cm/s for different reference scans [empty column with vertical internals, empty column without vertical internals, and no column (air)] are presented in Figure 19. These gas holdup radial profiles that displayed in Figure 19 were calculated by performing azimuthally average for the images of the gas holdup (Figure 16) without excluding the values of vertical internals (i.e., solid internals are present). It is apparent from the figure that gas holdup profiles calculated based on the empty column without vertical internals

and no column (i.e., air only) are close to each other. However, the gas holdup profiles computed based on the empty column with vertical internals as a reference scan displays a different trend from others, particularly at the positions of the vertical internals, due to the selection of an improper reference scan (empty column with vertical internals). For example, the value of gas holdup at the core region (r/R = 0.04) is 0.52 based on an empty column with vertical internals as the reference scan, while it is 0.05 for gas holdup calculated based on empty column and no column (air only) as reference scans with a relative percentage difference of 159%. This indicates that using the column with vertical internals as the reference scan, the old experimental scanning procedure (consider as scanning bubble column without vertical internal), and the old mathematical relationship for calculating gas holdup (consider as column without vertical internals) led to a significant error in the calculation of the gas holdup in the bubble column with vertical internals. Therefore, there is a need to exclude the vertical internals from the gas holdup distributions and the azimuthally averaging to reflect the actual and reliable gas holdup values. Unlike the obtained gas holdup profile in the bubble column without vertical internals, the gas holdup profile obtained in the bubble column with vertical internals was a wavy-like shape due to the presence of these vertical internals. Performing azimuthally (i.e., circumferentially average along the pixels of the image) averaging to the gas holdup distribution image to produce the radial profile in the presence of the vertical internals causes a significant error if those vertical internal tubes are not excluded from this averaging. The method of excluding the vertical internals from gas holdup distributions and their profiles will be explained in the next section.

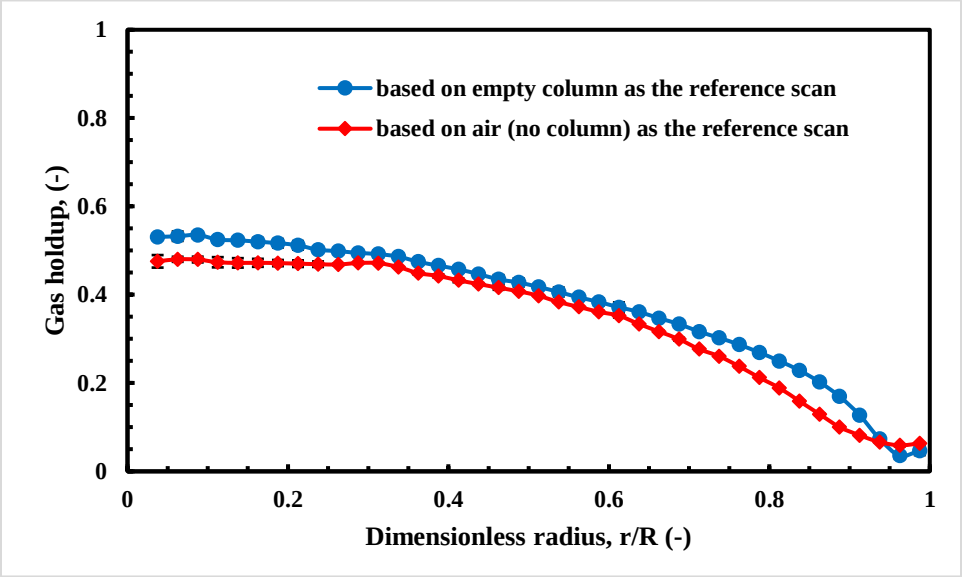

Figure 17: Comparison between the azimuthally gas holdups profiles of the bubble column without internals at a superficial gas velocity of 45 cm/s based on different reference scans (empty column, and air (no column))

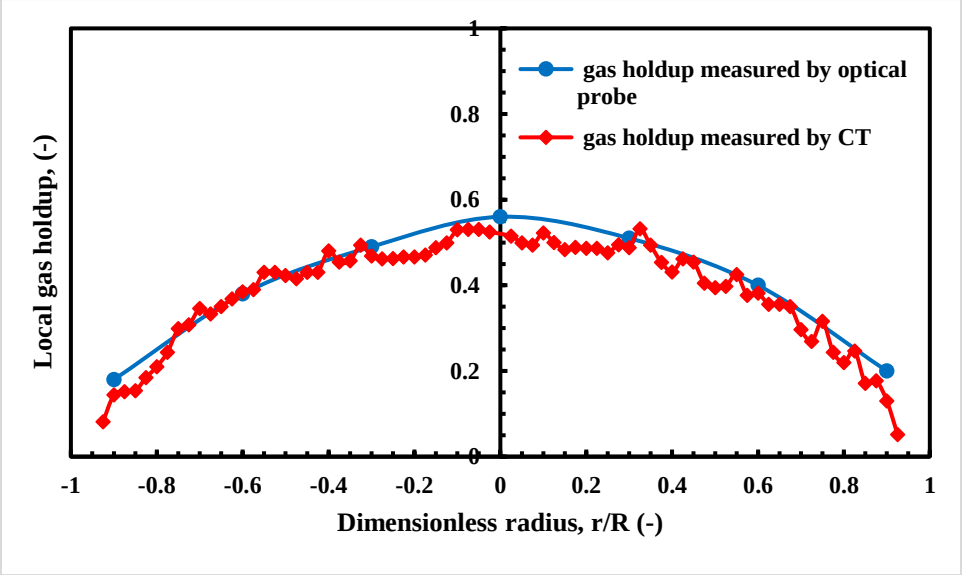

Figure 18: Comparison between local gas holdup values obtained by CT and optical probe techniques in the bubble column without vertical internals operating under a superficial gas velocity of 45 cm/s

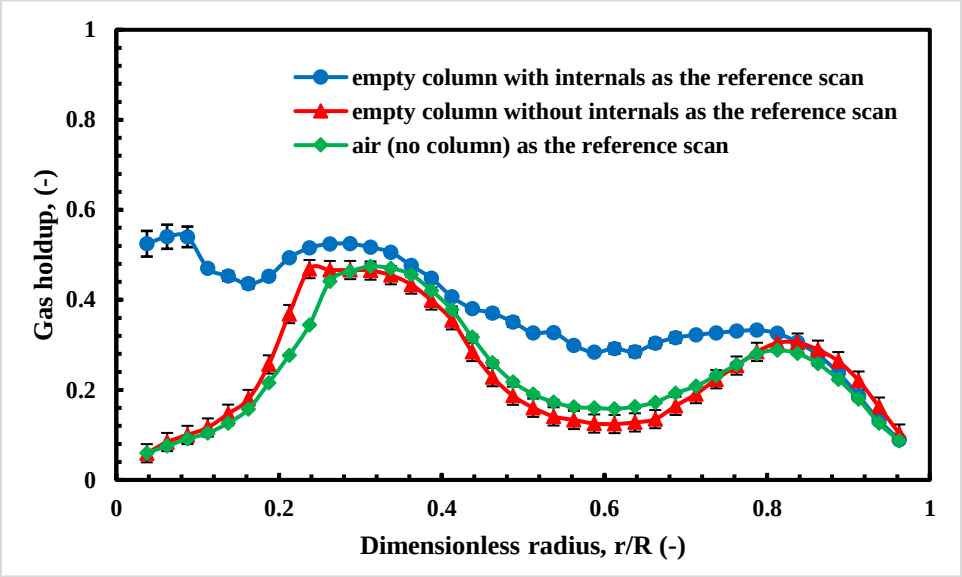

Figure 19: Comparison between the azimuthally gas holdup profiles in bubble column with internals at a superficial gas velocity of 45 cm/s based on different reference scans (empty column with internals, empty column without internals, and air (no column between gamma-ray source and its detectors))

5.5. NEW METHODOLOGY FOR EXCLUDING THE VERTICAL INTERNALS FROM THE GAS HOLDUP DISTRIBUTION IMAGES AND THEIR AZIMUTHAL AVERAGE PROFILES

Counting the values of the vertical internals in the calculation of the azimuthally averaging gas holdup profiles leads to propagating error if the same algorithms and programs in such calculations for columns without vertical internals are used for the column with vertical internals. Hence, there is a need to introduce a new algorithm or method to exclude the values of the vertical internals from the azimuthal averaging for these columns to achieve a reliable estimation of the radial profiles of the gas holdup. The values of the local gas holdup in the zones of the vertical internals should be zero, but according to Figure 16a, they are not zero (noise) at all. Hence, there is a need to precisely define the position of each of the vertical internals to exclude them from the azimuthal average of the gas holdup profiles. However, the cross-sectional image of the gas holdup

(Figure 16a) is very blurry as a result of using an improper reference scan (empty column with vertical internals), and the positions of the vertical internals cannot even be visually identified. Hence, the original configuration of the vertical internals (Figure 3) and the reconstructed linear attenuation coefficient image have been used (Figure 13h) to determine the exact locations of the vertical internals by applying the below procedure:

- Determining the center and boundaries of the column through the binarization process (converting a pixel image to a binary image)[70,71] of the reconstructed linear attenuation coefficient, as displayed in Figure 20. The center of the column is calculated by Eq. 35 and 36:

$$x_c = \frac{\sum_{(i,j)\in R} X_{ij}}{A} \tag{35}$$

$$y_c = \frac{\sum_{(i,j)\in R} y_{ij}}{A} \tag{36}$$

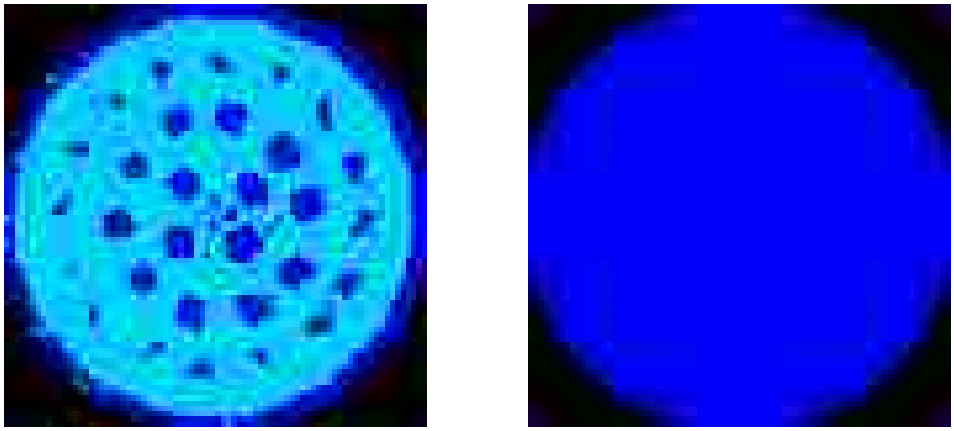

a) Reconstructed linear attenuation coefficient image for column containing air-water operated at superficial gas velocity of 45 cm/s (original image)

b) Reconstructed linear attenuation coefficient image for column containing air-water operated at superficial gas velocity of 45 cm/s (binary image)

Figure 20: Binarization process of the reconstructed linear attenuation coefficient image

- Defining the real position for each of the vertical internals in the gas holdup distribution image. Unfortunately for the low-resolution bitmap picture, even for the same circle of the vertical internals' arrangement, different centers show different shapes, as can be seen in Figure 21. Also, the vertical internals' circles should have the same size. Therefore, the actual dimensions of the configuration of the vertical internals (circular arrangement) were used (Figure 22a) to obtain an image for it and to impose this image on a reconstructed linear attenuation coefficient image (Figure 22b). However, the position of the vertical internals for the real image (configuration) does not match the reconstructed linear attenuation coefficient image. Therefore, in this work, a template matching technique has been used to identify an optimum radius and angles for the rotation, as shown in Figure 23. Additionally, the subpixel position accuracy was implemented to find the precise center of each of the vertical internals.[72] However, this template matching method is not universal and it has been applied case by case according to the vertical internals configurations and their sizes.

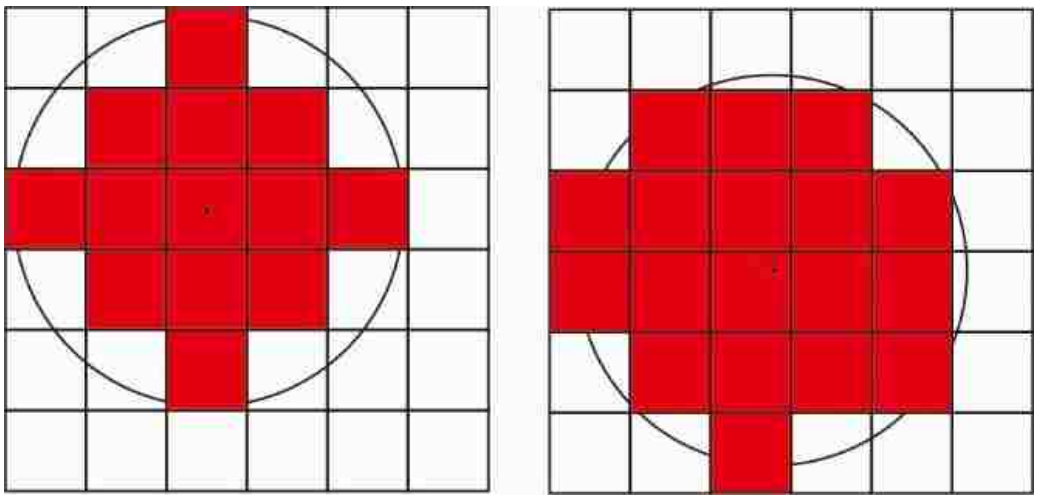

Figure 21: Different circle's shape because the checkerboard effect

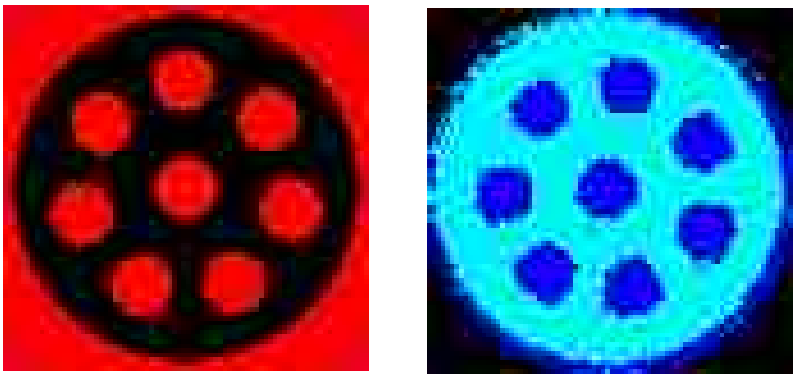

a) Real position of internals for circular arrangement (original configuration)

b) Reconstructed linear attenuation coefficient distribution for bubble column with internals operates at superficial gas velocity of 45 cm/s

Figure 22: Original configuration position and reconstructed linear attenuation coefficient images for bubble column with 1-in vertical internals operates at a superficial gas velocity of 45 cm/s

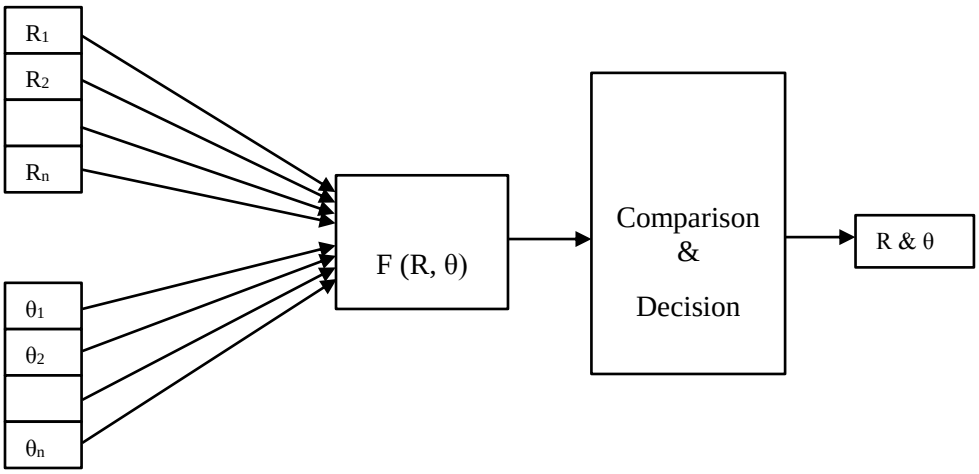

Figure 23: Illustration of the template matching method

➢ Deleting the noise (vertical internals zones), once the linear attenuation coefficient and real configuration images match. It is worth mentioning that this approach of exclusion of the vertical internals from gas holdup distribution images was implemented with different sizes of the vertical internals (0.5 in. and 1 in. diameter) and different configurations of vertical internals (circular and hexagonal shape), where it worked efficiently, as shown in Figure 24, Figure 25, and Figure 26.

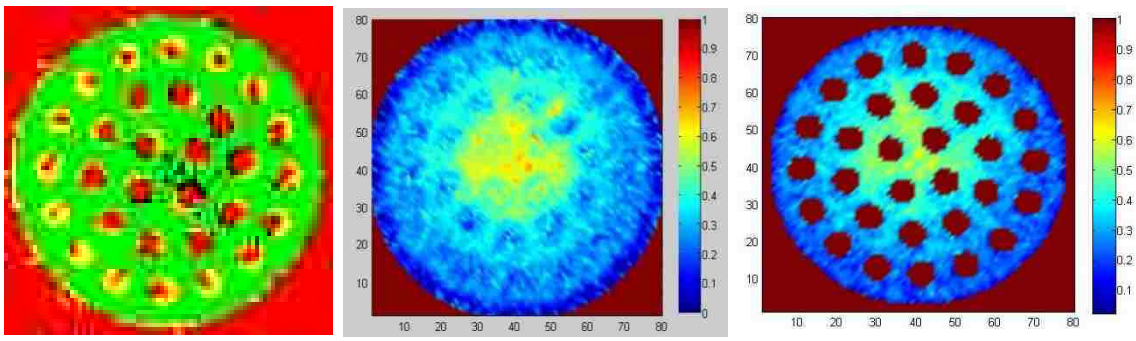

a) Matching between original configuration and reconstructed linear attenuation coefficient images

b) Gas holdup distribution at superficial gas velocity of 45 cm/s image before excluding the vertical internals

c) Gas holdup distribution at superficial gas velocity of 45 cm/s image after excluding the vertical internals

Figure 24: Cross-sectional gas holdup distributions for the bubble column with 0.5-in vertical internals arranged circularly and operated at a superficial gas velocity of 45 cm/s

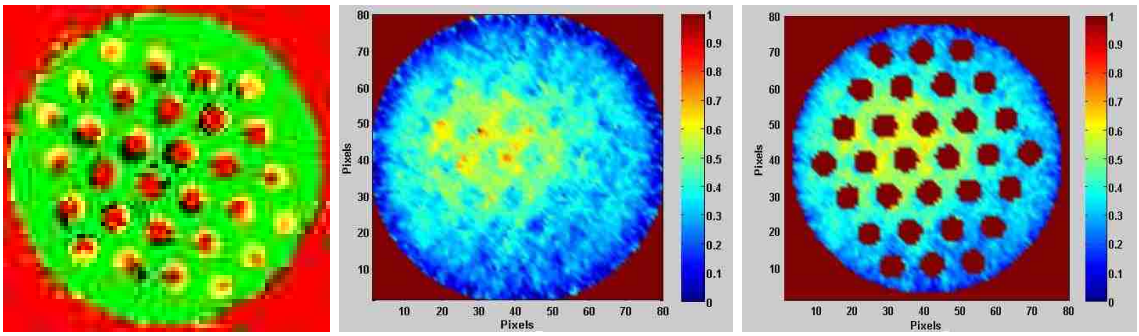

a) Matching between original configuration and reconstructed linear attenuation coefficient images

b) Gas holdup distribution at superficial gas velocity of 45 cm/s image before excluding the internals

c) Gas holdup distribution at superficial gas velocity of 45 cm/s image after excluding the internals

Figure 25: Cross-sectional gas holdup distributions for bubble column equipped with 0.5-in vertical internals arranged hexagonally at a superficial gas velocity of 45 cm/s

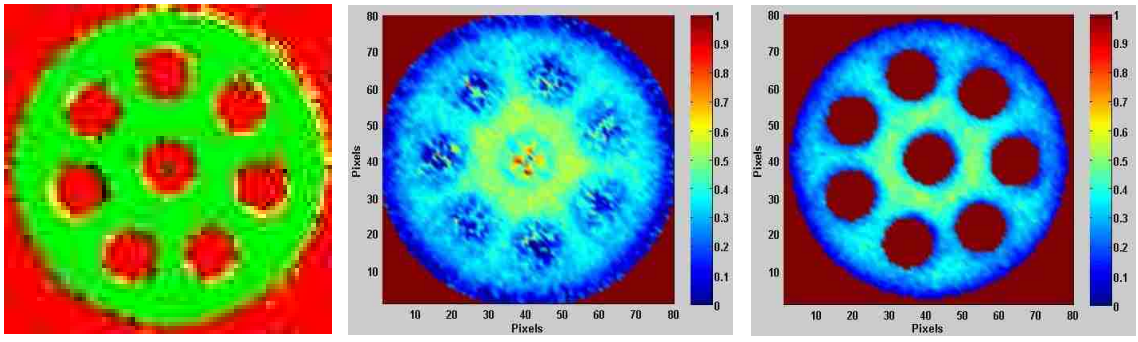

a) Matching between original configuration and reconstructed linear attenuation coefficient images

b) Gas holdup distribution at superficial gas velocity of 45 cm/s image before excluding the internals

c) Gas holdup distribution at superficial gas velocity of 45 cm/s image after excluding the internals

Figure 26: Cross-sectional gas holdup distributions for bubble column equipped with 1-in vertical internals arranged circularly at a superficial gas velocity of 45 cm/s

- Computation of the azimuthally averaged gas holdup profiles. This step is considered the most important step in the calculation of the azimuthally averaged gas holdup beacuase all simulation results and hydrodynamic models will be compared against and validated with experimental gas holdup profiles, and hence if the experimental azimuthally averaged gas holdup profiles, measured were wrong, then the validation process will be incorrect. Therefore, we excluded the values of the vertical internals from the averaging values of gas holdup to provide accurate and reliable gas holdup profiles. Once the vertical internal positions are excluded from the gas holdup distribution image, the azimuthally averaged gas holdup profiles can be easily computed, as shown in Figure 27, to produce an azimuthally averaged radial profile. Figure 28 displays the comparison between gas holdup profiles before and after excluding the internals. According to the Figure 28, the gas holdup profile after excluding the internals starts from the region at the dimensionless radius, r/R= 0.17 because before this region, there was an internal that was located at the center of the column. Additionally, there is a gap between the gas holdup profiles in the confined area by the dimensionless radius, r/R = 0.41, and r/R = 0.75, which represents the positions of internals. For example, the relative percentage difference between profiles is 59% at the dimensionless radius, r/R = 0.56. This difference in the gas holdup profiles results from excluding the internals from azimuthally averaged of gas holdup profile, and the obtained gas holdup in this region represents the azimuthally averaged of gas holdup values between the internals. These radial profiles of the gas holdup (Figure 28) were further processed to present them in the diametrical profiles, as exhibited in Figure 29. Furthermore, the diametrical gas holdup profiles obtained by CT technique for bubble column with vertical internals were compared with those obtained by other independent measurements using

four-point optical fiber probe. In this comparison, the local gas holdup values were measured in the same experimental setup (i.e., 6-inch bubble column with vertical internals) and under the same conditions (i.e., under a superficial gas velocity of 45 cm/s). The values of gas holdup along the diameter obtained by the optical probe were compared with local values of the gas holdup at the corresponding pixel locations of the CT image, as displayed in Figure 30. It is evident from this figure that the values of gas holdup obtained with CT and optical probe are close to each other with an average absolute relative difference of 6.2%, which confirms the fidelity of the CT measurements for bubble column with vertical internals. Finally, Figure 31 illustrates all steps of the methodology for excluding the internals from gas holdup distributions and their profiles.

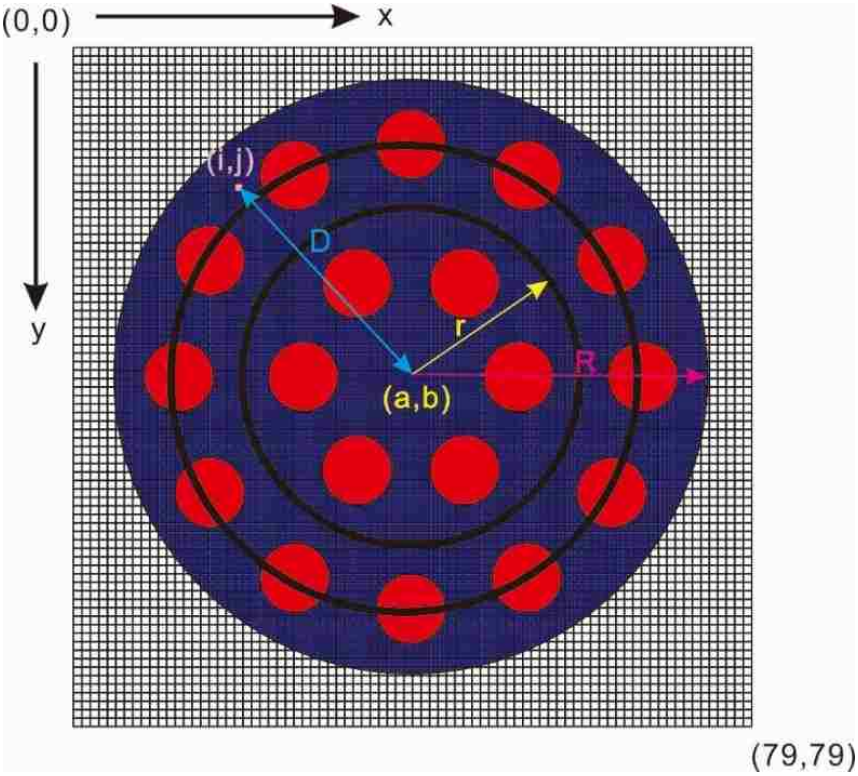

Figure 27: Azimuthally averaged for gas holdup in bubble column with vertical internals

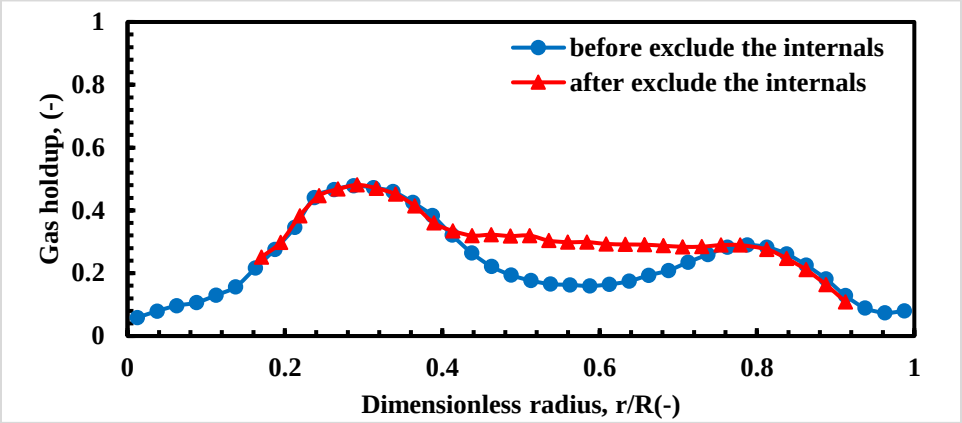

Figure 28: Radial profile of azimuthal gas holdup before and after excluding the internals for the bubble column with 1-in vertical internals at a superficial gas velocity of 45 cm/s

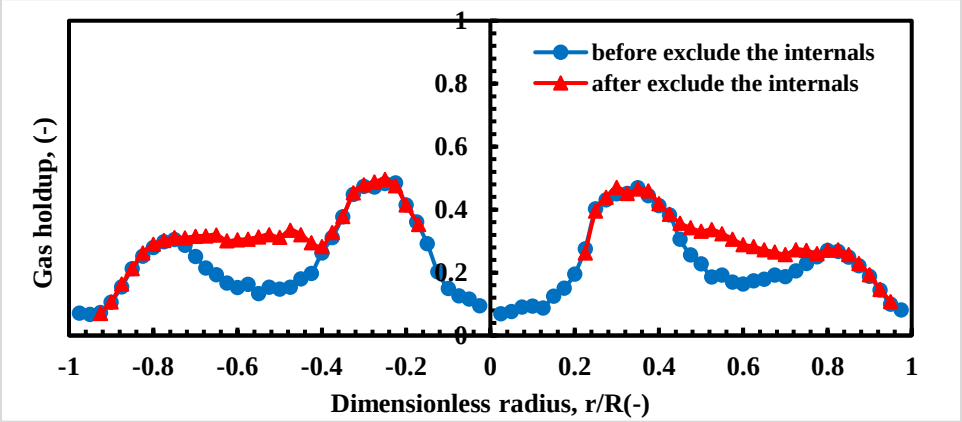

Figure 29: Diametrical profile of azimuthally gas holdup before and after excluding the internals for the bubble column with 1-in internals at a superficial gas velocity of 45 cm/s

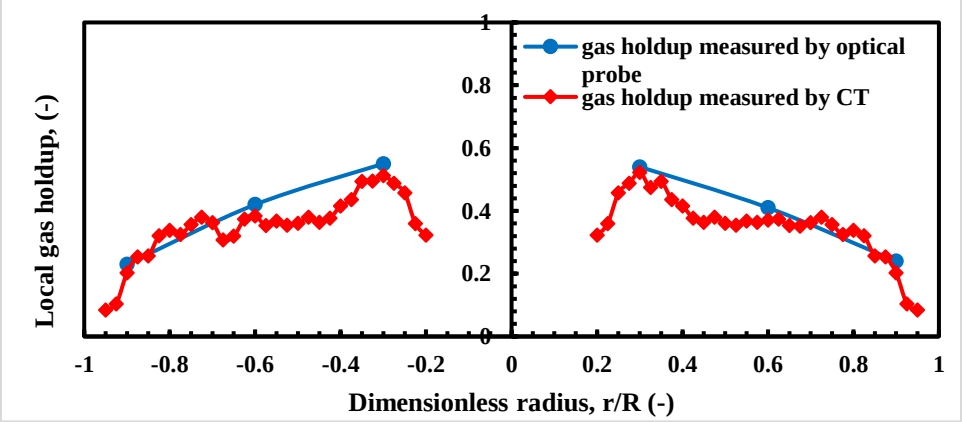

Figure 30: Comparison between the gas holdup values obtained by CT and optical probe techniques for the bubble column with internals operating at 45 cm/s

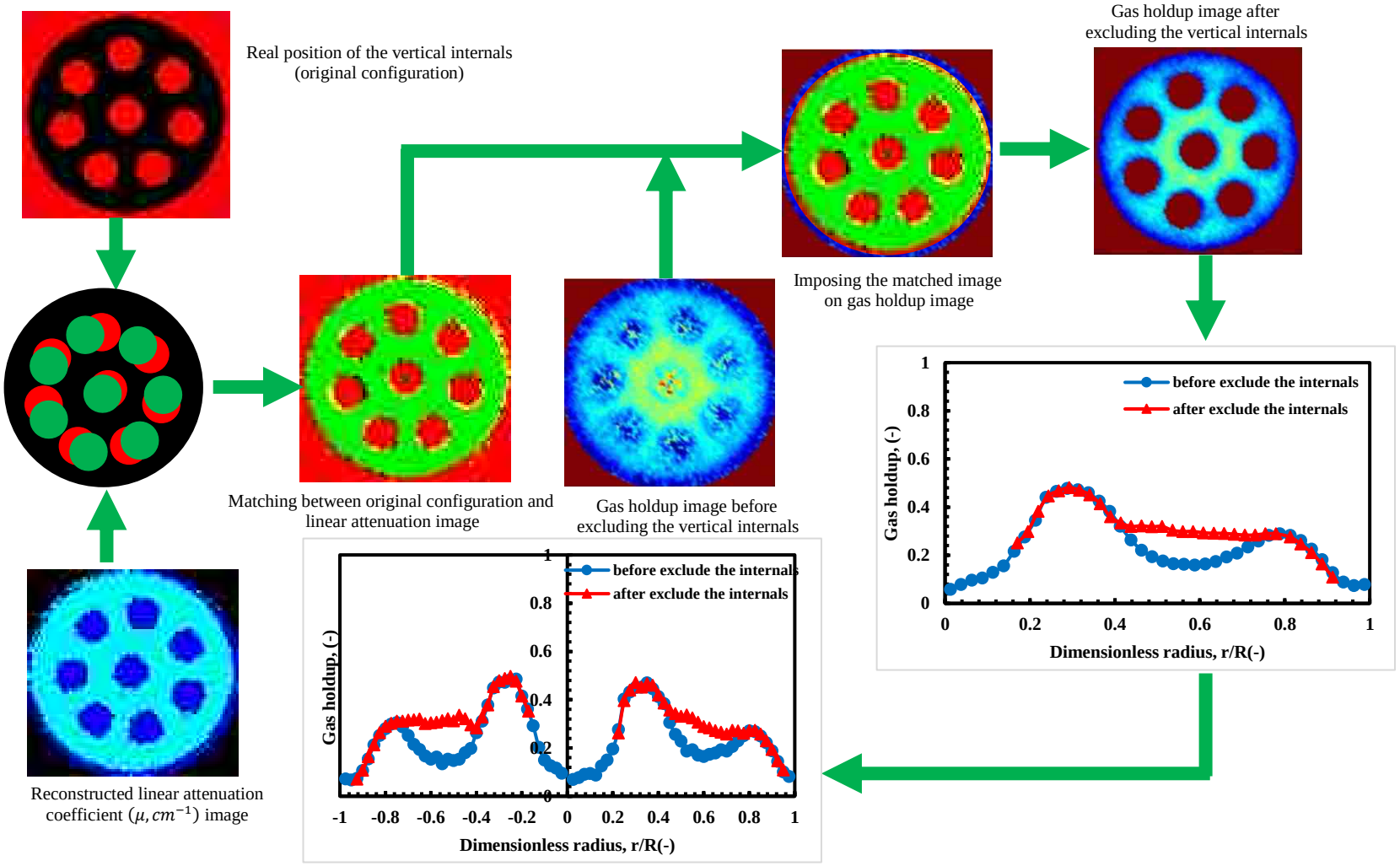

Figure 31: Illustration of excluding the internals from the gas holdup distribution image and its azimuthally averaging radial profile

6. REMARKS

The present work was performed to identify and address some major pitfalls in conducting and interpreting the results of the gamma ray computed tomography technique for the bubble column with vertical internal tubes to provide correct and reliable gas holdup distributions and their profiles at any operating condition. In this study, various pitfalls were identified, such as using an improper reference scan, attempting to estimate gas holdup distribution and their profiles in bubble column with vertical internals from the experimental scanning procedure and mathematical relationships used to determine gas holdup in bubble column without vertical internals, and failure to calculate the azimuthally gas holdup profile in the presence of the vertical internal tubes. This investigation was conducted in a 6 in. Plexiglas bubble column in the presence and absence of the vertical internals for the air–water system at a superficial gas velocity of 45 cm/s by utilizing an advanced gamma ray computed tomography (CT) technique. The key results are summarized as follows:

- A new experimental scanning procedure, mathematical equations for the estimation of gas holdup, and methodology of excluding the vertical internal tubes have been implemented to correctly and precisely visualize and quantify the gas holdup distribution and their profiles in the bubble column with vertical internals.
- Experimental results revealed that the reference scan significantly affects the values of the reconstructed linear attenuation coefficient and consequently the gas holdup results.
- The reconstructed linear attenuation coefficient values are compared with theoretical values and show good agreement when considering the empty column (without vertical internals) and air only (without putting column between the gamma-ray source and its

detectors) as reference scans, while showing disagreement when using the empty column with vertical internals as reference scan.

- Using air only (without column) as a reference scan has eliminated the error in gas holdup profiles at the wall region.
- The gamma ray computed tomography technique was capable of capturing the wall thickness of the column and the vertical internals when air only (without column) was used as a reference scan.
- The new experimental scanning procedure and method of excluding the vertical internals from the cross-sectional gas holdup distributions and their radial profiles have been successfully implemented with different sizes (0.5 and 1-inch diameters) of the vertical internals and different configuration of the vertical internals (circular and hexagonal shape).
- Identifying and addressing some issues and concerns that are associated with measuring gas holdup distributions and their profiles in the bubble columns with vertical internal tubes by using the CT technique will assist and guide those scanning bubble column with the vertical internals to avoid these pitfalls and provide reliable results for the gas holdup.
- Despite the presented experimental procedure, relationships for calculating gas holdup, and method of excluding the internals from gas holdup distribution and its profile were applied successfully based on a case by case for different sizes and configurations of vertical internals in this study. However, further algorithm development is required in the future to make this algorithm robust for any kinds of vertical internals.

ACKNOWLEDGMENT

The Higher Committee for Education Development in Iraq (HCED), Ministry of Higher Education and Scientific Research (Iraq), Missouri S&T, and Professor Dr. Muthanna Al-Dahhan are gratefully acknowledged for providing the funding for performing this study. The first author would like to thank Dr. Premkumar Kamalanathan and Dr. Mahmoud Moharam for valuable discussion and comments.

REFERENCES

[1] S. Degaleesan, M. Dudukovic, Y. Pan, *AIChE J.* **2001**, *47*, 1913.

[2] N. Kantarci, F. Borak, K. O. Ulgen, *Process Biochem.* **2005**, *40*, 2263.

[3] F. Laborde-Boutet, Cédric and Larachi, *AIChE J.* **2010**, *56*, 2397.

[4] L. S. Sabri, A. J. Sultan, M. H. Al-dahhan, *IEEE* **2017**, 3.

[5] C. Boyer, J. Gazarian, V. Lecocq, S. Maury, A. Forret, J. M. Schweitzer, V. Souchon, *Oil Gas Sci. Technol. – Rev. d'IFP Energies Nouv.* **2016**, *71*, 44.

[6] O. M. Basha, L. Sehabiague, A. Abdel-Wahab, B. I. Morsi, *Int. J. Chem. React. Eng.* **2015**, *13*, 201.

[7] M. Kölbel,H ;Ralek, *Catal. Rev. Eng.* **1980**, *21*, 225.

[8] M. Kagumba, M. H. Al-Dahhan, *Ind. Eng. Chem. Res.* **2015**, *54*, 1359.

[9] M. Al Mesfer, A. Sultan, M. Al-Dahhan, *Chem. Eng. J.* **2016**, *300*, 317.

[10] J. Chen, F. Li, S. Degaleesan, P. Gupta, M. H. Al-Dahhan, M. P. Dudukovic, B. A. Toseland, *Chem. Eng. Sci.* **1999**, *54*, 2187.

[11] A. Forret, J. M. Schweitzer, T. Gauthier, R. Krishna, D. Schweich, *Can. J. Chem. Eng.* **2003**, *81*, 360.

[12] F. Larachi, D. Desvigne, L. Donnat, D. Schweich, *Chem. Eng. Sci.* **2006**, *61*, 4195.

[13] A. K. Jhawar, A. Prakash, *Chem. Eng. Res. Des.* **2014**, *92*, 25.

[14] X. Guan, Y. Gao, Z. Tian, L. Wang, Y. Cheng, X. Li, *Chem. Eng. Res. Des.* **2015**, *102*, 196.

[15] G. Besagni, F. Inzoli, *Exp. Therm. Fluid Sci.* **2016**, *74*, 27.

[16] J. Chen, P. Gupta, S. Degaleesan, M. H. Al-Dahhan, M. P. Dudukovic, B. A. Toseland, *Flow Meas. Instrum.* **1998**, *9*, 91.

[17] Y. Wu, B. Cheng Ong, M. H. Al-Dahhan, *Chem. Eng. Sci.* **2001**, *56*, 1207.

[18] A. A. Mouza, G. K. Dalakoglou, S. V. Paras, *Chem. Eng. Sci.* **2005**, *60*, 1465.

[19] A. Behkish, R. Lemoine, L. Sehabiague, R. Oukaci, B. I. Morsi, *Chem. Eng. J.* **2007**, *128*, 69.

[20] M. D. Supardan, Y. Masuda, A. Maezawa, S. Uchida, *Chem. Eng. J.* **2007**, *130*, 125.

[21] B. C. Ong, P. Gupta, A. Youssef, M. Al-Dahhan, M. P. Duduković, *Ind. Eng. Chem. Res.* **2009**, *48*, 58.

[22] S. Dhanasekaran, T. Karunanithi, *Can. J. Chem. Eng.* **2012**, *90*, 126.

[23] H. Jin, Y. Lian, L. Qin, S. Yang, G. He, Z. Guo, *Can. J. Chem. Eng.* **2014**, *92*, 1444.

[24] R. F. Xue, J.;Al-Dahhan, M.;Dudukovic, M. P.;Mudde, *Flow Meas. Instrum.* **2008**, *19*, 293.

[25] S. Ojima, K. Hayashi, S. Hosokawa, A. Tomiyama, *Int. J. Multiph. Flow* **2014**, *67*, 111.

[26] J. Alvare, M. Al-dahhan, *Ind. Eng. Chem. Res.* **2006**, *45*, 3320.

[27] E. Fransolet, M. Crine, G. L. Homme, D. Toye, P. Marchot, *Meas. Sci. Technol.* **2001**, *12*, 1055.

[28] A. Bieberle, H.-U. Härting, S. Rabha, M. Schubert, U. Hampel, *Chemie Ing. Tech.* **2013**, *85*, 1002.

[29] A. Yadav, A. Kushwaha, S. Roy, *Can. J. Chem. Eng.* **2016**, *94*, 524.

[30] N. Rados, A. Shaikh, M. H. Al-dahhan, *Can. J. Chem. Eng.* **2005**, *83*.

[31] S. Roy, Quantification of two phase flow in liquid solid risers, PhD thesis, Washington University, St. Louis, MO, USA, **2000**.

[32] N. Rados, Slurry bubble column hydrodynamics, PhD thesis, Washington University, St. Louis, MO, USA, **2003**.

[33] S. Maurer, E. C. Wagner, J. R. van Ommen, T. J. Schildhauer, S. L. Teske, S. M. A. Biollaz, A. Wokaun, R. F. Mudde, *Int. J. Multiph. Flow* **2015**, *75*, 237.

[34] S. Maurer, E. C. Wagner, T. J. Schildhauer, J. R. van Ommen, S. M. A. Biollaz, R. F. Mudde, *Int. J. Multiph. Flow* **2015**, *74*, 118.

[35] S. Maurer, E. C. Wagner, T. J. Schildhauer, J. R. van Ommen, S. M. A. Biollaz, R. F. Mudde, *Int. J. Multiph. Flow* **2015**, *74*, 143.

[36] B. Ong, Experimental Investigation of Bubble Column Hydrodynamics - Effect of Elevated Pressure and Superficial Gas Velocity, PhD thesis, Washington University, St. Louis, MO, USA, **2003**.

[37] A. Youssef, Fluid Dynamics and Scale-up of Bubble Columns with Internals, PhD thesis, Washington University, St. Louis, MO, USA, **2010**.

[38] M. Kagumba, Heat Transfer and Bubble Dynamics in Bubble and Slurry, PhD thesis, Missouri university of science and technology, MO, USA, **2013**.

[39] a. V. Kulkarni, *Chem. Eng. Technol.* **2010**, *33*, 1015.

[40] Y. K. Doshi, A. B. Pandit, *Chem. Eng. J.* **2005**, *112*, 117.

[41] A. A. Youssef, M. H. Al-Dahhan, *Ind. Eng. Chem. Res.* **2009**, *48*, 8007.

[42] A. A. Youssef, M. E. Hamed, J. T. Grimes, M. H. Al-Dahhan, M. P. Duduković, *Ind. Eng. Chem. Res.* **2013**, *52*, 43.

[43] A. Jasim, The impact of heat exchanging internals on hydrodynamics of bubble column reactor, MSc thesis, Missouri university science and technology, MO, USA, **2016**.

[44] R. Varma, Characterization of anaerobic bioreactors for bioenergy generation using a novel tomography technique, PhD thesis, Washington University, St. Louis, MO, USA, **2008**.

[45] F. S. Al Falahi, Experimental investigation of the pebble bed structure by using gamma ray tomography, MSc thesis, Missouri university science and technology, MO, USA, **2014**.

[46] F. Al Falahi, M. Al-Dahhan, *Nucl. Eng. Des.* **2016**, *310*, 231.

[47] M. Al-Mesfer, Effect of Dense Heat Exchanging Internals on the Hydrodynamics of Bubble Column Reactors Using Non-Invasive Measurement Techniques, PhD thesis, Missouri university science and technology, MO, USA, **2013**.

[48] A. Efhaima, M. Al-Dahhan, *Int. J. Ind. Chem.* **2015**, *6*, 143.

[49] A. Efhaima, Scale-up investigation and hydrodynamics study of gas-solid fluidized bed reactor using advanced non- invasive measurement techniques, PhD thesis, Missouri university science and technology, MO, USA, **2016**.

[50] A. Efhaima, M. Al-Dahhan, *Can. J. Chem. Eng.* **2016**, *94*.

[51] A. Efhaima, M. H. Al-Dahhan, *Can. J. Chem. Eng.* **2017**, *95*, 656.

[52] N. Y. Ali, Evaluating of scale-up methodologies of gas-solid spouted beds for coating triso nuclear fuel particles using advanced measurement techniques, PhD thesis, Missouri university science and technology, MO, USA, **2016**.

[53] N. Ali, T. Al-Juwaya, M. Al-Dahhan, *Chem. Eng. Res. Des.* **2016**, *114*, 129.

[54] N. Ali, T. Al-Juwaya, M. Al-Dahhan, *Exp. Therm. Fluid Sci.* **2017**, *80*, 90.

[55] T. Al-Juwaya, N. Ali, M. Al-Dahhan, *Exp. Therm. Fluid Sci.* **2017**, *86*, 37.

[56] P. Gupta, Churn Turbulent bubble columns, PhD thesis, Washington University, St. Louis, MO, USA, **2002**.

[57] S. Roy, A. Kemoun, M. H. Al-Dahhan, M. P. Dudukovic, T. B. Skourlis, F. M. Dautzenberg, *Chem. Eng. Process. Process Intensif.* **2005**, *44*, 59.

[58] P. A. S. Vasquez, C. H. De Mesquita, G. A. C. LeRoux, M. M. Hamada, *Appl. Radiat. Isot.* **2010**, *68*, 658.

[59] J. A. O. Sullivan, D. L. Snyder, *IEEE Trans. Med. Imaging* **2007**, *26*, 144.

[60] R. Varma, S. Bhusarapu, J. O' Sullivan, M. Al-Dahhan, *Meas. Sci. Technol.* **2007**, *18*, 1.

[61] N. Ellis, H. T. Bi, C. J. Lim, J. R. Grace, *Chem. Eng. Sci.* **2004**, *59*, 1841.

[62] X. Yang, J. R. Van Ommen, J. Schoormans, R. F. Mudde, *Comput. Phys. Commun.* **2015**, *196*, 27.

[63] J. Gómez-Hernández, J. Ruud van Ommen, E. Wagner, R. F. Mudde, *Powder Technol.* **2016**, *290*, 33.

[64] I. Csiszar, *Ann. Stat.* **1991**, *19*, 2032.

[65] X. Yang, J. R. van Ommen, R. F. Mudde, *Powder Technol.* **2014**, *253*, 626.

[66] M. Al-Dahhan, *Atoms Peace – An Int. J.* **2009**, *2*, 324.

[67] M. H. Al-Dahhan, *Procedia Eng.* **2016**, *138*, 347.

[68] J. H. Hubbell, S. M. Seltzer, 'Tables of X-Ray Mass Attenuation Coefficients and Mass Energy-Absorption Coefficients. National Institute of Standards and Technology (NIST).', **1996**, https://www.nist.gov/pml/x-ray-mass-attenuation-coefficients.

[69] M. K. Al Mesfer, A. J. Sultan, M. H. Al-Dahhan, *Chem. Eng. J.* **2016**, *300*, 317.

[70] J. Sauvola, M. Pietikäinen, *Pattern Recognit.* **2000**, *33*, 225.

[71] B. Gatos, I. Pratikakis, S. J. Perantonis, *Pattern Recognit.* **2006**, *39*, 317.

[72] R. Brunelli, *Template Matching Techniques in Computer Vision: Theory and Practice*, Wiley, **2009**.

II. INFLUENCE OF THE SIZE OF HEAT EXCHANGING INTERNALS ON THE GAS HOLDUP DISTRIBUTION IN A BUBBLE COLUMN USING GAMMA-RAY COMPUTED TOMOGRAPHY

Abbas J. Sultan, Laith S. Sabri, Muthanna H. Al-Dahhan †

Multiphase Reactors Engineering and Applications Laboratory (mReal), *Department of Chemical and Biochemical Engineering, Missouri University of Science and Technology, Rolla, MO 65409-1230. USA*

ABSTRACT

The effects of the presence of the vertical internals of different sizes at a wide range of superficial gas velocity on the overall, local gas holdup distributions and their profiles have been studied and quantified in a 6-inch (0.14 m) Plexiglas® bubble column with air-water system using a non-invasive advanced gamma-ray computed tomography (CT) technique. In this study, two sizes of Plexiglas® vertical internals, having the same occupying area (~25%) of the column's cross-sectional area (CSA) that represents those used in Fischer-Tropsch synthesis, have been used within a range of superficial gas velocities that cover bubbly and churn turbulent flow regimes (0.05 to 0.45 m/s). The reconstructed CT scan images revealed that the bubble columns equipped with or without internals displayed a uniform cross-sectional gas holdup distribution (symmetric) for all studied superficial gas velocities. However, the bubble column equipped with 1-inch vertical internals exhibited more uniform gas holdup distribution than the column with 0.5-inch internals. Also, the visualization of the gas-liquid distributions for bubble columns with and without internals reveal that the well-known phenomenon of the core-annular liquid circulation pattern that observed in the bubble column without internals still exists in bubble column packed densely with vertical internals. Moreover, a remarkable increase in the gas holdup values at the wall region was achieved in the churn turbulent flow regime

based on the insertion of the vertical internals inside the column as compared with using a bubble column without obstacles. Furthermore, the values of the gas holdup in the core region of the bubble column with vertical internals are similar to those of the bubble column without vertical internals when they are operated at high superficial gas velocity (churn turbulent flow regime), based on the free cross-sectional area (CSA) for the flow. In general, the magnitude of the gas holdup increased significantly with increasing superficial gas velocity for the bubble columns with and without internals. However, the gas holdup profile was shaped like a wavy line in the bubble column with vertical internals, whereas it exhibited a parabolic gas holdup profile in the bubble column without obstacles.

Keywords: Bubble column, internals size, gas holdup distribution, computed tomography (CT).

†Correspondence author at Chemical & Biochemical Engineering Department, Missouri University of Science and Technology, Rolla, MO, 65409. Tel.: +1 573-578-8973. E-mail: aldahhanm@mst.edu

1. INTRODUCTION

Bubble and slurry bubble column reactors have several features that make them widely used in the industry such as chemical and biochemical, petroleum and petrochemical, and metallurgical processes [1–5]. Among these characteristics, they offer high heat and mass transfer rates, sufficient heat recovery by equipping them with a bundle of the heat exchanging tubes, invariant overall catalyst activity, an absence of moving parts and hence they are suitable for high-pressure operating conditions, and with their simple design and construction they save time and cost during construction, operation, and maintenance processes [6–10]. The main disadvantages of bubble/slurry bubble columns

are significant phase-back mixing and challenges for design and scale-up due to the complex interaction that exists between the gas-liquid or gas-solid-liquid (gas-slurry) phases, which affects the interface forces such as the drag force, lift force, turbulent dispersion force, and others [11].

Many of the chemical reactions conducted in bubble/slurry bubble columns are involving highly exothermic reactions such as acetic acid industry, acetone production, Fischer-Tropsch (FT) synthesis, and many others that require inserting a large number of vertical cooling tubes inside these reactors to absorb the excess heat generated and to maintain the desired temperature for the reaction to prevent local overheating of catalyst, decrease selectivity for desired products, and runaway of these reactors [12–17]. Equipping these reactors with a bundle of the heat exchanging tubes will impact the hydrodynamics and consequently the performance, productivity, and selectivity of these reactors [18].

Among these hydrodynamic factors, gas holdup distribution is considered one of the most important hydrodynamic parameters because it governs the liquid/slurry flow pattern, mixing, gas-liquid interfacial area and as a result the heat transfer rate from the heat exchange tubes of the gas-liquid or gas-slurry phases and the mass transfer rate between the phases [19–21]. Therefore, the efficient design, scale-up, operating, monitoring, and optimization of bubble/slurry bubble columns equipped with a bundle of the heat exchanging tubes requires the knowledge of gas holdup distributions and their profiles, which are lacking in the open literature.

In the past few decades, an extensive experimental and simulation studies have been performed on the hydrodynamics of the bubble/slurry bubble columns without internals [22–33]. However, very limited studies have considered the effect of the presence of the

vertical internals on the hydrodynamics of these reactors despite the fact that an intense vertical bundle of the heat exchanging tubes is equipped inside industrial bubble/slurry bubble columns to maintain the temperature of the reaction. Some of these experimental investigations and their key findings on bubble/slurry bubble columns equipped with vertical tubes are summarized in Table 1.

According to Table 1, noteworthy experimental studies that led to advance the understanding of the hydrodynamics and the bubble properties of the bubble/slurry bubble columns equipped with vertical internals [11,15,34–45]. Unfortunately, most of these investigations were carried out using visual observation or probe-based experimental techniques [34,37,39,41,43,44,46,47]. It is not usually feasible to make measurements based on visual observations because of the opaque nature of the flow pattern in a bubble column with internals [48]. Also, probe-based techniques are invasive, and even if they are reliable, but still they are providing point measurements that require extensive experimental work to address the effects of the operating and design parameters. Additionally, these probe techniques have access issues for all the cross-sectional area of the column during the measurements, especially with columns equipped with dense solid vertical internals due to there is not enough room to insert the probes. Moreover, the measured gas holdup profiles by these probes-based techniques cannot capture the non-symmetry of the measured parameters across the cross-sectional area of the bubble column since the flow behavior inside the bubble columns is turbulent and chaotic, especially in high superficial gas velocity (churn turbulent flow regime) [49,50]. Therefore, it was difficult to capture the maldistribution using these point measurement techniques.

Furthermore, the dimensions of the probe can affect the hydrodynamic data of the fluid being measured, as reported by Ellis et al. [51].

Recently, Whitemarsh et al. [52] studied the influence of the presence of a probe on the local gas holdup in a fluidized bed and concluded that there are significant variations in the gas holdup data at the probe tips and even in the flow above the inserted probe. Therefore, there is a need to use non-invasive techniques, such as gamma ray or x-ray computed tomography that can provide reliable phase holdups distribution data over the entire cross-sectional area of the bubble column in the presence and absence of the vertical internals without disturbing the flow pattern.

To the best of the authors' knowledge, there are no more than two published studies in the literature that have investigated the influence of the vertical internals on the time-averaged gas holdup distributions and their radial profiles by using gamma-ray computed tomography as a non-invasive technique. One such study performed by Chen et al. [38], measured in the fully developed region (132 cm above the gas distributor) the time and azimuthal averaged of the gas holdup profiles at the superficial gas velocities of 2, 5, and 10 cm/s in an 18-inch (44 cm) diameter bubble column without and with internals (occupying 5% of the total cross-sectional area (CSA) of the column) for both air-water and air-drake oil systems. They reported that in the fully developed region of the bubble column with or without internals for both systems, the gas holdup and the liquid recirculation flow pattern were axisymmetric. Also, they found that the gas holdup was higher in the air-water system as compared with the air-drake oil system for the same studied superficial gas velocities based on the total cross-sectional area of the column. However, their study was carried out at a low superficial gas velocity (up 10 cm/s), while

the industrial processes are interested in high volumetric productivity, which can only be achieved with high superficial gas velocity (typically in churn turbulent flow regime) [53,54]. Moreover, they utilized a vertical rods bundle that covered a little blocked cross-sectional area of the column (5 percent of the total cross-sectional area (CSA) of the column that targets methanol synthesis), which does not meet the requirement of FT synthesis to remove the generated heat. Furthermore, the reported slight increase in the gas holdup based on the insertion of the vertical rods may be the result of using the same superficial gas velocity, which is calculated based on the total CSA of the bubble columns without internals. Hence, the gas velocity through the gaps between the tubes is higher than that in the case of the bubble column without internals.

The other study that investigated the impact of the vertical internals on the gas holdup distributions and their profiles was published recently by Al-Mesfer et al. [45]. In this work, the time-averaged cross-sectional gas holdup distributions and their radial profiles in bubble columns for an air-water system with a broad range of superficial gas velocities from 5-45 cm/s were measured by using gamma-ray computed tomography (CT). They used a bundle of the vertical internals (tubes) of 0.5-inch (1.27 cm) diameter that arranged non-uniformly in a hexagonal configuration with wall clearance. These tubes were designed to cover about 25% of the CSA of the column, similar to those employed in FT synthesis. Their experimental results showed that the overall and local gas holdups were similar in both columns without or with internals when the superficial gas velocities were calculated based on the free CSA for the flow inside the column while higher overall and local gas holdups obtained in the column equipped with internals and this column operated at a superficial gas velocity computed based on the total cross-sectional area CSA of the

column. In this case, the same volumetric flow was flowing through a smaller cross-sectional area of the gaps between the internals as compared with what occurs in the column without internals. They also stated that the time-averaged cross-sectional gas holdup distributions were symmetric (uniform) for the bubble column without internals for all studied superficial gas velocities, whereas bubble column packed with dense vertical internals based on the configuration used exhibited a symmetric (uniform distribution) gas holdup distribution at low superficial gas velocities and an asymmetric (non-uniform distribution) at high superficial gas velocities. Furthermore, they reported that the total and local gas holdup profiles for a bubble column without internals can be extrapolated to determine the gas holdup profile in a bubble column with internals, if the superficial gas velocities are computed based on the free CSA available for the flow of the phases provided that the symmetric cross-sectional gas holdup distributions and geometrical similarity be achieved. However, this study was limited to one size of rods (0.5-inch diameter) and these rods were inserted inside the bubble column in a hexagonal configuration with uneven clearances between the wall of the column and the bundle of vertical rods.

Thus, due to lack of knowledge of the gas holdup distributions in bubble column with internals this work focus on quantifying the influence of the presence of the vertical internals with different sizes on the time-averaged cross-sectional gas holdup distribution and their profiles at a range of superficial gas velocity that covers the bubbly and churn turbulent flow regimes using advanced gamma-ray computed tomography (CT) technique.

The experimental results and finding of this work along with previous studies on the subject will significantly enhance and enrich the fundamental understanding of the influence of the presence of dense and sparse vertical internals as well as their diameter on

the gas-liquid distribution in a bubble column equipped with a bundle of the heat exchanging tubes (internals). Computational fluid dynamics (CFD) simulation studies for bubble columns with vertical internals [55–59] are still limited in the literature due to these bubble columns with vertical internals involving a very complex interaction among phase and due to the lack of experimental data for CFD validation. Therefore, this study will provide benchmark data not only for future experimental investigations in this field, but also for evaluation, tuning, and validation of a three-dimensional (3D) computational fluid dynamics (CFD) simulations and hydrodynamics models for a bubble column equipped with a bundle of the vertical internals. This assessment and validation process of the CFD simulations are much needed due to the turbulent models, and the closures of interfacial forces that use in these simulations are based on empirical correlations. Once CFD simulations of bubble columns equipped with vertical internals for air-water system at different superficial gas velocities are validated, then one can use the validated CFD to assess industrial related conditions and to conduct sensitivity analysis with various input feed, different operating conditions, different configurations of vertical internals, and with different sizes of reactors.

Thus this will facilitate the design and scale up of these types of reactors. It is noteworthy that air-water system has been selected in this work to have the base of comparison with the bulk of the work in the literature, which used air-water system. The development of the 3D CFD simulations of the bubble columns packed with vertical internals is currently in progress in our Laboratory and will be reported in subsequent publications.

Table 1: Summary of experimental investigations on bubble columns equipped with vertical internals

Author	System	Dimension of column	Type of configuration and size of internals	Occluded cross-sectional area of column (%)	Operating conditions	Measurement techniques	Investigated parameters	Key findings
Yamashita,1987 [34]	air-water	I.D.=8.0 cm H= 350 cm I.D.=16 cm, H= 270 cm I.D.=31 cm, H= 300 cm	the arrangement of internals was not defined D=1.4,2.2,6 cm	not defined	1.66-66.3 cm/s 1.66-47.0 cm/s 0.883-35.3 cm/s at ambient and atmospheric pressure	manometric method	overall gas holdup	•The overall gas holdup increased with the number of tubes and the outer diameter of the pipe and rod. •The overall gas holdup did not depend on the vertical internal arrangements.
Saxena and Rao, 1992 [37]	air-water air-solid-water	I.D.= 30.5 cm H=325 cm	different hexagonal arrangements with 37,5,7 tubes D=1.9 cm	1.9% 2.7 % 14.3%	2 to 30 cm/s at (T=298,323 ,343 K) and atmospheric pressure	temperature- and pressure-measuring instruments	overall gas holdup	•The bubble coalescence decreased with an increasing number of internals. •The gas holdup was higher in the bubble column equipped with 37 tubes than those with 7 or 5 tubes.
Chen et al., 1999 [38]	air-water and air-drakeoil	I.D.=44 cm, H= 244 cm	circular D= 2.54 cm	5%	2, 5, and 10 cm/s at ambient and atmospheric pressure	computer automat radioactive particle tracking (CARPT) and computed tomography (CT) techniques	gas holdup profiles, liquid velocity, turbulent stresses and eddy diffusivities	•The gas holdup of the bubble column with internals was a little higher than in the column without internals. •The gas holdup for air-drake oil was lower than for the air-water system. •At the fully developed region, with high superficial gas velocity (10 cm/s), the gas holdup distribution was axisymmetric for the bubble column with or without internals for all investigated systems.

Table 1: Summary of experimental investigations on bubble columns equipped with vertical internals (cont.)

Author	System	Dimension of column	Type of configuration and size of internals	Occluded cross-sectional area of column (%)	Operating conditions	Measurement techniques	Investigated parameters	Key findings
Forret et al., 2003 [11]	air-water	I.D.=100 cm, H= 370 cm	internals arranged in a square pitch of 10.8 cm D= 6.3 cm	22%	15 cm/s at ambient and atmospheric pressure	pitot tube, standard tracer method based on conductivity	liquid velocity profile, axial dispersion	• The presence of internals led to enhanced liquid recirculation intensity and reduced the fluctuation of the liquid velocity. • The two-dimensional (2-D) axial dispersion model (ADM) was developed for a bubble column with internals.
Youssef and Al-Dahhan, 2009 [39]	air-water	I.D.=19 cm, H= 200 cm	hexagonal and circular D= 1.27 cm	5% 25%	3 to 20 cm/s at ambient and atmospheric pressure	4-point fiber optical probe	local gas holdup, interfacial area, bubble chord length, and bubble velocity	• The results showed an increase in the local gas holdup and the specific interfacial area but a decrease in the chord length and bubble velocity based on the insertion of vertical internals into the bubble column.
Balamurugan et al., 2010 [40]	air-water	I.D.=15cm, H= 125 cm	helical springs D=1,1.9,4 cm vertical internals D=1.9 cm	0.23%-0.84% 14.4%	3.6 to 54.2 cm/s at ambient and atmospheric pressure	manometer	overall gas holdup	• 135% of the increase in gas holdup was found in the bubble column equipped with vibrating helical spring internals compared to the column without internals.
Youssef et al., 2013 [41]	air-water	I.D.= 45 cm, H= 376 cm	hexagonal and circular D= 2.54 cm	5% 25%	5 to 45 cm/s at ambient and atmospheric pressure	4-point fiber optical probe	local gas holdup, interfacial area, bubble frequency, bubble chord length, and bubble velocity	• The overall and local gas holdup increased based on equipping the bubble column with intense internals. • A significant increase in the specific interfacial area was obtained at the wall region of the column.

Table 1: Summary of experimental investigations on bubble columns equipped with vertical internals (cont.)

Author	System	Dimension of column	Type of configuration and size of internals	Occluded cross-sectional area of column (%)	Operating conditions	Measurement techniques	Investigated parameters	Key findings
Jhawar and Prakash, 2014 [42]	air-water	I.D.=15 cm, H= 250 cm	circular tube bundles concentric baffle circular tube bundles with baffle	not defined	3 to 35 cm/s at ambient and atmospheric pressure	pressure transducers heat transfer probe	gas holdup, local liquid velocity, and bubble fractions holdups	•The internals design significantly affected the gas holdup and the heat transfer coefficients.
Guan et al., 2015 [43]	air-water	I.D.=80 cm, H= 500 cm	uniform and non-uniform hexagonal D= 2.5	9.2%	8 to 62 cm/s at ambient and atmospheric pressure	electrical resistivity probe and Pavlov tub	overall and local gas holdup, and liquid velocity	•The presence of the pin-tube internals led to an increase in the total holdup and significantly affected the local gas holdup and liquid velocity. •Pin-tube internals reduced the distributor region in the bubble column.
Kagumba and Al-Dahhan, 2015 [44]	air-water air-solid-water	I.D.=14 cm, H=183 cm I.D.=44 cm, H=366 cm	hexagonal and circular D= 1.27 & 2.54 cm	25%	3-45 cm/s at ambient and atmospheric pressure	4-point fiber optical probe	overall and local gas holdup, interfacial area, bubble velocity, bubble passage frequency, and bubble chord lengths	•The bubble column with 0.5-inch internals had a higher gas holdup, specific interfacial area, and bubble passage frequency than the column equipped with 1-inch internals and the column without internals. •During the churn turbulent flow regime, the internal diameter's effect on the gas holdup was insignificant

Table 1: Summary of experimental investigations on bubble columns equipped with vertical internals (cont.)

Author	System	Dimension of column	Type of configuration and size of internals	Occluded cross-sectional area of column (%)	Operating conditions	Measurement techniques	Investigated parameters	Key findings
Al-Mesfer et al., 2016 [17,91]	air-water	I.D.=14 cm, H=183 cm	hexagonal D= 1.27 cm	25%	5 to 45 cm/s at ambient and atmospheric pressure	γ-ray computed tomography (CT), radioactive particle tracking (RPT) techniques	gas holdup distribution, liquid velocity field, and turbulent parameter profiles	• The presence of vertical internals significantly increased the overall and local gas holdup by increasing the superficial gas velocity calculated based on the total CSA of the column. • During the churn turbulent flow regime, the overall and local gas holdup obtained in the column without internals could be extrapolated to find the gas holdup in the column with internals by operating at a superficial gas velocity calculated based on the free CSA available for the flow. • Cross-sectional gas holdup distributions were approximately symmetric for the bubble column without internals but asymmetric for the bubble column with internals at high superficial gas velocities.
Kalaga et al., 2017 [92]	air-water	I.D.=12 cm, H=120 cm	Column with only one central internal (3.6 cm O.D) internals arranged circularly in one bundle with one central internal	9% 11.7%	1.5 to 26.5 cm/s at ambient and atmospheric pressure	radioactive particle tracking (RPT) technique	Overall gas holdup liquid velocity field, and turbulent parameter profiles	• The magnitude of the axial liquid velocity and turbulent parameters achieved in bubble columns with and without vertical internals were found to increase with increasing superficial gas velocity. • The presence of internals has a significant impact on the axial liquid velocity. • It was found that increasing the percentage of the covered cross-sectional area of the column by the internals caused an increase in the axial fluctuation.

Table 1: Summary of experimental investigations on bubble columns equipped with vertical internals (cont.)

Author	System	Dimension of column	Type of configuration and size of internals	Occluded cross-sectional area of column (%)	Operating conditions	Measurement techniques	Investigated parameters	Key findings
Kalaga et al., 2017 [93]	air-water	I.D.=12 cm, H=120 cm	the vertical internals arranged in five circular configurations with different percentages of coverage cross-sectional area of the column by these vertical internal tubes.	0-63%	4.4 to 26.5 cm/s for superficial gas velocity while liquid velocity ranging from 0.5 to 14 cm/s at ambient and atmospheric pressure	radioactive particle tracking (RPT) radiotracer (RTD) techniques	Gas holdup distribution Axial liquid velocity Liquid phase mixing	• Hydrodynamics information in terms of gas holdup distribution, axial mean liquid velocity, and liquid phase mixing characteristics are found influenced significantly by the presence of vertical internals. • The percentage of coverage cross-sectional area of the column by vertical internals was remarkably affected the local fluctuating kinetic energy which causes an increase in the local liquid velocity and liquid mixing intensity. • The increase in the superficial gas velocity, superficial liquid velocity and percentage of covering the cross-sectional area of the column by vertical internals caused an increase in the axial liquid phase dispersion coefficient.

2. EXPERIMENTAL WORK

2.1. EXPERIMENTAL SETUP

A Plexiglas® bubble column with an inner diameter of 5.5-inches (0.14 m) and a height of 72-inches (1.83 m) using an air-water system has been employed in this study, as displayed schematically in Figure 1. In this work, the air (gas phase) was supplied from an oil-free industrial compressor (Ingersoll Rand Company). The air was passed through filters and introduced to pre-calibrated flow meters. The gas flow rate was regulated and measured using a pressure regulator and two calibrated flow meters (Brooks Instrument) with a different scale where they are connected in parallel to cover the wide range of selected superficial gas velocities (0.05-0.45 m/s), particularly bubbly and churn turbulent flow regimes. The air was continuously introduced from the bottom of the column through the plenum and stainless steel perforated plate distributor, with 121 holes of 1.32 mm diameter, arranged in a triangular pitch, with the total free area of 1.09%, as shown in Figure 2.

Purified water provided by a reverse osmosis water filtration system was used for the liquid phase, in batch mode, for all experiments. As mentioned earlier, the reasons for the selecting air-water system in this present study owes to its simplicity in the experimental work and the abundance of previous experimental works of this system for bubble column with and without vertical internals that will be facilitated the comparison with obtaining results. Besides those reasons, the most important one was to complement Kagumba [60], Kagumba and Al-Dahhan [44] and Jasim [61] studies, which were included measuring the bubble properties (specific interfacial area, axial bubble velocity, bubble

passage frequency, and bubble chord lengths) in the same system by using a 4-point fiber optical probe technique.

In the present work, the dynamic level of the bed was maintained at 62-inches (1.6 m) (L/D = 10.3) above the gas distributor by changing the initial static liquid level in accordance with the operating superficial gas velocity. An adhesive measuring tape was attached to the column to monitor both the static liquid and dynamic levels during the experiments. It is important to note that the dynamic level was adjusted by adding water during the run due to water loss caused by evaporation, especially at high superficial gas velocities, as the result of humidification and the long duration of the experiment for each CT scan.

In this investigation, two sizes of the vertical internals were used: 0.5-inch (0.0127 m) and 1-inch (0.0254 m) diameter Plexiglas® tubes. These tubes were arranged vertically and uniformly distributed inside the bubble column in a circular configuration, as shown in Figure 3. The 0.5-inch internals were organized in three bundles that were positioned at three dimensionless radial positions, r/R (0.8, 0.5, and 0.2), while the 1-inch internals were arranged in one bundle that was located at r/R = 0.65, with one tube at the center of the column. In each case, these bundles of the vertical internals were designed to cover approximately 25% of the total cross-sectional area of the column to represent the bundle of heat exchanging tubes that used in FT synthesis to remove the heat generated by its exothermic reaction. The internals were inserted and secured vertically in the column starting with a 3-inch clearance from the gas distributor and extending up to the top of the column by using three circular spacers/supports as well as the top plate to eliminate the vibration and make the vertical internals more stable, as seen in Figure 3.

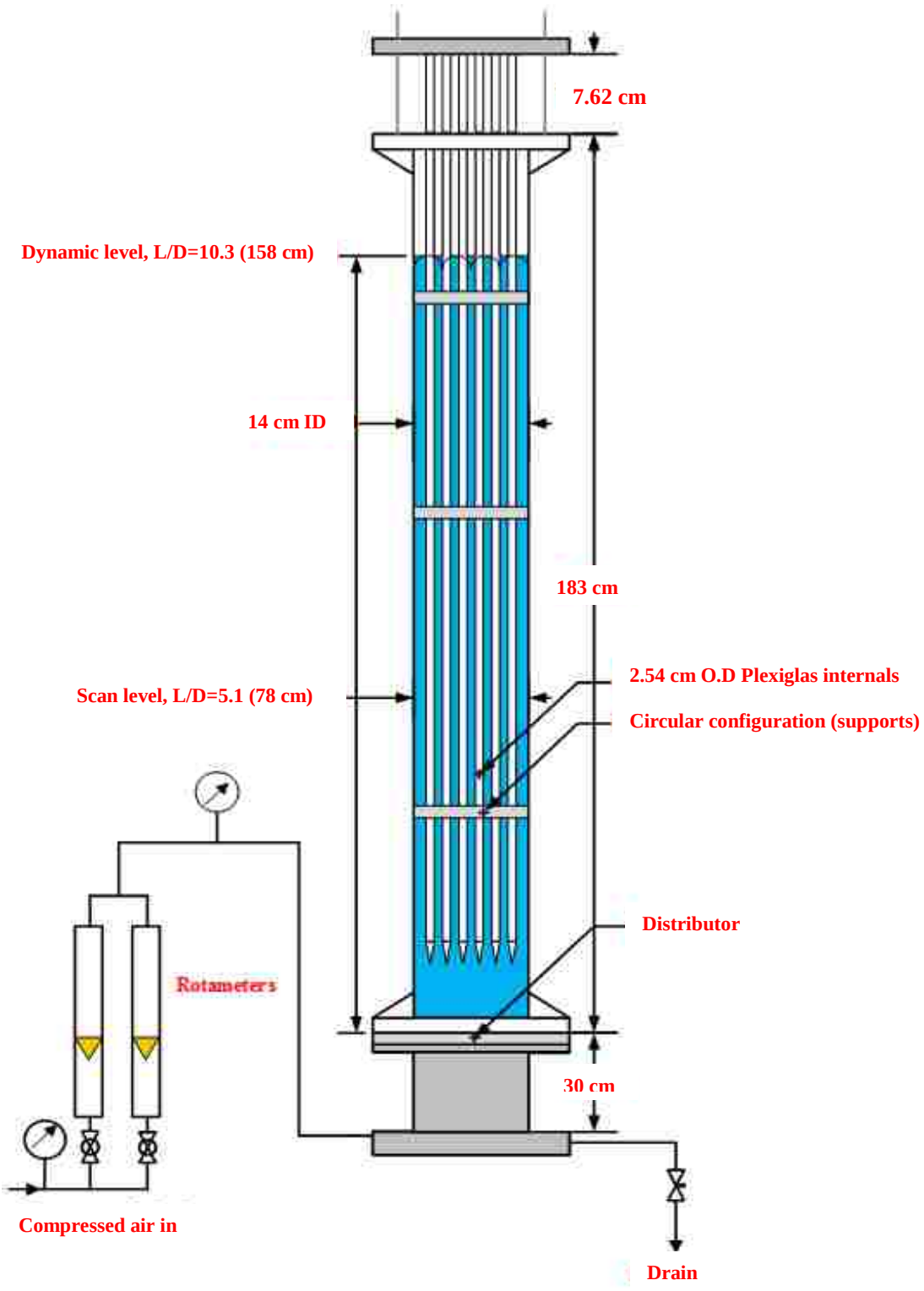

Figure 1: Schematic diagram of a bubble column equipped with vertical internals

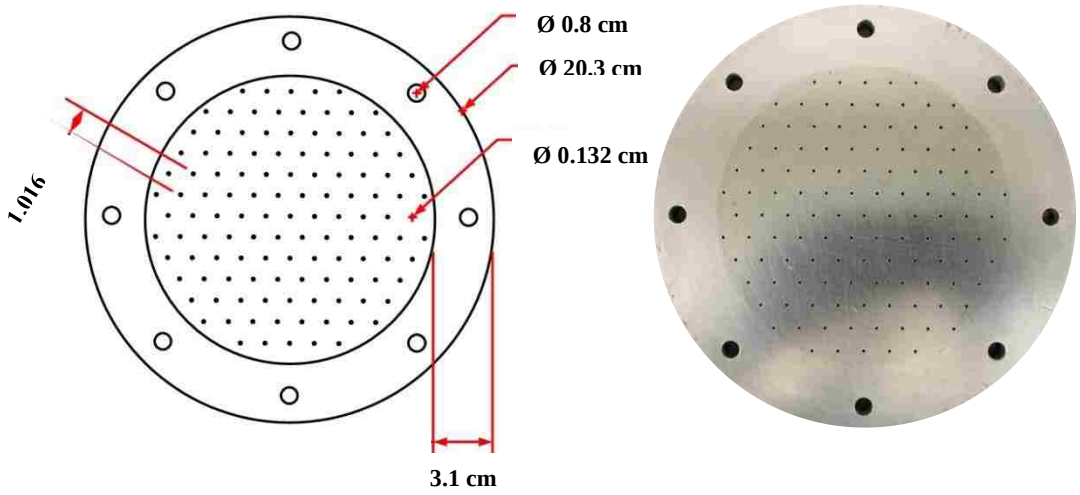

Figure 2: Schematic diagram and photo of the stainless-steel distributor (perforated plate)

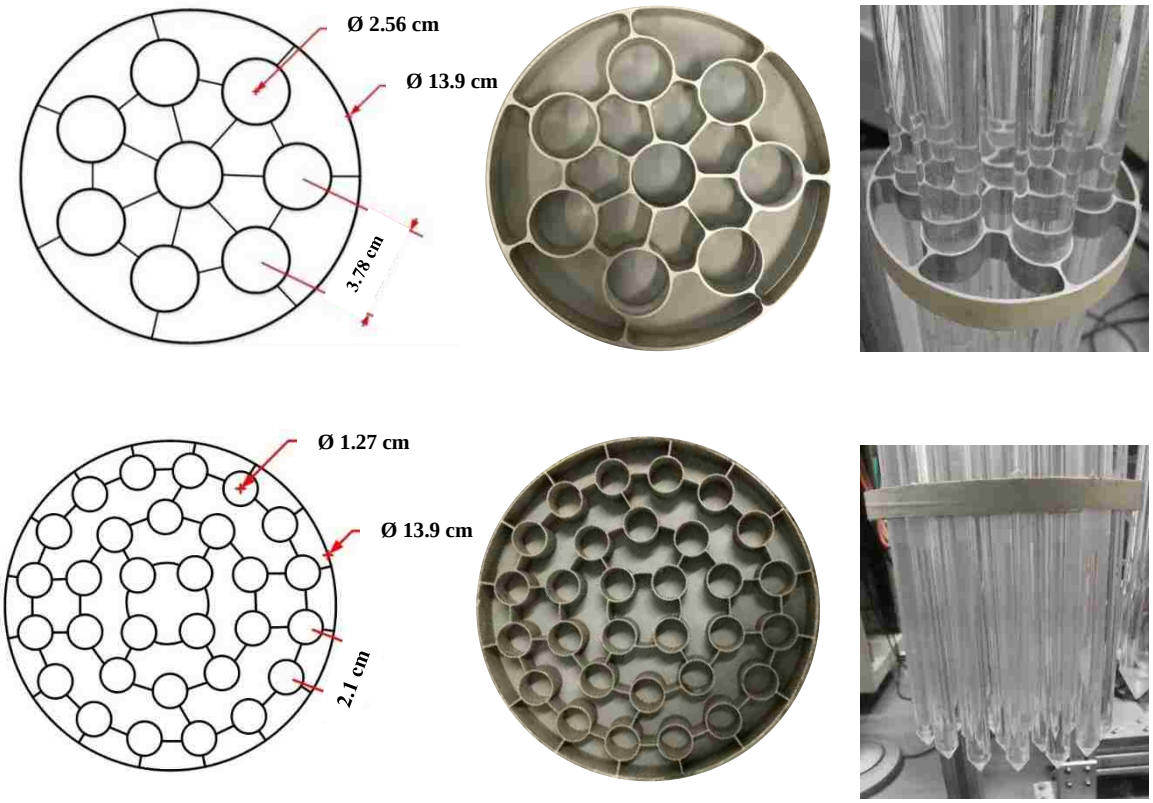

Figure 3: Schematic diagrams and pictures of the circular configurations (spacers/supports) for 0.5, and 1-inch internals

As mentioned earlier, the cooling tubes used in the FT synthesis are dense which covers 25% of the cross-sectional area of the column. Therefore, to establish dense internal tubes which represent FT synthesis, 0.5- inch vertical internals were used for the 6-inch column diameter. Additionally, to study the effect of internals size while keeping the same covering cross-sectional area and the same configuration of vertical internals, the 1-inch vertical internals were chosen where the number of tubes will be noticeably lower which gives rise to larger gaps between the vertical internals to demonstrate such effect. The bubble columns with or without vertical internals were well-balanced and centered in the middle of the gamma-ray computed tomography (CT) scanner, as seen in Figure 4. In addition, vertical and horizontal alignments were made for bubble columns to make sure the column was balanced. Furthermore, the bubble column was supported at the bottom and top by a rigid aluminum structure with a rubber piece to prevent any mechanical vibration during the operation that could affect the gas holdup measurements [62,63]. All experiments were carried out at room temperature and atmospheric pressure over a wide range of superficial gas velocities (0.05-0.45 m/s) based on the total CSA for the bubble column without vertical internals, while based on the free CSA for the flow in the case of the bubble column equipped with vertical internals. The free CSA for the flow is equal to:

$$(total\ cross\text{-}sectional\ area\ of\ the\ bubble\ column\ without\ vertical\ internals) - (cross\text{-}sectional\ area\ occupied\ by\ vertical\ internals)$$

The studied superficial gas velocities (5, 20, and 45 cm/s) were selected to have a velocity of 5 cm/s within the bubbly flow region [64], early churn turbulent of 20 cm/s, and deep in churn turbulent flow regime of 45 cm/s. The bubble columns with or without vertical internals were scanned in the fully developed region (L/D =5.1 above the gas

distributor). This axial level of the scan was chosen because the experimental results showed that the gas holdup profile remained relatively unchanged in this region [65]. Each CT scan was replicated twice to check for the reproducibility.

2.2. GAMMA-RAY COMPUTED TOMOGRAPHY (CT) TECHNIQUE

Our dual-source/energy gamma-ray computed tomography (DSCT) is an advanced non-invasive technique that provides qualitative and quantitative information about the time-averaged cross-sectional three phase distributions along the height of the reactor column when three phases that are dynamically moving [66]. However, for two-phase flow systems, a single source has been used.

At our laboratory (Multiphase Reactors Engineering and Application Laboratory, mReal) a single-source (Cs-137 (662 KeV)) gamma-ray computed tomography (CT) technique, which is part of the dual-source computed tomography (DSCT), was successfully used to measure the cross-sectional phase distributions and their radial profiles in a two-phase flow bubble column [45], pebble bed [67], fluidized bed [68–70], and spouted bed [71,72] at different operating conditions. The DSCT technique consists of two encapsulated sources, with initial activity ~ 250 mCi Cs-137 (half-life of about 37 years) and ~ 50 mCi Co-60 (half-life of about 5.24 years), which are well sealed and housed inside lead-shielded and tungsten, respectively containers as seen in Figure 4. In the present investigation, a single gamma-ray source (Cs-137) was used to investigate the time-averaged cross-sectional gas holdup distributions and their diameter profiles in the studied bubble columns with and without vertical internals. An arch created by 15 sodium iodide (NaI) scintillation detectors (2-inches (5 cm) in diameter) was positioned in front of each gamma-ray source as displayed in Figure 5. Both sources were collimated to provide a fan

beam with 40° in the horizontal plane and 5 mm height in the vertical plane. The detectors are also collimated with a lead collimator that has an open slit of dimension 2 mm × 5 mm to make sure lines (beams) passed through the detector's aperture and were recorded by the detectors. The collimator designs for both the gamma-ray sources and detectors were selected to acquire the highest number of counts with the minimum scattering effects [49].

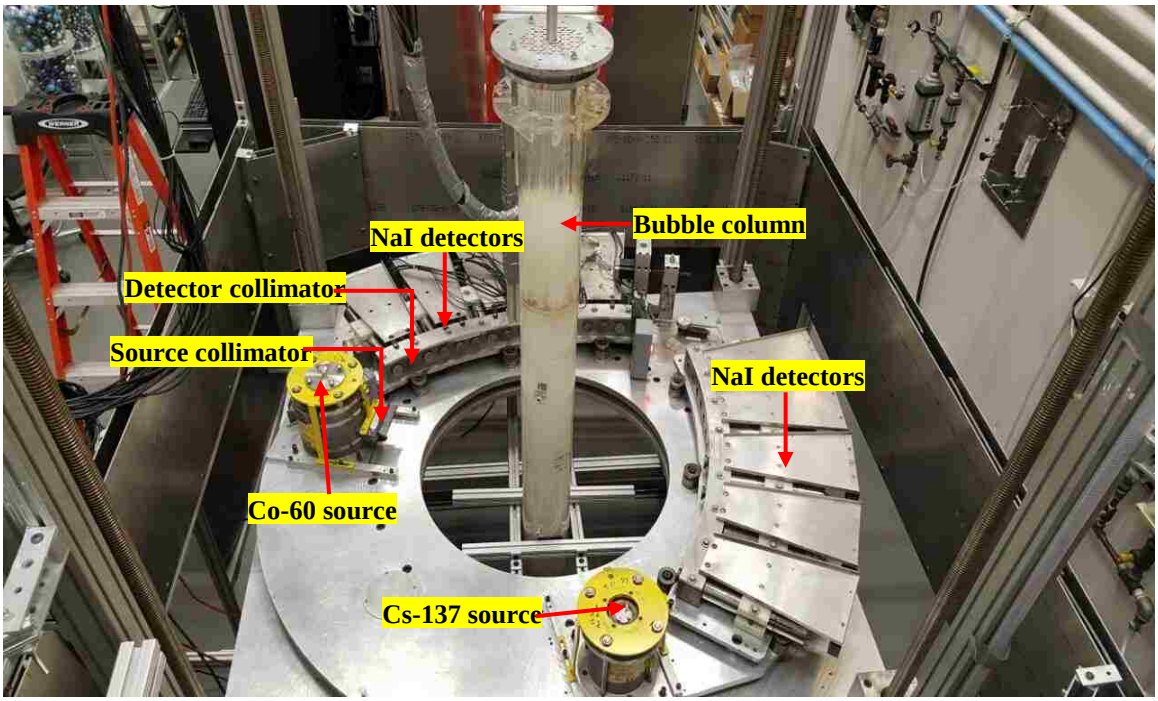

Figure 4: Dual source gamma ray computed tomography (CT) technique with a bubble column with internals

Together, the source and the detectors were placed on the rotatable, circular plate that was attached to the fixed square (base) plate by a circular rack and pinion. Both circular and square plates had 30-inch (0.762 m) circular open space, which designates to the reactor column being scanned. The square plate was connected to four threaded vertical rods that were joined at the top and bottom of the aluminum structure for the CT technique. On the lower part of each screwed rod, a pinion was located. These four pinions were linked

by a chain to the electric gear motor. When the electric motor is operated, the chain moves and rotates the threaded rods, which in turn moves the square plate upward or downward to allow the column to be scanned at different axial levels.

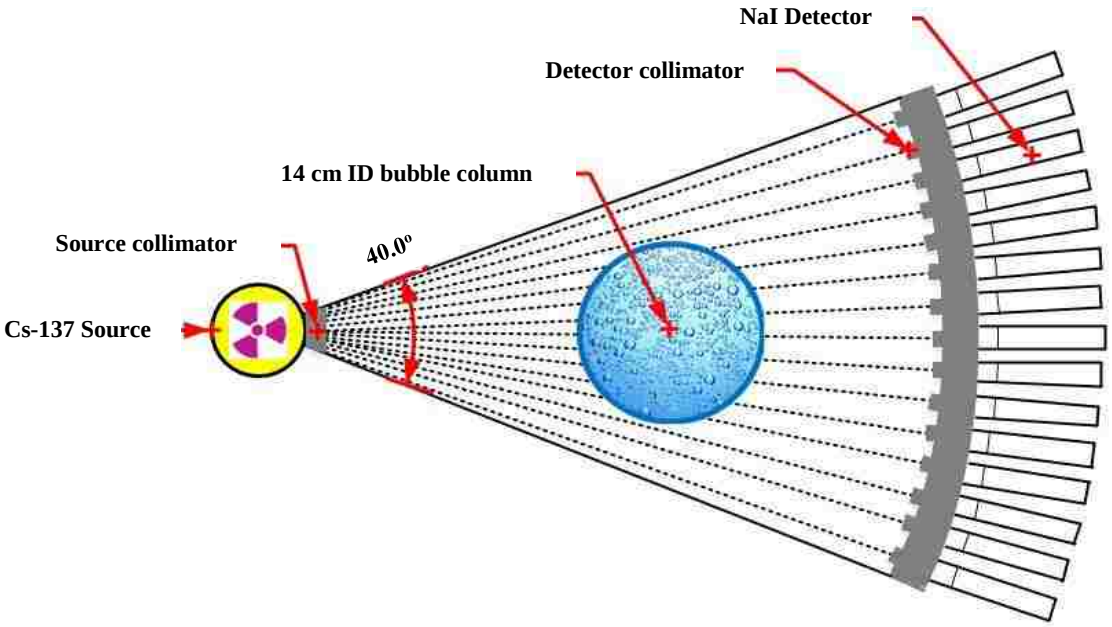

Figure 5: Schematic diagram of the Cs-137 source and configuration of the detectors

During CT scanning, the circular plate rotated around the studied column with a small angle (approximately 1.83°) per each rotation (view) by using the precise stepper motor. For each step on a rotating basis (one view), the array of detectors moved by using another stepper motor, with 21 steps and an angle of 0.13°, producing 315 detector positions (projections). Therefore, for full CT scans, there were 197 source positions (views) and 315 (21 × 15) projections. Hence, 62,055 (197 views × 315 projections) projections passed through the scanned object were recorded and used to calculate the transmission ratios, construct the sinograms, linear attenuation coefficient (μ, cm^{-1}) distribution, and gas holdup distribution images for the bubble columns with or without

vertical internals. In this study, the sampling rate for acquiring accounts was chosen to be 60 samples at 10 Hz, which took about 8.25 hours for a complete scan to achieve good statistics for the time-averaged gas holdup distributions.

Different scans for bubble columns with or without vertical internals, including empty columns, the column filled with water only, and the column under selected operating conditions (i.e., at the studied superficial gas velocity) were performed independently to obtain the cross-sectional distribution of the linear attenuation coefficients (μ, cm^{-1}) by applying alternating minimization (AM) algorithm, which was developed by O'Sullivan et al. [73] and implemented by Varma [66]. The AM algorithm is an iterative procedure that models the stochastic nature of gamma-rays and which uses the idea of the I-divergence introduced by Csiszar [74] to obtain a maximum-likelihood estimate. I-divergence represents the difference between the modeled transmission of photons by the Beer-Lambert's law and the measured transmission of gamma-rays through the studied domain. Therefore, the target of the AM algorithm is to find the value of the linear attenuation coefficient (μ, cm^{-1}) that minimizes the value of I-divergence. More details about the mathematical derivation and implementation of the AM algorithm for reconstructing images can be found elsewhere [66,73].

For image reconstruction, the domain of the studied bubble column cross section was divided into a resolution of 80×80 pixels and applied to all images that presented in this work. Therefore, each single pixel represents an area of 1.905 mm × 1.905 mm for 6-inch bubble columns with or without vertical internals. After the linear attenuation coefficient was reconstructed for an individual scan, the gas holdup distribution is calculated through a specific procedure that will be explained in the next section.

Furthermore, the line and azimuthal averaging are computed to represent the diameter profiles for the gas holdup. Before the CT scan begins, the bubble column is operated at a selected condition (i.e., the studied superficial gas velocity) for at least 20 minutes to allow the flow rate reading and the flow inside the column to reach a steady state. The moment that the selected operating conditions achieve a steady state, the CT scanner is turned on to scan the column at the selected axial level (L/D = 5.1). For radiation safety considerations, the CT technique is shielded with a lead on four sides to reduce and eliminate the radiation dose where the dose rate of one foot (0.3048 m) from the CT is less than 0.03 mR/hr. Hence, this CT technique is safe to use if all operational protocols are followed and applied. Note that these operations protocols were established and approved by the Department of Environmental Health and Safety at Missouri University Science and Technology. More details about the software and hardware used by the DSCT technique are available elsewhere Varma [75] and Varma et al. [66].

2.3. VALIDATION OF THE CT MEASUREMENTS

Two concentric cylinders of Plexiglas® were used as a phantom as illustrated in Figure 6 to validate our CT measurements. Both cylinders were glued onto the flat plate of Plexiglas®. The diameters of the inner and outer cylinders were 3 inches (0.0762 m) and 6 inches (0.1524 m), respectively. The Phantom was well centered and aligned in the middle of the CT technique as displayed in Figure 6. Individual scans have been performed for the phantom with different cases as follows:

- Case I: Empty Phantom
- Case II: The annular section was filled with water, whereas the inner section was empty

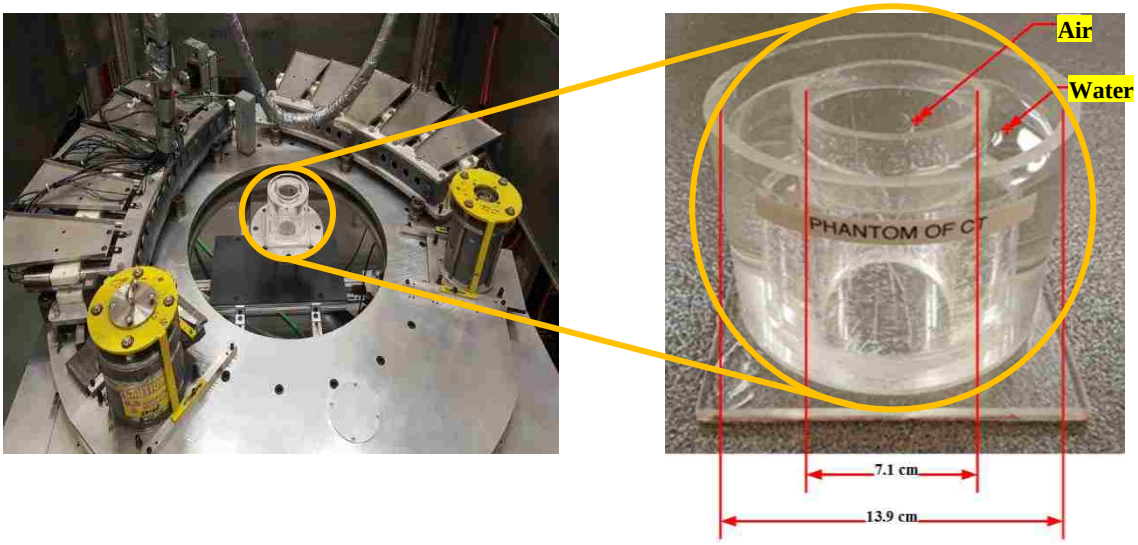

Figure 6: Dual-source gamma ray computed tomography (CT) technique with phantom

The following equation gives the transmission ratio [76,77]:

$$T = \frac{I}{I_\circ} = e^{-\rho\bar{\mu}l} \tag{1}$$

$$Ln\left(\frac{I}{I_\circ}\right) = -\rho\bar{\mu}l \tag{2}$$

$$Ln\left(\frac{I_\circ}{I}\right) = +\rho\bar{\mu}l \tag{3}$$

where (T) is the transmission ratio, $(I_\circ)$ is the initial intensity of the photons, (I) is the intensity of the photons transmitted across some distance l, ρ is density of medium (g/cm^3), $\bar{\mu}$ is the mass attenuation coefficient (cm^2/g), and l is the path length through the medium (cm). The measured quantity $Ln\left(\frac{I_\circ}{I}\right)$ is equal to the integral sum of the attenuation through the material along the beam path.

For the gamma-ray computed tomography technique, the attenuations are measured along a number of such beam paths through the bubble column from different

directions around it. Here, the transmission ratio and sinograms have been plotted for each scan to identify the artifacts in the beginning stage of performing the experiments and processing the data.

The x-axis of the transmission ratio plot represents the angular position of the projection in the fan beam, while the y-axis represents the transmission ratio (T), which is estimated from the incident count (no column between the source and its detectors) and the attenuated counts based on the materials used. Each pixel in the sinogram figures represents the transmission ratio for the corresponding projection number (y-axis) and the source position (view) (x-axis).

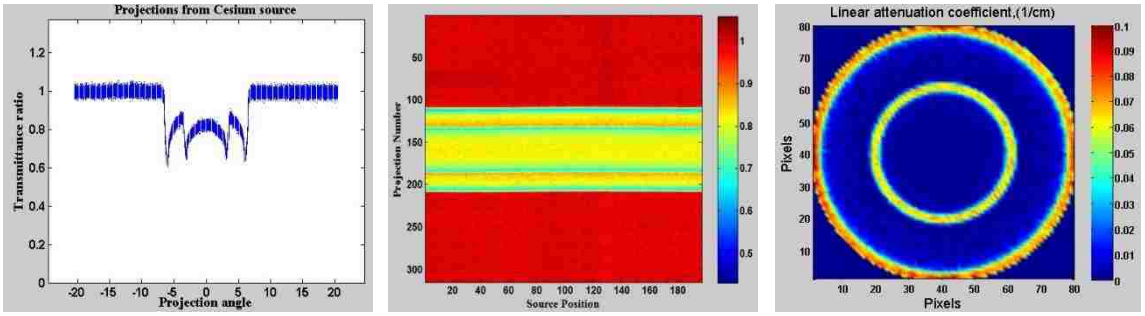

Transmission ratio **Sinogram** **Linear attenuation coefficient (cm^{-1})**

Figure 7: Transmission ratio, sinogram, and linear attenuation coefficient distribution for Case I

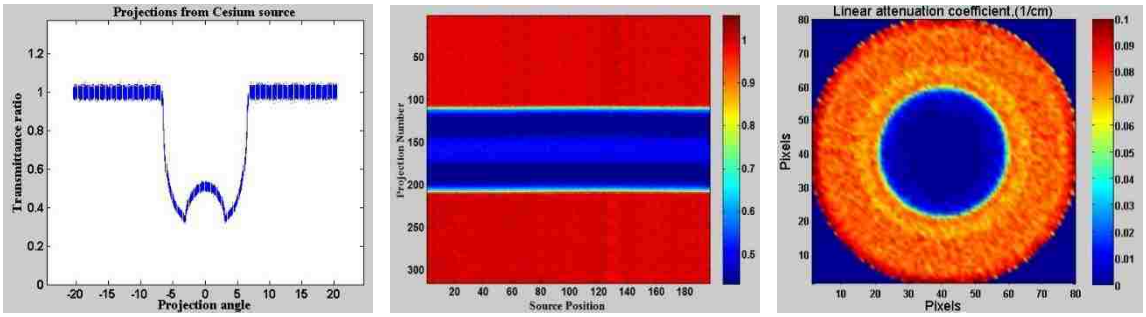

Transmission ratio **Sinogram** **Linear attenuation coefficient (cm^{-1})**

Figure 8: Transmission ratio, sinogram, and linear attenuation coefficient distribution for Case II

From Figure 7 and Figure 8 one can clearly distinguish the walls of the phantom for the cases I and II. Moreover, the transmission ratio figures appear smooth and, symmetric, with no detector artifacts. They confirm the quality of the measurement and the image reconstruction method.

Figure 7 and Figure 8 demonstrate the validation of CT measurements through scanning and reconstructing linear attenuation coefficient images for different cases of the phantom (see Figure 6). These figures show the linear attenuation coefficient distributions reconstructed by the AM algorithm for different cases of the phantom. In these figures, the dimensions and geometry of the phantom were reproduced by the scan, and the air-water were clearly distinguished. Also, the reconstructed linear attenuation coefficients for air, water, and Plexiglas® were compared with the theoretical linear attenuation coefficients of air (0.0001 cm^{-1}), water (0.0857 cm^{-1}), and Plexiglas® (0.0988 cm^{-1}), and they showed good agreement for all cases.

The figures demonstrate that the CT technique was capable of capturing the thickness of the inner and outer sections of the phantom. Furthermore, the linear attenuation images displayed in Figure 9, Figure 10, and Figure 11 clearly show that the CT technique was able to capture and reproduce the arrangement and location of each of the vertical internals as well as of the column wall.

These images confirm the quality of this CT technique and also the image reconstruction algorithm (AM). This means that the CT is capable of capturing a small maldistribution in the multiphase reactor if it exists.

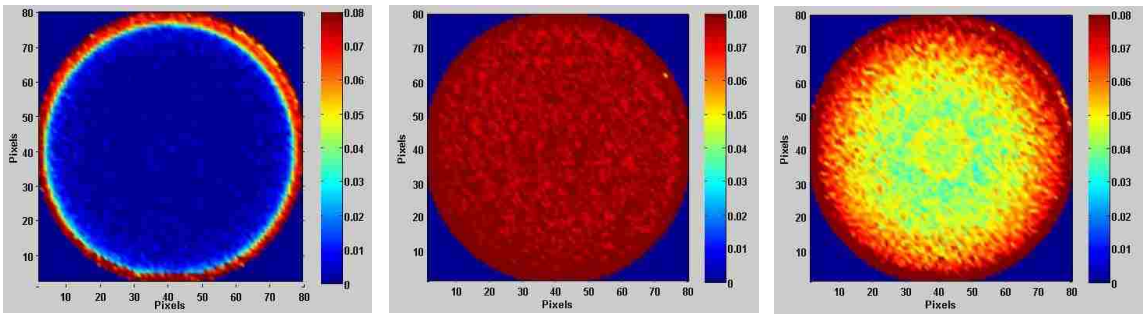

(a) **(b)** **(c)**

Figure 9: Linear attenuation coefficient distribution for a bubble column without internals: (a) empty column, (b) column filled with water, and (c) column with air-water at superficial gas velocity 45 cm/s

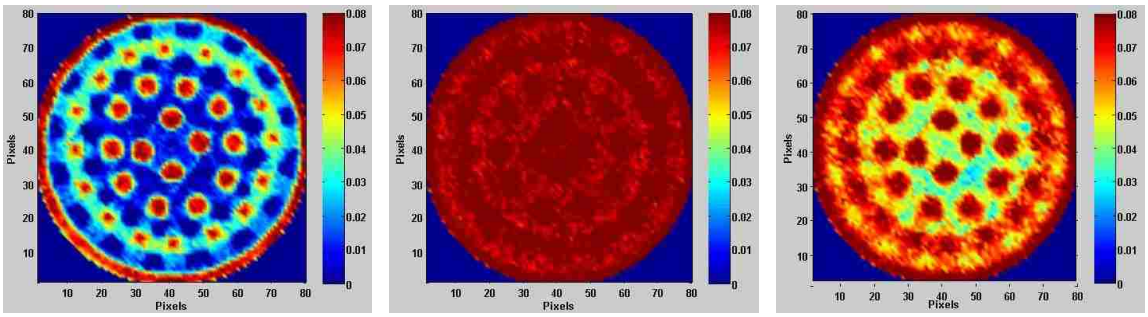

(a) **(b)** **(c)**

Figure 10: Linear attenuation coefficient distribution for a bubble column equipped with 0.5-inch internals: (a) empty column, (b) column filled with water, and (c) column with air-water at superficial gas velocity 45 cm/s

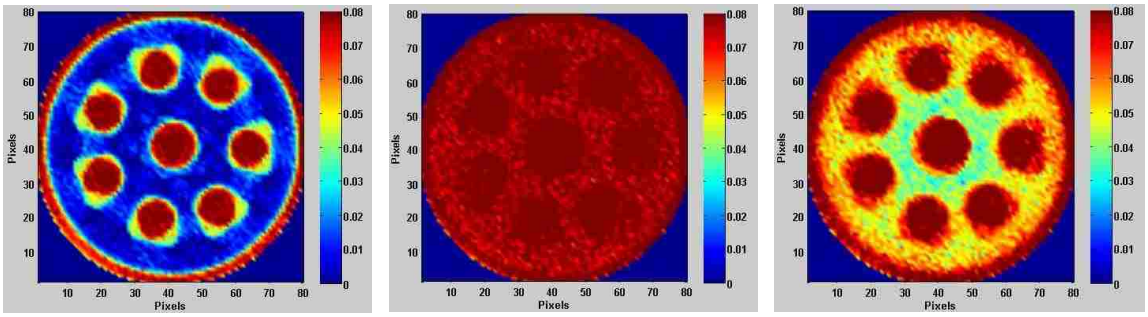

(a) **(b)** **(c)**

Figure 11: Linear attenuation coefficient distribution for a bubble column equipped with 1.0-inch internals: (a) empty column, (b) column filled with water, and (c) column with air-water at superficial gas velocity 45 cm/s

2.4. GAS HOLDUP ESTIMATION

2.4.1. Gas Holdup Estimation for a Bubble Column without Vertical Internals (Two-Phase System). For a two-phase bubble column without vertical internals (air-water) operating at any superficial gas velocity, the total attenuation in each pixel can be written as [78]

$$A_{g-l,ij} = \left(\rho_g \bar{\mu}_g l_g + \rho_l \bar{\mu}_l l_l\right)_{ij} \tag{4}$$

Since $l_g = \varepsilon_{g,ij} L_{ij}, and\ l_l = \varepsilon_{l,ij} L_{ij}, where\ L_{ij} = \left(l_g + l_l\right)_{ij}$

Eq. (4) becomes

$$A_{g-l,ij} = \rho_g \bar{\mu}_g \varepsilon_{g,ij} L_{ij} + \rho_l \bar{\mu}_l \varepsilon_{l,ij} L_{ij} \tag{5}$$

Since $\varepsilon_g + \varepsilon_l = 1$, Eq. (5) can be written as:

$$A_{g-l,ij} = \rho_g \bar{\mu}_g \varepsilon_{g,ij} L_{ij} + \rho_l \bar{\mu}_l (1 - \varepsilon_{g,ij}) L_{ij} \tag{6}$$

$$A_{g-l,ij} = \rho_g \bar{\mu}_g \varepsilon_{g,ij} L_{ij} + \rho_l \bar{\mu}_l L_{ij} - \rho_l \bar{\mu}_l L_{ij} \varepsilon_{g,ij} \tag{7}$$

For a bubble column filled with water only (single phase), the attenuation in each pixel can be written as

$$A_{l,ij} = \rho_l \bar{\mu}_l \varepsilon_{l,ij} L_{ij} = \rho_l \bar{\mu}_l L_{ij}\ , where\ \varepsilon_{l,ij} = 1 \tag{8}$$

By substituting Eq. (8) into Eq. (7), the following is obtained:

$$A_{g-l,ij} = \rho_g \bar{\mu}_g \varepsilon_{g,ij} L_{ij} + A_{l,ij} - A_{l,ij} \varepsilon_{g,ij} \tag{9}$$

Since

$$\rho_{air}, \mu_{air}(0.0012\ \ g/cm^3\ , 0.0001\ cm^{-1}) \ll\ \rho_{water}, \mu_{water}(0.997\ \ g/cm^3\ , 0.086\ cm^{-1})$$

The attenuation caused by the gas phase (air) is negligible. This is a general simplification that also applies to the FT synthesis reaction mixture where the attenuation

caused by the mixture of gases (CO and H_2) is still negligible compared to the liquid phase and catalyst (slurry) solid. Therefore, Eq. (9) becomes:

$$A_{g-l,ij} = A_{l,ij} - A_{l,ij}\varepsilon_{g,ij} \tag{10}$$

$$\varepsilon_{g,ij} = 1 - \frac{A_{g-l,ij}}{A_{l,ij}} \tag{11}$$

Since

$$A_{g-l,ij} = \rho_{g-l,ij}\bar{\mu}_{g-l,ij}L_{ij} = \mu_{g-l,ij}L_{ij}$$

$$A_{l,ij} = \rho_{l,ij}\bar{\mu}_{l,ij}L_{ij} = \mu_{l,ij}L_{ij}$$

Eq. (11) becomes

$$\varepsilon_{g,ij} = 1 - \frac{A_{g-l,ij}}{A_{l,ij}} = 1 - \frac{\mu_{g-l,ij}\,L_{ij}}{\mu_{l,ij}\,L_{ij}} = 1 - \frac{\mu_{g-l,ij}}{\mu_{l,ij}} \tag{12}$$

Also, the liquid holdup can be estimated directly from the following equation:

$$\varepsilon_{l,ij} = 1 - \varepsilon_{g,ij} \tag{13}$$

where $\varepsilon_{g,ij}$ is the gas holdup in each pixel, $\mu_{g-l,ij}$ is the linear attenuation of the gas-liquid in each pixel (cm^{-1}), $\mu_{l,ij}$ is the linear attenuation of the liquid in each pixel (cm^{-1}) which was obtained by scanning the column filled with liquid only, and L_{ij} is the length along which a particular gamma ray beam passes through this pixel.

According to the above equations, the time–averaged cross-sectional gas holdup distribution in bubble column without internals was obtained by applying the following scanning steps:

- Performing a scan without the column, which was considered a reference scan ($I_\circ$)

- Conducting a scan of the column filled with water only to get (I_l) and then calculating the transmission ratio (counts of the column filled with water/reference counts) to determine $A_{l,ij}$.
- Scanning the column with gas-liquid (in operation) $\left(I_{g-l}\right)$ at the desired conditions and then computing the transmission ratio (counts of the column gas-liquid/reference counts) to determine $A_{g-l,ij}$.

Applying the alternating minimization (AM) algorithm for each transmission $\left(I_{g-l}\right)$ and (I_l) individually, produces the linear attenuation coefficients for gas-liquid $\mu_{g-l,ij}$ and liquid $\mu_{l,ij}$ respectively. Finally, the local gas and liquid holdup can be directly calculated using Eqs. (12) and (13).

2.4.2. Gas Holdup Estimation for a Bubble Column with Vertical Internals (Three-Phase System). Determining the cross-sectional gas holdup distribution for three phases that are moving dynamically requires a dual gamma-ray. However, in this study for the bubble column with vertical internal (solid) (air-solid-liquid), one gamma-ray source is adequate to quantify the gas holdup because the vertical internals (solid) are stationary. Hence, for the bubble column with vertical internals (air-solid-liquid) operated at any superficial gas velocity, the total attenuation in each pixel can be written as

$$A_{g-l-s,ij} = \left(\rho_g \bar{\mu}_g l_g + \rho_l \bar{\mu}_l l_l + \rho_s \bar{\mu}_s l_s\right)_{ij} \tag{14}$$

Since $l_g = \varepsilon_{g,ij} L_{ij},\ l_l = \varepsilon_{l,ij} L_{ij},\ l_s = \varepsilon_{s,ij} L_{ij}$ $where\ L_{ij} = l_g + l_l + l_s$

Eq. (14) becomes

$$A_{g-l-s,ij} = \rho_g \bar{\mu}_g \varepsilon_{g,ij} L_{ij} + \rho_l \bar{\mu}_l \varepsilon_{l,ij} L_{ij} + \rho_s \bar{\mu}_s \varepsilon_{s,ij} L_{ij} \tag{15}$$

Since $\varepsilon_g + \varepsilon_l + \varepsilon_s = 1$, Eq. (15) can be written as

$$A_{g-l-s,ij} = \rho_g \bar{\mu}_g \varepsilon_{g,ij} L_{ij} + \rho_l \bar{\mu}_l L_{ij}(1 - \varepsilon_{g,ij} - \varepsilon_{s,ij}) + \rho_s \bar{\mu}_s \varepsilon_{s,ij} L_{ij} \quad (16)$$

Since $\rho_{air}, \mu_{air}(0.0012\ g/cm^3, 0.0001\ cm^{-1}) \ll$

$\rho_{\text{Plexiglas®}}, \mu_{\text{Plexiglas®}}\ (1.18\ g/cm^3, 0.098\ cm^{-1})$

$and\ \rho_{water}, \mu_{water}(0.997\ g/cm^3, 0.086\ cm^{-1}$. Therefore, the attenuation caused by the gas phase (air) is negligible. Hence, Eq. (16) becomes

$$A_{g-l-s,ij} = \rho_l \bar{\mu}_l L_{ij}(1 - \varepsilon_{g,ij} - \varepsilon_{s,ij}) + \rho_s \bar{\mu}_s \varepsilon_{s,ij} L_{ij} \quad (17)$$

Since $A_{l,ij} = \rho_l \bar{\mu}_l \varepsilon_{l,ij} L_{ij} = \rho_l \bar{\mu}_l L_{ij}\ , where\ \varepsilon_{l,ij} = 1$, for a bubble column without internals filled water only, Eq. (17) becomes

$$A_{g-l-s,ij} = A_{l,ij} - A_{l,ij}\varepsilon_{g,ij} - A_{l,ij}\varepsilon_{s,ij} + \rho_s \bar{\mu}_s \varepsilon_{s,ij} L_{ij} \quad (18)$$

For scanning bubble column with vertical internals (air-solid) only, the total attenuation in each pixel can be written as

$$A_{g-s,ij} = \rho_g \bar{\mu}_g \varepsilon_{g,ij} L_{ij} + \rho_s \bar{\mu}_s \varepsilon_{s,ij} L_{ij} \quad (19)$$

Since $\varepsilon_g + \varepsilon_s = 1$, Eq. (19) can be written as

$$A_{g-s,ij} = \rho_g \bar{\mu}_g (1 - \varepsilon_{s,ij}) L_{ij} + \rho_s \bar{\mu}_s \varepsilon_{s,ij} L_{ij} \quad (20)$$

Since $\rho_g, \mu_g \ll \rho_s, \mu_s$, the attenuation caused by the gas phase (air) is negligible therefore, $\rho_g \bar{\mu}_g (1 - \varepsilon_{s,ij}) L_{ij} \cong 0$. Eq. (20) becomes

$$A_{g-s,ij} = \rho_s \bar{\mu}_s \varepsilon_{s,ij} L_{ij} \quad (21)$$

For scanning column with vertical internals filled water (liquid-solid), the total attenuation in each pixel can be written as

$$A_{l-s,ij} = \rho_l \bar{\mu}_l \varepsilon_{l,ij} L_{ij} + \rho_s \bar{\mu}_s \varepsilon_{s,ij} L_{ij} \quad (22)$$

Since $\varepsilon_l + \varepsilon_s = 1$, Eq. (22) can be written as

$$A_{l-s,ij} = \rho_l \bar{\mu}_l L_{ij}(1 - \varepsilon_{s,ij}) + \rho_s \bar{\mu}_s \varepsilon_{s,ij} L_{ij} \quad (23)$$

Recall that $A_{l,ij} = \rho_l \bar{\mu}_l \varepsilon_{l,ij} L_{ij} = \rho_l \bar{\mu}_l L_{ij}$, $where\ \varepsilon_{l,ij} = 1$, for a bubble column without internals filled water only. Therefore, Eq. (23) becomes

$$A_{l-s,ij} = A_{l,ij} - A_{l,ij}\varepsilon_{s,ij} + \rho_s \bar{\mu}_s \varepsilon_{s,ij} L_{ij} \quad (24)$$

By further simplification, Eq. (24) becomes

$$\rho_s \bar{\mu}_s \varepsilon_{s,ij} L_{ij} = A_{l-s,ij} - A_{l,ij} + A_{l,ij}\varepsilon_{s,ij} \quad (25)$$

By substituting Eq. (25) into Eq. (18) results in

$$A_{g-l-s,ij} = A_{l,ij} - A_{l,ij}\varepsilon_{g,ij} - A_{l,ij}\varepsilon_{s,ij} + A_{l-s,ij} - A_{l,ij} + A_{l,ij}\varepsilon_{s,ij} \quad (26)$$

By canceling the similar terms from the above equation, the above equation becomes

$$\varepsilon_{g,ij} = \frac{A_{l-s,ij} - A_{g-l-s,ij}}{A_{l,ij}} \quad (27)$$

Eq. (27) becomes

since $A_{l-s,ij} = \rho_{l-s,ij} \bar{\mu}_{l-s,ij} L_{ij} = \mu_{l-s,ij} L_{ij}$

$$A_{g-l-s,ij} = \rho_{g-l-s,ij} \bar{\mu}_{g-l-s,ij} L_{ij} = \mu_{g-l-s,ij} L_{ij}$$

$$A_{l,ij} = \rho_{l,ij} \bar{\mu}_{l,ij} L_{ij} = \mu_{l,ij} L_{ij}$$

$$\varepsilon_{g,ij} = \frac{A_{l-s,ij} - A_{g-l-s,ij}}{A_{l,ij}} = \frac{\rho_{l-s,ij} \bar{\mu}_{l-s,ij} L_{ij} - \rho_{g-l-s,ij}\, \bar{\mu}_{g-l-s,ij}\, L_{ij}}{\rho_{l,ij} \bar{\mu}_{l,ij} L_{ij}}$$

$$= \frac{(\mu_{l-s,ij} - \mu_{g-l-s,ij}) L_{ij}}{\mu_{l,ij}\, L_{ij}} = \frac{(\mu_{l-s,ij} - \mu_{g-l-s,ij})}{\mu_{l,ij}}$$

$$\varepsilon_{g,ij} = \frac{\mu_{l-s,ij} - \mu_{g-l-s,ij}}{\mu_{l,ij}} \quad (28)$$

where $\varepsilon_{g,ij}$ is the local gas holdup in each pixel for a bubble column with vertical internals, $\mu_{l-s,ij}$ is the linear attenuation of liquid-solid only in each pixel (cm^{-1}), $\mu_{g-l-s,ij}$ is the linear attenuation of gas-liquid-solid (column under operating at any superficial gas

velocity) in each pixel (cm^{-1}), and $\mu_{l,ij}$ is linear attenuation of liquid only in each pixel (cm^{-1}). The time–averaged cross-sectional gas holdup distribution in a bubble column equipped with vertical internals was obtained by applying the following procedure:

- Performing a scan without the column as a reference scan ($I_\circ$).
- Conducting a scan for the column without internals filled with water only to get (I_l) and then calculating the transmission ratio ($I_l/I_\circ$) to determine $A_{l,ij}$.
- Scanning the column with vertical internals and filled with water $(I_{l,s})$ and then finding the transmission ratio ($I_{l,s}/I_\circ$) to calculate $A_{l-s,ij}$.
- Scanning the column with vertical internals operated at the studied superficial gas velocity $(I_{g,l,s})$ and then finding the transmission ratio ($I_{g,l,s}/I_\circ$) to calculate $A_{g-l-s,ij}$.

Using the alternating minimization (AM) algorithm for each transmission independently produces the linear attenuation coefficients for the liquid-solid $\mu_{l-s,ij}$, gas-liquid-solid $\mu_{g-l-s,ij}$, and liquid $\mu_{l,ij}$, respectively. Finally, the local gas holdup can be directly estimated using Eq. (28).

3. RESULTS AND DISCUSSION

Our advanced gamma-ray computed tomography (CT) technique was used in this present investigation to visualize and quantify the effect of the existence of the vertical internals and their sizes on the gas-liquid distribution in a 6-inch Plexiglas bubble column for the air-water cold flow system at different superficial gas velocities. All CT scans were performed in a fully developed flow region (L/D = 5.1). Two different sizes of the vertical internals were used, which were arranged in a circular-like shape for both sizes. In the

following subsections, the unprecedented results of the impact of the presence of dense and sparse vertical internals, internals diameters, and superficial gas velocity on the overall, local gas holdup distributions, and their diametrical profiles were analyzed, discussed, and presented in more details.

3.1. REPRODUCIBILITY OF THE CT MEASUREMENTS

For demonstrating the reproducibility of the CT scans, the measurements of the time-averaged cross-sectional gas holdup distribution and its diametrical profile in a bubble column were replicated. These replications were carried out in a 6-inch bubble column without vertical internals that operated under a superficial gas velocity of 20 cm/s. The CT scans were repeated at one axial level of 78 cm (L/D = 5.1) above the gas distributor, which represents the fully developed flow region.

The reconstructed cross-sectional gas holdup distributions for both experiments that are presented in Figure 12a and b show that the local gas holdup distribution for both scans (experiments 1 and 2) are similar. Moreover, the azimuthally averaged of the gas holdup diametrical profiles were computed from the cross-sectional gas holdup images by circumferential averaging the pixels to quantify the difference between the gas holdup profiles. It is evident from Figure 12c that the gas holdup profiles for both experiments are almost identical and similar in the magnitude for most diameter positions of the bubble column. For example, the percentage of relative differences in the gas holdup values for the two repeated experiments at the region close to the center (where the difference is high) is 3.3%.

These obtained results either for the reconstructed cross-sectional gas holdup distributions or diametrical profiles confirm the excellent reproducibility that was achieved

with the CT measurements. It is obvious that, there is no need to replicate CT scan for each operating condition. Despite that, in this present study, the CT scan was repeated twice for each operating condition to reduce the measurement error and check the reproducibility of gas holdup data. Therefore, the average of these two measurements was used to present the diametrical gas holdup profiles. Furthermore, the error bars were calculated and plotted for all gas holdup profiles that presented in this work.

As another independent method to check the accuracy of the gas holdup data obtained by our CT technique, the overall gas holdup obtained by bed expansion method at the same operating condition was compared with the average of the cross-sectional gas holdup obtained by CT technique. The cross-sectional mean gas holdup ($\overline{\varepsilon_g}$) was calculated from gas holdup distribution image by first azimuthally averaging and then performing another averaging by using the following equation:

$$\overline{\varepsilon_g} = \frac{2}{R^2}\int_0^R \varepsilon(r) r dr \tag{29}$$

The above equation was solved numerically by using Simpson's rule where R represents the radius of the bubble column and $\varepsilon(r)$ represents the values of a gas holdup at a specific radius (r). The percentage of relative difference between the mean of the cross-sectional gas holdup and the overall gas holdup was found to be 3.7%, which confirms the high accuracy and the reliability of the CT technique.

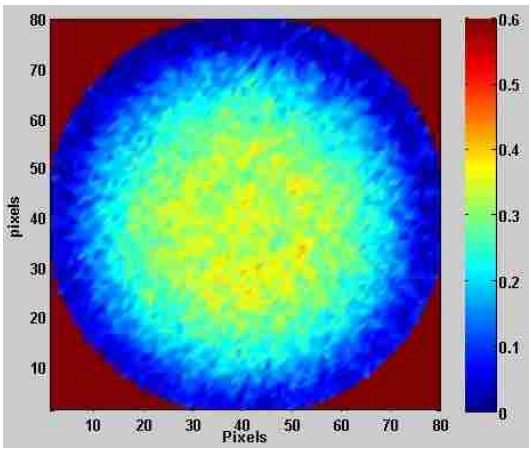

a) Time-averaged gas holdup distribution of experiment #1 in 6-inch bubble column without internal operated at superficial gas velocity of 20 cm/s

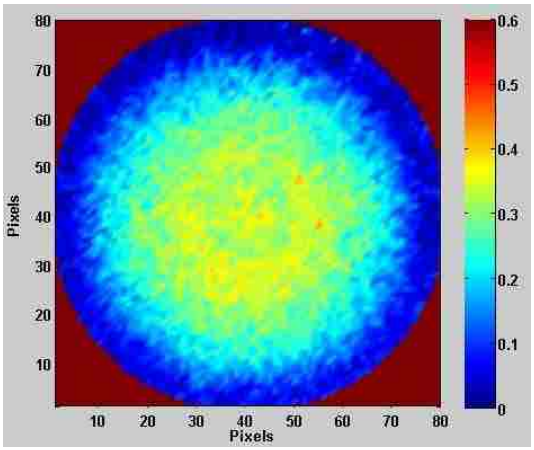

b) Time-averaged gas holdup distribution of experiment #2 in 6-inch bubble column without internal operated at superficial gas velocity of 20 cm/s

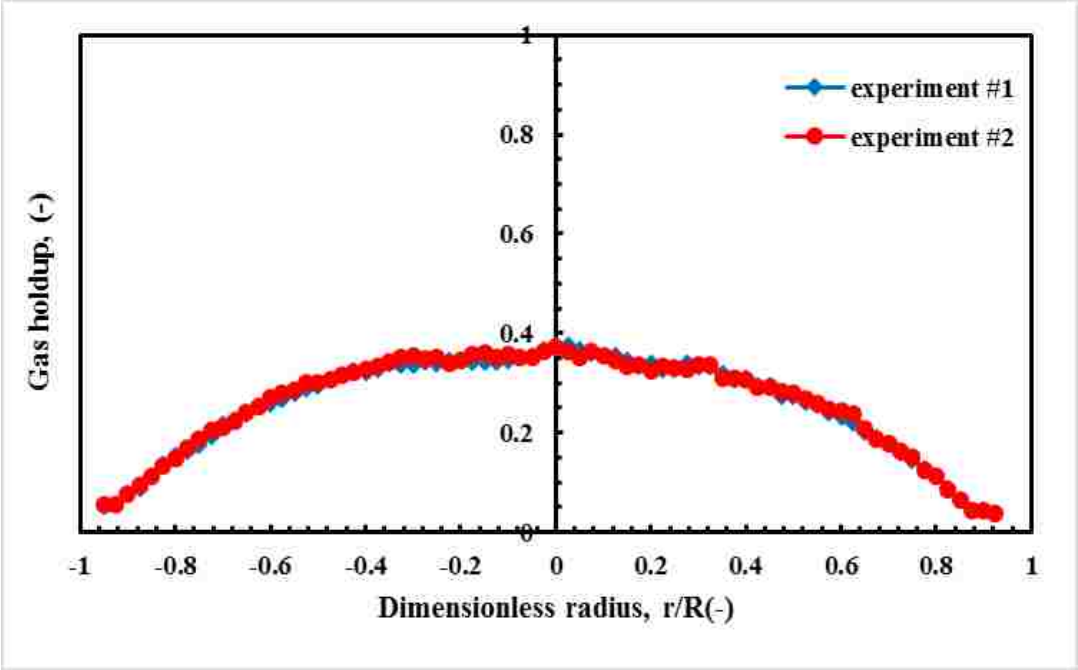

c) Azimuthally averaged of gas holdup profiles in 6-inch bubble column without vertical internals operated at superficial gas velocity of 20 cm/s

Figure 12: Reproducibility of the time-averaged cross-sectional gas holdup distributions and their diametrical profiles in 6-inch bubble column without vertical internals operated at superficial gas velocity of 20 cm/s

3.2. EFFECT OF THE PRESENCE OF VERTICAL INTERNALS AND THEIR SIZE ON THE OVERALL GAS HOLDUP

To demonstrate the impact of the presence of dense and sparse vertical internals as well as their size on the overall gas holdup, a method of the bed expansion (change in the bed height between dynamic and static) was used to quantify the overall gas holdup in a 6-inch Plexiglas bubble columns with and without vertical internals based on following the equation:

$$overall\ gas\ holdup = \frac{height\ of\ dynamic\ bed - height\ of\ static\ liquid}{height\ of\ dynamic\ bed} \quad (30)$$

The dynamic levels of the bed for all experiments were maintained at 62-inches (1.6 m) (L/D = 10.3) above the gas distributor by changing the initial static liquid levels corresponding to each operating superficial gas velocity. An adhesive measuring tape was attached to the column and used to visually monitor both the static liquid and dynamic levels during the experiments. Figure 13 depicts the effects of the presence of the vertical internals and their size as well as the superficial gas velocity on the overall gas holdup in bubble columns in the presence and absence of the vertical internals for the air-water system. Figure 13 shows a convergence in the values of the overall gas holdup obtained in the bubble column with 0.5 or 1-inch internals. This convergence between the values of the gas holdup can be explained by using almost the same free CSA for the flow, which was used to calculate superficial gas velocities where for both cases (with 0.5 or 1-inch internals) the bundle of vertical internals almost blocked 25% of the column cross-sectional area and hence the same superficial gas velocity was applied for both cases that lead to obtaining almost the same magnitude of the gas holdup. Furthermore, the values of the overall gas holdup obtained in bubble column in the absence of vertical internals were

achieved in bubble column equipped with 0.5 and 1-inch internals operated at a superficial gas velocity calculated based on free CSA for the flow. These results and findings of overall gas holdup are in line with the previously reported investigation for the air-water system [60,61,79].

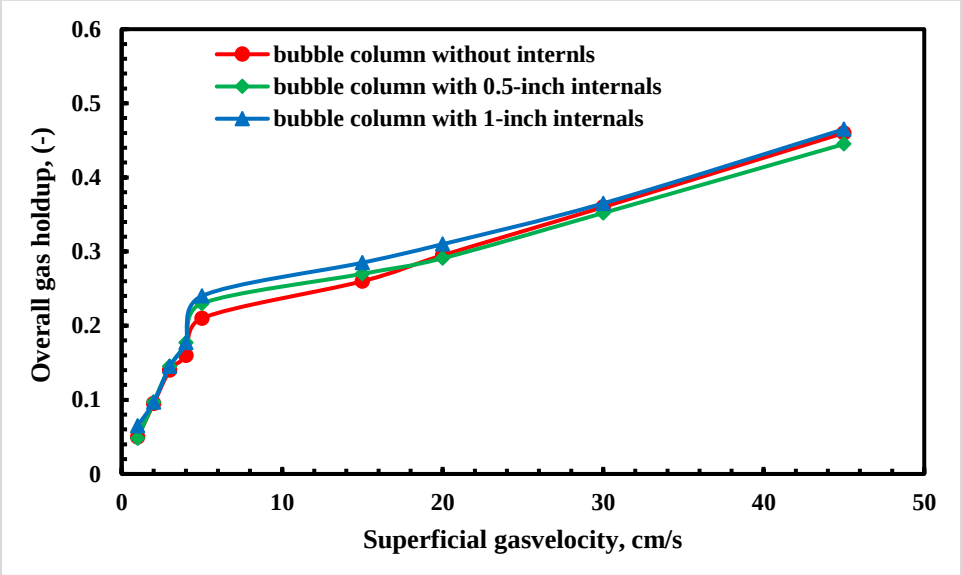

Figure 13: Effect of the vertical internals and their size on the overall gas holdup in 6-inch bubble column operated at different superficial gas velocities

3.3. EFFECT OF SUPERFICIAL GAS VELOCITY ON THE TIME-AVERAGED CROSS-SECTIONAL GAS HOLDUP DISTRIBUTION AND THEIR DIAMETRICAL PROFILES

The time-averaged gas holdup reconstructed CT images for the bubble columns with and without vertical internals are displayed in Figure 14. These images show the local gas holdup for each pixel, where each single pixel represents an area of 1.905 mm × 1.905 mm of a 6-inch (0.14 m) bubble column. The color bar in each image represents the range of gas holdup, where red indicates high gas holdup and blue signifies low gas holdup (high liquid holdup). The obtained two-dimensional scanned images visualize qualitatively how

the gas and liquid phases are distributed inside the bubble columns in the presence or not of the vertical internals at different operating conditions. As can be seen from the 2D images in Figure 14, the magnitude of the gas holdup rises with increases in the superficial gas velocities for bubble columns either with or without vertical internals. In addition, the well-known phenomena in a bubble column without obstacles (higher gas holdup in the core of the column and lower in the wall region) still obtains in the bubble column equipped with dense internals for both sizes of internals. However, based on the visualization of gas-liquid distributions for bubble columns with and without vertical internals at different superficial gas velocities, the bubble column with 1-inch vertical internals exhibits the common core-annulus (ascending of liquid in the center and liquid descending on wall region) liquid circulation very similar to the one obtained in the bubble column without vertical internals.

Additionally, the gas holdup distribution images further revealed that the higher gas holdup was achieved in the core region of bubble columns without vertical internals while the lowest gas holdup was obtained in the wall region because of the high shear stress (i.e., typically maximum at the wall of the column) in this region [17]. Such effect of shear stress induces the bubbles to move and breakup into smaller bubbles in the core of the column, which is characterized by less shear stress. Accordingly, these small bubbles rise with low velocity, causing an increase in the residence time for these bubbles and hence increasing the gas holdup magnitude in the center of the column. However, for bubble columns with vertical internals, the maximum gas holdup values are obtained in the center gaps between the vertical internals because the bubbles in this area are suffering from extra wall shear, which is generated by the walls of these vertical internal tubes. This wall shear of the

vertical internals forces the bubbles to move from the area of the vicinity of vertical internals toward the center of the space (i.e., gaps of internals). Consequently, the rising bubbles (i.e., bubbles confined in the gaps of vertical internals) are subject to more resistance to flow, especially under a high superficial gas velocity, causing slowly rising bubbles through these gaps and hence resulting high gas holdup in these regions (i.e., center of the gaps) and low in the vicinity of the vertical internals.

This phenomenon of increasing gas holdups in the gaps of vertical internals has been confirmed recently by the CFD simulation [58,59,80] for these bubble columns with vertical internals under the same operating conditions. Moreover, upon observing of each image, it is evident that all images exhibit a symmetric gas holdup distribution for all ranges of superficial gas velocities. However, the bubble column with 1-inch internals (sparse arrangement) gives a more symmetric distribution than the column equipped with 0.5-inch internals (dense arrangement). Furthermore, the most remarkable observation of the scanned images is that a bubble column equipped with 0.5-inch internals that arranged uniformly in a circular configuration can significantly reduce the maldistribution (asymmetrical distribution) that obtained in a bubble column equipped with 0.5-inch internals arranged non-uniformly in a hexagonal arrangement (Al-Mesfer et al. [45] and Al-Mesfer [79]), especially when using a high superficial gas velocity.

From the perspective of the industrial process, the performance of the bubble/slurry bubble columns will be enhanced significantly by reducing the maldistribution (non-uniform gas-liquid distribution) because it decreases the magnitude of the specific interfacial area and consequently decreases the mass transfer between phases. Moreover, the maldistribution increases the liquid back-mixing as well as the possibility of the

formation of hot and dead zones and eventually leads to a runaway of the reactor, in particular during exothermic reactions [81,82].

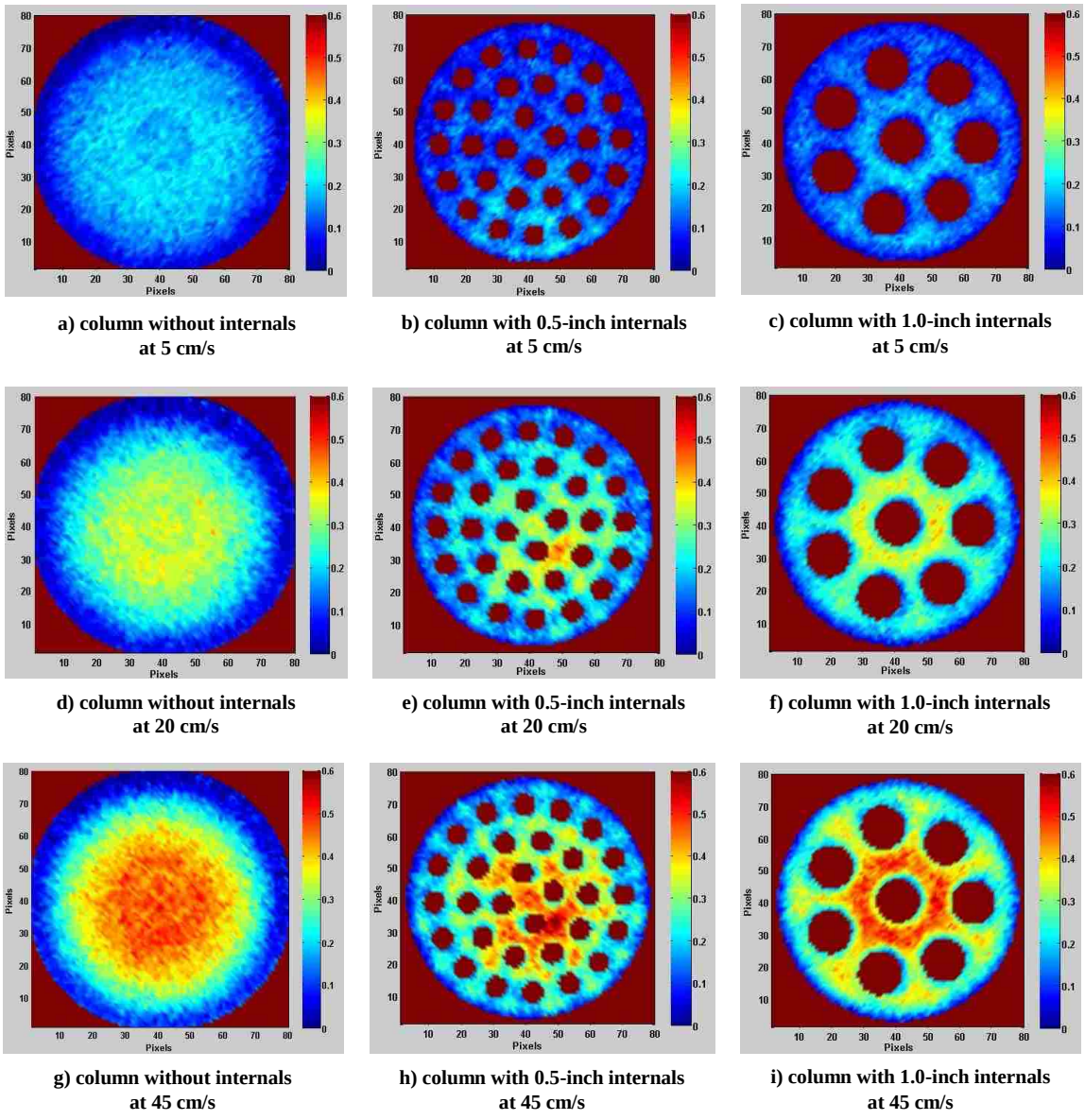

a) column without internals at 5 cm/s

b) column with 0.5-inch internals at 5 cm/s

c) column with 1.0-inch internals at 5 cm/s

d) column without internals at 20 cm/s

e) column with 0.5-inch internals at 20 cm/s

f) column with 1.0-inch internals at 20 cm/s

g) column without internals at 45 cm/s

h) column with 0.5-inch internals at 45 cm/s

i) column with 1.0-inch internals at 45 cm/s

Figure 14: Time-averaged cross-sectional gas holdup distributions for a bubble column with or without internals at different superficial gas velocities (5, 20, and 45 cm/s) based on the free cross-sectional area (CSA) for the flow

The obtained gas holdup distributions for a bubble column without vertical internals for air-water system scanned by the CT technique were qualitatively consistent with the gas holdup distribution reported by Chen et al. [38], Rados et al. [83], Shaikh [31], and Al-Mesfer et al. [45] for the same air-water system.

As mentioned earlier, the CT technique has been capable of capturing the configurations of the internal bundles and their positions inside the column for all CT scans. Hence, the CT technique can not only be used to provide knowledge about the phase distribution and consequently the performance of the reactor, but it can also be used as a diagnostic tool for identifying integrity issues with internals.

To provide quantifiable and easy to understand the results, further processing is needed for the time-averaged cross-sectional gas holdup distributions to obtain azimuthally, and line averaged gas holdup profiles as well as the local gas holdup in each pixel of the CT scan image. For each of the azimuthally averaged gas holdup profiles, the values of the gas holdup for the vertical internals before the averaging process were excluded so that not to affect the calculated average with the outlier's data. Moreover, to determine the azimuthally averaged profiles, a method was developed to divide the reconstructed image (80 × 80 pixels) in half (left and right; 40 × 40 pixels) and then average them separately not to smooth it out and to achieve a more precise representation of the results. Furthermore, the error bars were plotted for all figures in this work to quantify the reliability and reproducibility of the CT measurements, which represent one standard deviation from the average gas holdup at every radial position. The calculated error bars were very slight as shown in all presented figures. More details about the approach of excluding the vertical internals from gas holdup distribution and their azimuthally averaged

can be found elsewhere [84].The results of the azimuthally averaged gas holdup profiles for bubble columns without, with 0.5-inch, and 1.0-inch internals at different superficial gas velocities are exhibited in Figure 15, Figure 16 and Figure 17. Like a bubble column without obstacles, the magnitude of the gas holdup for a bubble column with vertical internals increased as the superficial gas velocity increased. These figures further reveal that the shape of the gas holdup profile is parabolic for the bubble column without vertical internals, while, the column with vertical internals displayed wavy line profiles. Additionally, each concave curvature in the gas holdup profile, whether for bubble columns equipped with 0.5-inch or 1.0-inch internals represents the azimuthally averaged values of the gas holdup among the gaps between internals for the same bundle. The different curvatures in the gas holdup profiles can be explained by the following factors: the internal bundle arrangement, gaps among the vertical internals, and the size of the vertical internals. For example, the bubble column equipped with 0.5-inch internals produced wavy line profiles with a small concave curvature, while the bubble column with 1.0-inch internals produced a larger concave curvature. Furthermore, Figure 16 and Figure 17 illustrate that the number and degree of concavity in the gas holdup profiles indicates the number of bundles and size of internals inside the bubble columns. For instance, the 0.5-inch internal configuration consisted of three bundles of internals; thus, the radial profile had three small concave sections for each side. In contrast, the radial profile of the 1-inch internals had one large concave area and one area that was half concave in the center due to the 1.0-inch internals configuration being composed of one bundle and one internal in the center. The same wavy line gas holdup profiles were reported by Al-Mesfer et al. [45] for a bubble column equipped with a 0.5-inch dense internals.

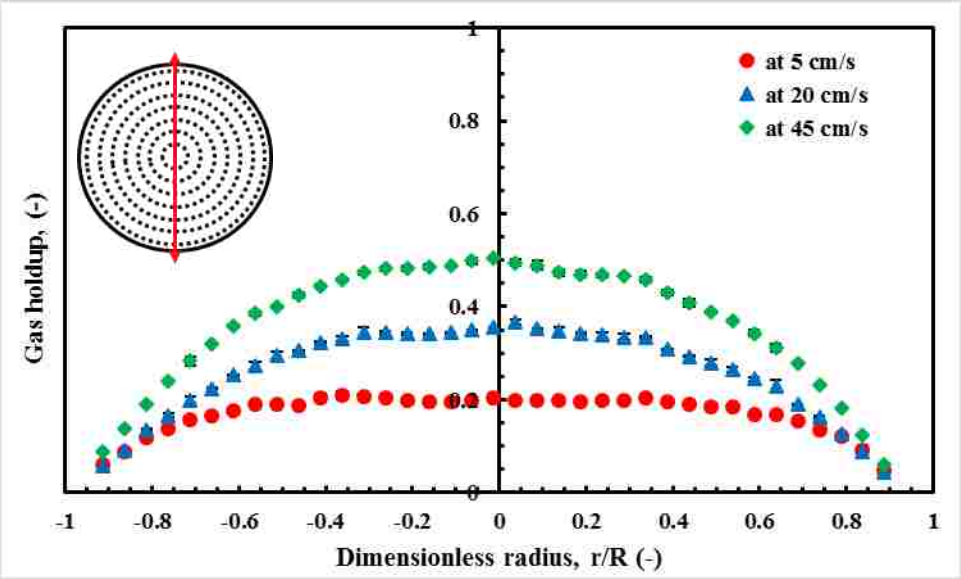

Figure 15: Time and azimuthally averaged gas holdup profiles in a bubble column without internals at different superficial gas velocities based on the free cross-sectional area (CSA) for the flow

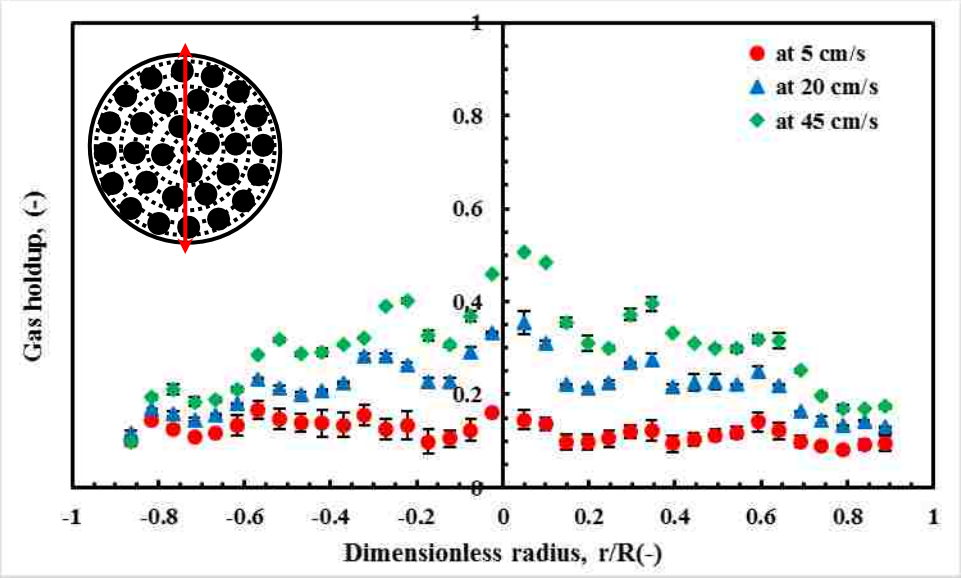

Figure 16: Time and azimuthally averaged gas holdup profiles in a bubble column equipped with 0.5-inch internals at different superficial gas velocities based on the free cross-sectional area (CSA) for the flow

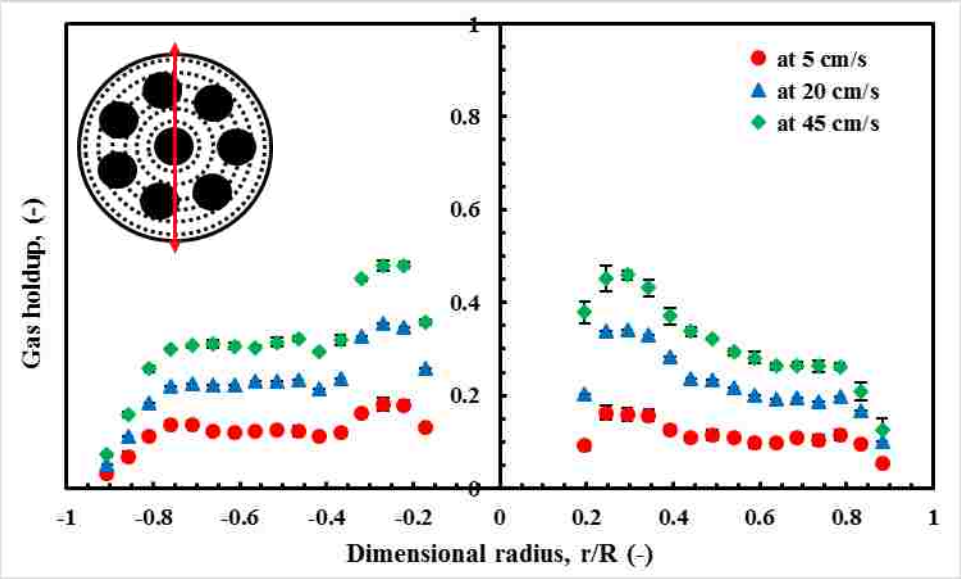

Figure 17: Time and azimuthally averaged of gas holdup profiles in a bubble column equipped with 1.0-inch internals at different superficial gas velocities based on the free cross-sectional area (CSA) for the flow

3.4. THE IMPACT OF THE VERTICAL INTERNAL DIAMETERS ON THE GAS HOLDUP PROFILES AT DIFFERENT SUPERFICIAL GAS VELOCITIES

Figure 18, Figure 19, and Figure 20 present the comparison of the azimuthally averaged of the gas holdup diametrical profiles the total CSAe columns with or without vertical internals at different superficial gas velocities, which were calculated based on total CSA for bubble column without vertical internals while were computed based on free CSA for bubble column equipped with vertical internals (0.5 and 1-inch internals). According to these figures, the bubble column equipped with 1.0-inch internals produced a higher gas holdup than the bubble column with 0.5-inch internals at the region between r/R = 0.25-0.45 and the region between r/R = 0.7-0.9 for different superficial gas velocities. Also, the gas holdup values of the bubble column with 1.0-inch internals approach the values of the gas holdup for the column without vertical internals in the region r/R = 0.25-0.4. However, at the churn turbulent flow regime (at a superficial gas of 20, and 45 cm/s),

a significant increase in the gas holdup values was obtained in the bubble column equipped with 1.0-inch internals at the wall region as compared with the bubble columns without or with 0.5-inch internals. The variation in the figures for the gas holdup profiles due to the presence more vertical internals for 0.5-inch internals (30 of vertical internals) than 1-inch internals (8 of vertical internals).

Quantitatively, at a superficial gas velocity of 45 cm/s, the gas holdup value increased by 52% for the bubble column with the 1-inch internal bundle at the wall region (r/R = 0.8) when compared with the bubble column without internals, while it increased by 39% when compared with the bubble column equipped with 0.5-inch internals. During the churn turbulent flow regime (heterogeneous flow), the presence of dense vertical internals in the bubble column enhanced the bubble breakup, and bubble passage frequency [85]. As a result, a significant number of small bubbles will be formed in the column with vertical internals.

This phenomenon was also confirmed by a recent study conducted in our mReal lab that measured the bubble properties, such as specific interfacial area, bubble rise velocity, bubble passage frequency, and bubble chord lengths by using a four-point fiber optical probe on the same column for the air-water system [47]. The availability of a significant number of tiny bubbles in the column leads to an increase in the gas holdup magnitude due to the small bubbles having a low bubble rise velocity (high drag force), and this leads to an increase in the residence time of gas (bubbles) as compared with large bubbles, which have a higher bubble rise velocity (less drag force).

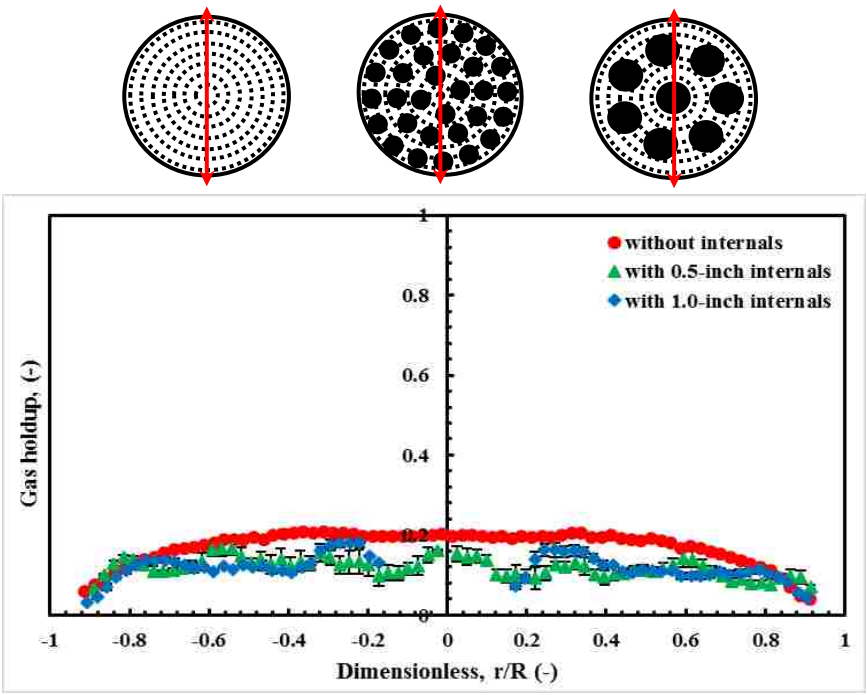

Figure 18: Comparison between the azimuthally averaged gas holdup profiles for bubble columns with or without internals at superficial gas velocity (5 cm/s) based on the free cross-sectional area (CSA)

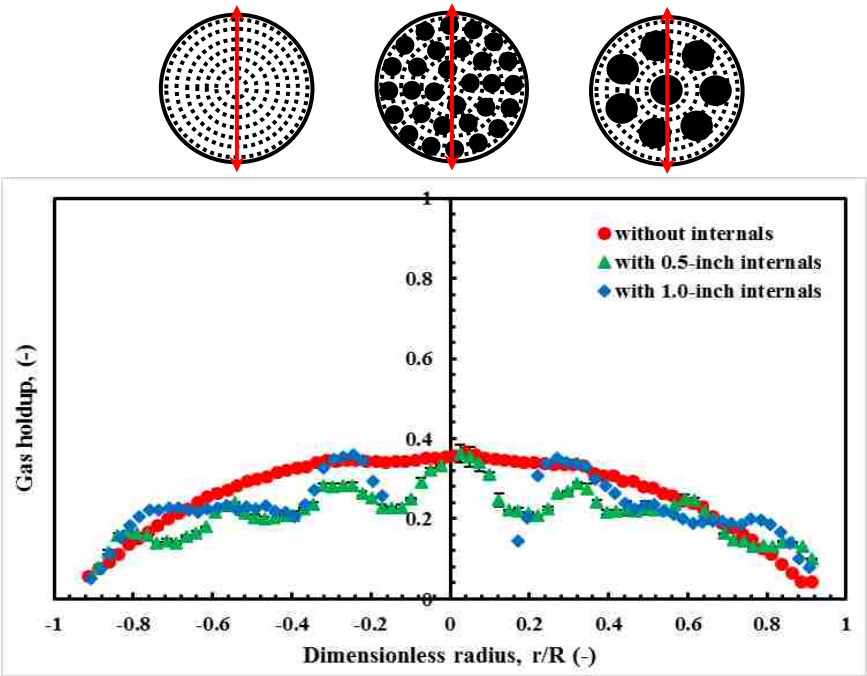

Figure 19: Comparison between the azimuthally averaged gas holdup profiles for bubble columns with or without internals at superficial gas velocity (20 cm/s) based on the free cross-sectional area (CSA)

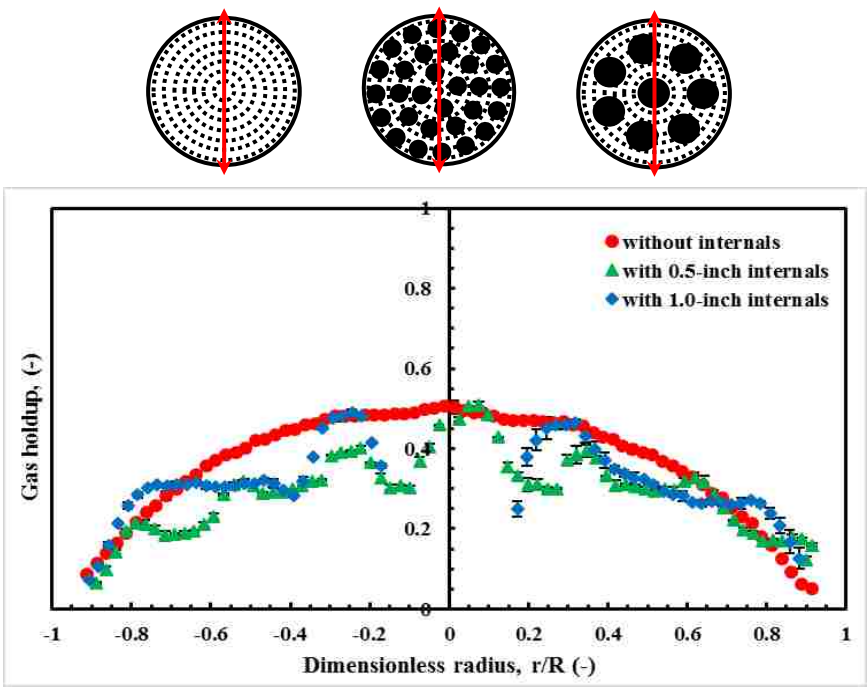

Figure 20: Comparison between the azimuthally averaged gas holdup profiles for bubble columns with or without internals at superficial gas velocity (45 cm/s) based on the free cross-sectional area (CSA) for the flow

However, it is evident from the presented figures that the gas holdup values obtained in bubble column packed densely with vertical internals reaches the values of the gas holdup in the core region of bubble column without vertical internals while displaying a considerable increase near the wall region of the column. This might be explained by the fact that at a high superficial gas velocity (churn turbulent flow regime) bubbles do not only move axially with varying bubble rise velocities but also radially (perpendicular to the flow) toward the wall region due to the effect of interfacial forces, such as lift and dispersion forces. These forces depend mainly on bubble size; and hence, for a bubble column equipped with vertical internals, the presence of bundle of the vertical internals will allow to small bubbles (bubbles smaller than the gaps among the vertical internals) to pass through and circulate with liquid in the wall region, but the vertical internals will trap

any large bubbles (bigger than the gap between the internals) in the core region. For that reason, the gas holdup in the bubble column with internals is similar to the gas holdup values at the center region of the bubble column without internals while larger gas holdup near the wall. This significant increase in the gas holdup in the wall region for the bubble columns equipped with vertical internals can also be seen distinctly in Figure 22, Figure 23, Figure 25, and Figure 26 for the vertical and horizontal line averaged gas holdup profiles. This increase in gas holdup magnitude becomes more pronounced with bubble column equipped with 1-inch vertical internals due to the geometric configuration (circular-like shape) for 1-inch internals that has one central tube while the 0.5-inch vertical internals configuration does not have a central tube. However, from Figure 21 and Figure 24, one can observe that the line average (i.e., gas holdup averaging along vertical and horizontal lines of pixels over the cross-sectional image) of the gas holdup diametrical profiles in bubble columns with and without vertical internals are relatively similar to each other under the studied superficial gas velocity of 5 cm/s based on free CSA for flow despite using different size of vertical internals. This convergence of gas holdup values indicates that the presence of vertical internals and their sizes do not affect the gas holdup magnitude under this superficial gas velocity within bubbly flow regime condition (i.e., at a superficial gas velocity of 5 cm/s). This bubbly flow regime is characterized by the presence of uniform small bubble sizes with almost the same bubble rise velocity. Accordingly, these bubbles while they are formed at the distributor region and rise, they are not subjected to coalescence and break up due to bubble-bubble and bubble-vertical internals interactions under this condition, especially the gaps between the vertical internals are bigger than the sizes of the rising bubbles.

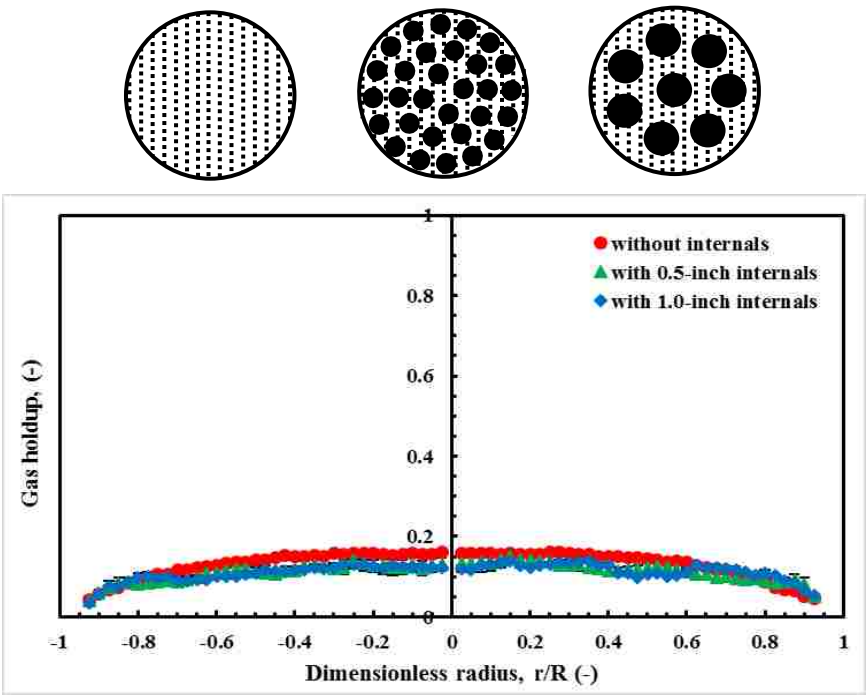

Figure 21: Comparison between the vertical line averaged gas holdup profiles for bubble columns with or without internals at superficial gas velocity (5 cm/s) based on the free cross-sectional area (CSA) for the flow

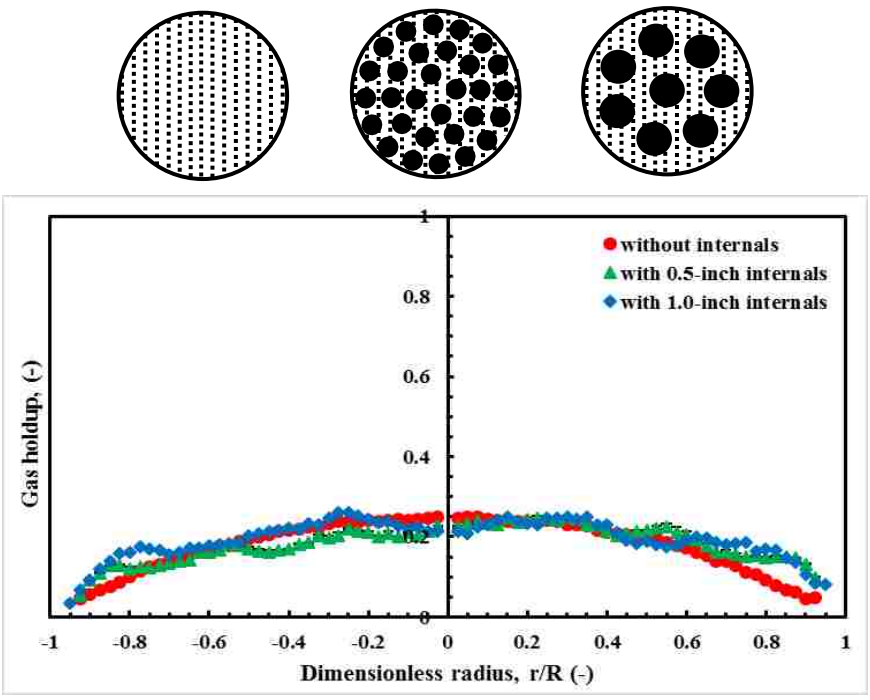

Figure 22: Comparison between the vertical line averaged gas holdup profiles for bubble columns with or without internals at superficial gas velocity (20 cm/s) based on the free cross-sectional area (CSA) for the flow

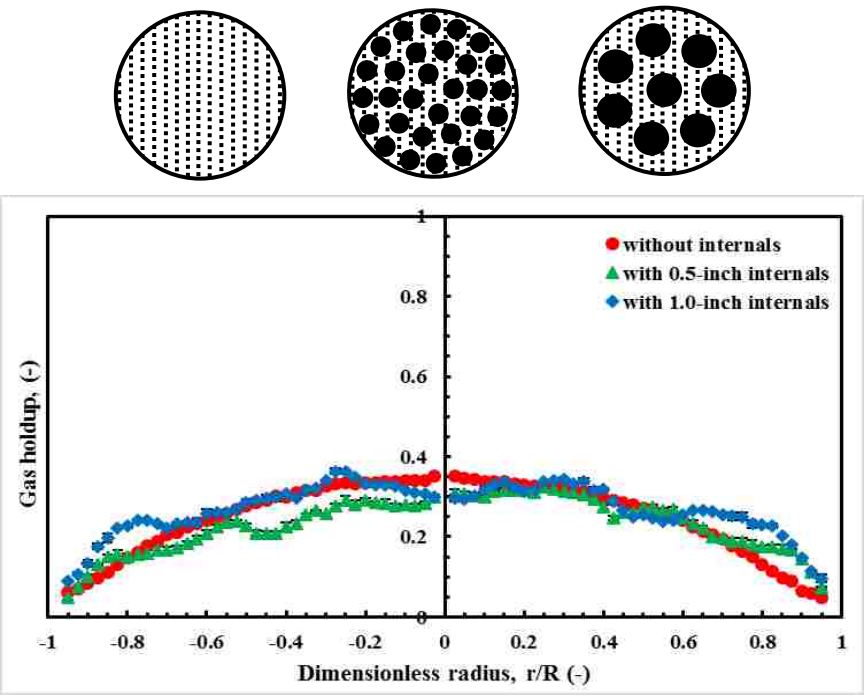

Figure 23: Comparison between the vertical line averaged gas holdup profiles for bubble columns with or without internals at superficial gas velocity (45 cm/s) calculated based on the free cross-sectional area (CSA) for the flow

The existence of the central tube with 1-inch vertical internals arrangement plays an important role in distributing the gas-liquid flow inside the column where it helps to push and displaces the gas-liquid toward the wall region. Also, the size of a pitch for 1-inch internal configuration (3.8 cm) approximately twice larger than 0.5-inch internals (2.1 cm) as shown in Figure *3*, which provides a large compartment among the vertical internals as compared with 0.5-inch internals and hence will facilitate the passing of bubbles from the core of the column toward the wall region. Moreover, at the churn turbulent flow regime, the bubbles that move radially from the center of column toward the wall region will face one bundle of the 7 vertical internals in the case of bubble column with 1-inch internals while face three bundles of the 30 vertical internals in the case of the bubble column with 0.5-inch vertical internals and hence more resistance to movement of the

bubbles associated with the bubble column equipped with 0.5-inch internals. This difference between the gas holdup values obtained in the bubble columns with 0.5-inch and 1-inch vertical internal at wall region is expected to change the magnitude of the large-scale liquid circulation and intensity of the liquid mixing but unfortunately, this information is vastly unknown. Therefore, further experimental investigations are required to quantify the local liquid velocity for both sizes of vertical internals. These experimental studies are ongoing in our laboratory to quantify the impact of the different diameters of the vertical internals on the 3D liquid velocity field and turbulent parameters by using advanced radioactive particle tracking (RPT) technique and will be reported in the future manuscripts.

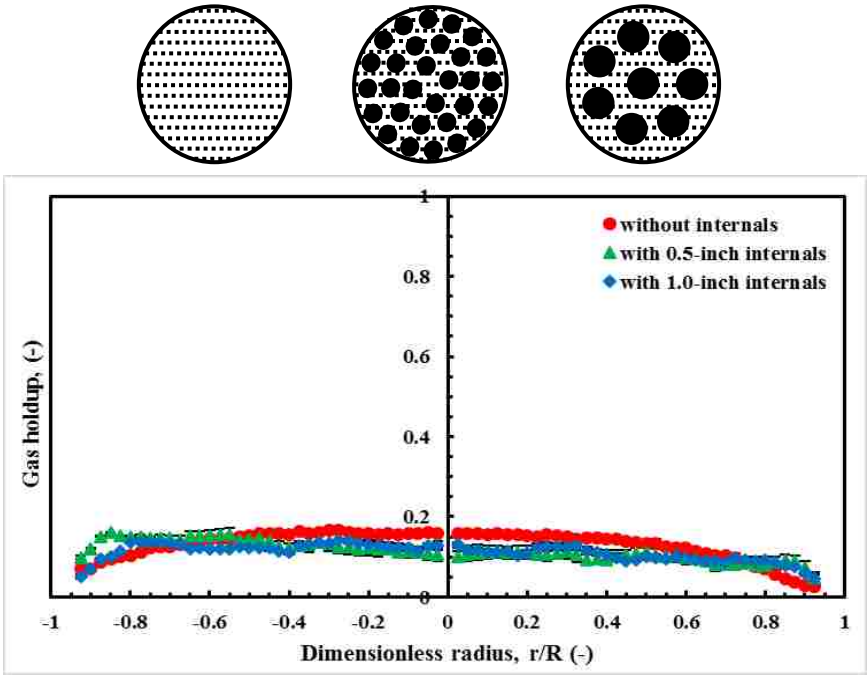

Figure 24: Comparison between the horizontal line averaged gas holdup profiles for bubble columns with or without internals at superficial gas velocity (5 cm/s) based on the free cross-sectional area (CSA) for the flow

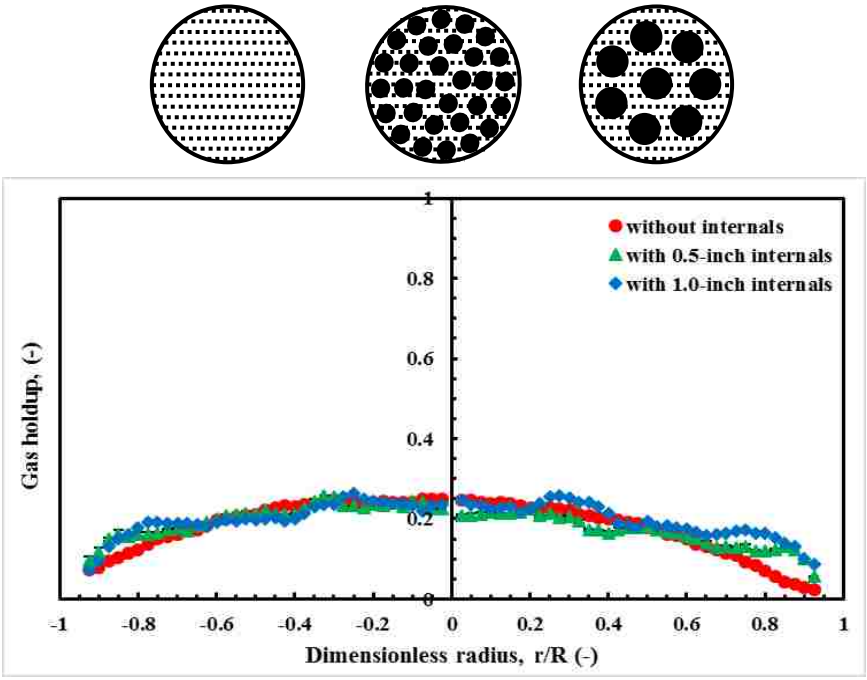

Figure 25: Comparison between the horizontal line averaged gas holdup profiles for bubble columns with or without internals at superficial gas velocity (20 cm/s) based on the free cross-sectional area (CSA) for the flow

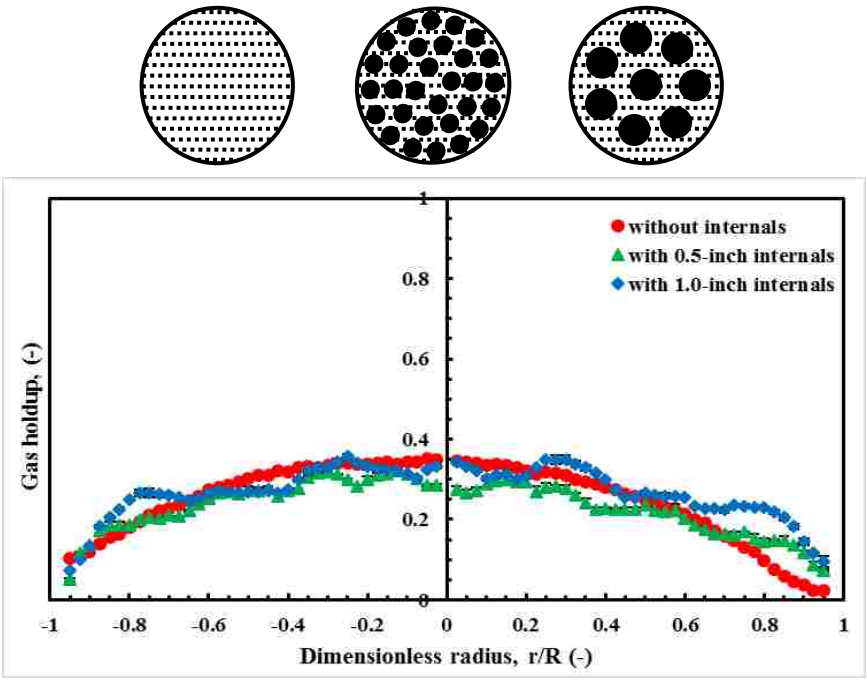

Figure 26: Comparison between the horizontal line averaged gas holdup profiles for bubble columns with or without internals at superficial gas velocity (45 cm/s) based on the free cross-sectional area (CSA) for the flow

In this study, the gas holdup profiles were presented in two ways, azimuthally (circularly) and line (vertically or horizontally) averaged gas holdup profiles. The azimuthally averaged gas holdup was computed by averaging the pixels of the 2D gas holdup distribution circumferentially after excluding the values of the vertical internals. The azimuthally averaged usually performs to any systems based on an axisymmetric assumption (i.e., the values of gas holdup are constant in θ-direction) of the 2D gas holdup distribution and this works properly for columns without internals such as bubble column [86], fluidized bed [87], spouted bed [88], pebble bed [89] and trickle bed [90]. However, the axisymmetric of gas-liquid distribution rarely maintains in columns packed densely with vertical internals. Therefore, a line averaged gas holdup profile was applied here as an alternative representation for gas holdup data.

The vertical and horizontal lines averaged gas holdup profiles were calculated by averaging the pixels of gas holdup distribution in vertical and horizontal order. To make sure which type of profiles more representative to gas holdup data, the arithmetic mean of the cross-sectional gas holdup distribution was calculated and compared with arithmetic means of azimuthal and line profiles. The results of comparison reveal that the line averaged gas holdup either vertically or horizontally profiles in more representative than azimuthally one.

For instance, it was found that the percentages of relative difference between the mean of the cross-sectional gas holdup distribution and the average for azimuthally gas holdup profile at a superficial gas velocity of 45 cm/s for bubble columns without internals, with 0.5-inch internals, and with 1-inch internals were 26.7%, 14.8%, and 9.8% respectively. While the percentages of relative difference were 8%, 8.3%, and 7.14% when

it was calculated between the mean of the cross-sectional gas holdup and the average of line gas holdup profile at the same superficial gas velocity. Furthermore, during the churn turbulent flow regime, particularly at a superficial gas velocity of 20 and 45 cm/s, the gas holdup values obtained in the bubble columns equipped with 0.5-inch or 1-inch vertical internals have approached the values of the gas holdup of the bubble column without vertical internals at the core region of the column. This only can be accomplished through operating the bubble column equipped with dense of the vertical internals under a superficial gas velocity calculated based on free CSA of the column.

This key finding of the results was also observed previously by Al Mesfer [91], Al Mesfer et al. [45], and Kagumba [44] when they studied the effect of using superficial gas velocity calculated based on the total and free CSA for the flow on the magnitude of the gas holdup for the air-water system in bubble column equipped with dense vertical internals.

To further highlight the influence of vertical internals on the gas holdup, the local gas holdup along the center line of pixels over the cross-sectional image (i.e., horizontal and vertical lines) for bubble columns with and without vertical internals operated under a superficial gas velocity of 45 cm/s are shown in Figure 27 and Figure 28. From these figures, one can notice that the parabolic gas holdup profile obtained in the bubble column without vertical internals has replaced by wavy gas holdup profile with maximum gas holdup values in the center of the gaps for the vertical internals. This significant increase in the gas holdup values in these gaps is due to each vertical internal providing extra wall shear [92,93], which induces bubbles to move away from the vicinity of the internal walls and accumulate in the gaps between the internals, causing an increase in the gas holdup

values in these regions. Additionally, from the gas holdup distributions and local gas holdup profiles, one can deduce the behavior of liquid circulation and axial liquid velocity due to the gas phase driving the liquid phase in the bubble columns (i.e., driving the liquid phase by imbalance in buoyancy force and rising bubbles of gas phase) [40,94].

For example, the regions of the maximum gas holdup in the cross-sectional of gas holdup distribution indicate regions of ascending liquid, whereas regions of minimum gas holdup mark for descending liquid. Accordingly, the axial liquid velocity profiles in bubble column without vertical internals breakup into the ascending areas in the center of the gaps and descending regions in the vicinity of the walls for the vertical internals. Therefore, the observed large eddies in the bubble column without vertical internals have segregated into small eddies within the size of gaps for vertical internals.

Hence, it can be obviously concluded that the presence of vertical internals and their sizes have a substantial effect not only on the gas holdup distribution over the entire cross-sectional area of the columns but also on the velocity field. However, a study of the effect of the sizes of vertical internals, which covering 25% of the cross-sectional area to represent the heat-exchanging internals used in the industrial FT synthesis, on the liquid velocity field and turbulent parameters (Reynolds normal stress, Reynolds shear stress, and turbulent kinetic energy) is not available in the literature.

This lack of data for liquid velocity field and turbulent parameters has been addressed in our laboratory (MReal) by using advanced radioactive particle tracking (RPT) technique and will be reported soon.

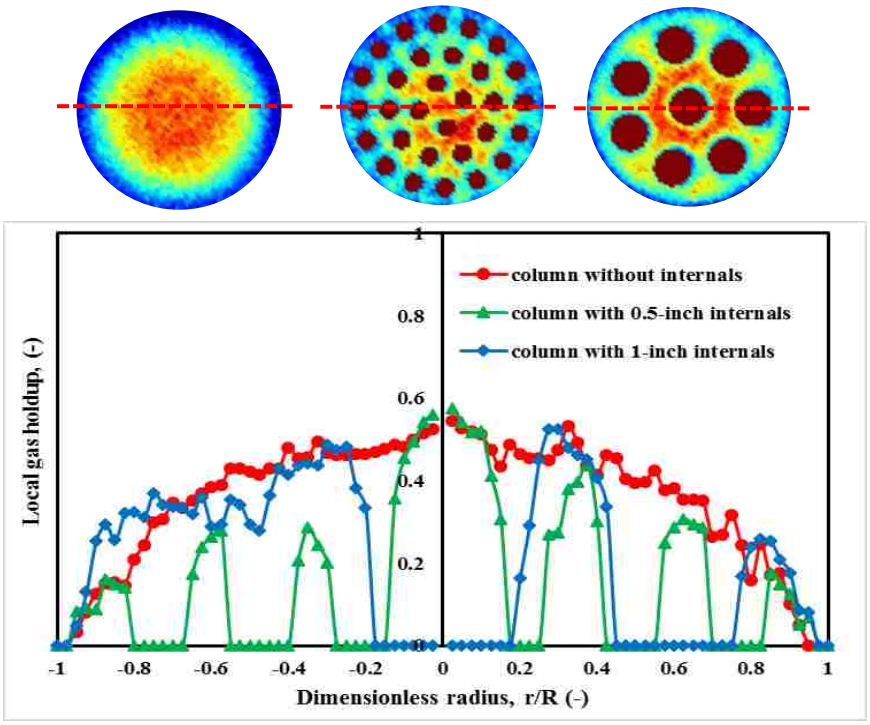

Figure 27: Horizontal centerline gas holdup profile for bubble columns with and without vertical internals operated under a superficial gas velocity of 45 cm/s

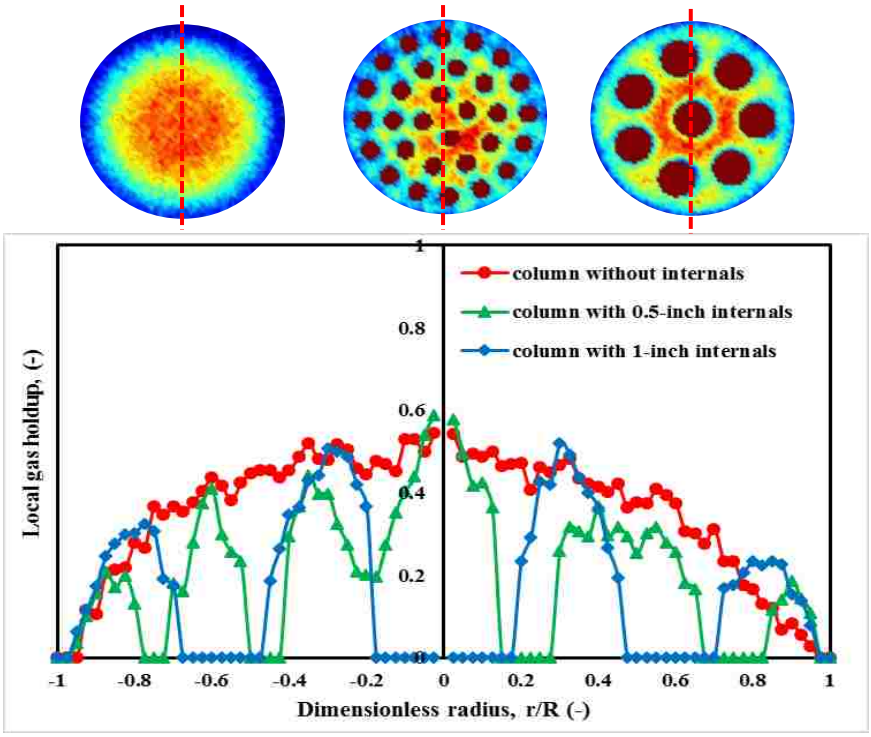

Figure 28: Vertical centerline gas holdup profile for bubble columns with and without vertical internals operated under a superficial gas velocity of 45 cm/s

4. REMARKS

The influences of the presence of the bundle of the vertical internals and their size on the overall, local gas-liquid distributions and their profiles have been investigated in a 6-inch (0.14 m) Plexiglas bubble column for the air-water system by using an advanced gamma-ray computed tomography (CT) technique. The vertical internals for both sizes were arranged circularly and fitted uniformly inside the bubble column where both diameters were having the same occluded area (~25%) of the column's CSA to represent the blocking percentage of area in FT synthesis. The time-averaged cross-sectional gas holdup distributions and their profiles were visualized and quantified at different superficial gas velocities, which covering the homogeneous and heterogeneous flow regimes. The summary of the remarks of this study is as follows:

- No significant effect was observed when using either 0.5-inch or 1-inch vertical internals in 6-inch bubble column on the overall gas holdup values (i.e., measured by bed expansion) at different superficial gas velocities. This is due to the operating superficial gas velocities for bubble column with vertical internals (either for 0.5-inch or 1-inch in diameter) were estimated based on the free cross-sectional area for the flow (i.e., both sizes of the internals covering the same CSA) where the volumetric flow rate will be the same in both cases and lower than in the column without internals. Also, the overall gas holdup values that were achieved in the bubble column without vertical internals at different superficial gas velocity are similar to those obtained in bubble columns equipped with 0.5-inch and 1-inch of the vertical internals if these columns with vertical internals operated under the same superficial gas velocity but calculated

based on free CSA for the flow. However, the size of vertical internals has a significant effect on the gas holdup distribution over the entire cross-sectional area of the column.

- The imaging of the gas-liquid distribution inside the bubble columns with and without vertical internals reveal that the phenomenon of the core-annular liquid circulation pattern, which commonly observed in the bubble column without vertical internals still exist in bubble column packed densely with vertical internals.
- The circular configurations for either 0.5 or 1-inch of the vertical internals inside the column significantly reduce the maldistribution, which was reported in the literature.
- The reconstructed CT images show that the bubble columns equipped with or without vertical internals displayed a uniform cross-sectional gas holdup distribution (symmetric) for all studied superficial gas velocities. However, the bubble column packed with 1-inch of the vertical internals (sparse arrangement) produced more symmetric distributions than the column equipped with 0.5-inch of the vertical internals (dense arrangement).
- The magnitude of the gas holdup increases significantly with the superficial gas velocity for bubble columns with or without vertical internals. However, the gas holdup profile took on the wavy line shape in the bubble column with vertical internals due to the design and the number of the vertical internals, whereas the column without obstacles exhibits a parabolic gas holdup profile.
- At the churn turbulent flow regime, especially in the superficial gas velocities 20 and 45 cm/s, a noticeable increase in the magnitude of the gas holdup near the wall (in the dimensionless radius, r/R=0.8) region is obtained based on the insertion bundle of the vertical internals in the column as compared with a bubble column without obstacles.

However, the bubble column with 1-inch internals exhibited higher gas holdup than the column equipped with 0.5-inch internals.

- The presence of the central tube with 1-inch internals configuration, pitch size as well as the number of vertical internals plays a major role in the distribution of gas-liquid over the cross-sectional area of the column.
- The values of the gas holdup obtained in the core of the bubble column without vertical internals are found to be similar to those in the bubble column equipped with vertical internals when these columns with vertical internals operate at a high superficial gas velocity (churn turbulent flow regime) and calculated based on the free cross-sectional area (CSA) for the flow.
- The originality of the obtained data and findings is worthy as benchmark data for developing and validating a 3D CFD simulation and hydrodynamic model for the air-water system.
- The present study was limited to one type of configuration (a circular arrangement of tubes) and a lab-scale bubble column. Therefore, further investigations are recommended to visualize, measure, analyze, and quantify the effect of the different tube bundle arrangements on gas holdup distributions and their profiles in the various scales of bubble columns. Such kind of analysis can be conducted using properly validated CFD code and models.

ACKNOWLEDGMENTS

The authors gratefully acknowledge the financial support in the form of a scholarship provided by the Higher Committee for Education Development in Iraq (HCED), Ministry of Higher Education and Scientific Research (Iraq), and the funds

provided by Missouri S&T and Professor Dr. Muthanna Al-Dahhan to develop the CT technique, the experimental set-up and to perform the present study. Also, the authors would like to thank, Dr. Fadha Ahmed for his help with the gamma-ray computed tomography (CT) technique.

REFERENCES

[1] F. Yamashita, Effect of Shape of Baffle Plates and Mesh and Cross-Sectional Area of Wire Gauzes on Gas Holdup and Pressure Drop in a Bubble column, J. Chem. Eng. Japan. (1987) 201–204.

[2] S.C. Saxena, N.S. Rao, N.. Saxena, S. C. and Rao, Estimation of gas holdup in a slurry bubble column with internals: nitrogen-Therminol-magnetite system, Poweder Technol. 75 (1993) 153–158. doi:10.1016/0032-5910(93)80076-M.

[3] S. Degaleesan, M. Dudukovic, Y. Pan, Experimental study of gas-induced liquid-flow structures in bubble columns, AIChE J. 47 (2001) 1913–1931. doi:10.1002/aic.690470904.

[4] A. Yadav, A. Kushwaha, S. Roy, An algorithm for estimating radial gas holdup profiles in bubble columns from chordal densitometry measurements, Can. J. Chem. Eng. 94 (2016) 524–529. doi:10.1002/cjce.22412.

[5] L.S. Sabri, A.J. Sultan, M.H. Al-dahhan, Assessment of RPT Calibration Need during Microalgae Culturing and other Biochemical Processes, IEEE. (2017) 3–8.

[6] N. Kantarci, F. Borak, K.O. Ulgen, Bubble column reactors, Process Biochem. 40 (2005) 2263–2283. doi:10.1016/j.procbio.2004.10.004.

[7] A. Shaikh, M.H. Al-Dahhan, A Review on Flow Regime Transition in Bubble Columns, Int. J. Chem. React. Eng. 5 (2007). doi:10.2202/1542-6580.1368.

[8] R.S. Abdulmohsin, M.H. Al-Dahhan, Impact of internals on the heat-transfer coefficient in a bubble column, Ind. Eng. Chem. Res. 51 (2012) 2874–2881. doi:10.1021/ie2018096.

[9] A.A. Youssef, M.H. Al-Dahhan, M.P. Dudukovic, Bubble columns with internals: A review, Int. J. Chem. React. Eng. 11 (2013) 169–223. doi:10.1515/ijcre-2012-0023.

[10] A. Esmaeili, S. Farag, C. Guy, J. Chaouki, Effect of elevated pressure on the hydrodynamic aspects of a pilot-scale bubble column reactor operating with non-Newtonian liquids, Chem. Eng. J. 288 (2016) 377–389. doi:10.1016/j.cej.2015.12.017.

[11] A. Forret, J.M. Schweitzer, T. Gauthier, R. Krishna, D. Schweich, Liquid dispersion in large diameter bubble columns, with and without internals, Can. J. Chem. Eng. 81 (2003) 360–366. doi:10.1002/cjce.5450810304.

[12] P. Gupta, M. H. Al-Dahhan, M. P. Dudukovic, B. A. Toseland, Comparison of single- and two-bubble class gas-liquid recirculation models - Application to pilot-plant radioactive tracer studies during methanol synthesis, Chem. Eng. Sci. 56 (2001) 1117–1125. doi:10.1016/S0009-2509(00)00329-8.

[13] E.D. Larson, R. Tingjin, Synthetic fuel production by indirect coal liquefaction, Energy Sustain. Dev. 7 (2003) 79–102. doi:10.1016/S0973-0826(08)60381-6.

[14] R. Guettel, U. Kunz, T. Turek, Reactors for Fischer-Tropsch synthesis, Chem. Eng. Technol. 31 (2008) 746–754. doi:10.1002/ceat.200800023.

[15] M. Kölbel,H ;Ralek, The Fischer-Tropsch Synthesis in Liquid Phase, Catal. Rev. Eng. 21 (1980) 225–274.

[16] S. Saeidi, M.K. Nikoo, A. Mirvakili, S. Bahrani, N.A. Saidina Amin, M.R. Rahimpour, Recent advances in reactors for low-temperature Fischer-Tropsch synthesis: process intensification perspective, Rev. Chem. Eng. 31 (2015) 19–21. doi:10.1515/revce-2014-0042.

[17] M.K. Al Mesfer, A.J. Sultan, M.H. Al-Dahhan, Study the effect of dense internals on the liquid velocity field and turbulent parameters in bubble column for Fischer–Tropsch (FT) synthesis by using Radioactive Particle Tracking (RPT) technique, Chem. Eng. Sci. 161 (2017) 228–248. doi:10.1016/j.ces.2016.12.001.

[18] A. Forret, J.M. Schweitzer, T. Gauthier, R. Krishna, D. Schweich, Scale up of slurry bubble reactors, Oil Gas Sci. Technol. 61 (2006) 443–458. doi:10.2516/ogst:2006044a.

[19] Y. Wang, W. Fan, Y. Liu, Z. Zeng, X. Hao, M. Chang, C. Zhang, Y. Xu, H. Xiang, Y. Li, Modeling of the Fischer-Tropsch synthesis in slurry bubble column reactors, Chem. Eng. Process. Process Intensif. 47 (2008) 222–228. doi:10.1016/j.cep.2007.02.011.

[20] Y. Wu, B. Cheng Ong, M.H. Al-Dahhan, Predictions of radial gas holdup profiles in bubble column reactors, Chem. Eng. Sci. 56 (2001) 1207–1210. doi:10.1016/S0009-2509(00)00341-9.

[21] H. Jin, Y. Lian, Y. Qin, S. Yang, G. He, Distribution characteristics of holdups in a multi-stage bubble column using electrical resistance tomography, Particuology. 11 (2013) 225–231. doi:10.1016/j.partic.2012.05.005.

[22] O.N. Manjrekar, M.P. Dudukovic, Application of a 4-point optical probe to a Slurry Bubble Column Reactor, Chem. Eng. Sci. 131 (2015) 313–322. doi:10.1016/j.ces.2015.03.027.

[23] L. Han, M.H. Al-Dahhan, Gas-liquid mass transfer in a high pressure bubble column reactor with different sparger designs, Chem. Eng. Sci. 62 (2007) 131–139. doi:10.1016/j.ces.2006.08.010.

[24] Y. Wu, M.H. Al-Dahhan, Prediction of axial liquid velocity profile in bubble columns, Chem. Eng. Sci. 56 (2001) 1127–1130. doi:10.1016/S0009-2509(00)00330-4.

[25] A. Behkish, R. Lemoine, L. Sehabiague, R. Oukaci, B.I. Morsi, Gas holdup and bubble size behavior in a large-scale slurry bubble column reactor operating with an organic liquid under elevated pressures and temperatures, Chem. Eng. J. 128 (2007) 69–84. doi:10.1016/j.cej.2006.10.016.

[26] C. Laborde-Boutet, F. Larachi, N. Dromard, O. Delsart, D. Schweich, CFD simulation of bubble column flows: Investigations on turbulence models in RANS approach, Chem. Eng. Sci. 64 (2009) 4399–4413. doi:10.1016/j.ces.2009.07.009.

[27] K. Ekambara, M.T. Dhotre, J.B. Joshi, CFD simulations of bubble column reactors: 1D, 2D and 3D approach, Chem. Eng. Sci. 60 (2005) 6733–6746. doi:10.1016/j.ces.2005.05.047.

[28] M. Pourtousi, J.N. Sahu, P. Ganesan, Effect of interfacial forces and turbulence models on predicting flow pattern inside the bubble column, Chem. Eng. Process. Process Intensif. 75 (2014) 38–47. doi:10.1016/j.cep.2013.11.001.

[29] M. Pourtousi, P. Ganesan, A. Kazemzadeh, S.C. Sandaran, J.N. Sahu, Methane bubble formation and dynamics in a rectangular bubble column: A CFD study, Chemom. Intell. Lab. Syst. 147 (2015) 111–120. doi:10.1016/j.chemolab.2015.08.003.

[30] N. Rados, A. Shaikh, M.H. Al-Dahhan, Solids flow mapping in a high pressure slurry bubble column, Chem. Eng. Sci. 60 (2005) 6067–6072. doi:10.1016/j.ces.2005.04.087.

[31] A. Shaikh, M. Al-Dahhan, A new methodology for hydrodynamic similarity in bubble columns, Can. J. Chem. Eng. 88 (2010) 503–517. doi:10.1002/cjce.20357.

[32] R.S. Abdulmohsin, B.A. Abid, M.H. Al-Dahhan, Heat transfer study in a pilot-plant scale bubble column, Chem. Eng. Res. Des. 89 (2011) 78–84. doi:10.1016/j.cherd.2010.04.019.

[33] M. Gheni, Saba;Abdulaziz, I.;Al-Dahhan, Effect of L / D Ratio on Phase Holdup and Bubble Dynamics in Slurry Bubble Column using Optical Fiber Probe Measurements, Int. J. Chem. React. Eng. (2016).

[34] F. Yamashita, Effects of Vertical Pipe and Rod Internals on Gas Holdup in Bubble Columns., J. Chem. Eng. Japan. 20 (1987) 204–206.

[35] J. Fox, Fischer-Tropsch Reactor Selection, Catal. Letters. 7 (1990) 281–292.

[36] J. Fox, B. Degen, G. Cady, F. Deslate, R. Summers, A. Akgerman, Slurry reactor design studies, San Francisco, CA, 1990.

[37] S.. C. Saxena, N.. S. Rao, P.R. Thimmapuram, Gas Phase Holdup in Slurry Bubble Column for Two- and Three-Phase Systems, Chem. Eng. J. 49 (1992) 151–159. http://dx.doi.org/10.1016/0300-9467(92)80051-B.

[38] J. Chen, F. Li, S. Degaleesan, P. Gupta, M.H. Al-Dahhan, M.P. Dudukovic, B.A. Toseland, Fluid dynamic parameters in bubble columns with internals, Chem. Eng. Sci. 54 (1999) 2187–2197. doi:10.1016/S0009-2509(99)00003-2.

[39] A.A. Youssef, M.H. Al-Dahhan, Impact of internals on the gas holdup and bubble properties of a bubble column, Ind. Eng. Chem. Res. 48 (2009) 8007–8013. doi:10.1021/ie900266q.

[40] V. Balamurugan, D. Subbarao, S. Roy, Enhancement in gas holdup in bubble columns through use of vibrating internals, Can. J. Chem. Eng. 88 (2010) 1010–1020. doi:10.1002/cjce.20362.

[41] A.A. Youssef, M.E. Hamed, J.T. Grimes, M.H. Al-Dahhan, M.P. Duduković, Hydrodynamics of pilot-scale bubble columns: Effect of internals, Ind. Eng. Chem. Res. 52 (2013) 43–55. doi:10.1021/ie300465t.

[42] A.K. Jhawar, A. Prakash, Bubble column with internals: Effects on hydrodynamics and local heat transfer, Chem. Eng. Res. Des. 92 (2014) 25–33. doi:10.1016/j.cherd.2013.06.016.

[43] X. Guan, Y. Gao, Z. Tian, L. Wang, Y. Cheng, X. Li, Hydrodynamics in bubble columns with pin-fin tube internals, Chem. Eng. Res. Des. 102 (2015) 196–206. doi:10.1016/j.cherd.2015.06.028.

[44] M. Kagumba, M.H. Al-Dahhan, Impact of internals size and configuration on bubble dynamics in bubble columns for alternative clean fuels production, Ind. Eng. Chem. Res. 54 (2015) 1359–1372. doi:10.1021/ie503490h.

[45] M.K. Al Mesfer, A.J. Sultan, M.H. Al-Dahhan, M.H.A.-D. Mohammed K. Al Mesfer , Abbas J. Sultan, Impacts of dense heat exchanging internals on gas holdup cross-sectional distributions and profiles of bubble column using gamma ray Computed Tomography (CT) for FT synthesis, Chem. Eng. J. 300 (2016) 317–333. doi:10.1016/j.cej.2016.04.075.

[46] P. Pradhan, Anil K.;Parichha,R.;De, A.K. Pradhan, R.K. Parichha, P. De, Gas Holdup in Non-Newtonian Solutions in a Bubble Column with Internals, Can. J. Chem. Eng. 71 (1993) 468–471. doi:10.1002/cjce.5450710319.

[47] A. Jasim, The impact of heat exchanging internals on hydrodynamics of bubble column reactor, Missouri university science and technology, 2016.

[48] J. Xue, Bubble Velocity , Size and Interfacial Area Measurements in Bubble Columns, Washington University, 2004. doi:10.1002/aic.

[49] S. Roy, A. Kemoun, M.H. Al-Dahhan, M.P. Dudukovic, T.B. Skourlis, F.M. Dautzenberg, Countercurrent flow distribution in structured packing via computed tomography, Chem. Eng. Process. Process Intensif. 44 (2005) 59–69. doi:10.1016/j.cep.2004.03.010.

[50] S. Ghasemi, M. Sohrabi, M. Rahmani, A comparison between two kinds of hydrodynamic models in bubble column slurry reactor during Fischer-Tropsch synthesis: Single-bubble class and two-bubble class, Chem. Eng. Res. Des. 87 (2009) 1582–1588. doi:10.1016/j.cherd.2009.04.015.

[51] N. Ellis, H.T. Bi, C.J. Lim, J.R. Grace, Influence of probe scale and analysis method on measured hydrodynamic properties of gas-fluidized beds, Chem. Eng. Sci. 59 (2004) 1841–1851. doi:10.1016/j.ces.2004.01.037.

[52] E.A. Whitemarsh, D.R. Escudero, T.J. Heindel, Probe effects on the local gas holdup conditions in a fluidized bed, Powder Technol. 294 (2016) 191–201. doi:10.1016/j.powtec.2016.02.035.

[53] P. Chen, J. Sanyal, M.P.P. Duduković, Numerical simulation of bubble columns flows: Effect of different breakup and coalescence closures, Chem. Eng. Sci. 60 (2005) 1085–1101. doi:10.1016/j.ces.2004.09.070.

[54] M. Al-Dahhan, Radioisotope Applications in the Petrochemical Industry : An Overview, Int. Symp. Peac. Appl. Nucl. Technol. GCC Ctries. (2008) 10.

[55] F. Larachi, D. Desvigne, L. Donnat, D. Schweich, Simulating the effects of liquid circulation in bubble columns with internals, Chem. Eng. Sci. 61 (2006) 4195–4206. doi:10.1016/j.ces.2006.01.053.

[56] F. Laborde-Boutet, Cédric and Larachi, CFD Simulations of Hydrodynamic/Thermal Coupling Phenomena in a Bubble Column with Internals, AIChE J. 56 (2010) 2397–2411. doi:10.1002/aic.

[57] X. Guan, Z. Li, L. Wang, Y. Cheng, X. Li, CFD simulation of bubble dynamics in bubble columns with internals, Ind. Eng. Chem. Res. 53 (2014) 16529–16538. doi:10.1021/ie502666y.

[58] X. Guan, N. Yang, CFD simulation of pilot-scale bubble columns with internals: Influence of interfacial forces, Chem. Eng. Res. Des. 126 (2017) 109–122. doi:10.1016/j.cherd.2017.08.019.

[59] V.H. Bhusare, M.K. Dhiman, D. V. Kalaga, S. Roy, J.B. Joshi, CFD simulations of a bubble column with and without internals by using OpenFOAM, Chem. Eng. J. 317 (2017) 157–174. doi:10.1016/j.cej.2017.01.128.

[60] M. Kagumba, Heat Transfer and Bubble Dynamics in Bubble and Slurry, Missouri university of science and technology, 2013.

[61] A. Jasim, The impact of heat exchanging internals on hydrodynamics of bubble column reactor, Missouri University of Science and Technology, 2016.

[62] J. Ellenberger, J.M. Van Baten, R. Krishna, Intensification of bubble columns by vibration excitement, Catal. Today. 79–80 (2003) 181–188. doi:10.1016/S0920-5861(03)00003-8.

[63] R. Krishna, J. Ellenberger, Influence of low-frequency vibrations on bubble and drop sizes formed at a single orifice, Chem. Eng. Process. 42 (2003) 15–21. doi:10.1016/S0255-2701(02)00012-0.

[64] A. Shaikh, M. Al-Dahhan, Characterization of the hydrodynamic flow regime in bubble columns via computed tomography, Flow Meas. Instrum. 16 (2005) 91–98. doi:10.1016/j.flowmeasinst.2005.02.004.

[65] B.C. Ong, P. Gupta, A. Youssef, M. Al-Dahhan, M.P. Duduković, Computed Tomographic Investigation of the Influence of Gas Sparger Design on Gas Holdup Distribution in a Bubble Column, Ind. Eng. Chem. Res. 48 (2009) 58–68. doi:10.1021/ie800516s.

[66] R. Varma, S. Bhusarapu, J.A.O. Sullivan, M. Al-Dahhan, A comparison of alternating minimization and expectation maximization algorithms for single source gamma ray tomography, Meas. Sci. Technol. 18 (2007) 1–13. doi:10.1088/0957-0233/19/1/015506.

[67] F. Al Falahi, M. Al-Dahhan, Experimental investigation of the pebble bed structure by using gamma ray tomography, Nucl. Eng. Des. 310 (2016) 231–246. doi:10.1016/j.nucengdes.2016.10.009.

[68] A. Efhaima, M. Al-Dahhan, Local time-averaged gas holdup in fluidized bed reactor using gamma ray computed tomography technique (CT), Int. J. Ind. Chem. 6 (2015) 143–152. doi:10.1007/s40090-015-0048-6.

[69] A. Efhaima, M. Al-Dahhan, Assessment of Scale-up Dimensionless Groups Methodology of Gas-Solid Fluidized beds using Advanced Non-Invasive Measurement Technique (CT and RPT), Can. J. Chem. Eng. 94 (2016).

[70] A. Efhaima, M. Al-Dahhan, Bed Diameter Effect on the Hydrodynamics of Gas-Solid Fluidized Beds via Radioactive Particle Tracking (RPT) Technique, Can. J. Chem. Eng. 94 (2016).

[71] M. Al-Dahhan, S. Aradhya, F. Zaid, N. Ali, T. Aljuwaya, Scale-up and On-line Monitoring of Gas-solid Systems Using Advanced and Non-invasive Measurement Techniques, Procedia Eng. 83 (2014) 469–476. doi:10.1016/j.proeng.2014.09.080.

[72] N. Ali, T. Al-Juwaya, M. Al-Dahhan, Demonstrating the non-similarity in local holdups of spouted beds obtained by CT with scale-up methodology based on dimensionless groups, Chem. Eng. Res. Des. 114 (2016) 129–141. doi:10.1016/j.cherd.2016.08.010.

[73] J.A.O. Sullivan, D.L. Snyder, Alternating Minimization Problems for Transmission Tomography Using Energy Detectors, IEEE Trans. Med. Imaging. 26 (2007) 144–147.

[74] I. Csiszar, Why Least Squares and Maximum Entropy ? An Axiomatic Approach to Inference for Linear Inverse Problems Author (s): Imre Csiszar Source : The Annals of Statistics , Vol . 19 , No . 4 (Dec ., 1991), pp . 2032-2066 Published by : Institute of Mathematica, Ann. Stat. 19 (1991) 2032–2066.

[75] R. Varma, Characterization of anaerobic bioreactors for bioenergy generation using a novel tomography technique, Washington University, 2008.

[76] U.P. Veera, J.B. Joshi, MEASUREMENT OF GAS HOLD-UP PROFILES IN BUBBLE COLUMN BY GAMMA RAY TOMOGRAPHY Effect of Liquid Phase Properties, Trans. Inst. Chem. Eng. 78 (2000) 425–434. doi:10.1205/026387699526232.

[77] P.A.S. Vasquez, C.H. De Mesquita, G.A.C. LeRoux, M.M. Hamada, Methodological analysis of gamma tomography system for large random packed columns, Appl. Radiat. Isot. 68 (2010) 658–661. doi:10.1016/j.apradiso.2009.11.077.

[78] J. Chen, P. Gupta, S. Degaleesan, M.H. Al-Dahhan, M.P. Dudukovic, B.A. Toseland, Gas holdup distributions in large-diameter bubble columns measured by computed tomography, Flow Meas. Instrum. 9 (1998) 91–101. doi:10.1016/S0955-5986(98)00010-7.

[79] M. Al-Mesfer, Effect of Dense Heat Exchanging Internals on the Hydrodynamics of Bubble Column Reactors Using Non-Invasive Measurement Techniques, Missouri University of Science and Technology, Rolla, MO, 2013.

[80] X. Guo, C. Chen, Simulating the impacts of internals on gas–liquid hydrodynamics of bubble column, Chem. Eng. Sci. 174 (2017) 311–325. doi:10.1016/j.ces.2017.09.004.

[81] J. Hanika, Safe operation and control of trickle-bed reactor, Chem. Eng. Sci. 54 (1999) 4653–4659. doi:10.1016/S0009-2509(98)00532-6.

[82] a. V. Kulkarni, Design of a Pipe/Ring Type of Sparger for a Bubble Column Reactor, Chem. Eng. Technol. 33 (2010) 1015–1022. doi:10.1002/ceat.200800347.

[83] N. Rados, A. Shaikh, M.H. Al-dahhan, Phase Distribution in a High Pressure Slurry Bubble Column via a Single Source Computed Tomography, Can. J. Chem. Eng. 83 (2005).

[84] A.J. Sultan, L.S. Sabri, M.H. Al-Dahhan, Overcoming the Gamma-Ray Computed Tomography Data Processing Pitfalls for Bubble Column Equipped with Vertical Internals, Can. J. Chem. Eng. (2017).

[85] A. Youssef, Fluid Dynamics and Scale-up of Bubble Columns with Internals, Washington University, Saint Louis, Missouri, 2010. doi:10.1017/CBO9781107415324.004.

[86] S.B. Kumar, D. Moslemian, M.P. Duduković, Gas-holdup measurements in bubble columns using computed tomography, AIChE J. 43 (1997) 1414–1425. doi:10.1002/aic.690430605.

[87] A. Efhaima, Scale-up investigation and hydrodynamics study of gas-solid fluidized bed reactor using advanced non- invasive measurement techniques, (2016).

[88] N.Y. Ali, Evaluating of scale-up methodologies of gas-solid spouted beds for coating triso nuclear fuel particles using advanced measurement techniques, (2016).

[89] F.S. Al Falahi, Experimental investigation of the pebble bed structure by using gamma ray tomography, Missouri University of Science and Technology, 2014.

[90] M. Schubert, C. Zippe, Liquid flow texture analysis in trickle bed reactors using high-resolution gamma ray tomography, Chem. Eng. J. 140 (2008) 332–340. doi:10.1016/j.cej.2007.10.006.

[91] M. Al Mesfer, A. Sultan, M. Al-Dahhan, Impacts of dense heat exchanging internals on gas holdup cross-sectional distributions and profiles of bubble column using gamma ray Computed Tomography (CT) for FT synthesis, Chem. Eng. J. 300 (2016) 317–333. doi:10.1016/j.cej.2016.04.075.

[92] D. V. Kalaga, H.J. Pant, S. V. Dalvi, J.B. Joshi, S. Roy, Investigation of hydrodynamics in bubble column with internals using radioactive particle tracking (RPT), AIChE J. 63 (2017) 4881–4894. doi:10.1002/aic.15829.

[93] D. V. Kalaga, A. Yadav, S. Goswami, V. Bhusare, H.J. Pant, S. V. Dalvi, J.B. Joshi, S. Roy, Comparative analysis of liquid hydrodynamics in a co-current flow-through bubble column with densely packed internals via radiotracing and Radioactive Particle Tracking (RPT), Chem. Eng. Sci. 170 (2017) 332–346. doi:10.1016/j.ces.2017.02.022.

[94] U.P. Veera, K.L. Kataria, J.. Joshi, Gas hold-up profiles in foaming liquids in bubble columns, Chem. Eng. J. 84 (2001) 247–256. doi:10.1016/S1385-8947(00)00287-4.

III. IMPACT OF HEAT-EXCHANGING TUBE CONFIGURATIONS ON THE GAS HOLDUP DISTRIBUTION IN BUBBLE COLUMNS USING GAMMA-RAY COMPUTED TOMOGRAPHY

Abbas J. Sultan, Laith S. Sabri, Muthanna H. Al-Dahhan[†]

Multiphase Reactors Engineering and Applications Laboratory (mReal), *Department of Chemical and Biochemical Engineering, Missouri University of Science and Technology, Rolla, MO 65409-1230. USA*

ABSTRACT

An advanced gamma-ray computed tomography (CT) technique was used for the first time to visualize and quantify the impacts of the presence of heat-exchanging tubes and their configurations on the gas-liquid distributions and their profiles in a 6-inch (0.1524 m O.D.) Plexiglas® bubble column in an air-water reactor. Two superficial gas velocities (i.e., 0.2 and 0.45 m/s) were employed to simulate the churn turbulent flow regime. To investigate the impact of vertical internals configurations, three arrangements (i.e., hexagonal, circular without a central internal, and circular with a central internal) were employed in addition to the column with no internals. Using the same sized vertical internals and the same occluded cross-sectional area (CSA), it was found that the configuration of the vertical internals significantly impacted the gas holdup distribution over the CSA of the column. All studied superficial gas velocities resulted in symmetrical gas holdup distributions over the CSA of the bubble columns without vertical internals; however, the columns equipped densely with vertical internals did not have symmetrical gas holdup distributions. The presence of an extra central tube in the circular configuration played a key role in the gas-liquid distribution over the CSA of the bubble column. The hexagonal configuration had the advantage of providing the best spread of the gas phase over the entire CSA of the column. Gas holdup values at the wall region of the bubble

column increased with the addition of vertical tubes in all investigated configurations. However, a remarkable increase in the gas holdup values was obtained with the hexagonal configuration. The experimental data (i.e., gas holdup distributions and their diametrical profiles) can help to evaluate and validate three-dimensional (3-D) computational fluid dynamics (CFD) simulations to better predict the hydrodynamic parameters involved in these types of reactors.

Keywords: Bubble column with vertical internals, tube configurations, gas holdup distribution, computed tomography (CT).

[†]Correspondence author at Chemical & Biochemical Engineering Department, Missouri University of Science and Technology, Rolla, MO, 65409. Tel.: +1 573-578-8973. E-mail: aldahhanm@mst.edu

1. INTRODUCTION

In the chemical [1], biochemical [2], petroleum [3], petrochemical [4], metallurgical [5], and waste treatment industries [6] as well as in many industrial processes [7], bubble/slurry bubble column reactors are used due to their advantages over other multiphase reactors in terms of reactions and chemistry. Some of these processes are associated with highly exothermic reactions that require inserting dense heat-exchanging tubes inside these reactors to remove the excess heat and to maintain the desired conditions of these reactors, such as for the production of benzoic acid (with a heat of reaction of −628 kJ/mol) [8], production of cyclohexanol (with a heat of reaction of −294 kJ/mol) [9], production of acetone (with a heat of reaction of −255 kJ/mol) [10], Fischer-Tropsch (FT) synthesis (with heat of reaction of −210 kJ/mol) [11–13], and many others. The existence of such dense bundle of cooling tubes strongly impacts and alters the reactor's fluid

dynamics in a very complex manner that affects the phases distributions of the reactants (gas-liquid in bubble column or gas-catalyst-liquid in a slurry bubble column) and thus affects the performance of these reactors [14,15]. The non-uniform distribution of gas-liquid in a bubble column or gas-solid-liquid in slurry bubble column during the chemical reaction creates liquid/slurry circulation, radial and axial temperature gradients, and hot spots, where in the worst case scenario, a reactor runaway may occur, thereby reducing the activity of the catalyst [16,17].

Understanding the influence of heat-exchanging tubes and their arrangements (configurations) on the phase distribution in these reactors is essential to improving the design of these heat-exchanging tubes to enhance the gas-liquid or gas-slurry distributions and the dynamics inside these reactors. This enhancement of phase' distributions inside these reactors offers better contact between reactant phases, which enhance the heat, mass transfer, and chemical reaction rates, and ultimately affects the overall performance of the reactor. However, comprehending such complexity has been hampered due to lack of implementing advanced measurement techniques [12,18]. Therefore, fundamental knowledge of the impacts of the heat-exchange tubes on the hydrodynamics of bubble/slurry bubble columns is necessary to enhance the performance, design, and scale-up of these reactors.

The hydrodynamic studies of bubble/slurry bubble columns equipped with vertical internals have been reviewed in depth by Youssef et al. [8]. Their review revealed few investigations of the effect of heat-exchanging tubes (i.e., vertical internals) on the hydrodynamics of these columns, showing more experimental data is needed on this subject. Recently, Basha et al. [19] also reviewed and summarized current experimental

and modeling works conducted in bubble/slurry bubble columns, and recommended that further experimental studies be conducted to address the effect of the cooling tubes arrangements on the hydrodynamics of these reactors.

To design and scale up high-performance bubble/slurry bubble columns equipped with heat-exchanging tubes, the gas holdup distribution is one of the most crucial hydrodynamic parameters because the gas phase dictates the fluid dynamics of these reactors. The gas holdup distribution turns the liquid or the slurry (liquid-solid) phase circulation and controls the movement and mixing of the liquid/slurry; consequently, it governs the mixing characteristics and the mass and heat transfer rates, in essence, the overall performance of these reactors [20,21]. However, only a small number of experimental studies account for the effects of these vertical cooling tube bundle on the gas holdup distribution [22,23].

Among these few studies, Yamashita [24] investigated the impacts of vertical pipes and rods on the overall gas holdup in three bubble column diameters (i.e., 0.08, 0.16, and 0.31 m) using an air-water system. The experimental results indicated an increase in the magnitude of the overall gas holdup as the number of tubes and their sizes increased, while the overall gas holdup decreased with reductions in the distance between the internals.

Saxena et al. [25] also employed a 12-inch (0.305-m) diameter bubble column equipped with internals blocking 1.9, 2.7, and 14.3% of the total cross-sectional area (TCSA) of the column to address the impacts of the vertical internals on the overall gas holdup for an air-water-glass beads system. It was found that the overall gas holdup in the slurry bubble column equipped with 37 tubes (occupying 14.3% of the TCSA of the column) was higher than that of the column with seven tubes (blocking 2.7% of the TCSA

of the column). Nevertheless, the overall gas holdup, as in the aforementioned studies, is considered a global parameter, and hence, provides no information about how the vertical internal tubes affect the phase distributions and flow pattern inside bubble/slurry bubble column reactors.

Chen et al. [26] were the first group that applied gamma-ray computed tomography (CT) to investigate the effect of the vertical internals on the gas holdup distribution in an 18-inch (0.44 m) bubble column for air-water and air-drakeoil systems at superficial gas velocities with a range of 0.02-0.1 m/s that were calculated based on the TCSA of the column. The internals bundle represented the process of liquid-phase methanol (LPMeOH) synthesis, where it occupied 5% of the TCSA of the reactor. Their results showed that the existence of the vertical internals caused a slight increase (about 10%) in the gas holdup at the core region of the column. In addition, the experimental data revealed that the gas holdup distribution was axisymmetric in the fully developed flow region for systems in bubble columns both with and without internals. Moreover, the measured gas holdup for the air-drakeoil system was lower than the gas holdup for the air-water system due to the former system having a much higher viscosity than the latter. This leads to the formation large bubbles that have higher bubble rise velocities, which causes a decrease in the residence time of the gas (bubbles) as compared with the small bubbles in an air-water system. However, the range of superficial gas velocity used in this study was low (not deeply into the churn turbulent flow regime); hence, they did not address and evaluate the effect of the vertical internal tubes on the gas holdup distributions and their profiles at high superficial gas velocities, which is of industrial interest in achieving high volumetric productivity in these reactors. Additionally, the bundle of vertical internals used in their

work obstructed a low fraction of the bubble column, which did not reflect the presence of the dense heat-exchanging tubes that are employed in high exothermic reactions as mentioned earlier. Furthermore, the obtained increase in the gas holdup magnitude for the bubble column with vertical internals could not be explained only by the presence of these internals, but by the fact that the superficial gas velocities were calculated on the basis of the TCSA of the column, where a similar amount of the gas phase (air) was only applied to the column with vertical internal tubes. Therefore, the existence of vertical internal tubes in the bubble column reduced the cross-sectional area of the flow and subsequently increased the interstitial gas velocity in the column, which eventually caused an increase in the magnitude of the gas holdup.

There is a lack of modeling and simulation of bubble columns equipped with vertical tubes due to the high complexity of the multiphase flow in these reactors, especially when they are equipped with dense vertical internals. Among the very few simulation studies, Larachi et al. [27] built 3D computational fluid dynamics (CFD) simulations for five pilot-scale plant bubble columns (1 m in diameter), with and without vertical internals, for an air-water system at a superficial gas velocity of 0.12 m/s to investigate the impacts of these tubes on the flow pattern in these columns. Their simulation showed that the configurations of the tube bundles significantly affected the flow pattern of the bubble columns. This impact was particularly remarkable when the tubes were non-uniformly arranged over the cross-sectional area of the column. However, these simulation results for bubble columns with internals were not validated and compared against any benchmark experimental data because there is little experimental data for bubble columns equipped with bundle of heat-exchanging tubes.

Youssef and Al-Dahhan [28] for the first time used a 4-point fiber optical probe technique to assess the effects of the vertical internals bundle on the local gas holdup profiles in an 8-inch (0.2-m) diameter bubble column for an air-water system at superficial gas velocities of 0.03-0.2 m/s, which were computed based on the TCSA of the column. These internals covered 5% and 22% of the TCSA of the column to represent the heat-exchanging tubes employed in industrial LPMeOH and FT processes, respectively. Their findings revealed that internals covering 5% of the TCSA had no significant effect on the gas holdup, while internals covering 22% of the TCSA of the column led to a significant increase in the gas holdup magnitude.

Balamurugan et al. [29] enhanced the overall gas holdup in a 6-inch (0.15-m) bubble column in an air-water system by designing, developing, and testing helical spring as vertical internals. They reported significant increases of 230% and 150% for the overall gas holdup values in the bubble column operated at superficial gas velocities of 0.12 m/s and 0.4 m/s (calculated based on the TCSA of the column), respectively. Additionally, they concluded that geometry, the material of construction, and properties of the helical spring internals had a significant effect on the overall gas holdup.

Youssef et al. [30] extended their investigation to a large-scale bubble column (0.44 m in diameter) equipped with a bundle of vertical internals to study the impact of these internals on the local gas holdup profiles in an air-water system under the churn turbulent flow regime (0.2, 0.3, and 0.45 m/s of superficial gas velocity computed based on the TCSA of the column) by using a 4-point fiber optical probe. In this investigation, they used different designs of the internals that included circular (5% of the TCSA of the column) and hexagonal (25% of the TCSA of the column) arrangements. Analysis of the local gas

holdup data revealed that the presence of intense internals (25% of the TCSA of the column) led to a remarkable increase in the magnitude of the local gas holdup values.

Guan et al. [31] presented experimental results of the gas holdup profiles measured by an electrical resistivity probe in a 0.8 m diameter bubble column equipped with pin fin tubes (covering 9.2% of the TCSA of the column) for an air-water system in a wide range of superficial gas velocities (0.08-0.62 m/s calculated based on the free cross-sectional area [FCSA] of the flow). The authors observed that the presence of the pin fin tubes increased the overall gas holdup and altered the local gas holdup profiles. Also, they reported that the height of the distributor region decreased in the presence of the pin fin tubes. Moreover, arranging the internals non-uniformly over the cross-sectional area of the column (having removed two internals) caused strong gas short-circuiting, even without downward liquid flow.

Kagumba and Al-Dahhan [32] examined the influence of different sizes and configurations of vertical tubes on the local gas holdup in a 5.5-inch (0.14-m) inner diameter Plexiglas® bubble column with and without internals at a wide range of superficial gas velocities (0.03-0.45 m/s) for an air-water system using a 4-point fiber optical probe. Also in their experimental work, they investigated the effect of using a superficial gas velocity that was calculated based on the TCSA and FCSA of the column on the overall and local gas holdup in a bubble column equipped with vertical internal tubes. Two sizes of internals (0.0127 and 0.0254 m in diameter) were employed, where both sizes of the internals were designed to occupy 25% of the TCSA of the column to simulate industrial FT reactor's heat-exchanging tubes. The overall and local gas holdup at the center of the column significantly increased in the bubble columns equipped with

vertical internal tubes when these columns operated at a superficial gas velocity calculated based on the TCSA of the column. Additionally, compared to the column without vertical internals, the local gas holdup values were higher in bubble column equipped with 0.0127 m vertical internals operated in the bubbly flow regime, particularly at a superficial gas velocity of 0.03 m/s computed based on the FCSA of the flow. Moreover, size of the vertical internals was insignificant in affecting the gas holdup values when the bubble columns with vertical internals operated at a high superficial gas velocity (0.45 m/s), which was calculated based on the FCSA of the flow. Furthermore, the gas holdup values obtained in the bubble column without internals can be extrapolated to a column equipped with internals if it operates at superficial gas velocities calculated based on the FCSA of the flow. However, in this work, the vertical internals were designed differently for each size of internals. For example, the 0.0127 m internals were arranged in a hexagonal shape, while the 0.0254 m internals were arranged in a circular shape. Hence, the change in the magnitude of the local gas holdup profiles might have been caused by the different configuration of the internals, not by the difference in the size of the internals. Therefore, further investigations are needed to determine which variable was responsible for the change in the local gas holdup values.

Jasim [33] investigated the effect of internals configurations and their size on the gas holdup measured in the same experimental setup and conditions as Kagumba and Al-Dahhan [32]. He designed and developed a circular configuration for 0.5-inch (0.0127-m) internals, where all the internals were arranged and distributed uniformly across the CSA of the column to compare it with the hexagonal configuration to assess the impact of the configurations (i.e., circular and hexagonal) on the gas holdup. To investigate the impact

of the size of the internals Jasim [33] compareded the gas holdup values measured with 0.5-inch (0.0127-m) and 1-inch (0.0254-m) internals arranged in a circular shape, concluding that the 0.5-inch (0.0127-m) internals with a circular configuration gave symmetric gas holdup profiles along the diameter of the column, while the 0.5-inch (0.0127-m) internals with the hexagonal arrangement led to a distinct asymmetric gas holdup diameter profile. Also, the 1-inch (0.0254-m) internals enhanced the local gas holdup at the wall region more than the 0.5-inch internals arranged in a circular shape.

Recently, to investigate and quantify the influence of these tubes on the cross-sectional gas holdup distributions and their radial profiles, Al-Mesfer et al. [34] employed for the first time an advanced gamma-ray computed tomography (CT) technique for scanning a 6-inch (0.1524-m O. D.) Plexiglas® bubble column equipped with intense heat-exchanging tubes (about 25% of the TCSA of the reactor), representing the Fischer-Tropsch synthesis (FTS) reactor's internals. These vertical internal tubes were arranged in a hexagonal-like shape, with a pitch of 21 mm over the CSA of the bubble column. They used an air-water system with a broad range of superficial gas velocities (0.05-0.45 m/s), calculated based on the total and free CSAs. Thus, they demonstrated the effect of the manner in which the superficial gas velocity is calculated, compared to columns without vertical internals. The CT scan images showed that the gas holdup distributions were symmetrical (uniform) over the CSA in the bubble column without internals but asymmetrical (nonuniform) at higher superficial gas velocities (0.3 and 0.45 m/s) for a bubble column with internals. Also, gas holdup values increased significantly when the bubble column operated at superficial gas velocities that were calculated based on the TCSA of the reactor, while little effect was noticed when the same superficial gas velocities

were computed based on the FCSA of the flow. Another key finding was that the overall and local gas holdup results under a churn turbulent flow regime in the column without vertical internal tubes could be extrapolated to those reactors with vertical internal tubes if the superficial gas velocity based on the FCSA of the flow was applied to those columns with vertical internal tubes.

Thus far, the influence of dense heat-exchanging tubes configurations on the gas holdup distributions and their profiles has not been investigated, and whether the presence of different designs of vertical internal tubes affects the gas-liquid distribution over the entire cross-sectional area of the bubble column remains an open question. Therefore, this work aims to target this issue for the first time by investigating the effects of tube configurations on the gas-liquid distribution and their profiles at different superficial gas velocities (particularly at the high superficial gas velocities of 0.2 and 0.45 m/s calculated based on the FCSA of the column) by using advanced gamma-ray computed tomography. The particular goals of this work were to (1) visualize and quantify the effect of the internals configurations on the gas holdup distributions and their profiles; (2) examine the effect of the superficial gas velocity on the gas holdup distributions and their profiles, and (3) identify which configuration provides a better distribution of the gas holdup over the entire CSA of the column.The knowledge gained by conducting this research will improve the level of fundamental understanding of the effect of the design of heat-exchanging tubes on the gas holdup distributions in a bubble column. Also, the obtained experimental results will enlarge the database related to bubble columns with vertical internal tubes, such that they can then be used to evaluate and validate 3-D CFD simulations.

2. EXPERIMENTAL WORK AND MEASUREMENT TECHNIQUE

2.1. BUBBLE COLUMN SETUP

The Plexiglas® bubble column used in this study has an outer diameter of 6 inches (0.1524 m) and a height of 72 inches (1.83 m). The schematic diagram of bubble column equipped with vertical internals displays in Figure 1. The fluids used in the present work are dry air as the continuous gas phase, whereas purified water (i.e., provided by a reverse osmosis water filtration system) was employed as the liquid phase in batch mode. According to the most recent hydrodynamic study [35], which was conducted in a counter-current gas-liquid bubble column with two vertical internal tubes, operating the bubble column in counter-current mode for the liquid phase causes a significant increase in the gas holdup magnitude, while also decreasing the bubble velocity. Therefore, it would be interesting in future work to study the influence of vertical internals and their configurations on the gas holdup distribution when these columns operate under co-current or counter-current modes. For easier comparison to the literature, this study used an air-water system. The air was fed continuously to two calibrated flow meters connected in parallel to cover a wide range of superficial gas velocities. The gas entered the bubble column at the bottom of a plenum 0.3-m in height, was sparged through a perforated plate (gas distributor), and dispersed continuously in the form of bubbles in the bulk of the liquid phase. The gas distributor was stainless steel, with 121 holes, each 1.32 mm in diameter, distributed uniformly in a triangular pitch and offering 1.09% of the open area as exhibited in Figure 1.

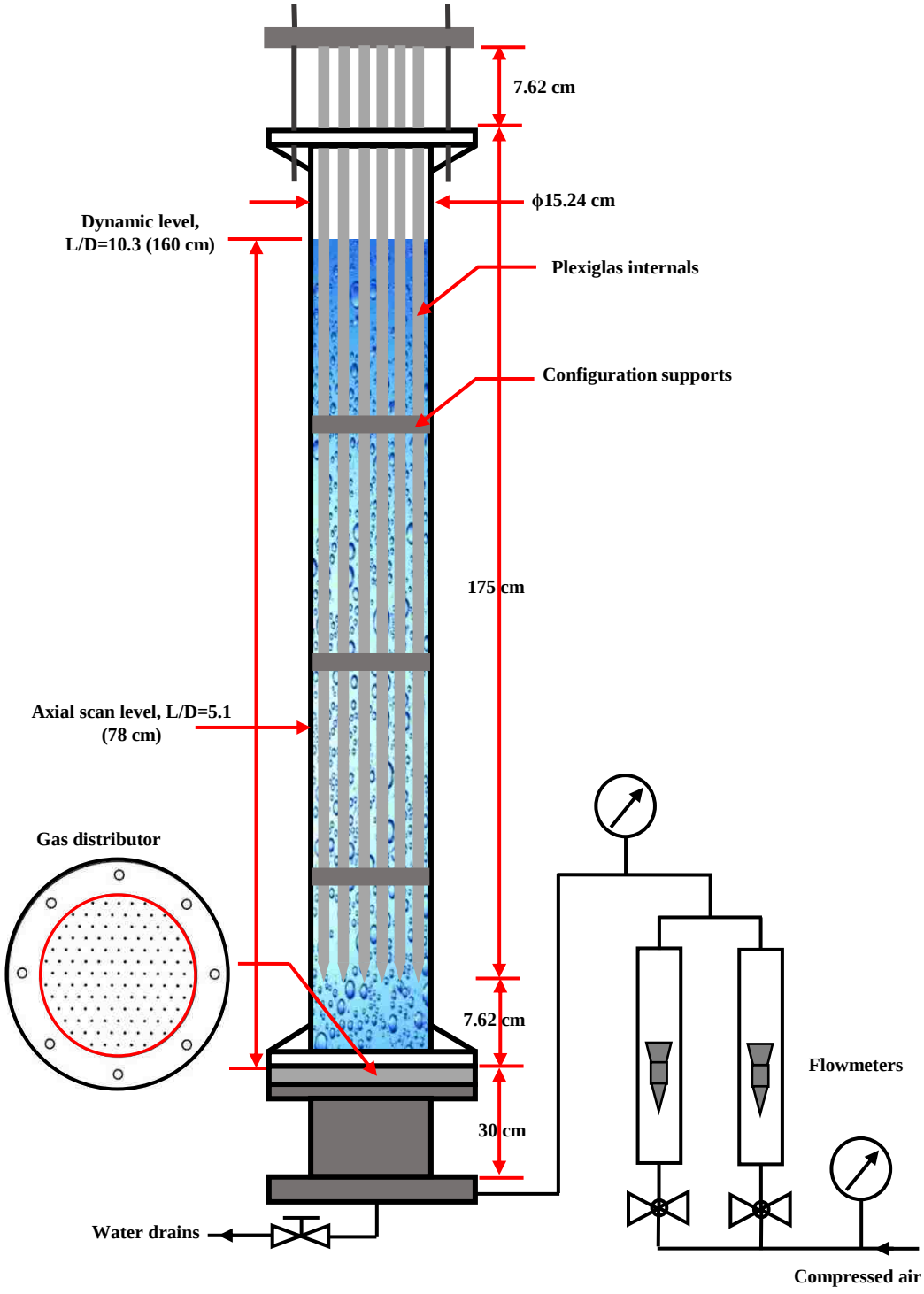

Figure 1: Schematic diagram of the experimental setup for a 6-inch bubble column with a bundle of vertical internal tubes

The dimensions of the column (H = 1.83 m, and D = 0.1524 m), aspect ratio (H/D=12), and gas distributor design (hole diameter = 1.32 mm) indicate that the gas holdup distribution and their profiles were independent of the column and gas distributor design, according to Wilkinson et al. [36], who reported that the gas holdup depends on the gas distributor design if the distributor holes are greater than 1 mm (i.e., coarse gas distributor). Additionally, Ong et al. [37] stated that under the churn turbulent flow regime (i.e., the condition of the current study), the influence of the gas distributor design with various sizes of holes (0.4, 0.5, and 1.25 mm) on the gas holdup distribution was negligible.

Three configurations of vertical internal tubes (i.e., hexagonal and circular without a central tube, and circular with a central tube) were employed in this work, as shown in Figure 2. Both the hexagonal and circular without central tube configurations consisted of 30 of vertical internal tubes while circular with central tube comprises 31 of 0.5-inch (0.0127-m) Plexiglas® vertical internal tubes. These vertical internals tubes covered 25% of the TCSA of the column to represent the same area that was occupied by industrial heat-exchanging tubes in FT synthesis [38–40]. The vertical internals in the hexagonal configuration were arranged in a triangular pitch of 2.1 cm over the CSA of the column, while the vertical internals of the circular configuration were organized in three concentric circles of 1-cm, 3.5-cm, and 5.5-cm diameters. Also, one tube was inserted vertically in the center of the circular configuration to assess the effect of adding a central tube on the gas holdup distributions. In this investigation, the internals for all configurations were housed and fixed vertically inside the column with a 3-inch (0.076-m) distance (i.e., the gap between the internals and the distributor) from the gas distributor, using three spacers/supports as well as the head plate, to prevent the vibration of the vertical internals

during the operation of the bubble columns. All experiments were conducted at ambient conditions as well as at the constant dynamic level of the gas-liquid dispersion (1.6 m above the distributor, H/D = 10.3, where H = dynamic level and D = diameter). Therefore, the initial liquid levels varied according to the studied superficial gas velocities. For example, the initial liquid height above the gas distributor in the bubble columns without internals, which operated at the superficial gas velocities 0.2 and 0.45 m/s was 1.1 and 0.92 m respectively, while the height was 1 and 0.85 m for the columns with internals operating at the same superficial gas velocities but calculated based on the free CSA of the flow. According to the dynamic level (H) and diameter (D) of the column used in this study, the bubble columns with and without vertical internals were operated with the aspect ratio (i.e., H/D) of 10.5, which is greater than the critical aspect ratio (5-10) [41] to ensure that the measured gas holdup distributions and their profiles were not influenced by the column size and the gas distributor design [42].

Depending on the nature of the industrial process, bubble columns can be operated in different flow regimes such as bubbly (homogeneous) and churn turbulent (heterogeneous) flow regimes. For example, the bubble columns in biochemical applications are operated in a bubbly flow regime, while they operate in the churn turbulent flow regime in a highly exothermic process [43]. A bubbly flow regime occurs at a low gas flow rate, and it is characterized by small uniform bubbles (i.e., no interaction and coalescence between bubbles) [44], while the churn turbulent flow regime occurs at a high gas flow rate and is characterized by the presence of a wide range of bubble size distribution (i.e., severe coalescence and break-up between bubbles).

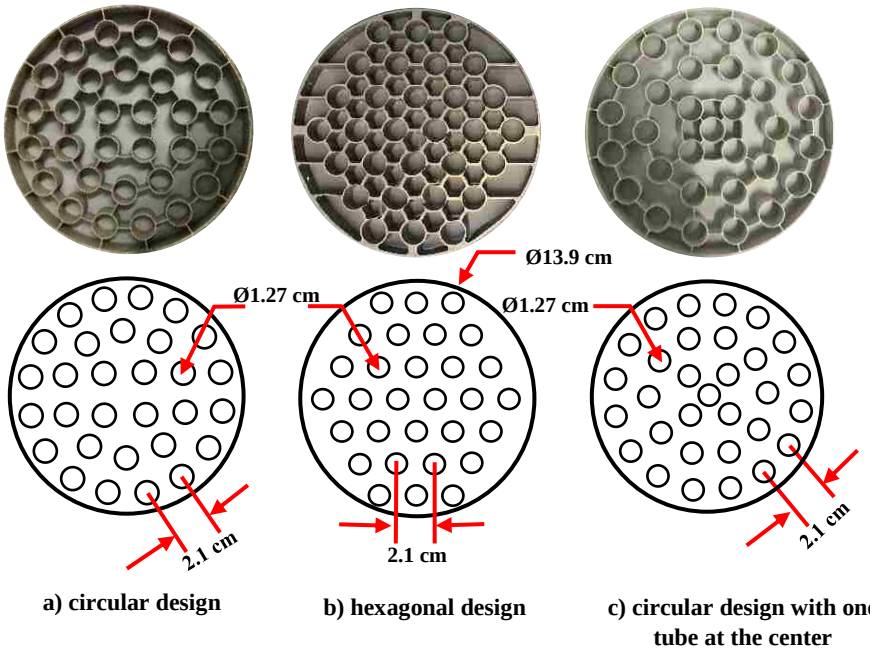

Figure 2: Schematic and photos of the top view of the investigated configurations of the vertical internal tubes

The cross-sectional gas holdup distributions and their profiles were measured at the churn turbulent flow regime, particularly at 0.2 and 0.45 m/s superficial gas velocities. These superficial gas velocities were selected based on simulating industrial interest conditions, which usually employ high superficial gas velocities (typically in the heterogeneous regime) to achieve high productivity [45–47]. It is important to note that the superficial gas velocity of the bubble column without vertical internal tubes was calculated based on the TCSA of the column, while it was computed based on the FCSA of the flow in the case of the bubble column equipped with bundles of internals. The FCSA of the flow was calculated as follows:

$$\begin{aligned} &Free\ cross\text{-}sectional\ area\ (FCSA)\ for\ the\ flow \\ &= total\ cross\text{-}sectional\ area\ (TCSA)\ of\ the\ column\ without\ tubes \\ &- cross\text{-}sectional\ area\ occupied\ by\ tubes \end{aligned} \quad (1)$$

It is important to mention that the static pressure inside the bubble column decreases when the gas flows upward (i.e., the gas expands). As a result, the superficial gas velocity could vary with the elevation of the bubble column [48]. However, due to experimental limitations, it was not possible to quantify the change in the superficial gas velocity in relation to column's height. Therefore, the superficial gas was calculated based on the empty column (i.e., the column not filled with water).

All the gas-liquid distributions and their diametrical profile measurements were performed at one axial level (L/D = 5.1) in the fully developed flow region where the gas holdup did not change axially for the bubble column without vertical internals [37,49]. Additionally, a recent hydrodynamic study [50] was conducted in a bubble column (0.1 m inner diameter) with vertical internals using ultrafast X-ray tomography to assess the effect of the internals layout on the gas holdup and bubble size distributions under bubbly and churn turbulent flow regimes.

In this study, the author scanned the column at three axial heights (H/D = 0.04, 5, and 7) to identify the height of the fully developed flow regime (i.e., equilibrium region) at two superficial gas velocities (i.e., 0.02 and 0.1 m/s).

The gas holdup and bubble size distributions in the fully developed flow regime reached an axial height from H/D = 5 to H/D = 7 (which is the same axial CT scan level used in the current study) in bubbly (i.e., at 0.2 m/s) and churn turbulent (i.e., 0.1 m/s) flow regimes where the gas holdup and bubble size distributions were found to be independent of the axial level within the fully developed flow region.

2.2. GAMMA-RAY COMPUTED TOMOGRAPHY (CT)

A novel dual-source gamma-ray computed tomography (CT) technique was designed, developed, and validated by Varma [51] to visualize and quantify the phase holdup distribution in three phases flowing in a multiphase flow system in a nondestructive way. This CT technique which is currently available at Multiphase Reactors Engineering and Applications Laboratory (mReal) in the Chemical and Biochemical Engineering Department, Missouri University of Science and Technology (Missouri S&T) was successfully implemented for imaging and measuring the phase distributions in different multiphase reactors including very dense systems (with high attenuation materials), opaque systems (with high gas holdup), and large-scale columns (up to 0.46 m,). Examples of these implementations of this CT scanner are visualized, and quantified of void fraction distribution in pebble bed [52], gas holdup distribution in a bubble column [53], solid and gas holdups distribution in spouted [54,55] and fluidized beds [56], etc. A photo and schematic diagram of the CT technique used in the present study are illustrated in Figure 3 and Figure 4. This CT scanner is composed of two gamma-ray encapsulated sources, namely cesium (^{137}Cs, with initial activity of ~250 mCi) and cobalt (^{60}Co with initial activity of ~50 mCi), which are well sealed and shielded by lead and tungsten containers, respectively, developed by Oak Ridge National Laboratory (ORNL). For each of these gamma-ray sources, there are 15 sodium iodide (NaI) detectors, which are located corresponding to each source with a distance of 1.2 m from the source as shown in Figure 3. In the present study, only a single gamma-ray source (^{137}Cs, with 662 keV photon energy), which is a part of this technique, was used to visualize and quantify the cross-sectional gas holdup distributions and their diametrical profiles in bubble columns with

and without a bundle of heat-exchanging tubes. The ^{137}Cs source was collimated by installing a window in the lead collimator to form a fan beam of gamma photons 5 mm in height and 40^{o} in width, oriented toward the detectors.

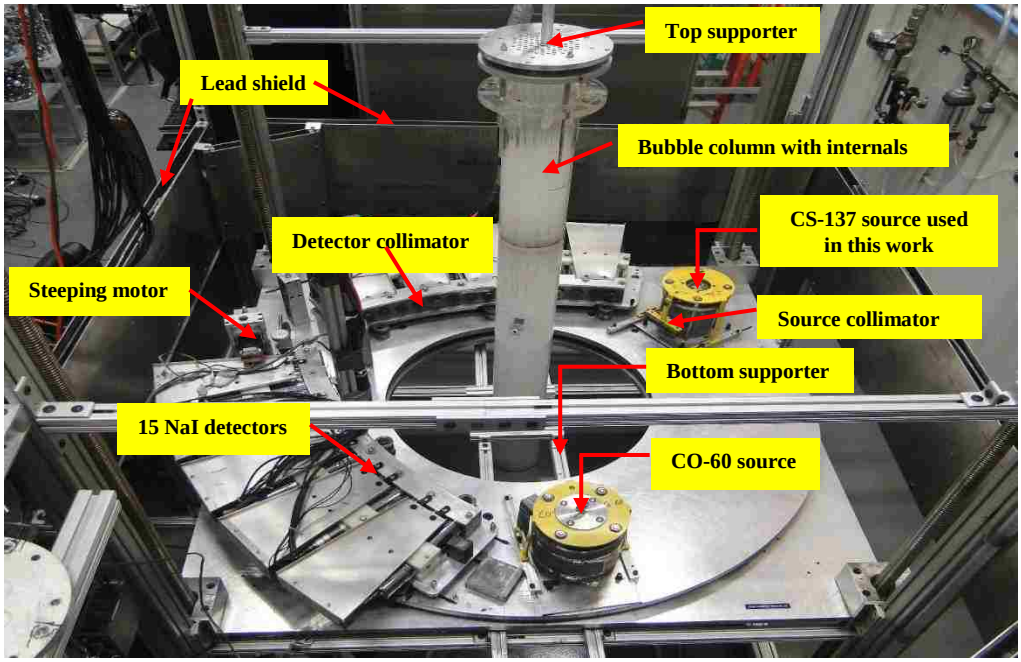

Figure 3: Photo of the dual source gamma-ray computed tomography (DSCT) technique at the Multiphase Reactors Engineering and Applications Laboratory (mReal), while scanning a bubble column equipped with a bundle of vertical internal tubes

These detectors were also collimated with lead, where each collimator had an open rectangular area (2 mm × 5 mm) to receive and record only the lines (beams) of gamma rays that passed through this open slit, thus reducing the effects of gamma scattering [57]. The collimated ^{137}Cs source and its array of detectors were installed on a stainless steel rotating circular plate that was connected from the bottom to a fixed square plate. These plates had a circular opening 30 inches (0.75 m) in diameter dedicated for objects to be scanned. These square and circular plates could be moved axially to scan the objects along their heights to provide 2-D cross-sectional images at specific axial elevations. The

capability to move up or down enabled this CT technique to create a 3-D image of the phase distribution if many scans were taken along the column's height, allowing for scans at various axial levels up to 2.75 m in height and 0.75 m in diameter. A detailed description of the hardware and software used in this CT technique can be found elsewhere [51].

During CT scanning of the bubble columns in the presence and absence of the vertical internals, the collimated ^{137}Cs source shot narrow beams of gamma-rays as it rotated automatically around the column using a stepping motor that controlled the angular movement (view) of the circular plate. For each view of rotation (^{137}Cs source position), the array of detectors, which are located opposite the source, also moved automatically through 21 fine steps (detector positions or projections) at an angle of 0.13° from the ^{137}Cs source using another independent stepping motor. Thus, for a complete scan (360^{o}), this CT technique offers 197 views, and for each of those views, there are a 315 (21 step × 15 detectors) projections. As a result, more than 62,000 projections pass through the column at different angles. As these projections of gamma-rays, pass through the column, they are recorded and transmitted to the computer as counts. These counts were acquired with a sampling rate of 60 samples of data at a frequency of 10 Hz, with a full scan requiring 8.5 hours. The acquired projections data are usually processed by a computer using a number of reconstruction algorithms such as Fourier transform (FT) [58], back projection (BP) [59], filtered back projection (FBP) [60], simultaneous iterative reconstruction technique (SIRT) [61], expectation maximization (EM) [62], and alternating minimization [63], to reconstruct the linear attenuation coefficients (μ, cm^{-1}) distribution of the medium that was scanned. Among these reconstruction algorithms, the EM algorithm has been widely used to reconstruct the phase distributions of various multiphase reactors [37,64,65].

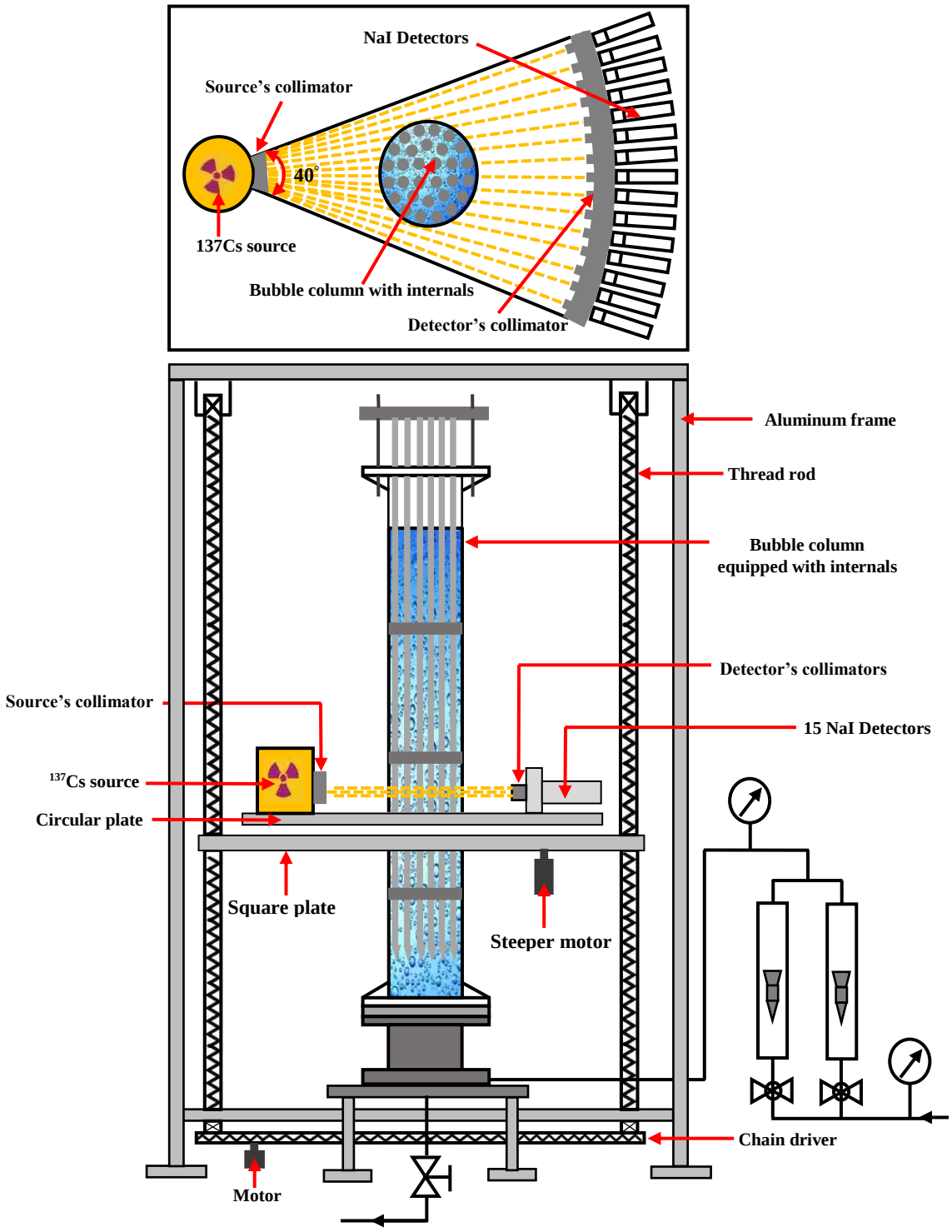

Figure 4: Schematic diagram of a single source gamma-ray computed tomography (CT) technique and bubble column equipped with a bundle of vertical internal tubes

However, the AM algorithm, developed by O'Sullivan and Benac [63] and applied and introduced successfully by Varma [51] to create images of the phase distribution, is currently used instead of the EM algorithm because the AM algorithm exhibits overall better enhancement in the quality of images, according to the comparative study performed by Varma et al. [66]. Therefore, in the present work, the AM algorithm was implemented to reconstruct all phase distributions images in the bubble columns in the presence and absence of vertical internals.

The experimental steps for scanning the bubble column without vertical internal tubes is as follows:

- Perform a scan without the column between the ^{137}Cs source and its detectors to obtain a reference scan ($I_\circ$).
- Conduct a scan of the column filled only with water to get (I_l); then, calculate the transmission ratio ($I_l/I_\circ$) to find $A_{l,ij}$, as follows:

$$A_{l,ij} = \mu_{l,ij} L_{ij} \tag{2}$$

- Scan the bubble column without vertical internals operated at the studied superficial gas velocity $(I_{g\text{-}l})$; then, compute the transmission ratio $(I_{g\text{-}l}/I_\circ)$ to determine $A_{g\text{-}l,ij}$, as follows:

$$A_{g\text{-}l,ij} = \mu_{g\text{-}l,ij} L_{ij} \tag{3}$$

In contrast, the experimental procedure for scanning a bubble column equipped with vertical internal tubes is as follows:

- Perform a scan without the column as a reference scan ($I_\circ$).
- Conduct a scan for the column without vertical internals and only filled with water to get (I_l); then, calculate the transmission ratio ($I_l/I_\circ$) to determine $A_{l,ij}$.

- Scan the column equipped with vertical internal tubes and filled with water $(I_{l,s})$; then, find the transmission ratio ($I_{l,s}/I_{\circ}$) to calculate $A_{l\text{-}s,ij}$; as follows:

$$A_{l\text{-}s,ij} = \mu_{l\text{-}s,ij} L_{ij} \tag{4}$$

Scan the column with vertical internal tubes operated at the studied superficial gas velocity $(I_{g,l,s})$ and then finding the transmission ratio ($I_{g,l,s}/I_{\circ}$) to calculate $A_{g\text{-}l\text{-}s,ij}$.

$$A_{g\text{-}l\text{-}s,ij} = \mu_{g\text{-}l\text{-}s,ij} L_{ij} \tag{5}$$

After scanning the bubble columns with and without vertical internal tubes according to the above experimental steps, the transmission ratios for the individual scans were initially calculated based on the reference scans. Then, these transmission ratios were fed as input data for the alternating minimization (AM) algorithm to reconstruct the linear attenuation coefficients for each scan separately. Subsequently, the local gas holdup distributions in bubble columns with and without vertical internals were calculated using the following equations.

$$\varepsilon_{g,ij} = 1 - \frac{A_{g\text{-}l,ij}}{A_{l,ij}} = 1 - \left(\frac{\mu_{g\text{-}l,ij}}{\mu_{l,ij}}\right) \tag{6}$$

To calculate the local gas holdup in the bubble column equipped with vertical internal tubes, use Eq. 7:

$$\varepsilon_{g,ij} = \frac{A_{l\text{-}s,ij} - A_{g\text{-}l\text{-}s,ij}}{A_{l,ij}} = \frac{\mu_{l\text{-}s,ij} - \mu_{g\text{-}l\text{-}s,ij}}{\mu_{l,ij}} \tag{7}$$

where $\varepsilon_{g,ij}$ represents the local gas holdup in each pixel for the bubble column with and without vertical internal tubes; $\mu_{g\text{-}l,ij}$ is the linear attenuation coefficient of the gas-liquid in each pixel (cm^{-1}); $\mu_{l,ij}$ is the linear attenuation coefficient of the liquid without vertical internals in each pixel (cm^{-1}); $\mu_{l\text{-}s,ij}$ is the linear attenuation coefficient of the liquid-solid

in each pixel (cm^{-1}); and $\mu_{g\text{-}l\text{-}s,ij}$ is the linear attenuation coefficient of the gas-liquid-solid in each pixel (cm^{-1}). Further processing of the gas holdup distributions by removing the values of the vertical internals from the gas holdup distributions produced azimuthally and line-averaged gas holdup profiles.

More details about the method of calculating gas holdup based on the linear attenuation coefficients as well as the scan procedures for bubble columns with and without internals and the approach of excluding the vertical internals from the gas holdup distribution can be found in our previous publications. Recently we have validated this CT technique by scanning different cases of Plexiglas® phantom and have verified the reliability of this CT technique to visualize and quantify the phase distributions with high precision.

This CT technique has another feature that can also work as a gamma-ray densitometry (GRD) technique to measure (1) the line-averaged phase holdup, (2) identify flow regimes, (3) detect the maldistribution of phases, and (4) monitor and characterize the flow pattern of multiphase reactors by fixing (not rotating) the ^{137}Cs source and using only the middle detector, which is positioned opposite the center of the ^{137}Cs source [67].

2.3. THE ACCURACY AND REPRODUCIBILITY OF CT SCANS

Before scanning the bubble columns with and without vertical internals tubes, phantom (i.e., two concentric Plexiglas® cylinders) scanning was performed to adjust all the electronics, detectors, and related parameters to ensure the reliability of the technique and readiness for measurement at the desired conditions. Additionally, the accuracy of the CT results was checked and confirmed through various scanning cases for the phantom (i.e., empty phantom; the inner cylinder filled with water, while the outer cylinder was

empty) and the linear attenuation was reconstructed for different cases of the phantom. Compared to the theoretical values, the measured linear attenuation coefficient of water, air, and Plexiglas® were within 2.3% [34,52]. Then, to check the reliability of the CT measurements, the reproducibility of the measurement was evaluated for the cross-sectional gas holdup distributions and their profiles. Therefore, in the present study, CT scans were conducted at the axial level of the fully developed flow region (H/D = 5.1) for the 6-inch bubble column without vertical internal tubes under two operating conditions (0.05 and 0.45 m/s superficial gas velocities). For each superficial gas velocity, the CT scan was repeated twice on two successive days, and the cross-sectional gas holdup and its diametrical profiles were constructed as shown in Figure 5 and Figure 6. As can be noted these figures, the obtained gas holdups for two replications (runs No.1 and 2) of each condition (0.05 and 0.45 m/s) were identical qualitatively and quantitatively. To quantify the difference between the gas holdup profiles, the statistical difference in terms of the average absolute relative difference (AARD) was calculated using the following equation:

$$AARD = \frac{1}{N}\sum_{1}^{N}\left|\frac{\varepsilon_1(r) - \varepsilon_2(r)}{\varepsilon_1(r)}\right| \quad (8)$$

where $\varepsilon_1(r)$ and $\varepsilon_2(r)$ represent the gas holdup values of experiments No. 1 and 2, respectively, at the corresponding dimensionless radial positions. N represents the number of data points along the radius of the column. It was found that the AARD in the percentage between the gas holdup profiles for a superficial gas velocity of 0.05 and 0.45 m/s was approximately 2.62% and 1.74%, respectively. These outcomes display the attainment of excellent reproducibility, thus, confirming the reliability of the CT technique and its capability to reproduce gas holdup measurements. Thus, there was no need to replicate

many scans. However, in this work, all the gas holdup profiles were based on an average of two repeated measurements (two scans) of the gas holdup. The error bars were plotted in all subsequent diametrical profiles, but they cannot be seen clearly due to their small values, which lie within the data points along the diameter of the columns.

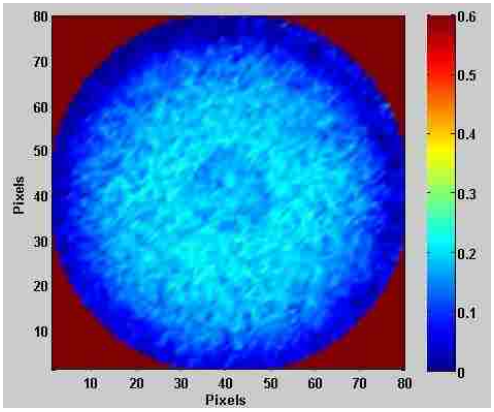

(a)Time-averaged cross-sectional gas holdup distribution in a 0.14 m inside diameter column without vertical internals for run#1 at a superficial gas velocity of 0.05 m/s

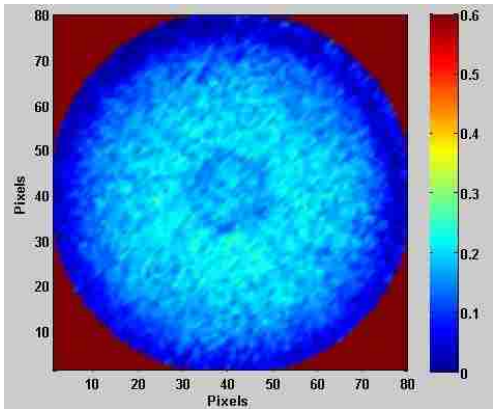

(b)Time-averaged cross-sectional gas holdup distribution in a 0.14 m inside diameter column without vertical internals for run#2 at a superficial gas velocity of 0.05 m/s

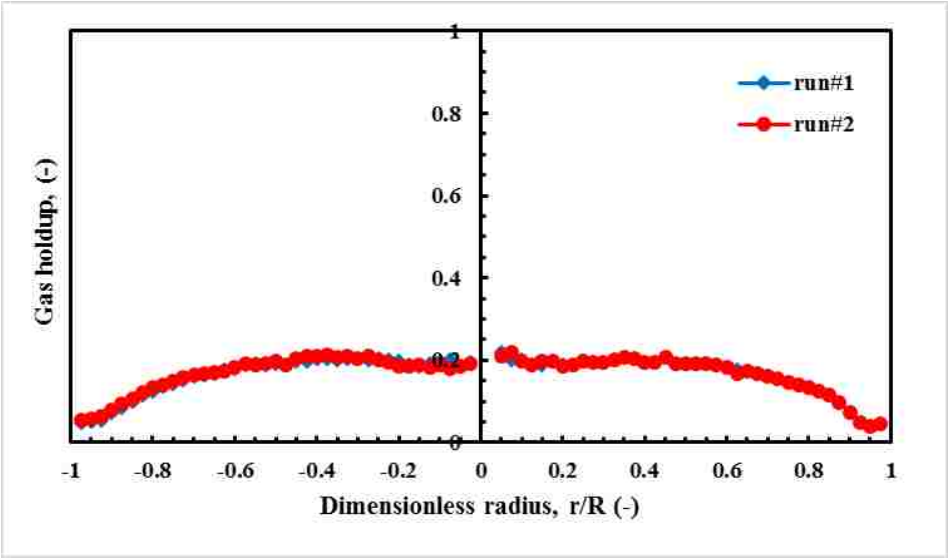

(c) Reproducibility of the diametrical gas holdup profiles measured in a 0.14 m inside diameter column without vertical internals at a superficial gas velocity of 0.05 m/s

Figure 5: Reproducibility of the cross-sectional gas holdup distributions and their diametrical profiles in a 0.14 m inside diameter column without vertical internal tubes at a superficial gas velocity of 0.05 m/s

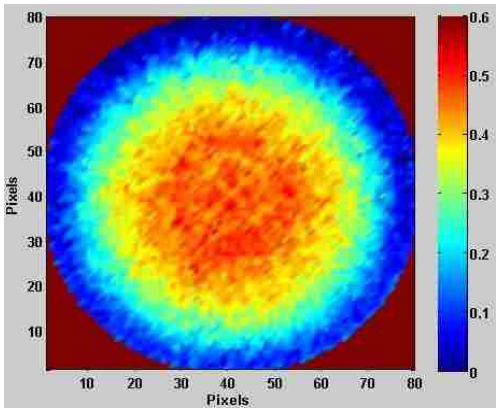

(a)Time-averaged cross-sectional gas holdup distribution in a 0.14 m inside diameter column without vertical internals for run#1 at a superficial gas velocity of 0.45 m/s

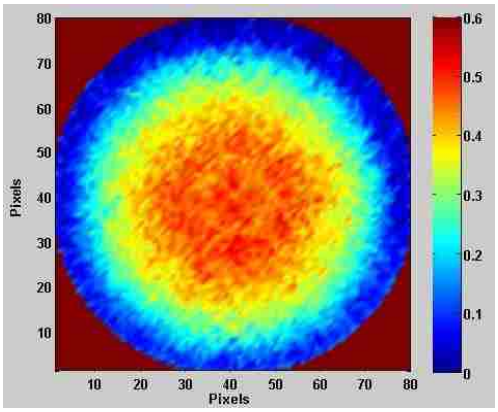

(b)Time-averaged cross-sectional gas holdup distribution in a 0.14 m inside diameter column without vertical internals for run#2 at a superficial gas velocity of 0.45 m/s

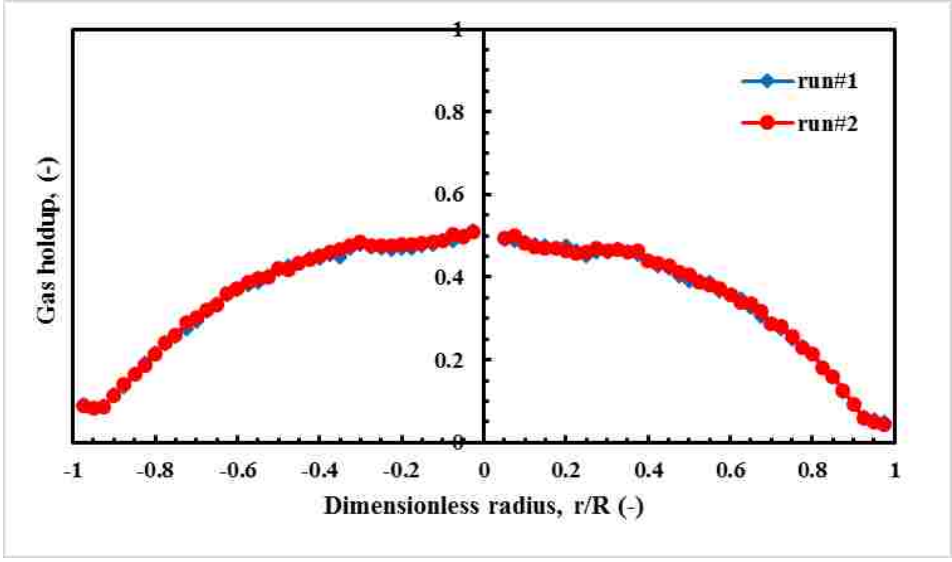

(c) Reproducibility of the diametrical gas holdup profiles measured in a 0.14 m inside diameter column without vertical internals at a superficial gas velocity of 0.45 m/s

Figure 6: Reproducibility of the cross-sectional gas holdup distributions and their diametrical profiles in a 0.14 m inside diameter column without vertical internal tubes at a superficial gas velocity of 0.45 m/s

Moreover, the means of the cross-sectional gas holdup distribution for the bubble column without vertical internals operated at superficial gas velocities of 0.05 and 0.45 m/s were calculated and compared with the overall gas holdup for the same operating conditions to check the accuracy of the measured gas holdup data using the CT technique.

The overall gas holdup was measured using the bed expansion method and calculated based on the change in the bed height as follows:

$$Overall\ gas\ holdup = \frac{(dynamic\ height\ of\ the\ bed\ (H_d) - static\ liquid\ height(H_s))}{dynamic\ height\ of\ the\ bed\ (H_d)} \quad (9)$$

The relative differences between the mean of the cross-sectional gas holdup and the overall gas holdup obtained by the bed expansion technique were 3.6% and 4.1% for the superficial gas velocities of 0.05 and 0.45 m/s, respectively. In terms of validating the CT technique, the reproducibility of the CT data, and its comparison with another independent method, these results confirmed the validity and reliability of the CT measurements for bubble columns with and without vertical internals.

3. RESULTS AND DISCUSSION

An analysis of the results of the time-averaged cross-sectional gas holdup distributions, azimuthally and line-averaged gas holdup profiles, and the extent of the gas holdup dispersion over the entire CSA of the column are presented in this section. The cross-sectional gas holdup distributions and their profiles were obtained by scanning at the fully developed flow region (L/D = 5.1) with four configurations of bubble columns, including bubble columns without vertical internals and bubble columns with three arrangements of vertical internal tubes (hexagonal, circular without a central tube, and circular with an extra central tube) operated the under churn turbulent flow regime (particularly at superficial gas velocities of 0.2 and 0.45 m/s). These results are analyzed and discussed in more detail in the following subsections.

3.1. VISUALIZING THE EFFECTS OF THE PRESENCE OF THE VERTICAL INTERNALS AND THEIR CONFIGURATION DESIGNS ON THE GAS HOLDUP DISTRIBUTIONS

Figure 7 displays the reconstructed time-averaged cross-sectional gas holdup distributions for all four studied bubble column configurations and superficial gas velocity. The color bar of these figures represents the magnitude of the gas holdup in each pixel, where the red color marks more gas, whereas the blue color means less gas holdup (more liquid holdup). The gas holdup distributions for bubble columns with vertical internals of different configurations were entirely dissimilar, despite their use of the same size vertical internal tubes and the same percentage of the occluded CSA (about 25% of the TCSA of the column) occupied by vertical internal tubes. This dissimilarity could result from using different geometric configurations of vertical internal tubes and their inter-tube gaps (spaces among vertical internals). Additionally, it is evident from the gas holdup distribution images that the presence of the vertical internal tubes and their arrangements alter the quality of the gas-liquid distribution over the CSA of the columns. Moreover, the CT technique was capable of visualizing qualitatively the gas and liquid phase behavior over the entire CSA of the columns as well as capturing the local variation of the gas holdup with superficial gas velocities in bubble columns in the presence and absence of a bundle of vertical internal tubes. The time-averaged cross-sectional gas holdup distributions present in Figure 7 clearly exhibit almost symmetric gas holdup distributions in bubble columns without vertical internals for all studied superficial gas velocities. On the other hand, the symmetric gas holdup distributions do not occur in the bubble columns equipped densely with vertical internal tubes.

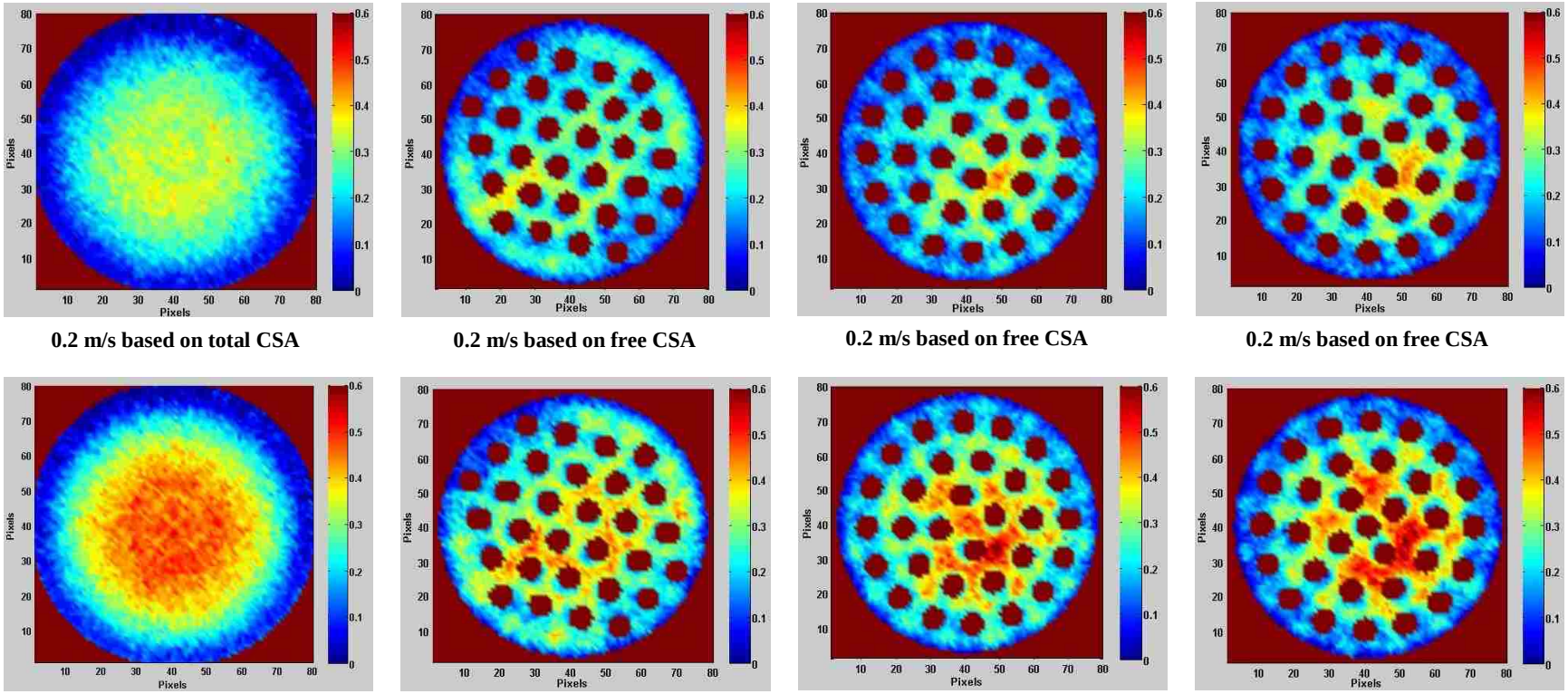

Figure 7: Effect of the internals configuration and superficial gas velocity on the time-averaged cross-sectional gas holdup distributions

However, the bubble column with vertical internals arranged circularly with the extra central tube had distinct asymmetric gas holdup distributions. This asymmetric (non-homogeneous spread of the gas phase over the CSA of the column) of the gas holdup distribution tended to increase as the superficial gas velocity rose. In addition, the well-known phenomenon in bubble column without internals, where there is more gas at the center and less gas near the wall region of the column, still occurred in the bubble column equipped with an intense bundle of vertical internals (blocking about 25% of the TCSA of the column) for all studied configurations. However, the gas holdup distributions varied according to the configuration used in these columns, and that means the large liquid circulation will be different. Therefore, further experimental investigations are necessary to address this issue, especially since there is no local liquid velocity data available in the literature for bubble column equipped with dense vertical internals arranged in different configurations; this is under consideration in our laboratory and will be the subject of future manuscripts.

Moreover, the presence of the vertical internal tubes enhanced the gas holdup near the wall region because the hexagonal and circular arrangements of these tubes spreads more gas towards the wall region. However, this enhancement was more pronounced for bubble column with a hexagonal arrangement of vertical internals because that arrangement provided the most clearance area (no vertical tubes were present in this area) between the bundle of internal tubes and the wall of the column. This clearance space could facilitate and allow for the accumulation of small bubbles because small bubbles have a lower bubble rise velocity than large bubbles. As a result, the residence time of the bubbles increased, causing increases in the gas holdup. Furthermore, the CT images disclose that

the existence of an extra central tube with a circular configuration reduced the gas holdup magnitude at the center of the column by pushing the gas out of this area. However, the absence of the central tube caused a remarkable increase in the gas holdup in this area, as shown in the circular configuration without a central vertical tube. This new and unusual finding needs to be considered in designing heat-exchanging tubes of pilot and commercial bubble/slurry bubble column reactors.

Qualitatively, the gas holdup distribution images revealed that the bubble column with vertical tubes arranged in a hexagonal shape provided more even (homogeneously distributed over the CSA of the column) gas holdup distributions over the entire CSA of the column than other configurations. From an industrial point of view, this finding is significant because the cross-sectional distribution of the gas holdup and liquid flow field and its circulation affect the quality and efficiency of the chemical reaction; hence, reactor performance is affected due to the contact between gas-liquid or gas-slurry phases in bubble/slurry bubble columns. These differences in the cross-sectional gas holdup distributions are mainly caused by the arrangements of the vertical internal tubes, whose diametrical profiles are quantified in the following section.

The reconstructed cross-sectional gas holdup distributions for bubble column without vertical internals are qualitatively in agreement with those obtained in the experiments using the same system (air-water) and reported in the literature [34,68,69]. However, the reconstructed gas holdup distributions images for bubble columns equipped with a bundle of vertical internal tubes arranged in different configurations have never before been reported. Therefore, these results add to the body of knowledge about the effect of heat-exchanging tubes on the gas-liquid structure over the CSA of a bubble column. In

addition, these experimental results serve as baseline data for the future assessment and validation of CFD simulations and phenomenological models towards better prediction of the performance of these reactors.

3.2. INFLUENCE OF THE PRESENCE OF VERTICAL INTERNALS AND THEIR ARRANGEMENTS ON THE AZIMUTHALLY AND LINE-AVERAGED GAS HOLDUP PROFILES

The influence of vertical internal tubes and their configurations as well as superficial gas velocities on the phases distribution was further demonstrated by the azimuthally and line-averages of the gas holdups in the cross-sectional images that illustrate the diametrical gas holdup profiles. The azimuthally averaged diametrical profiles for a 2-D image of the gas holdup distributions were computed by circularly averaging the pixel values of the gas holdup image after excluding the values of the tubes from the azimuthally and line-averaged profiles.

The methodology used to exclude the vertical internal tubes from these profiles was described in more detail in our previous publication. These azimuthally averaged profiles and the impacts of the configuration on the gas holdup are displayed in Figure 8 and Figure 9 for superficial gas velocities corresponding to the flow in the churn turbulent flow regime (0.2 and 0.45 m/s).

These azimuthal profiles demonstrate that the gas holdup values near the wall region of the columns increased in the presence of vertical tubes for the studied superficial gas velocities. However, the bubble column with the hexagonal configuration of tubes showed a noticeable increase in the gas holdup near the wall region, which did not occur for the other configurations. For example, using a superficial gas velocity of 0.45 m/s and

at the wall region (dimensionless radius, r/R = 0.8), an increase of 105% was obtained in the bubble column with the hexagonal configuration.

Additionally, a significant decrease was observed in the gas holdup values at the center of the column with the tubes arranged hexagonally. The possible cause of this phenomenon is the presence of the vertical internal tubes that enhance the bubbles' break-up rate under the churn turbulent flow regime inside the bubble column, which hinders the lateral movement of the bubbles. Consequently, the vertical internals allow only for smaller bubbles (smaller than the space between the vertical internals) to move radially toward the wall region, while these internals restrict and trap the larger bubbles at the center of the column. Such a phenomenon can be clearly distinguished in the bubble column with the hexagonal configuration because this arrangement had smaller inter-tube gaps and a large space (clearance) between the wall of the column and the vertical internals.

This observation was recently confirmed by conducting a comparative investigation and analysis in our laboratory to measure the bubble passage frequency and bubble chord length in the same experimental setup and operating conditions, using a 4-point fiber optical probe for the air-water system [33]. The experimental results showed that the bubble passage frequency (number of bubbles passing through a unit volume in the column per unit time) in the center of the column with the hexagonal configuration was lower than in the column with a circular configuration, while it was higher than in the column with the circular arrangement in the wall region.

This was due to the absence of tubes in this region, which could facilitate bubble rising, thereby increasing the gas holdup. For example, at the wall region and at a superficial gas velocity of 0.45 m/s, the percentage of increase in the bubble passage

frequency was 140%, while the percentage of decrease was 15.2% at the center of the column with the hexagonal configuration. Additionally, the bubble chord length (bubble size) in the bubble column with the hexagonal arrangement was smaller than in the column with the circular configuration at the center and the wall regions by 18% and 1.5%, respectively. Moreover, the bubble chord length was greater in the center than in the wall area for the column with the hexagonal configuration; and this strongly confirms the phenomenon of trapping the large bubbles in the center of the column and accumulating the small bubbles at the wall region. These experimental results, obtained using a 4-point fiber optical probe, showed increasing bubble passage frequency at the wall region, with decreasing frequency at the center.

Reducing the bubble chord length in the column with the hexagonal configuration was a factor that led to the gas holdup in the bubble column with the hexagonal configuration having a significant increase in the wall region, while it had a noticeable decrease at the center of the column. As discussed earlier, inserting an extra central tube in the circular configuration played an important role in the gas holdup distribution, where a significant decrease was observed in the gas holdup values at the center of the column in the case with the central vertical tube, while a noticeable increase was obtained in the absence of the central tube.

The underlying reason behind this variation in the gas holdup may result from effect of the wall lubrication force, which drives the bubbles away from the wall of the vertical internal tubes, thereby decreasing the gas holdup in the vicinity of the vertical internals and increasing the gas holdup in the gaps between the vertical internals.

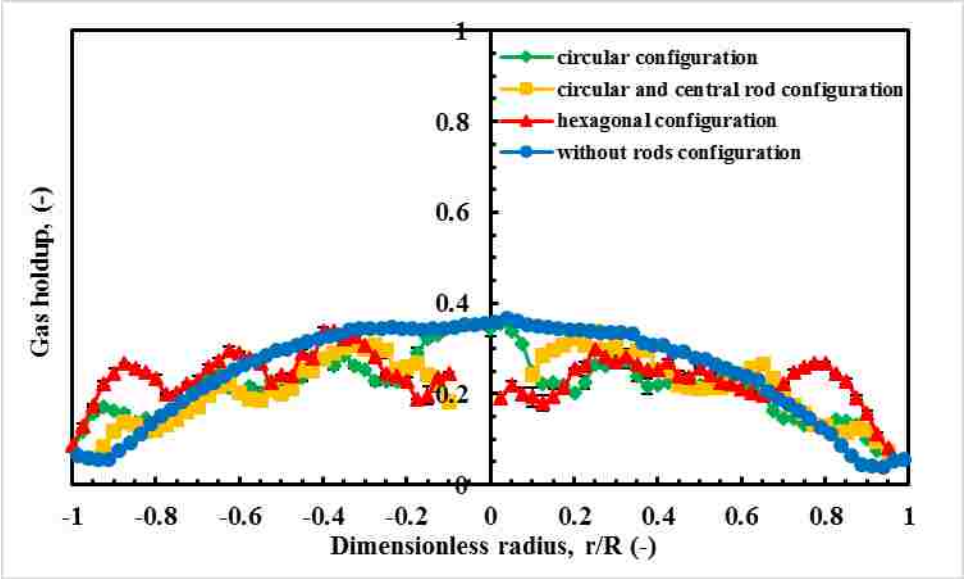

Figure 8: Effect of configuration on the azimuthally averaged gas holdup diametrical profiles at a superficial gas velocity of 0.20 m/s

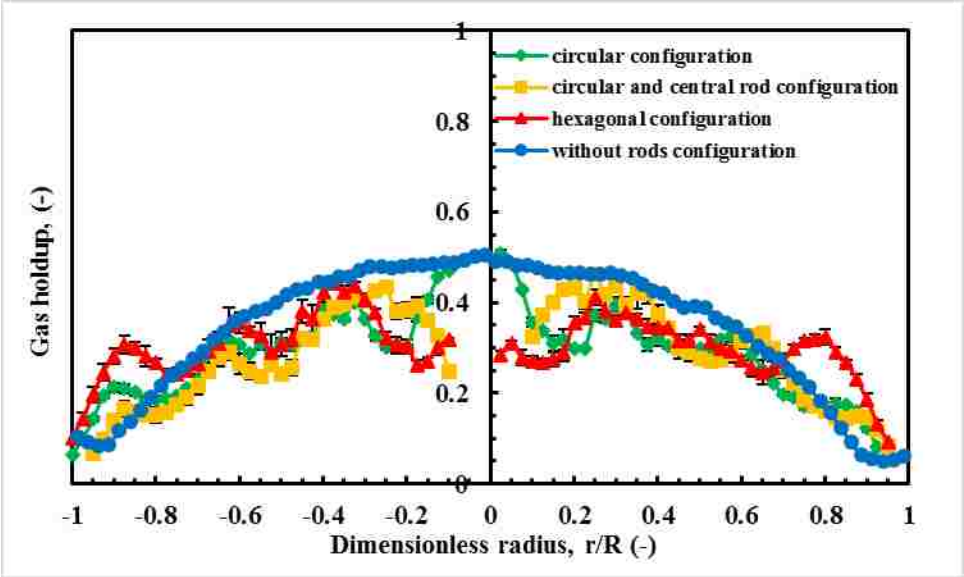

Figure 9: Effect of configuration on the azimuthally averaged gas holdup diametrical profiles at a superficial gas velocity of 0.45 m/s

In addition, the bubble column without vertical internal tubes exhibited a gas holdup profile for all studied superficial gas velocities shaped as a smooth parabola. The parabolic gas holdup profile of the bubble column without vertical internals, which was obtained in the current study and reported in the literature [64,70] under the churn turbulent

flow regime also followed a similar profile (i.e., parabolic shape), which is typical of coarse gas distributor (i.e., holes diameter greater than 1 mm) [71]. However, the bubble columns equipped with dense vertical internal tubes displayed wavy-shaped profiles along with a parabolic trend for all investigated configurations with vertical internals. These wavy profiles for the bubble columns with vertical internal tubes varied according to the configurations of the vertical internals in the bubble column. This variation in the gas holdup profiles among the bubble columns with vertical internals was due to the different arrangements of tubes over the CSA of the column, the shape of the pitch for each configuration, and the space (clearance) between the bundle of vertical internals and the column wall. Each concave area of these profiles represents the azimuthal average of the values of the gas holdup in the spaces among the vertical internal tubes. These kinds of wavy gas holdup profiles have not been reported in the literature for a bubble column with dense vertical internals when measured by optical probes. In the literature, parabolic profiles were only obtained in the columns with vertical internals, which were similar to those achieved in the bubble column without vertical internal tubes. However, wavy profiles were reported by Al Mesfer [40] and Al Mesfer et al. [34] when they measured the gas holdup in the bubble column with dense vertical internals using the CT technique. The difference between the gas holdup profiles measured by the optical probe and the CT technique are due to the limitations of the optical probe technique, such as the local point measurements and access issues for the probe, in particular in the bubble column equipped densely with vertical internals. For example, the gas holdup measurements made using an optical probe were usually conducted at four points (at the dimensionless radius, r/R (-) of 0, 0.3, 0.6, and 0.9) along the radius of the column and in the gaps (which usually had high

gas holdup values) between the vertical internal tubes. Hence, it was difficult to measure the local gas holdup in the vicinity of the internals, where there were usually low gas holdup values. However, this can be achieved by the CT technique, which measures the local gas holdup in an area not exceeding 3.62 mm^2 (area of each pixel in the gas holdup images) due to the size of the detector collimators that are used in this study (2 mm × 5 mm). For that reason, the wavy gas holdup profiles in the bubble column equipped with vertical internal tubes were not obtained using the optical probe.

Line-averaged gas holdup profiles in this study were calculated by averaging all the pixels of a gas holdup image in the vertical and horizontal directions, after excluding the tubes, to provide diametrical line-average profiles, as displayed in Figure 10, Figure 11, Figure 12, and Figure 13. In this study, the vertical and horizontal gas holdup profiles were also computed using another method because the azimuthally averaged profiles usually are calculated for symmetric systems over the entire CSA (i.e., gas holdup values are invariant along the pixels in the θ-direction). However, the bubble columns equipped densely with vertical internal tubes hardly maintained a perfect symmetric distribution as observed in the bubble column with vertical tubes because these vertical internals and their arrangements played a significant role in the gas-liquid distribution. Therefore, line-averaged profiles were computed. The line-averaged gas holdup profiles verify, the phenomenon of increasing gas holdup in the wall region of the column due to the insertion of dense vertical internal tubes. Interestingly, the diametrical profiles of the line-averaged (vertical and horizontal) gas holdup of the bubble columns with different configurations of vertical tubes were more similar to the gas holdup profiles in the core region of the bubble column without tubes, particularly with the dimensionless radius, r/R = 0-0.6).

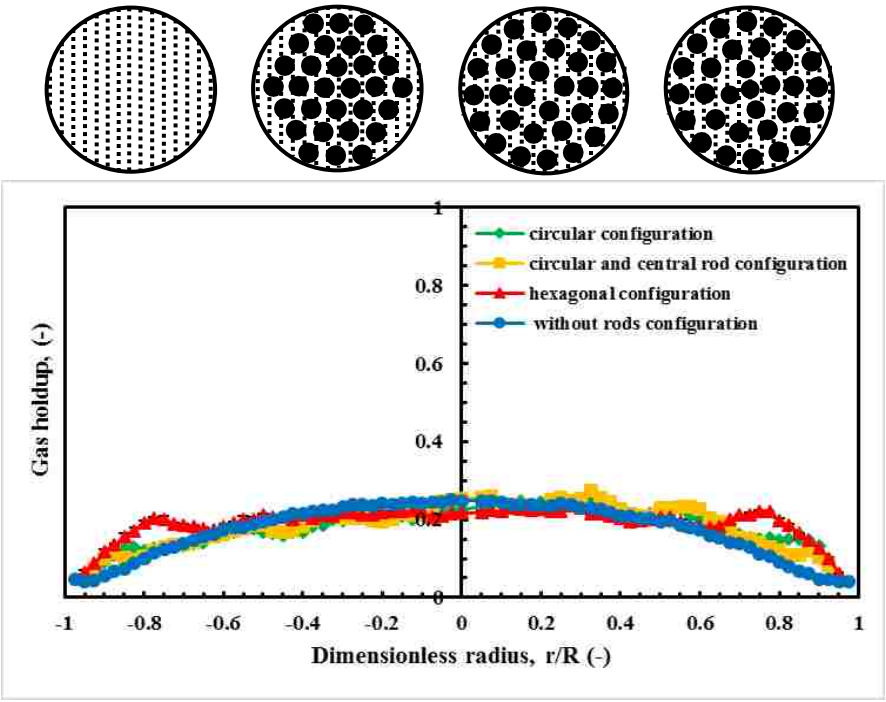

Figure 10: Comparison of the line-averaged (along the vertical pixels in the cross-sectional image, as shown schematically at the top of this figure) gas holdup profiles between different configurations of bubble columns at a superficial gas velocity of 0.2 m/s

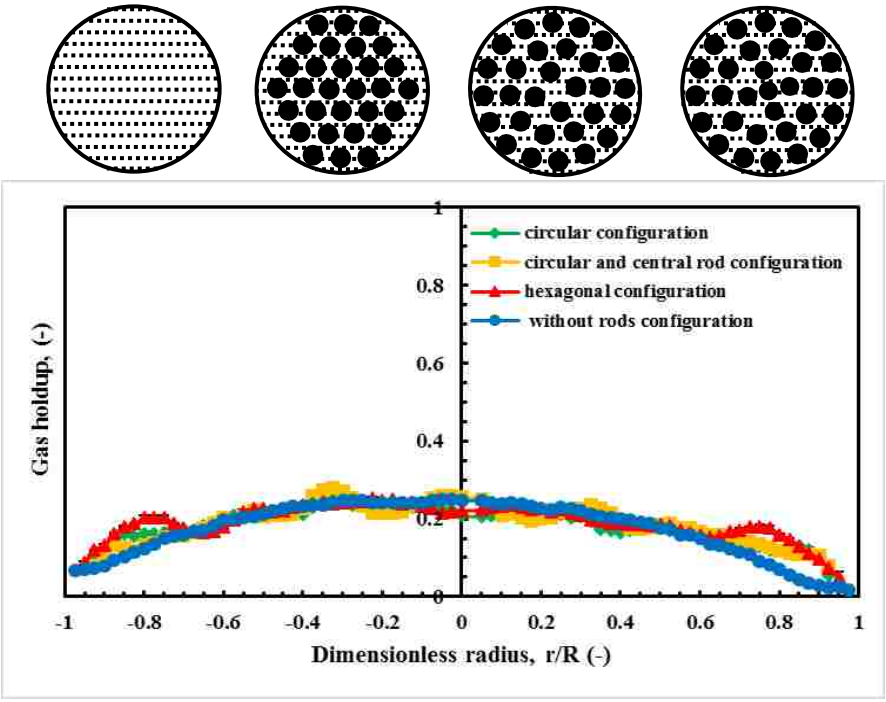

Figure 11: Comparison of line-averaged (along the horizontal pixels in the cross-sectional image, as shown schematically at the top of this figure) gas holdup profiles between different configurations of bubble columns at a superficial gas velocity of 0.2 m/s

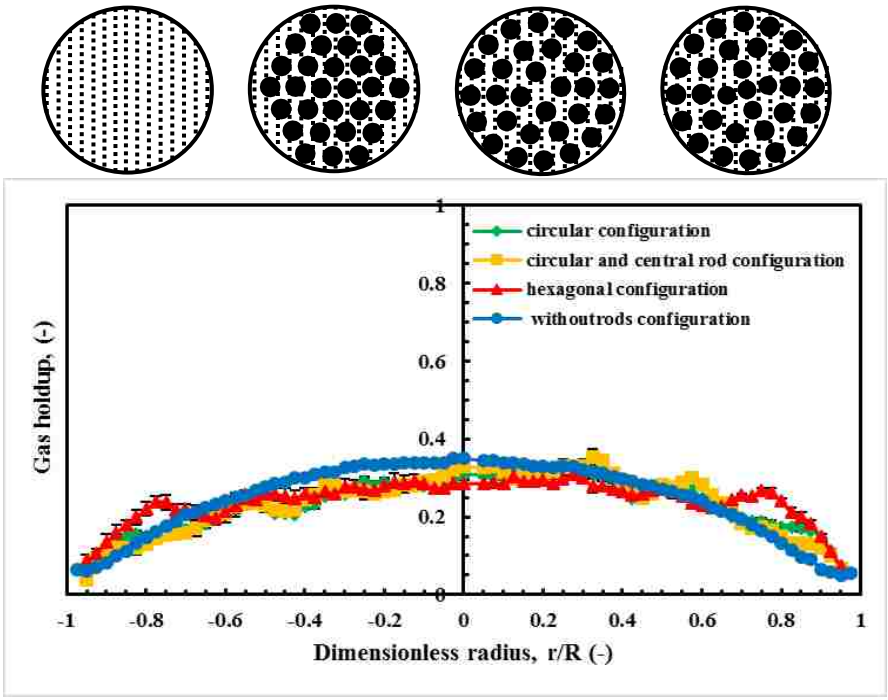

Figure 12: Comparison of line-averaged (along the vertical pixels in the cross-sectional image, as shown schematically at the top of this figure) gas holdup profiles between different configurations of bubble columns at a superficial gas velocity of 0.45 m/s

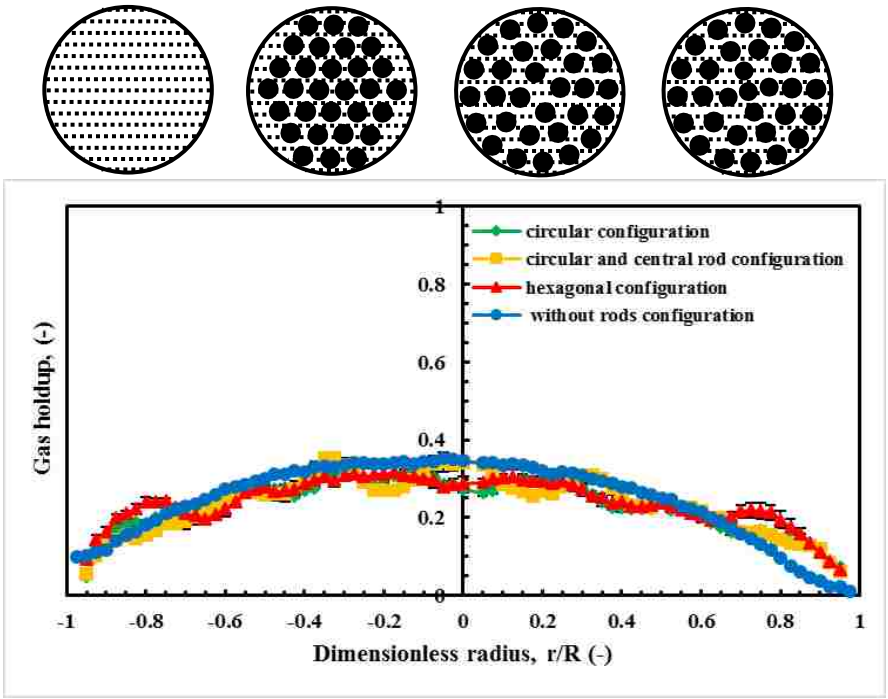

Figure 13: Comparison of line-averaged (along the horizontal pixels in the cross-sectional image as shown schematically at the top of this figure) gas holdup profiles between different configurations of bubble columns at a superficial gas velocity of 0.45 m/s

Therefore, the values of the gas holdup obtained in the core region of the bubble column without tubes operating under a high superficial gas velocity based on the TCSA of the column can be achieved in the bubble columns with dense vertical tubes if these columns operate at the same superficial gas velocity, but if it is calculated based on the FCSA of the flow. However, significant increases in gas holdup values can be obtained in the bubble column equipped with vertical internal tubes if these columns operated at the same high superficial gas velocity but are calculated based on the TCSA of the column, as investigated and demonstrated recently at mReal by Al Mesfer [40] and Kagumba [72]. Local gas holdup profiles along the horizontal and vertical pixels of the cross-sectional image also were obtained in this study for bubble columns with and without vertical internals operated at a superficial gas velocity of 0.45 m/s, as displayed in Figure 14 and Figure 15.

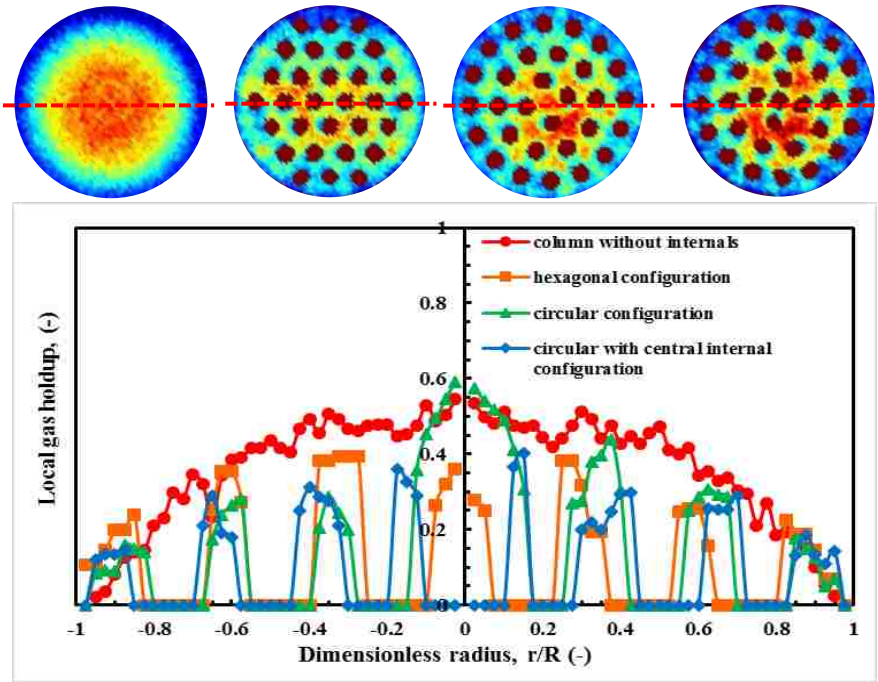

Figure 14: Comparison of the local gas holdup profiles along the horizontal pixels of the cross-sectional images for bubble columns with different configurations of vertical internals operated at a superficial gas velocity of 0.45 cm/s

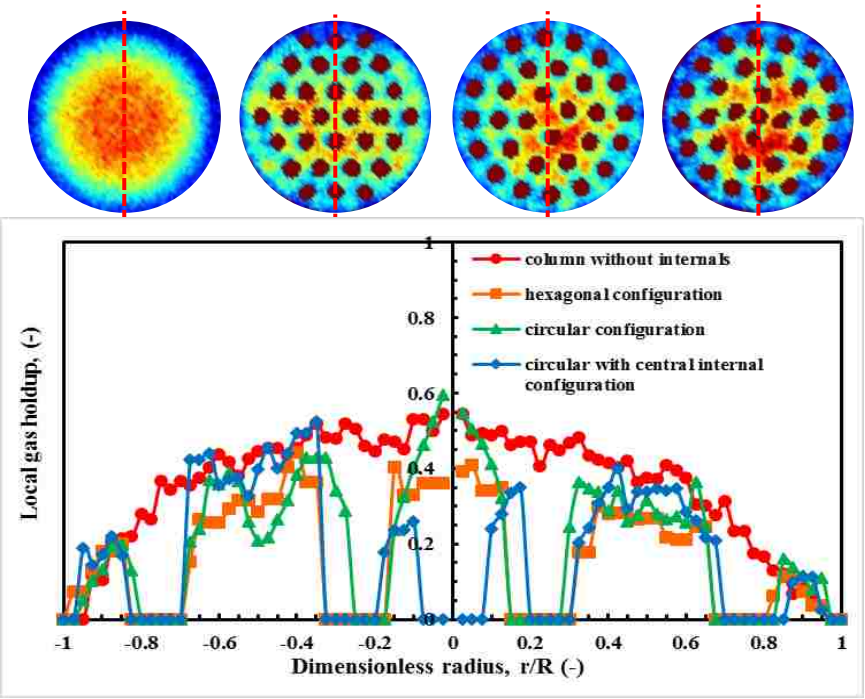

Figure 15: Comparison of the local gas holdup profiles along the vertical pixels of the cross-sectional images for bubble columns with different configurations of vertical internals operated at a superficial gas velocity of 0.45 cm/s

As shown in these figures, the local gas holdup profiles decreased across the bundle of vertical internals as compared to the parabolic gas holdup profile for a bubble column without vertical internals. However, the highest gas holdup was observed in the center of the column ($-0.15 \leq r/R \leq 0.15$) with the circular configuration without the central internal, due to the absence of the central internal in this region. Additionally, pronounced peaks in the gas holdup were observed in the inner gaps between the vertical internals due to the wall shear of these vertical internals, which induced the bubbles to accumulate at the center of the gap and to cause an increase in the gas holdup in this region [13,50]. Moreover, a close analysis of the gas holdup distributions and their profiles in the central compartments (i.e., at $r/R = 0$) for the bubble columns with different configurations of vertical internals (i.e., the area enclosed by four vertical internals) revealed that the highest gas holdup

magnitude was obtained with the central compartment of a circular configuration (i.e., circular without the central internal). This increase in the gas holdup magnitude can be attributed to the circular configuration (without the central internal), where a larger compartment (square pitch) in the center allows for more bubbles to rise inside this compartment as compared to the hexagonal configuration which is more compact, with triangular pitch. These results indicate that the geometry of the compartment (size and type of pitch) greatly affects the gas holdup distribution between the compartments [73]. Hence, the effect of the geometry of the compartment should be considered when developing a model or correlation to predict gas holdup in a bubble column with vertical internals. The arithmetic means of the cross-sectional gas holdup, presented in Table 1, were calculated to show the effects of the arrangement of vertical tubes on the gas holdup. The calculation of the arithmetic means of the cross-sectional gas holdup distributions $\left(\overline{\varepsilon_g}\right)$ is outlined as below.

- Conducting azimuthally (circumferentially) averaged radial profile from the 2D image of the gas holdup distribution.
- Performing numerical integration based on Simpson's rule for the following equation:

$$\overline{\varepsilon_g} = \frac{2}{R^2}\int_0^R \varepsilon(r) r dr \tag{10}$$

where R represents the radius of the bubble column and $\varepsilon(r)$ represents the values of a gas holdup at a specific radius (r). Table 1 represents the values of arithmetic means for the cross-sectional gas holdup as a function of the superficial gas velocity for different configurations of bubble columns. The values of the arithmetic mean of the cross-sectional

gas holdup for all configurations were similar, confirming that the values of the gas holdup in the bubble column equipped with vertical internal tubes and operated under high superficial gas velocities (churn turbulent flow regime) calculated based on the FCSA of the flow can be estimated by using the values of the gas holdup in the bubble column without internals, except for the values close to the wall region.

Table 1: Arithmetic mean of the cross-sectional gas holdup as a function of the configurations of internals and superficial gas velocity

	Arithmetic mean of cross-sectional gas holdup		
Types of configurations	**0.05 m/s**	**0.2 m/s**	**0.45 m/s**
Bubble column without internals	0.134	0.188	0.264
Bubble column with circular configuration	0.117	0.194	0.247
Bubble column with circular and central tube configuration	0.116	0.198	0.251
Bubble column with hexagonal configuration	0.121	0.202	0.255

3.3. INFLUENCE OF THE CONFIGURATION DESIGNS OF VERTICAL INTERNALS ON THE DEGREE OF THE UNIFORMITY OF THE GAS HOLDUP DISTRIBUTION

After the visualization (i.e., gas-liquid distribution map) described in the previous section qualitatively demonstrated which configurations provided uniform gas holdup distributions over the CSA of the columns, a quantitative analysis was needed to characterize the effect of the arrangement on the gas holdup. Therefore, in the present work, the maldistribution factor (MDF) was computed to assess the uniformity (homogeneity) of

the gas-liquid distribution quantitatively. Hoek et al. [74] introduced the following formula (Eq. 11) to calculate the MDF, which has been implemented in many studies [75–77].

$$MDF = \frac{1}{N}\sum_{i,j=1}^{N}\left(\frac{\varepsilon_{g,ij} - \varepsilon_{avg}}{\varepsilon_{avg}}\right)^2 \quad (11)$$

$$\varepsilon_{avg} = \frac{1}{N}\sum_{i,j=1}^{N}\varepsilon_{g,ij} \quad (12)$$

Eq. 11 is based on the deviation of the gas holdup in each pixel ($\varepsilon_{g,ij}$) from the cross-sectional mean (ε_{avg}) gas holdup where smaller values (closer to zero) indicate the uniform gas holdup distribution.

The existence of vertical internal tubes arranged in different configurations (i.e., hexagonal, circular, and circular with a central tube) significantly reduced the maldistribution factor for all ranges of studied superficial gas velocities (i.e., enhanced the gas holdup distributions) as exhibited in Figure 16. Additionally, the MDF for the bubble column with the hexagonal arrangement of vertical internals was the lowest, meaning that the hexagonal configuration offered a better gas holdup distribution. The maldistribution factors confirmed the results obtained by visual analysis, which were explained earlier. Moreover, for all studied superficial gas velocities, the circular configuration without a tube at the center had a lower MDF than the circular design with an extra central tube. Furthermore, Figure 16 illustrates that the MDF rose as the superficial gas velocities increased for all configurations of bubble columns. However, the MDF of the bubble column with the hexagonal arrangements of internals remained almost constant as the superficial gas velocity rose.

The nonuniform (maldistribution) gas phase distribution over the entire CSA of the bubble and slurry bubble column reactors led to (1) a decrease in the interfacial areas for the mass transfer rate, (2) an increase in the magnitude of the liquid backmixing, and (3) an increase in the possibility of forming a hotspot, any of which would significantly affect the conversion and selectivity of these reactors [17]. Therefore, from an industrial perspective, enhancing the quality of the gas-liquid distribution over the bubble column's CSA will improve the heat and mass transfer rates between the gas-liquid phases in a bubble column or the gas-catalyst-liquid phases in a slurry bubble column. This is true because these transport phenomena depend mainly on the interaction between phases. Besides improving the heat and mass transfer characteristics, the liquid backmixing will decrease, which is desired in the churn turbulent flow regime to achieve the optimal performance of these reactors.

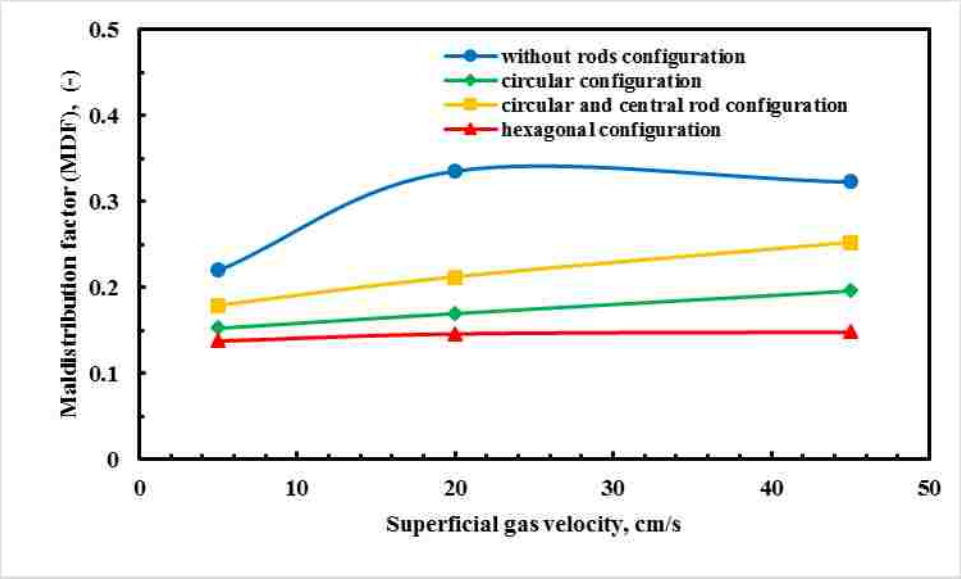

Figure 16: Effect of configuration and superficial gas velocity on the uniformity of gas holdup distributions

4. REMARKS

A unique comparative investigation was performed in a 6-inch bubble column using an advanced CT technique to visualize and quantify the impacts of the presence of the vertical internal tubes and their different configurations on the cross-sectional gas holdup distribution and its diametrical profiles under the churn turbulent flow regime. Three geometrical configurations of vertical tubes (i.e., hexagonal, circular without a central tube, circular with an extra central tube), which had the same size and the same occluded area (~25% of the TCSA of the column targeting FTS) were employed in this study as well as a bubble column without vertical tubes. The key results and findings of this work are briefly listed below:

- The reconstructed CT images disclose that the gas holdup distributions over the entire CSA of the bubble columns with internals are entirely different, despite using the same size vertical internals and the same percentage of the CSA occluded by the internals.
- Two-dimensional gas holdup distribution images clearly exhibit a symmetrical gas holdup distribution over the CSA for the bubble column without vertical internal tubes for all studied superficial gas velocities. On the other hand, the symmetric gas holdup distribution phenomenon was not sustained in the bubble column equipped densely with vertical internal tubes. However, the bubble column with tubes arranged in a circular configuration with an extra central tube displayed distinctly asymmetric gas holdup distributions.
- The well-known phenomenon (more gas at the center of the column and less gas at the wall region) in the bubble column without vertical internal tubes still occurred for all

studied configurations in the bubble columns equipped densely with vertical internal tubes that occluded about 25% of the TCSA of the columns.

- Inserting an extra tube at the center of a circular configuration played a vital role in the gas-liquid distribution over the CSA of the bubble column, where it caused significant decreases in the gas holdup at the center of the column as well as an increase in the degree of non-uniformity of the gas holdup distribution as compared to the circular configuration without a central tube.
- The hexagonal configuration of internals had the advantage of providing the best spread of the gas phase over the entire column's CSA, particularly in the wall region.
- Gas holdup values at the wall region of the bubble columns increased with the insertion of a bundle of internals for all investigated configurations. However, a remarkable increase in the gas holdup was obtained only with the hexagonal configuration.
- Unlike parabolic gas holdup profiles obtained in the bubble column without vertical internal tubes, wavy gas holdup profiles were achieved in the bubble columns with vertical internal tubes using the CT technique. However, these kinds of wavy profiles were not obtained in the bubble column with internals when the gas holdup was measured by the optical probe-based technique as had been reported in the literature.
- Interestingly, the gas holdup values achieved in the core (r/R = 0-0.6) of the bubble column without vertical internal tubes operated at the churn turbulent flow regime were similar to those obtained in the bubble columns equipped densely with vertical internal tubes if those columns operated at the same superficial gas velocity calculated based on the free (open) cross-sectional area (FCSA) of the flow. Therefore, the gas holdup values of the bubble column with vertical internal tubes can be estimated using the

values of the gas holdup of the bubble column without vertical internals at the core region.

- The maldistribution factor (MDF) decreased with the existence of vertical internals that were arranged differently (i.e., hexagonal, circular without central internal, circular with central internal) over the bubble column's CSA. However, the hexagonal configuration provided lowest values of the MDF than all other vertical internals arrangements (i.e., bubble column without vertical internals, circular with and without central internal) for all studied superficial gas velocities. Additionally, the MDF increased significantly with an increase in the superficial gas velocities for all configurations except the hexagonal configuration, which remained almost constant as the superficial gas velocities increased.
- Beyond the visualization and quantification of the impact of the vertical internal tube configurations on the gas-liquid distribution by the CT technique, this study provides reliable benchmarking data tom evaluate and validate CFD simulations and phenomenological models to better predict the hydrodynamic factors involved in a bubble column with and without a bundle of heat-exchanging tubes, thereby facilitating the design and scale-up of these reactors.
- The current study was performed using a 6-inch (0.1524 m O.D.) bubble column with and without vertical internal tubes; hence, further studies are needed to address the impact of the presence of these tubes and their arrangements in a large-scale bubble column on the gas-liquid distributions. These investigations are in progress in the mReal laboratory.

ACKNOWLEDGMENTS

The first and second authors are deeply thankful for the financial support in the form of scholarships awarded by the Higher Committee for Education Development in Iraq (HCED) and Ministry of Higher Education and Scientific Research (Iraq). Also, the authors gratefully acknowledge the funds presented by Missouri S&T and Professor Dr. Muthanna Al-Dahhan to develop the CT technique, the experimental set-up, and to conduct the current work.

REFERENCES

[1] S. Ojima, K. Hayashi, S. Hosokawa, A. Tomiyama, Distributions of void fraction and liquid velocity in air–water bubble column, Int. J. Multiph. Flow. 67 (2014) 111–121. doi:10.1016/j.ijmultiphaseflow.2014.05.008.

[2] A. Ojha, M. Al-Dahhan, Investigation of Local Gas Holdup and Bubble Dynamics using Four-Point Optical Probe Technique in a Split-Cylinder Airlift Reactor, Int. J. Multiph. Flow. 0 (2017) 1–15. doi:10.1016/j.ijmultiphaseflow.2017.12.001.

[3] P. Rollbusch, M. Becker, M. Ludwig, A. Bieberle, M. Grünewald, U. Hampel, R. Franke, Experimental investigation of the influence of column scale, gas density and liquid properties on gas holdup in bubble columns, Int. J. Multiph. Flow. 75 (2015) 88–106. doi:10.1016/j.ijmultiphaseflow.2015.05.009.

[4] G. Besagni, A. Di Pasquali, L. Gallazzini, E. Gottardi, L.P.M. Colombo, F. Inzoli, The effect of aspect ratio in counter-current gas-liquid bubble columns: Experimental results and gas holdup correlations, Int. J. Multiph. Flow. 94 (2017) 53–78. doi:10.1016/j.ijmultiphaseflow.2017.04.015.

[5] M. Pourtousi, P. Ganesan, J.N. Sahu, Effect of bubble diameter size on prediction of flow pattern in Euler–Euler simulation of homogeneous bubble column regime, Measurement. 76 (2015) 255–270. doi:10.1016/j.measurement.2015.08.018.

[6] L.S. Sabri, A.J. Sultan, M.H. Al-dahhan, Assessment of RPT Calibration Need during Microalgae Culturing and other Biochemical Processes, IEEE. (2017) 3–8.

[7] S.K. Majumder, Hydrodynamics and Transport Processes of Inverse Bubbly Flow, Elsevier, 2016.

[8] A.A. Youssef, M.H. Al-Dahhan, M.P. Dudukovic, Bubble columns with internals: A review, Int. J. Chem. React. Eng. 11 (2013) 169–223. doi:10.1515/ijcre-2012-0023.

[9] R. Pohorecki, W. Moniuk, P. Bielski, P. Sobieszuk, Diameter of Bubbles in Bubble Column Reactors Operating with Organic Liquids, Chem. Eng. Res. Des. 83 (2005) 827–832. doi:10.1205/cherd.04340.

[10] P.M.W. S. Schlfiter , A. Steiff, Heat transfer in two- and three-phase bubble column reactors with internals, Chem. Eng. Process. 34 (1995) 157–172.

[11] M. Kölbel,H ;Ralek, The Fischer-Tropsch Synthesis in Liquid Phase, Catal. Rev. Eng. 21 (1980) 225–274.

[12] M.K. Al Mesfer, A.J. Sultan, M.H. Al-Dahhan, Study the effect of dense internals on the liquid velocity field and turbulent parameters in bubble column for Fischer–Tropsch (FT) synthesis by using Radioactive Particle Tracking (RPT) technique, Chem. Eng. Sci. 161 (2017) 228–248. doi:10.1016/j.ces.2016.12.001.

[13] D. V. Kalaga, A. Yadav, S. Goswami, V. Bhusare, H.J. Pant, S. V. Dalvi, J.B. Joshi, S. Roy, Comparative analysis of liquid hydrodynamics in a co-current flow-through bubble column with densely packed internals via radiotracing and Radioactive Particle Tracking (RPT), Chem. Eng. Sci. 170 (2017) 332–346.

[14] A. Forret, J.M. Schweitzer, T. Gauthier, R. Krishna, D. Schweich, Scale up of slurry bubble reactors, Oil Gas Sci. Technol. 61 (2006) 443–458.

[15] K.J.H. George, A.K. Jhawar, A. Prakash, Investigations of flow structure and liquid mixing in bubble column equipped with selected internals, Chem. Eng. Sci. 170 (2016) 297–305. doi:10.1016/j.ces.2017.03.018.

[16] C. Boyer, B. Fanget, Measurement of liquid ow distribution in trickle bed reactor of large diameter with a new gamma-ray tomographic system, 57 (2002) 1079–1089.

[17] a. V. Kulkarni, Design of a Pipe/Ring Type of Sparger for a Bubble Column Reactor, Chem. Eng. Technol. 33 (2010) 1015–1022. doi:10.1002/ceat.200800347.

[18] O.M. Basha, L. Weng, Z. Men, B.I. Morsi, CFD Modeling with Experimental Validation of the Internal Hydrodynamics in a Pilot-Scale Slurry Bubble Column Reactor, Int. J. Chem. React. Eng. 14 (2016) 599–619. doi:10.1515/ijcre-2015-0165.

[19] O.M. Basha, L. Sehabiague, A. Abdel-Wahab, B.I. Morsi, Fischer-Tropsch Synthesis in Slurry Bubble Column Reactors: Experimental Investigations and Modeling - A Review, Int. J. Chem. React. Eng. 13 (2015) 201–288. doi:10.1515/ijcre-2014-0146.

[20] S. Rabha, M. Schubert, M. Wagner, D. Lucas, U. Hampel, Bubble size and radial gas hold-up distributions in a slurry bubble column using ultrafast electron beam X-ray tomography, AIChE J. 59 (2013) 1709–1722. doi:10.1002/aic.13920.

[21] B.K. Singh, A. Quiyoom, V. V. Buwa, Dynamics of gas-liquid flow in a cylindrical bubble column: Comparison of electrical resistance tomography and voidage probe measurements, Chem. Eng. Sci. 158 (2017) 124–139. doi:10.1016/j.ces.2016.10.006.

[22] S. Degaleesan, M.P. Duduković, Liquid backmixing in bubble columns and the axial dispersion coefficient, AIChE J. 44 (1998) 2369–2378. doi:10.1002/aic.690441105.

[23] Y. Wu, B. Cheng Ong, M.H. Al-Dahhan, Predictions of radial gas holdup profiles in bubble column reactors, Chem. Eng. Sci. 56 (2001) 1207–1210. doi:10.1016/S0009-2509(00)00341-9.

[24] F. Yamashita, Effects of Vertical Pipe and Rod Internals on Gas Holdup in Bubble Columns., J. Chem. Eng. Japan. 20 (1987) 204–206.

[25] S.. C. Saxena, N.. S. Rao, P.R. Thimmapuram, Gas Phase Holdup in Slurry Bubble Column for Two- and Three-Phase Systems, Chem. Eng. J. 49 (1992) 151–159. http://dx.doi.org/10.1016/0300-9467(92)80051-B.

[26] J. Chen, F. Li, S. Degaleesan, P. Gupta, M.H. Al-Dahhan, M.P. Dudukovic, B.A. Toseland, Fluid dynamic parameters in bubble columns with internals, Chem. Eng. Sci. 54 (1999) 2187–2197. doi:10.1016/S0009-2509(99)00003-2.

[27] F. Larachi, D. Desvigne, L. Donnat, D. Schweich, Simulating the effects of liquid circulation in bubble columns with internals, Chem. Eng. Sci. 61 (2006) 4195–4206. doi:10.1016/j.ces.2006.01.053.

[28] A.A. Youssef, M.H. Al-Dahhan, Impact of internals on the gas holdup and bubble properties of a bubble column, Ind. Eng. Chem. Res. 48 (2009) 8007–8013. doi:10.1021/ie900266q.

[29] V. Balamurugan, D. Subbarao, S. Roy, Enhancement in gas holdup in bubble columns through use of vibrating internals, Can. J. Chem. Eng. 88 (2010) 1010–1020. doi:10.1002/cjce.20362.

[30] A.A. Youssef, M.E. Hamed, J.T. Grimes, M.H. Al-Dahhan, M.P. Duduković, Hydrodynamics of pilot-scale bubble columns: Effect of internals, Ind. Eng. Chem. Res. 52 (2013) 43–55. doi:10.1021/ie300465t.

[31] X. Guan, Y. Gao, Z. Tian, L. Wang, Y. Cheng, X. Li, Hydrodynamics in bubble columns with pin-fin tube internals, Chem. Eng. Res. Des. 102 (2015) 196–206. doi:10.1016/j.cherd.2015.06.028.

[32] M. Kagumba, M.H. Al-Dahhan, Impact of internals size and configuration on bubble dynamics in bubble columns for alternative clean fuels production, Ind. Eng. Chem. Res. 54 (2015) 1359–1372. doi:10.1021/ie503490h.

[33] A. Jasim, The impact of heat exchanging internals on hydrodynamics of bubble column reactor, Missouri University of Science and Technology, 2016.

[34] M.K. Al Mesfer, A.J. Sultan, M.H. Al-Dahhan, Impacts of dense heat exchanging internals on gas holdup cross-sectional distributions and profiles of bubble column using gamma ray Computed Tomography (CT) for FT synthesis, Chem. Eng. J. 300 (2016) 317–333. doi:10.1016/j.cej.2016.04.075.

[35] G. Besagni, F. Inzoli, Influence of internals on counter-current bubble column hydrodynamics: Holdup, flow regime transition and local flow properties, Chem. Eng. Sci. 145 (2016) 162–180. doi:10.1016/j.ces.2016.02.019.

[36] P. Wilkinson, A. Spek, L. Van, Design parameters estimation for scale-up of high-pressure bubble columns, AIChE J. 38 (1992) 544–554.

[37] B.C. Ong, P. Gupta, A. Youssef, M. Al-Dahhan, M.P. Duduković, Computed Tomographic Investigation of the Influence of Gas Sparger Design on Gas Holdup Distribution in a Bubble Column, Ind. Eng. Chem. Res. 48 (2009) 58–68. doi:10.1021/ie800516s.

[38] A. Youssef, Fluid Dynamics and Scale-up of Bubble Columns with Internals, Washington University, Saint Louis, Missouri, 2010. doi:10.1017/CBO9781107415324.004.

[39] M. Hamed, Hydrodynamics, mixing, and mass transfer in bubble columns with internals, Washington University in St. Louis, 2012.

[40] M. Al-Mesfer, Effect of Dense Heat Exchanging Internals on the Hydrodynamics of Bubble Column Reactors Using Non-Invasive Measurement Techniques, Missouri University of Science and Technology, Rolla, MO, 2013.

[41] G. Besagni, A. Di Pasquali, L. Gallazzini, E. Gottardi, L.P.M. Colombo, F. Inzoli, The effect of aspect ratio in counter-current gas-liquid bubble columns: Experimental results and gas holdup correlations, Int. J. Multiph. Flow. 94 (2017) 53–78. doi:10.1016/j.ijmultiphaseflow.2017.04.015.

[42] T. Wang, J. Wang, Y. Jin, Slurry reactors for gas-to-liquid processes: A review, Ind. Eng. Chem. Res. 46 (2007) 5824–5847. doi:10.1021/ie070330t.

[43] A. Shaikh, M.H. Al-Dahhan, A Review on Flow Regime Transition in Bubble Columns, Int. J. Chem. React. Eng. 5 (2007). doi:10.2202/1542-6580.1368.

[44] G. Besagni, F. Inzoli, T. Ziegenhein, D. Lucas, The pseudo-homogeneous flow regime in large-scale bubble columns: experimental benchmark and computational fluid dynamics modeling, Petroleum. (2017). doi:10.1016/j.petlm.2017.12.004.

[45] P. Chen, J. Sanyal, M.P.P. Duduković, Numerical simulation of bubble columns flows: Effect of different breakup and coalescence closures, Chem. Eng. Sci. 60 (2005) 1085–1101. doi:10.1016/j.ces.2004.09.070.

[46] B.H. Davis, Fischer-Tropsch synthesis: Overview of reactor development and future potentialities, Top. Catal. 32 (2005) 143–168. doi:10.1007/s11244-005-2886-5.

[47] S. Saeidi, M.K. Nikoo, A. Mirvakili, S. Bahrani, N.A. Saidina Amin, M.R. Rahimpour, Recent advances in reactors for low-temperature Fischer-Tropsch synthesis: process intensification perspective, Rev. Chem. Eng. 31 (2015) 19–21. doi:10.1515/revce-2014-0042.

[48] S. Sasaki, K. Hayashi, A. Tomiyama, Effects of liquid height on gas holdup in air-water bubble column, Exp. Therm. Fluid Sci. 72 (2016) 67–74. doi:10.1016/j.expthermflusci.2015.10.027.

[49] S.B. Kumar, D. Moslemian, M.P. Duduković, Gas-holdup measurements in bubble columns using computed tomography, AIChE J. 43 (1997) 1414–1425. doi:10.1002/aic.690430605.

[50] F. Möller, Y.M. Lau, T. Seiler, U. Hampel, M. Schubert, A Study on the Influence of the Tube Layout on Sub-channel Hydrodynamics in a Bubble Column with Internals, Chem. Eng. Sci. 179 (2018) 265–283. doi:10.1016/j.ces.2018.01.008.

[51] R. Varma, Characterization of anaerobic bioreactors for bioenergy generation using a novel tomography technique, Washington University, 2008.

[52] F. Al Falahi, M. Al-Dahhan, Experimental investigation of the pebble bed structure by using gamma ray tomography, Nucl. Eng. Des. 310 (2016) 231–246. doi:10.1016/j.nucengdes.2016.10.009.

[53] M.K. Al Mesfer, A.J. Sultan, M.H. Al-Dahhan, M.H.A.-D. Mohammed K. Al Mesfer , Abbas J. Sultan, Impacts of dense heat exchanging internals on gas holdup cross-sectional distributions and profiles of bubble column using gamma ray Computed Tomography (CT) for FT synthesis, Chem. Eng. J. 300 (2016) 317–333. doi:10.1016/j.cej.2016.04.075.

[54] N. Ali, T. Al-Juwaya, M. Al-Dahhan, Demonstrating the non-similarity in local holdups of spouted beds obtained by CT with scale-up methodology based on dimensionless groups, Chem. Eng. Res. Des. 114 (2016) 129–141. doi:10.1016/j.cherd.2016.08.010.

[55] T. Al-Juwaya, N. Ali, M. Al-Dahhan, Investigation of cross-sectional gas-solid distributions in spouted beds using advanced non-invasive gamma-ray computed tomography (CT), Exp. Therm. Fluid Sci. 86 (2017) 37–53. doi:10.1016/j.expthermflusci.2017.03.029.

[56] A. Efhaima, M. Al-Dahhan, Local time-averaged gas holdup in fluidized bed reactor using gamma ray computed tomography technique (CT), Int. J. Ind. Chem. 6 (2015) 143–152. doi:10.1007/s40090-015-0048-6.

[57] S. Roy, A. Kemoun, M.H. Al-Dahhan, M.P. Dudukovic, T.B. Skourlis, F.M. Dautzenberg, Countercurrent flow distribution in structured packing via computed tomography, Chem. Eng. Process. Process Intensif. 44 (2005) 59–69. doi:10.1016/j.cep.2004.03.010.

[58] X. Yang, J.R. van Ommen, E. Wagner, R.F. Mudde, Time-resolved characterization of a flat-base spouted bed with a high speed X-ray system, Chem. Eng. J. 254 (2014) 143–152. doi:10.1016/j.cej.2014.05.050.

[59] S.B. Bhusarapu, Solids Flow Mapping In Gas-Solid Risers, WASHINGTON UNIVERSITY SEVER, 2005.

[60] J. Gómez-Hernández, J. Ruud van Ommen, E. Wagner, R.F. Mudde, A fast reconstruction algorithm for time-resolved X-ray tomography in bubbling fluidized beds, Powder Technol. 290 (2016) 33–44. doi:10.1016/j.powtec.2015.08.038.

[61] F.S. Al Falahi, Experimental investigation of the pebble bed structure by using gamma ray tomography, Missouri University of Science and Technology, 2014.

[62] M.H. Al-Dahhan, Trends in Minimizing and Treating Industrial Wastes for Sustainable Environment, Procedia Eng. 138 (2016) 347–368. doi:10.1016/j.proeng.2016.02.095.

[63] J.A. O'Sullivan, J. Benac, Alternating minimization algorithms for transmission tomography, IEEE Trans. Med. Imaging. 26 (2007) 283–297.

[64] N. Rados, A. Shaikh, M.H. Al-dahhan, Phase Distribution in a High Pressure Slurry Bubble Column via a Single Source Computed Tomography, Can. J. Chem. Eng. 83 (2005).

[65] S. Roy, A. Kemoun, M.H. Al-Dahhan, M.P. Dudukovic, Experimental investigation of the hydrodynamics in a liquid-solid riser, AIChE J. 51 (2005) 802–835. doi:10.1002/aic.10447.

[66] R. Varma, S. Bhusarapu, J.A.O. Sullivan, M. Al-Dahhan, A comparison of alternating minimization and expectation maximization algorithms for single source gamma ray tomography, Meas. Sci. Technol. 18 (2007) 1–13.

[67] M. Al-Dahhan, Radioisotopes applications in industry: an overview, Atoms Peace – An Int. J. 2 (2009) 324–337.

[68] J. Chen, P. Gupta, S. Degaleesan, M.H. Al-Dahhan, M.P. Dudukovic, B.A. Toseland, Gas holdup distributions in large-diameter bubble columns measured by computed tomography, Flow Meas. Instrum. 9 (1998) 91–101. doi:10.1016/S0955-5986(98)00010-7.

[69] J.L. Hubers, A.C. Striegel, T.J. Heindel, J.N. Gray, T.C. Jensen, X-ray computed tomography in large bubble columns, Chem. Eng. Sci. 60 (2005) 6124–6133. doi:10.1016/j.ces.2005.03.038.

[70] A. Shaikh, M. Al-Dahhan, Characterization of the hydrodynamic flow regime in bubble columns via computed tomography, Flow Meas. Instrum. 16 (2005) 91–98. doi:10.1016/j.flowmeasinst.2005.02.004.

[71] G. Besagni, F. Inzoli, Bubble size distributions and shapes in annular gap bubble column, Exp. Therm. Fluid Sci. 74 (2016) 27–48. doi:10.1016/j.expthermflusci.2015.11.020.

[72] M. Kagumba, Heat Transfer and Bubble Dynamics in Bubble and Slurry, Missouri university of science and technology, 2013.

[73] K. Hayashi, S. Hosokawa, A. Tomiyama, Void distribution and bubble motion in bubbly flows in a 4×4 rod bundle. Part II: Numerical simulation, J. Nucl. Sci. Technol. 51 (2014) 580–589. doi:10.1080/00223131.2014.882802.

[74] P.J. Hoek, J.A. Wesselingh, F.J. Zuiderweg, Small scale and large scale liquid maldistribution in packed columns, Chem. Eng. Res. Des. 64 (1986) 431–449.

[75] M.H. Al-Dahhan, A. Kemoun, A.R. Cartolano, S. Roy, R. Dobson, J. Williams, Measuring gas-liquid distribution in a pilot scale monolith reactor via an Industrial Tomography Scanner (ITS), Chem. Eng. J. 130 (2007) 147–152. doi:10.1016/j.cej.2006.06.022.

[76] A. Bieberle, H.-U. Härting, S. Rabha, M. Schubert, U. Hampel, Gamma-Ray Computed Tomography for Imaging of Multiphase Flows, Chemie Ing. Tech. 85 (2013) 1002–1011. doi:10.1002/cite.201200250.

[77] C. Meitzner, G. Hilpmann, T. Schäfer, S. Haase, M. Lange, U. Hampel, Homogeneous gas-liquid distribution for monolithic structures via a needle distributor, Chem. Eng. Technol. (2017) 1–20. doi:10.1002/ceat.201700125.

IV. INVESTIGATING THE INFLUENCE OF THE CONFIGURATION OF THE BUNDLE OF HEAT EXCHANGING TUBES AND COLUMN SIZE ON THE GAS HOLDUP DISTRIBUTIONS IN BUBBLE COLUMNS VIA GAMMA-RAY COMPUTED TOMOGRAPHY

Abbas J. Sultan, Laith S. Sabri, Muthanna H. Al-Dahhan[†]

[†]Multiphase Reactors Engineering and Applications Laboratory (mReal), *Department of Chemical and Biochemical Engineering, Missouri University of Science and Technology, Rolla, MO 65409-1230, USA*

ABSTRACT

The impact of dense vertical internal tubes and their configurations on the gas holdup distributions and their diametrical profiles in pilot-scale bubble column is visualized and quantified for the first time ever using an advanced gamma-ray computed tomography (CT) technique. Two arrangements of vertical internals (circular and hexagonal configurations) occupying the same cross-sectional area (CSA) of the column (about 25% of the total cross-sectional area to represent the heat exchanging tubes that are used in the Fischer-Tropsch synthesis), were examined in addition to the measurement in the bubble column without vertical internals. Moreover, the gas holdup distribution results of the 18-inch bubble column are compared with an available data of 6-inch bubble columns with and without vertical internals. CT scans have been conducted for 18-inch bubble columns with and without vertical internals for the air-water system under a wide range of superficial gas velocity (5-45 cm/s). The experimental results indicate that an improvement in the gas holdup distribution over the column's cross-sectional area is obtained when the vertical internal tubes (arranged in either a circular or a hexagonal configuration) were used. However, better cross-sectional gas holdup distribution was achieved in the bubble column with vertical internals arranged in a hexagonal configuration as compared to the bubble column without and with vertical internals arranged in a circular

arrangement. Additionally, the averages of the cross-sectional gas holdup and their profiles for bubble column with and without vertical internals are close to each other when the bubble column with vertical internals is operating at a high superficial gas velocity, which is calculated based on the free cross-sectional area for the flow. Furthermore, the gas holdup distributions are further improved when the larger bubble column with vertical internals was used as compared to the 6-inch bubble columns without and with internals.

Keywords: Bubble column, vertical internal tubes, vertical internals configurations, scale up, gas holdup distribution, computed tomography (CT).

†Correspondence author at the Chemical & Biochemical Engineering Department, Missouri University of Science and Technology, Rolla, MO, 65409. Tel.: +1 573-578-8973. E-mail: aldahhanm@mst.edu

1. INTRODUCTION

Bubble/slurry bubble columns with a bundle of heat-exchanging tubes are well-fitted reactors for conducting highly exothermic reactions, such as Fischer-Tropsch (FT) synthesis, acetic acid production, cyclohexanol manufacturing, and many others [1–5]. The reason these reactors were selected for wide applications in industry is that they possess superior advantages in facilitating sufficient heat removal and temperature control (close to isothermal condition), which allow for a secure and high reactor performance [6–12].

Despite the wide variety of applications of bubble/slurry bubble columns (e.g., in industry), the design and scale-up of these reactors is a difficult engineering task due to the complex behavior of multiphase flow patterns and the absence of a phenomenological model that can reliably predict the flow patterns for these columns [13–16]. Additionally, the presence of the dense geometry of vertical tubes inside these reactors further alters the flow

structure and the intensity of the mixing [17–21]. As a result, these vertical internal tubes make the design and scale-up even more challenging and complicated. Therefore, a comprehensive understanding of the impacts of vertical tubes on the hydrodynamics of these reactors is much needed to the successful design, scale-up, and optimize performance of a bubble/slurry bubble column with a bundle of the intense heat exchanging tubes.

One of the most critical hydrodynamic parameters for the design, scale-up, and modeling of bubble/slurry bubble columns is the gas holdup because of its impacts on the momentum, heat, and mass transfer rates between phases; hence, it characterizes the performance of these reactors [22–26]. Also, local gas holdup distribution has a significant effect on the reactor's performance. For example, the high degree of non-uniform gas holdup distribution inside these columns causes a significant reduction in the specific interfacial area between the gas-liquid or gas-slurry phases, thereby reducing the mass transfer rate. Moreover, this uneven distribution could increase the liquid back-mixing and thus may promote a temperature gradient that could lead to a greater chance that local hot spots will form [27–29]. Furthermore, improving the gas holdup distribution by presenting different designs or arrangements of heat-exchanging tubes will increase the contact area between the gas-liquid phases in a bubble column or the gas-catalyst-liquid phases in a slurry bubble column; this allows for a high mass transfer rate, which consequently enhances the reaction rate.

The proper arrangement of the heat-exchanging tubes is crucial to maintaining the uniformity of the gas-liquid distribution over the column's cross-sectional area. This will provide better contact and interaction between phases, which enhances the productivity of these reactors. Eventually, understanding the influence of vertical tubes on gas-liquid

distribution inside bubble columns is vital for the safe operation and efficient design of these reactors. Unfortunately, up-to-date, information of gas-liquid distribution for large-scale bubble column with intense vertical internals is not available in the literature.

So far, much researcher has focused extensively on the hydrodynamics of bubble columns without vertical tubes to achieve high performance in these reactors. However, few studies have investigated the effects of vertical tubes on the hydrodynamics of these reactors, while many of the industrial applications for the bubble/slurry bubble columns involve inserting bundle of vertical tubes to (1) remove the released heat of the reaction, (2) enhance the breakup of bubbles, or (3) reduce a degree of back-mixing of a liquid phase [30–34]. As pointed out earlier, the existence of the bundle of vertical tubes significantly affects the fluid dynamics of these reactors, and quantifying and predicting these impacts is difficult without experimental work. Therefore, the current investigation focuses on bubble columns equipped with dense vertical tubes.

To the best of the authors' knowledge, the local gas holdup distribution over the entire cross-sectional area of the bubble column equipped with vertical tubes has been measured using gamma-ray computed tomography (CT) in no more than two studies in the literature. One of these studies was performed by Chen et al. [35], where the authors measured for the first time the gas holdup distribution and related radial profiles in a pilot-scale bubble column (44 cm in diameter) with and without vertical internals for air-water and air-drakeoil systems operated under a range of superficial gas velocities from 2-10 cm/s. To simulate the heat-exchanging tubes used in industrial methanol synthesis, the 1-inch aluminum vertical internals in their work were designed and arranged sparsely in a circular configuration that blocked only 5% of the column's cross-sectional area. Their

experimental results revealed that the gas holdup distributions at the highest superficial gas velocity (i.e., 10 cm/s) were axisymmetric at the fully developed region for both systems in the bubble columns with and without vertical internals. Additionally, the gas holdup values obtained in the bubble column without vertical internals for the air-drakeoil system were lower than those measured in the same column for the air-water system. Furthermore, the authors pointed out that the effects of the internals were not significant on the gas holdup for both systems.

The second of the two studies was recently conducted by Al Mesfer et al. [36]. They imaged and quantified the gas holdup distributions in bubble columns (14 cm in diameter) with and without vertical internals for the air-water system under a wide range of superficial gas velocity (5-45 cm/s) calculated based on the free and the total cross-sectional area (CSA) of the column. The authors used 0.5-inch Plexiglas® vertical internals that were arranged densely in a hexagonal shape over the CSA of the column. These vertical internals were designed to cover 25% of the column's CSA to represent the heat-exchanging tubes that were used in Fischer-Tropsch (FT) synthesis. The CT images revealed that the gas holdup distributions were almost axisymmetric in the bubble columns with and without vertical internals for all studied superficial gas velocities except for the high superficial gas velocities of 30 and 45 cm/s, where distributions exhibited asymmetrically. Moreover, the authors found that the overall and local gas holdups rose significantly with increasing superficial gas velocities when the gas velocity was calculated based on the total CSA of the bubble column. Furthermore, they reported that the overall and local gas holdup profiles that were achieved in the bubble column without vertical internals operated under high superficial gas velocity could be extrapolated to the columns

with vertical internals if these columns worked under the same superficial gas velocity if it was calculated based on the free CSA of the column. However, the intensity of mixing and local liquid/slurry velocity and turbulent parameters cannot be similarly extrapolated [5].

According to the prior discussion, it is evident that the characteristics of gas holdup distributions in a large-scale bubble column equipped with dense (covering 25% of the total CSA) vertical tubes have not yet been visualized and quantified. Therefore, this study is the first attempt to fill this gap through visualization and quantification of the gas-liquid distribution over the entire CSA of large-scale bubble columns with and without vertical internals using an advanced gamma-ray computed tomography (CT) technique. An air-water system was used in this work because there in quite a large database related to air-water systems that can be applied for comparison and to properly report the effect of vertical internals in a large pilot-scale column (44 cm in diameter). To achieve this goal, the following objectives were set for this study:

(i) Investigating the impact of the bundle of vertical internals on the gas holdup distributions and their profiles in a large scale bubble column.

(ii) Examining the effect of tubes configurations (i.e., hexagonal and circular arrangements) on the gas holdup distributions and their profiles.

(iii) Assessing the effect of the superficial gas velocity on the gas holdup distributions and their diametrical profiles.

(iv) Comparing the obtained results in 18-inch bubble columns with those of 6-inch bubble columns to assess and address the impact of using different sizes of columns on the gas holdup distributions and their profiles.

The knowledge gained from this work and from previous studies will further improve the fundamental understanding of the influence of vertical tubes on the gas-liquid distribution not only in bubble/slurry bubble columns but also for the equipment, which is utilized in power generation such as boilers, boiling and pressurized water nuclear reactors. Additionally, the obtained experimental data will expand the database for the bubble columns with vertical tubes and serve as benchmarking data for the evaluation and validation of three-dimensional (3-D) computational fluid dynamics (CFD) simulations to enhance the prediction of the hydrodynamics of these columns. Only after CFD models are validated against reliable benchmark data for various operating conditions and scales of bubble/slurry bubble columns equipped with dense vertical tubes for the air-water system, can the validated models be employed as useful tools to predict the hydrodynamics for different scales of bubble/slurry bubble columns operated under various feed inputs and running conditions, including those of interest to industry. Finally, the current work will support the design and scale-up processes by providing baseline data for different scales of bubble columns using a bundle of dense heat-exchanging tubes.

2. EXPERIMENTAL WORK

2.1. EXPERIMENTAL SETUP

Gas-liquid distribution and gas holdup profiles were visualized and quantified in a pilot-scale Plexiglas® bubble column of 18-inch (0.46 m) diameter and with a height of 144 inches (3.66 m). A schematic diagram of the pilot-scale bubble column equipped with dense vertical internals is displayed in Figure 1. In this study, the bubble column was fitted with a gas distributor, which was placed above the gas chamber (plenum).

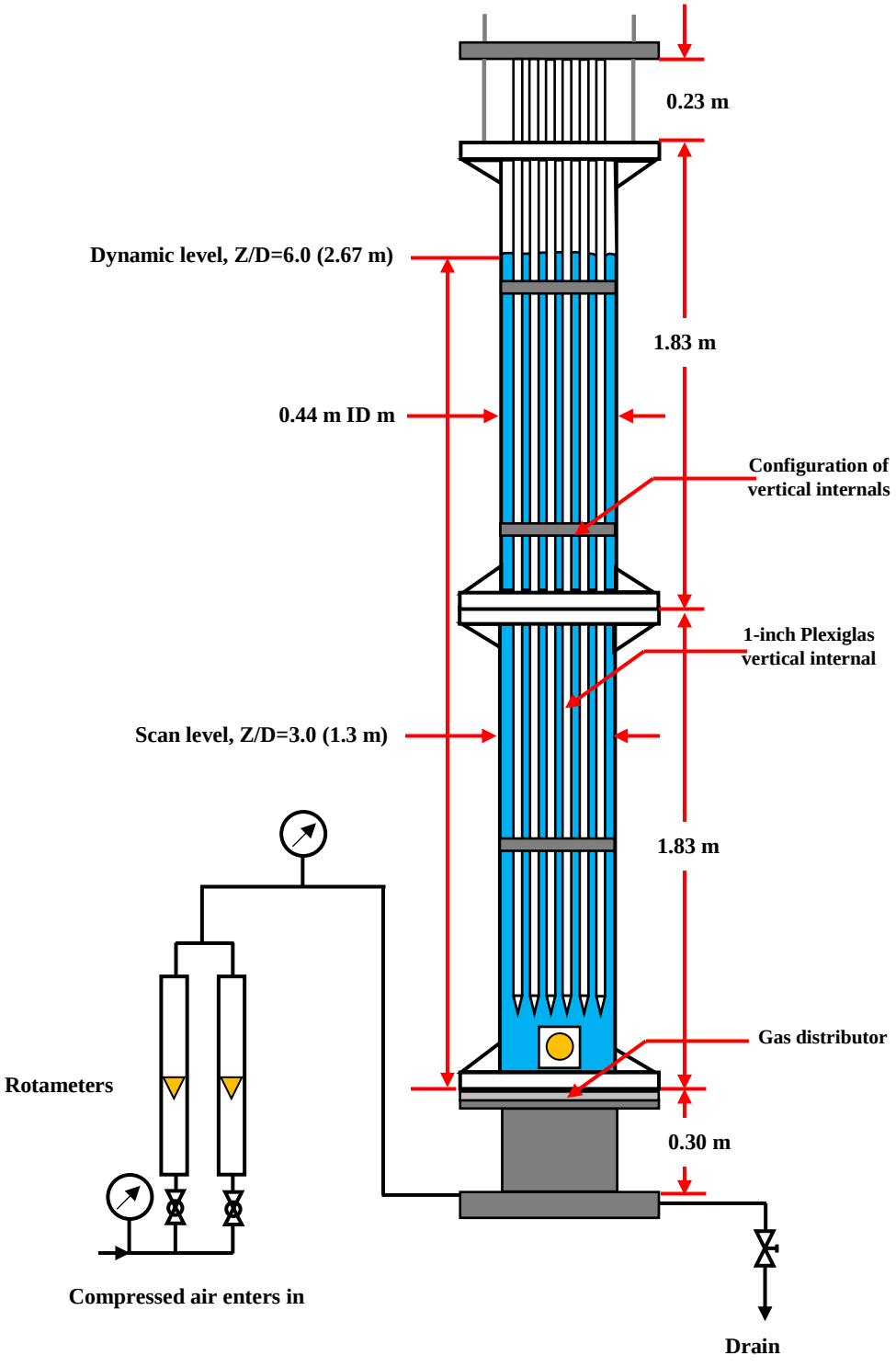

Figure 1: Schematic diagram of the 18-inch bubble column equipped with dense internals

This gas distributor is a stainless steel perforated plate designed with 241 holes, each 3 mm in diameter, as exhibited in Figure 2. These holes were designed in a triangular pitch of 2.5 cm over the CSA of the perforated plate, forming an open area of 1.09%. A bundle of 75 Plexiglas® vertical internals filling 25% of the CSA of the column was used in this study to represent the heat-exchanging tubes used in FT synthesis [37–40]. Each Plexiglas® vertical internal had a diameter of 1 inch (2.54 cm) and a height of 4 m.

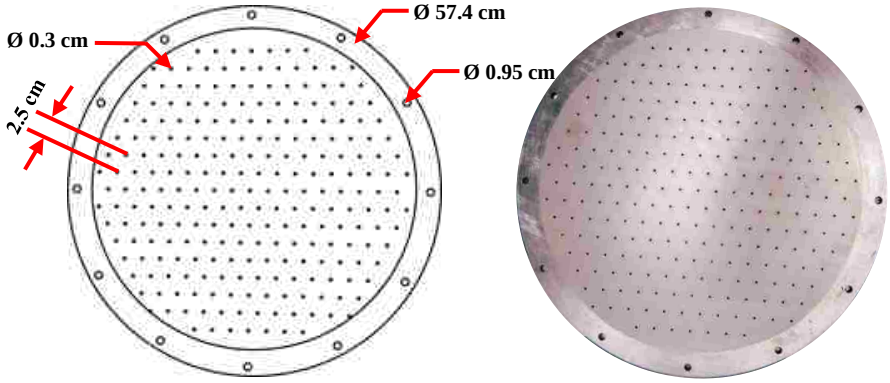

Figure 2: Schematic diagram and photo of the 18-inch stainless steel gas distributor (perforated plate)

Two geometric arrangements for these vertical internals, namely hexagonal and circular configurations, were examined in the current work, as shown in Figure 3. The vertical internals with a hexagonal configuration were designed and arranged in an equilateral (triangular) pitch of 4.5 cm, whereas the vertical internals with a circular configuration were organized in one central internal, and the rest of the internals were distributed in five concentric circles, located in a dimensionless radius (*r/R*) of 0.2, 0.4, 0.5, 0.7, and 0.9. With 9-inch clearance from the gas distributor, the vertical internals were housed and held tightly inside the bubble column using four aluminum spacers (configurations) and a top plate.

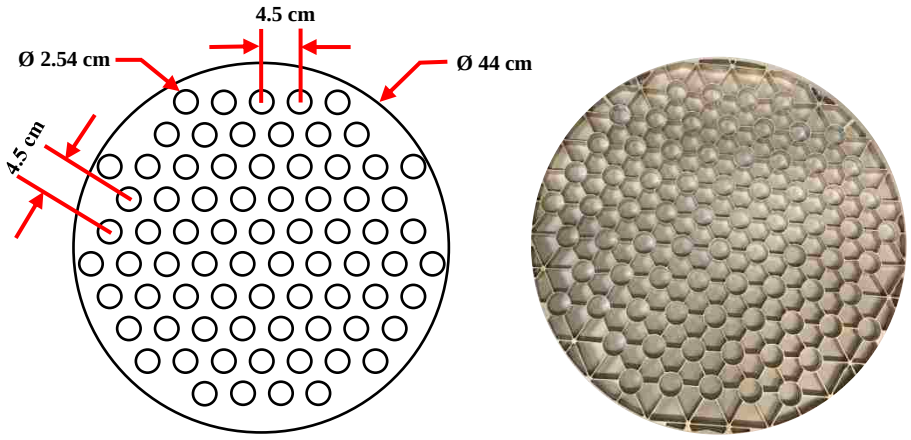

a) Hexagonal configuration (tube arrangements)

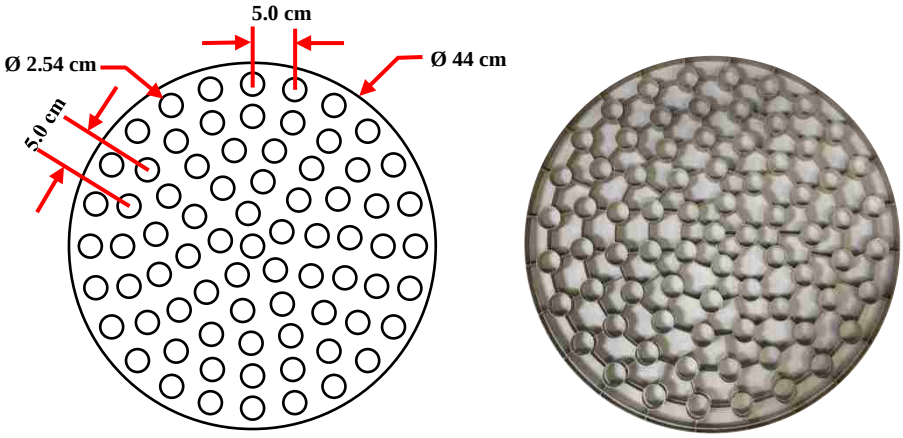

b) Circular configuration (tube arrangements)

Figure 3: Schematics and photos of the hexagonal and circular configurations of the heat exchanging tubes (vertical internals)

In this work, the bubble columns with and without vertical internals were operated at ambient pressure and temperature using continuous mode for the gas (air) phase and batch mode for the liquid (water) phase. The air was supplied by an industrial compressor (Ingersoll Rand) and passed through a flow measurement system that included an air dryer, filters, pressure gauges, and a pressure regulator to ensure only dry, oil-free air entered and sparged continuously through a pool of purified water during the operation of the bubble columns. The volumetric flow rate of the gas phase was monitored and controlled by a set

of pre-calibrated rotameters that were connected in a parallel configuration, which enabled this study to be conducted at a broad range of superficial gas velocities. These gas velocities were examined to fulfill the industrial needs for a high superficial gas velocity (i.e., in the churn turbulent flow regime) because most applications of these reactors operate under churn turbulent flow regime to achieve high productivity [41,42]. The computations of the superficial gas velocity for the bubble column without vertical internals were based on the total CSA of the column; however, for the column equipped densely with vertical internals, the computation was based on the free (open) CSA for the flow. The free CSA for the flow represents the difference between the total CSA of the column without vertical internals and the area occupied by all vertical internals, as shown below:

$$\begin{pmatrix} free \\ cross\text{-}sectional\ area \\ for\ the\ flow \end{pmatrix} = \begin{pmatrix} total \\ cross\text{-}sectional\ area \\ of\ the\ column\ without\ tubes \end{pmatrix} - \begin{pmatrix} occupied \\ cross\text{-}sectional\ area \\ by\ tubes \end{pmatrix}$$

During all experiments, the average of the dynamic (dispersion) level of the gas-liquid was kept constant at 2.67 m (H/D = 6) away from the gas distributor, which was monitored using a measuring tape attached to the Plexiglas® bubble column. It was shown in our studies that the variation in the dynamic height will not affect the reactor's hydrodynamics in its fully developed flow region. All CT scans for pilot-scale bubble columns with and without vertical internals were performed at one axial level, 1.3 m (H/D = 3) above the gas distributor. This axial level for the scans was chosen because within this region, a fully developed flow would exist, and according to many researchers [22,43,44], the local gas holdup and bubble properties (bubble rise velocity, bubble chord length, and bubble frequency) would be almost invariant. The other reason for selecting this level was to complement the available data about bubble properties measured in the same

experimental setup for the air-water system at the same axial level using the four-point fiber optical probe technique, which was developed, manufactured, and tested in our laboratory (Multiphase Reactors Engineering and Applications Laboratory, mReal) [39]. The integration of these results, which were obtained by advanced techniques (i.e., CT and four-point fiber optical probe), will improve the qualitative and quantitative understanding of fluid dynamics in a bubble column with vertical internals.

The pilot-scale bubble columns with and without dense vertical internals were well centered and balanced inside the open circular space when using the CT technique. Additionally, the columns were well supported in two places, at the bottom and top of the column, using an aluminum frame with pieces of rubber to eliminate the mechanical vibration that that would otherwise significantly affects the measurement of the gas holdups [45–48].

2.2. GAMMA-RAY COMPUTED TOMOGRAPHY (CT) TECHNIQUE

A single gamma-ray computed tomography (CT) technique, which is a part of a unique dual-source gamma-ray computed tomography (DSCT) scanner, was used in this study. In a noninvasive way, the DSCT images and quantifies the internal distributions of two- or three-phase flows, which are extensively encountered in different types of multiphase reactors or flow systems at various operating conditions. This technique has been applied successfully to different multiphase flow systems in our laboratory (mReal) at the Chemical and Biochemical Engineering Department at Missouri University of Science and Technology (Missouri S&T). Examples of such applications are in pebble bed [49,50], bubble column [36,38], fluidized bed [51–53], and spouted bed [54–56]. Detailed descriptions of

the fundamental underlying principle, hardware, and software related to the DSCT have been reported elsewhere in Varma [57] and are briefly described in this section.

In summary, the DSCT technique is comprised of two gamma-ray sources, namely cesium (Cs-137, with a half-life of about 37 years) and cobalt (Co-60, with a half-life of about 5.24 years), with an initial activity of ~250 and 50 mCi, respectively. Each of these sources was designed to face the center of an array of 15-sodium iodide (NaI) detectors to acquire emitted photons. However, for the present work, a single gamma-ray source (Cs-137, with 662 keV photon energy) and its arc of detectors were used to visualize and quantify for the first time the time-averaged cross-sectional gas-liquid distributions and their profiles in a pilot-scale bubble column equipped with and without dense vertical internals, as depicted in Figure 4.

This Cs-137 point source was well housed inside a lead-shielded container and further collimated using a lead collimator 5 mm in height and 40° in a horizontal plane to provide a fan beam of gamma radiation focusing toward the detector arc. Similarly, 15 lead collimators with an open rectangular slit of 5 mm in width and 10 mm in height were installed in front of each detector to collimate the detectors to ensure each detector receive lines (beams) of gamma rays with sufficient counts and less of a scattering effect [58]. The dimensions of collimators for the Cs-137 source and their detectors were designed to provide enough open area to acquire counts (photons) with sufficient statistics (high signal-to-noise ratio) at the selected frequency and sampling rate [59–61].

Both gamma-ray sources and their arrays of detectors were mounted and installed on a motorized rotatable circular plate. This circular plate was attached to a lift unit (square plate), which allowed for the whole system (i.e., circular plate, gamma-sources, and their

detectors) to perform CT scans in different selected axial planes automatically. The circular and square plates have a central opening space, which is dedicated to the objects to be examined.

During the scanning of the investigated bubble column, which was well balanced and centered inside the circular opening area of the CT technique, the Cs-137 source and its detectors were rotated around the column by repositioning the circular plate in a stepwise movement (approximately 1.83° for each step) that was controlled by a programmed, automated step motor. For a given step of rotation (each source view), the array of the Cs-137 source detectors was moved automatically 21 times in an arc of 0.13°/step, which was achieved by another independent automated stepping motor. These 21 steps of movements in one view were developed to produce more beams of gamma-ray (about 315 [21 × 15] projections per each view of the Cs-137 source) to improve the spatial resolution of images. Therefore, for a complete scan (197 views), the detectors acquired 62,055 (315 × 197) projections that passed through the column from different angles. These acquired projections were recorded at a frequency of 10 Hz with a sampling rate of 60 samples and sent to a computer where they were used as input data in a reconstruction algorithm to create a linear attenuation coefficient distribution of the scanned levels.

Rather than use other reconstruction algorithms (e.g., filter back-filtration, Fourier, algebraic, and expectation maximization [EM]), alternating minimization (AM) algorithm was selected for this study to reconstruct the cross-section of linear attenuation distribution for the various scans. The AM algorithm was chosen and applied in this work due to its capability to account for the stochastic nature of gamma-rays over the CSA of the objects as compared with other algorithms. This AM algorithm was initially proposed by

O'Sullivan and Benac [62] and applied for the first time by Varma et al. [63] to reconstruct an image of the phase holdup distribution in a two-phase system. Varma et al. [63] conducted a comparative study to reconstruct the gas holdup distribution in a two-phase system (phantom) by using the EM and AM algorithms.

Their reconstructed images revealed that the images obtained using the AM algorithm exhibit qualitatively and quantitatively more enhancement in the gas holdup distribution than those produced by the EM algorithm. These reconstructed linear attenuation coefficients for different cases of scans were subsequently used to calculate and produce the gas holdup distribution images by using special relationships, which were developed to estimate gas holdup distributions and their profiles in bubble columns with and without internals. The details of these relationships for calculating gas holdup as well as the methodology for excluding the vertical internals from the gas holdup distributions and their profiles are available in our previous paper [64,65].

One of the benefits of this CT technique is the possibility of using it as a gamma-ray densitometry (GRD) technique [66,67] to monitor online the flow behavior inside different multiphase reactors, demarcate flow regimes, detect the maldistribution (e.g., bypassing and stagnancy, hot spots), and measure phase holdup profiles. This GRD method employs only the central collimated detector opposite the source, without rotating the source and detector (both fixed) [68,69]. Another important feature is the ability of CT to scan large columns up to 30 inches (0.762) in diameter and 108 inches (2.743 m) in height. Furthermore, 3-D visualization of phase distributions can be achieved by scanning the object at multiple planes of the column's height.

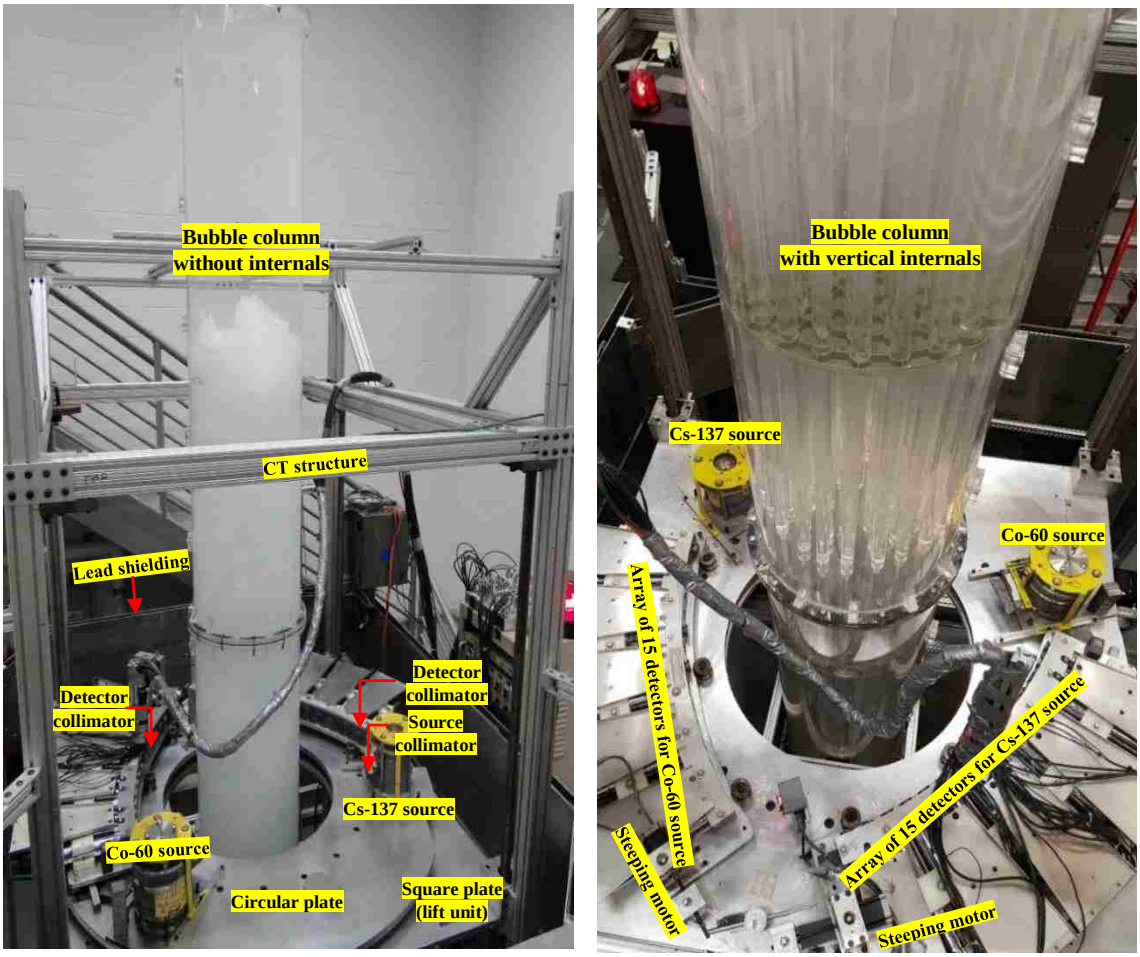

Figure 4: Photos of the DSCT technique with a pilot-scale bubble column with and without vertical internals

3. RESULTS AND DISCUSSION

3.1. ACCURACY AND REPRODUCIBILITY OF THE GAMMA-RAY COMPUTED TOMOGRAPHY (CT) MEASUREMENTS

The accuracy of the CT measurements was recently addressed and quantified in our previous publication [65] through a scanning Plexiglas® phantom that consisted of two concentric cylinders (inner cylinder of 3-inch diameter; outer cylinder of 6-inch diameter). Four cases of this phantom (i.e., empty phantom; inner cylinder filled with water, while the space between the coaxial cylinders was empty; empty inner cylinder, while the space

between the coaxial cylinders was only filled with water; both cylinders filled with water) were scanned independently, after which the linear attenuation coefficients (μ, cm^{-1}) for these cases of the phantom were reconstructed using the alternating minimization (AM) algorithm.

The experimental results of scanning the phantom in terms of the linear attenuation coefficient (μ, cm^{-1}) images and their diametrical profiles show the capability of the CT technique to reproduce the dimensions of the phantom with a discrepancy of only 1.39%. Additionally, the reconstructed linear attenuation coefficients of air, water, and Plexiglas® materials were compared to the theoretical linear attenuation coefficient (μ, cm^{-1}) of these materials, and it was found that they are in good agreement with theoretical values. For example, the absolute relative error (ARE) between the reconstructed linear attenuation coefficients (μ, cm^{-1}) and the theoretical values of air, water, and Plexiglas® were 1.3%, 2.4%, and 3.2%, respectively.

The reproducibility of the CT measurements was also checked and assessed systemically in this study. In this reproducibility assessment, an 18-inch bubble column with an air-water system and no vertical internal tubes was scanned at the fully developed flow regime (i.e., at an axial level of H/D = 3) to obtain the gas holdup distribution and their profiles. Two superficial gas velocities (5 and 30 cm/s) were examined in this assessment, where the CT scan was repeated twice in two different times to demonstrate the reproducibility of the CT experimental results.

The obtained experimental results in terms of the time-averaged cross-sectional gas holdup distributions and their azimuthal average diametrical profiles are presented in Figure 5 and Figure 6. As seen in these figures, the cross-sectional gas holdup distributions

that were measured and reconstructed for experiments Nos. 1, and 2 for either superficial gas velocities of 5 or 30 cm/s were qualitatively identical. Moreover, the azimuthal average of the gas holdup profiles of experiments Nos. 1, and 2 for the same operating conditions (at either superficial gas velocity 5 or 30 cm /s) were very similar along the diameter of the bubble column, indicating the high precision and reliability of the CT measurements.

For instance, the average absolute relative difference (*AARD*) between two profiles for each superficial gas velocity was calculated using Eq. 2, and it was found to be 2.17% and 3.47% for superficial gas velocities of 5 and 30 cm, respectively.

$$AARD = \frac{1}{N}\sum_{i=1}^{N}\left|\frac{\varepsilon_1(r) - \varepsilon_2(r)}{\varepsilon_1(r)}\right| \quad (2)$$

where $\varepsilon_1(r)$ and $\varepsilon_2(r)$ represent the gas holdup values of experiment No. 1 and No. 2, respectively, at the corresponding dimensionless radius positions, while N represents the number of data points along the diameter of the column.

Furthermore, the standard deviation (*SD*), which represents the deviation of the measured values of the gas holdup from the mean $\langle\varepsilon\rangle$ of these values along the diametrical profiles, was also calculated by Eq. 3.

$$SD = \sqrt{\frac{1}{N-1}\sum_{i=1}^{N}(\varepsilon_i - \langle\varepsilon\rangle)^2} \quad (3)$$

It was found that *SD* values were minimal, within 0.005 and 0.011 for the superficial gas velocities of 5 and 30 cm/s, respectively. The values of SD for the gas holdup profiles were inconsiderable, as exhibited in Figure 7; therefore, the error bars, which represent the standard deviation, are not plotted in the subsequent figures of the gas holdup profiles.

However, each scan was replicated twice, and the average of the gas holdup of these replications was estimated and plotted in this study to check the reproducibility of every experiment. The obtained values of the AARD and SD for the gas holdup profiles indicate that the CT measurements are highly reproducible (i.e., highly precise).

The bed expansion technique for calculating the overall gas holdup (Eq. 4) was also employed in this work as another independent method to check the accuracy of the CT results.

$$overall\ gas\ holdup = \frac{height\ of\ dynamic\ bed - height\ of\ static\ liquid}{height\ of\ dynamic\ bed} \quad (4)$$

The cross-sectional average of the gas holdup ($\bar{\varepsilon_g}$), can be also estimated by Eq. 5:

$$\bar{\varepsilon_g} = \frac{2}{R^2}\int_0^R \varepsilon(r) r dr \quad (5)$$

where *R* represents the radius of the bubble column and $\varepsilon(r)$ represents the values of the gas holdup at a specific radius (*r*).

There was good agreement between the results of the comparison between the overall and the average of the cross-sectional gas holdup values, with an absolute relative difference of 2.63% and 3.28% for the superficial gas velocities of 5 and 30 cm/s, respectively.

The dynamic height of the bed was held constant at an axial level of 2.67 m above the gas distributor, while the static height of the liquid was varied according to the operating conditions (i.e., at a superficial gas velocity of 5 or 30 cm/s).

It was demonstrated in our previous work that this will not affect the hydrodynamics of the fully developed flow region. The static and dynamic heights in these experiments were monitored and measured visually using a measuring tape, which was attached and pasted to the wall of the bubble column.

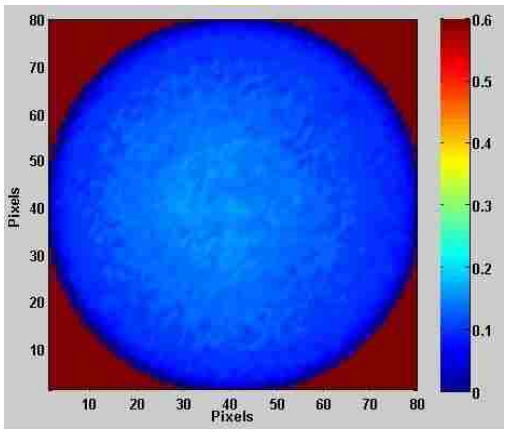

a) Time-averaged gas holdup distribution of experiment No. 1 in an 18-inch bubble column without vertical internal tubes operated at a superficial gas velocity of 5 cm/s

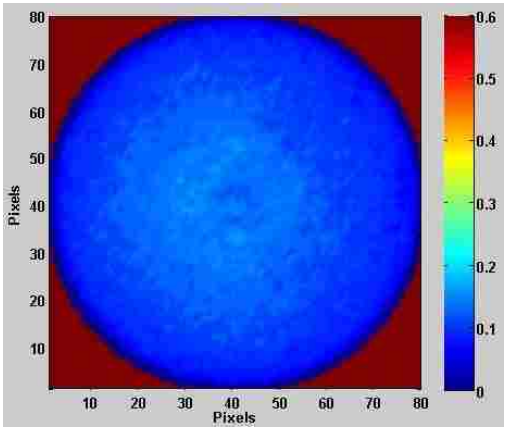

b) Time-averaged gas holdup distribution of experiment No. 2 in an 18-inch bubble column without vertical internal tubes operated at a superficial gas velocity of 5 cm/s

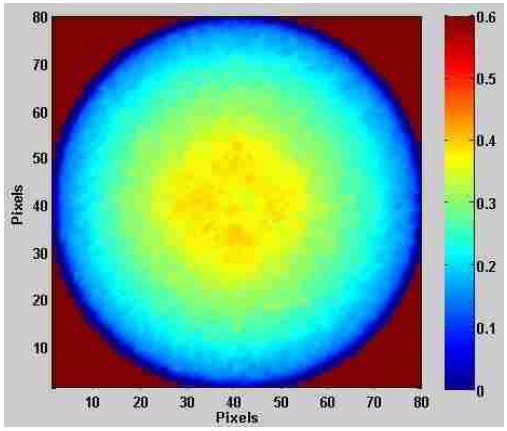

c)Time-averaged gas holdup distribution of experiment No. 1 in an 18-inch bubble column without vertical internal tubes operated at a superficial gas velocity of 30 cm/s

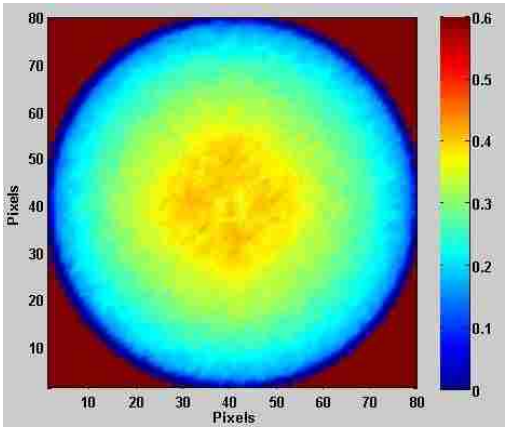

d)Time-averaged gas holdup distribution of experiment No. 2 in an 18-inch bubble column without vertical internal tubes operated at a superficial gas velocity of 30 cm/s

Figure 5: Reproducibility of the time-averaged cross-sectional gas holdup distributions in an 18-inch bubble column without vertical internal tubes operated at superficial gas velocities of 5 and 30 cm/s

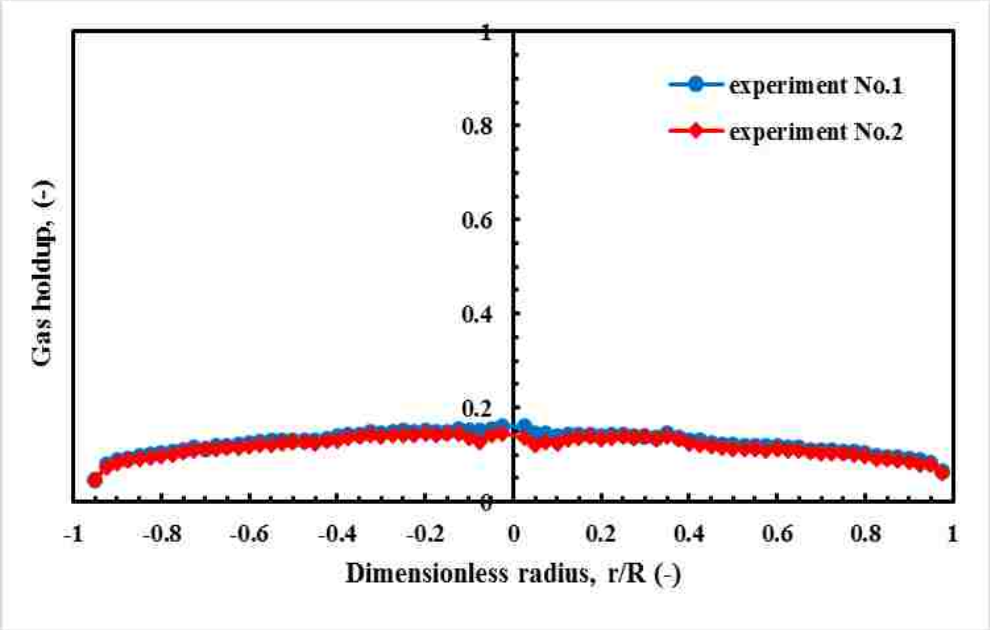

a) Azimuthal average of the gas holdup diametrical profiles in an 18-inch bubble column without vertical internal tubes operated at a superficial gas velocity of 5 cm/s

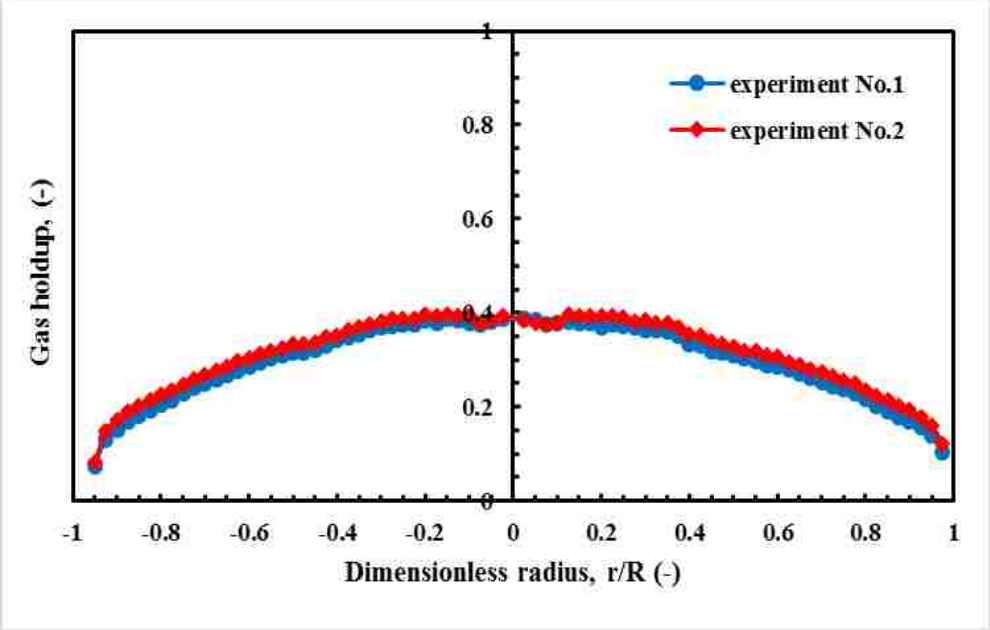

b) Azimuthal average of the gas holdup diametrical profiles in an 18-inch bubble column without vertical internal tubes operated at a superficial gas velocity of 30 cm/s

Figure 6: Reproducibility of the diametrical profiles of the gas holdup in an 18-inch bubble column without internals operated at superficial gas velocities of 5 and 30 cm/s

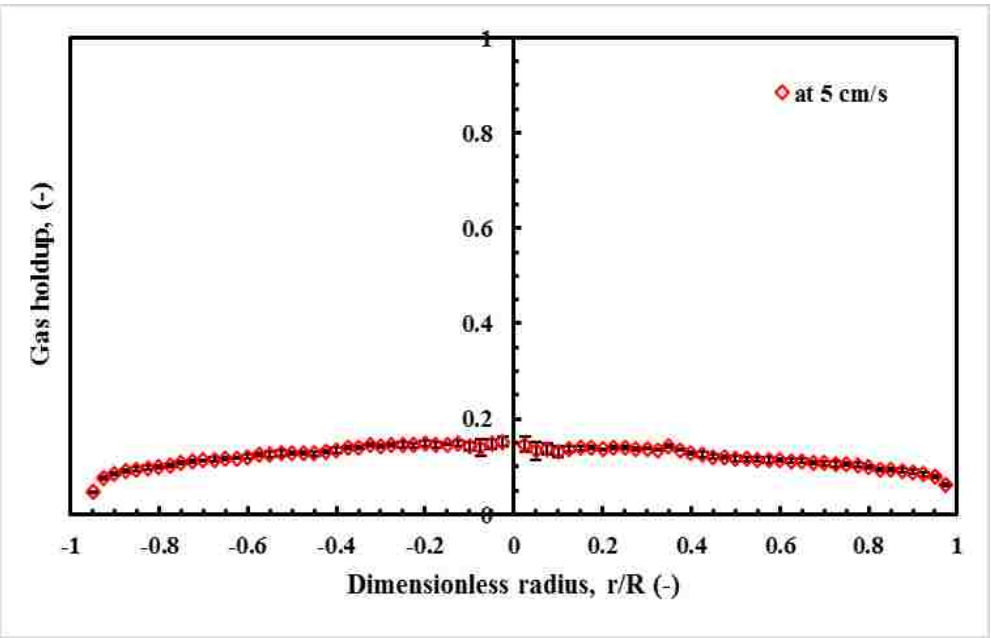

a) Azimuthal average of the gas holdup diametrical profiles in an 18-inch bubble column without vertical internal tubes operated at a superficial gas velocity of 5 cm/s (the error bars in this figure represent the standard deviation about the mean)

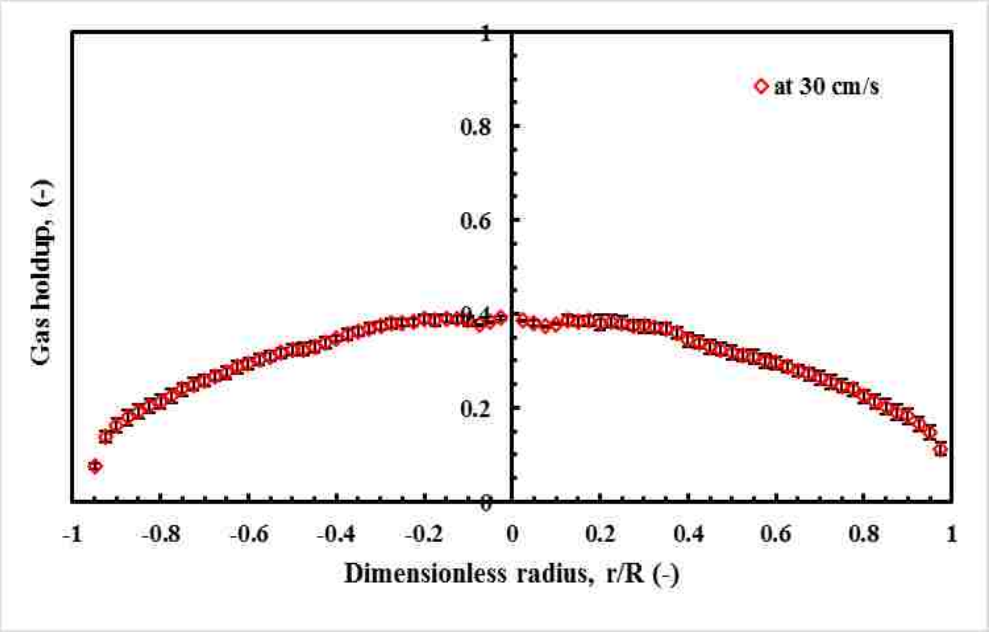

b) Azimuthal average of the gas holdup diametrical profiles in an 18-inch bubble column without vertical internal tubes operated at a superficial gas velocity of 30 cm/s (the error bars in this figure represent the standard deviation about the mean)

Figure 7: Reproducibility of the diametrical profiles of the gas holdup in an 18-inch bubble column without vertical internals operated at superficial gas velocities of 5 and 30 cm/s (the error bars in these figures represent the standard deviation about the mean)

3.2. IMAGING GAS-LIQUID DISTRIBUTIONS IN 18-INCH BUBBLE COLUMNS EQUIPPED WITH AND WITHOUT INTERNALS AT DIFFERENT SUPERFICIAL GAS VELOCITIES

One of the most important features of the CT technique in the field of multiphase flow is its capability to visualize and quantify the phase distribution over the column CSA, which is essential for evaluating the performance of reactors. Therefore, for the first time, the gas holdup distributions in a large-scale bubble column equipped densely with vertical internals were visualized in a noninvasive way using an advanced CT technique. Figure 8 displays the time-averaged cross-sectional gas holdup distributions for 18-inch diameter bubble columns with and without vertical internals arranged in a circular or hexagonal shape over the CSA of the column at different operating conditions (i.e., at superficial gas velocities of 5, 30, and 45 cm/s). It is evident from Figure 8 that the gas holdup distributions of the bubble columns with and without vertical internals were almost distributed symmetrically over the entire CSA of the bubble column for all the studied superficial gas velocities. Still, the phenomena of more gas at the center and less gas in the wall region of the bubble column in the absence of vertical internals persisted in the large-scale bubble column equipped densely with vertical internals, for both circular and hexagonal configurations.

For hexagonally arranged vertical internals, a notable increase in the gas holdup magnitude was observed in the wall region of the column, which is located in the space between the bundle of vertical internals and the wall of the column, unlike in the circular configuration. This available space (i.e., the clearance between the column wall and the bundle of internals, which is larger than that of the circular configuration) provides less resistance to the flow; hence, this might allow small bubbles to move to the region and rise

more freely than when bubbles move in the gaps between the vertical internals. As a result, the accumulation of small bubbles in this clearance leads to an increase in the gas holdup in this region. A similar observation was also reported by Youssef et al. [32] and Kagumba [39] when they measure the local gas holdup in an 18-inch bubble column with vertical internals for an air-water system using a four-point optical fiber probe.

In comparison with the bubble column without vertical internal tubes, the uniformity of the gas holdup distribution over the entire CSA of the columns in the presence of the vertical internals was enhanced for both configurations of internals. However, the hexagonal arrangement of the vertical internals provided a more homogeneous gas distributed over the column's CSA as compared to the column with the circular arrangement or without vertical internals.

To provide a further confirmation of this observation, a uniformity factor (*F*) of the gas holdup distribution over the entire CSA of the bubble columns with and without vertical internals was calculated by using the following equation:

$$F = \frac{1}{N}\sum_{i,j=1}^{N}\left(\frac{\varepsilon_{g,ij} - \varepsilon_{avg}}{\varepsilon_{avg}}\right)^2 \tag{6}$$

$$\varepsilon_{avg} = \frac{1}{N}\sum_{i,j=1}^{N}\varepsilon_{g,ij} \tag{7}$$

Eq. 6 was built based on the deviation of a gas holdup in each pixel ($\varepsilon_{g,ij}$) from the average of the cross-sectional (ε_{avg}) gas holdup, where the smaller values of the uniformity factor (close to zero) indicate a uniform gas holdup distribution. The presence of vertical internal tubes arranged either circularly or hexagonally significantly improved the distribution of the gas phase over the CSA of the columns at the churn turbulent flow

regime (i.e., particularly at the superficial gas velocities of 30 and 45 cm/s). This observed enhancement in the uniformity of the gas holdup distribution could be attributed to the existence of these vertical internal tubes, which help to spread the gas towards the column wall. However, the bubble column with a circular configuration provided nonuniform distribution at a low superficial gas velocity (5 cm/s) compared to the other bubble columns (i.e., the column without vertical internals or the column with the hexagonal arrangement). This might result from the geometric configuration because a flow does not fully develop under this condition (i.e., the effect of the entrance of column and the vertical internals still dominate at a low superficial gas velocity). According to the uniformity factor (*F*) of gas holdup distribution values, which are calculated and tabulated in Table 1, better distribution of the gas holdup over the entire CSA was achieved with the hexagonal configuration, which had low *F* values compared to the other bubble columns (i.e., with a circular configuration or without vertical internals). From an industrial point of view, a uniform distribution (i.e., gas distributed homogeneously over the entire cross-sectional area of the column) is essential to achieve optimal reactor performance. For instance, a high-quality and efficient chemical reaction can only be achieved through homogeneous gas holdup distribution along the liquid phase in the bubble column or slurry phase (liquid-catalyst) in a slurry bubble column. This occurs because the homogeneous gas holdup distribution leads to better interaction between phases, which is necessary for the chemical reaction. In contrast, the nonhomogeneous gas holdup distribution over the entire CSA of the column causes poor contact between other phases (liquid or slurry phases), which accelerates the reaction in some regions, while slowing in other areas of the reactor, which consequently negatively affects the reactor's performance.

More interestingly, the average of the cross-sectional gas holdup distributions for bubble columns with and without vertical internal tubes were very similar, as presented in Table 2. Therefore, these results confirm the findings obtained recently by Kagumba and Al-Dahhan [33] and Al Mesfer et al. [36], who reported that at the churn turbulent flow regime, the gas holdup that was achieved in the bubble column in the absence of vertical internals could be extrapolated to the columns with vertical internals. However, this could only occur when these columns with internals were operated at the same superficial gas velocity but calculated based on the free CSA for the flow. This finding is particularly noteworthy because it was achieved in 6-inch bubble columns, while in the current work the same observation was obtained in 18-inch bubble columns.

Table 1: Uniformity factor of the gas holdup distribution for bubble columns with and without internals

Superficial gas velocity, cm/s	Without vertical internals	Circular configuration	Hexagonal configuration
5	0.133	0.192	0.097
30	0.195	0.136	0.102
45	0.180	0.120	0.082

Table 2: Mean of the cross-sectional gas holdup distribution for bubble columns with and without internals

Superficial gas velocity, cm/s	Without vertical internals	Circular configuration	Hexagonal configuration
5	0.103	0.070	0.096
30	0.233	0.233	0.255
45	0.300	0.288	0.328

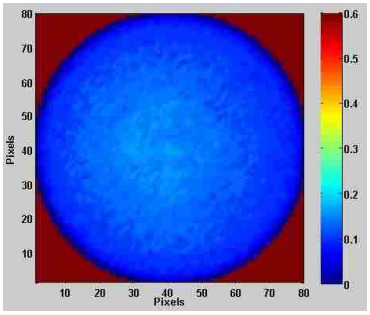

a) Gas holdup distribution in the bubble column without internals at a superficial gas velocity of 5 cm/s

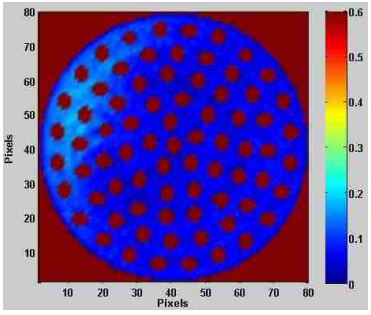

b) Gas holdup distribution in the bubble column with internals arranged in a circular configuration and operated at a superficial gas velocityof 5 cm/s

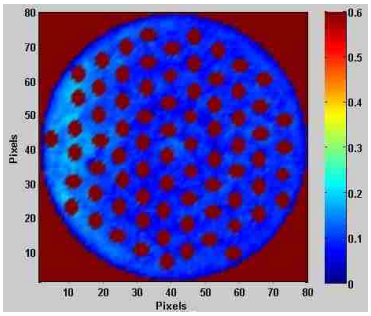

c) Gas holdup distribution in the bubble column with internals arranged in a hexagonal configuration and operated at a superficial gas velocity of 5 cm/s

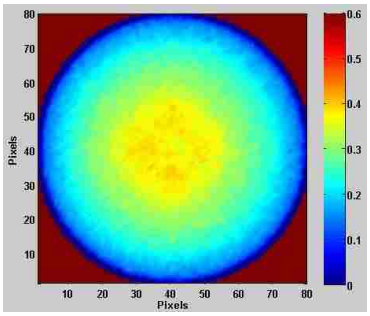

d) Gas holdup distribution in the bubble column without internals at a superficial gas velocity of 30 cm/s

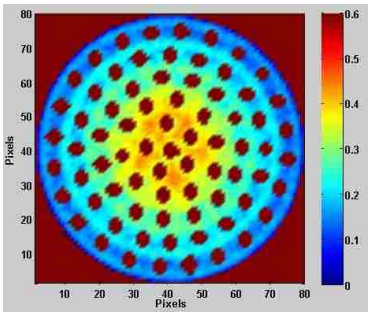

e) Gas holdup distribution in the bubble column with internals arranged in a circular configuration and operated at a superficial gas velocity of 30 cm/s

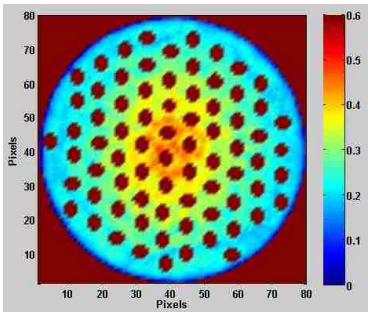

f) Gas holdup distribution in the bubble column with internals arranged in a hexagonal configuration and operated at a superficial gas velocity of 30 cm/s

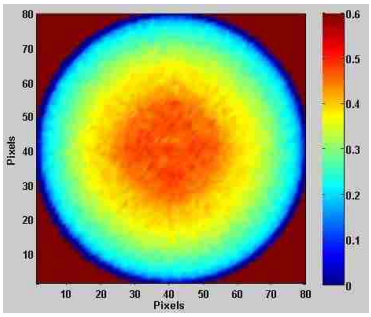

g) Gas holdup distribution in the bubble column without internals at a superficial gas velocity of 45 cm/s

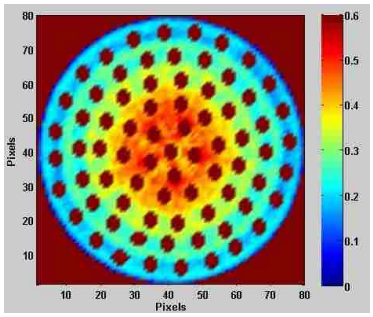

h) Gas holdup distribution in the bubble column with internals arranged in a circular configuration and operated at a superficial gas velocity of 45 cm/s

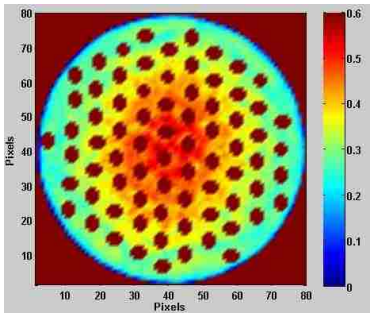

i) Gas holdup distribution in the bubble column with internals arranged in a hexagonal configuration and operated at a superficial gas velocity of 45 cm/s

Figure 8: Time-averaged cross-sectional gas holdup distributions for 18-inch bubble columns with and without vertical internal tubes (circular and hexagonal configurations) operated under different superficial gas velocities (5, 30, and 45 cm/s)

3.3. EFFECT OF THE VERTICAL INTERNAL TUBES AND THEIR ARRANGEMENTS ON THE DIAMETRICAL GAS HOLDUP PROFILES IN AN 18-INCH DIAMETER BUBBLE COLUMN AT DIFFERENT SUPERFICIAL GAS VELOCITIES

Figure 9-11 show the comparison between the azimuthal average of the gas holdup profiles for the 18-inch bubble columns in the presence or absence vertical internal tubes (i.e., circular and hexagonal arrangements) at different superficial gas velocities, namely 5, 30, and 45 cm/s. The superficial gas velocity for the bubble column without vertical internal tubes was calculated based on the total CSA of the column, while it was computed with respect to the free passing CSA for the columns equipped with vertical internal tubes. From Figure 9, it is evident that the circular and hexagonal configurations of the vertical internals at a superficial gas velocity of 5 cm/s provided lower diametrical gas holdup profiles compared to those of the bubble column without vertical internals, which produced a higher gas holdup profiles at all radial positions. However, the hexagonal configuration produces higher gas holdup than the circular configuration. Both the circular and hexagonal configurations had the same number of vertical internals and the same size of vertical internals (i.e., 1-inch diameter); also, the vertical internals occluded the same CSA (approximately 25% of the total CSA of the column). Therefore, the means of the gas holdup profiles for these configurations as well as for the column without vertical internals were computed to analyze whether they provided similar gas holdup profiles at a studied superficial gas velocity. For instance, at a superficial gas velocity of 5 cm/s, the mean of the gas holdup profile in the bubble column with the hexagonal configuration increased by 36% with respect to the column with the circular arrangement. As seen in Figure 9, the behavior of the circular configuration was significantly different than the hexagonal configuration, which had the same occupied CSA and the same diameter of vertical

internals. This observed difference in the behavior of the configurations could result from the difference in the geometry of the configurations (i.e., the compartment between tubes, the pitch of tubes). Figure 10 and Figure 11 display the azimuthal average of the gas holdup profiles for the bubble columns with and without vertical internals in the deep churn turbulent flow regime at superficial gas velocities of 30 and 45 cm/s. A closer analysis of these figures reveals that the configuration's impact on the gas holdup profiles is insignificant under a deep churn turbulent flow regime. For example, the absolute relative difference between the means of the gas holdup profiles for the bubble column with the circular configuration and the column without vertical internals was 0.13% and 4.16%, respectively, at a superficial velocity of 30 and 45 cm/s, respectively. However, for the hexagonal arrangement, the absolute relative difference was 8.94% and 9.38%, respectively, for the column without vertical internals at a superficial gas velocity of 30 and 45 cm/s, respectively. This convergence of the gas holdup values between the bubble columns with and without vertical internals suggests that the impact of the presence of vertical internals and their configurations on the gas holdup profiles is insignificant under deep churn turbulent flow regime. This is particularly true at the superficial gas velocities of 30 and 45 cm/s, when it was calculated based on the free CSA for the flow, not based on the total CSA of the column. These findings of convergence between the values of the gas holdup in the 18-inch bubble column with and without vertical internals were also obtained in a 6-inch bubble column as reported by Kagumba [33] and Al Mesfer [38]. Additionally, Figure 10 and Figure 11 illustrate that the gas holdup values for the bubble column with the hexagonal configuration were comparatively higher than those in either the column with the circular shape or the column without vertical internals near the wall

region. For instance, it was found that at a superficial gas velocity of 45 cm/s, the percentage of increase in the gas holdup in the wall region (r/R = 0.925) of the bubble column with the hexagonal configuration was 40.82% compared to the column with the circular arrangement and 50.82% in relation to the column without vertical internals. The reason for this enhancement of gas holdup values with the hexagonal configuration in the wall region could relate to the larger space (i.e., missing tubes in this area; see Figure 12) that exists between the vertical internals bundle and the column wall compared to the circular configuration, as explained earlier. This observation agrees with Kagumba's study, which included measuring the bubble properties (e.g., the specific interfacial area, axial bubble velocity, bubble passage frequency, and bubble chord length) in an 18-inch bubble column equipped densely with vertical internals using a four-point optical fiber probe. Kagumba [39] reported that smaller bubbles chord lengths were obtained in the wall region of the bubble column based on the insertion of vertical internals. Additionally, a notable decrease in the bubble rise velocity was obtained in the wall region of the bubble column with vertical internals. This reduction in the bubble cord length and bubble rise velocity caused an increase in the residence time of the bubbles, which explains the increase in the gas holdup in the wall region.

The gas holdup profiles show that the bubble column with the hexagonal arrangement of vertical internals provided higher gas holdup values at the center region and under a high superficial gas velocity (i.e., under a churn turbulent flow regime) as compared to other bubble columns. For instance, at a superficial gas velocity of 45 cm/s and dimensionless radius (r/R) of 0.075, there was a 13.94% increase in the gas holdup with the hexagonal as compared to the circular configuration. The rise in the gas holdup

for the hexagonal arrangement in the center region could result from the missing vertical tube (gap) in this area in the hexagonal configuration compared to the circular configuration, which has a central tube in this region. This observation was also reported by Kagumba [33], who measured the local gas holdup and bubble properties (e.g., specific interfacial area, axial bubble velocity, bubble passage frequency, and bubble chord lengths) in the same system and operating condition using a four-point fiber optical probe technique. Additionally, the shapes of the gas holdup profiles of the bubble columns were different; For example, the bubble column without vertical internals produced a parabolic shape profile, while the bubble column with vertical internals generated a wavy shape profile. However, the shape of the gas holdup profile in the bubble column with the circular configuration produced a wavier curve than the hexagonal configuration. This variation in the degree of the wavy curve between the gas holdup profiles resulted from (1) different arrangements of the vertical internals, and (2) the fact that the hexagonal configuration had compartments of uniform size, and (3) the degree of pitch between the internals as compared to the circular configuration. For industrially important arrangements of vertical internal tubes, the influence of a configuration can be considered significant at a low superficial gas velocity, whereas it is deemed insignificant at high superficial gas velocities (deep in the churn turbulent flow regime); these velocities should be calculated based on the free CSA for the flow.

The design and scale-up of bubble/slurry bubble columns are challenging tasks due to the complex interaction that exists among the phases in these reactors. However, the presence of a bundle of heat-exchanging tubes inside these reactors for highly exothermic reactions further increases this complexity and also alters the hydrodynamics, intensity of

the liquid or slurry mixing, and heat and mass transfer rates, all of which affect the performance of these reactors. Therefore, further experimental investigations must be performed to investigate, analyze, and quantify the impact of the presence of vertical internals on the hydrodynamics of these reactors. These investigations are necessary for the design and scale-up of these reactors as well as to develop and validate reactor simulations or models. Lab-scale, pilot-scale, and industrial scale experimental studies are under investigation in our mReal laboratory, where an advanced radioactive particle tracking (RPT) technique is used to investigate the impact of these vertical internal tubes and their arrangements on the liquid velocity field and turbulence parameters (e.g., Reynolds stresses, turbulent kinetic energy, and turbulent eddy diffusivities). These experimental investigations will be reported in future papers.

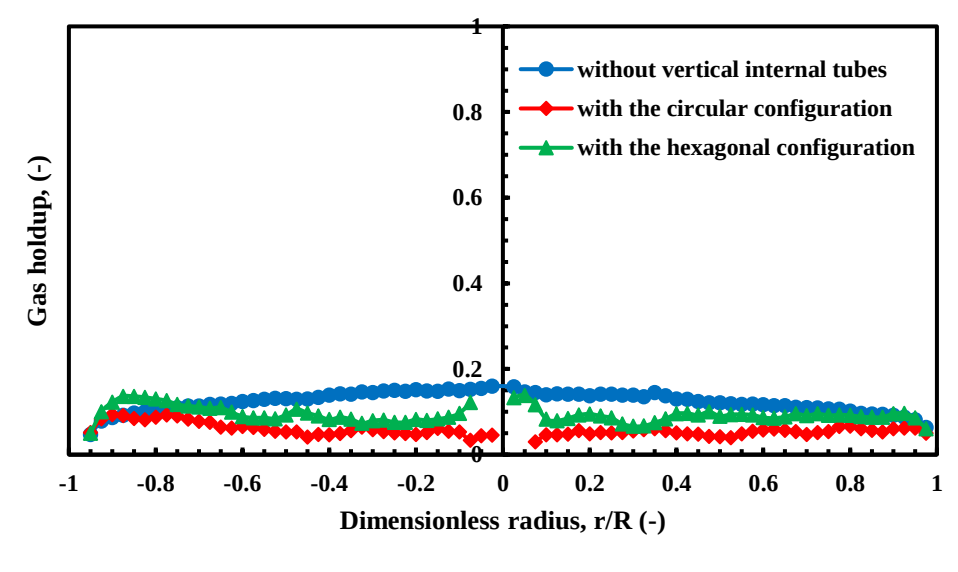

Figure 9: Comparison between the azimuthal average of the gas holdup profiles measured at a superficial gas velocity of 5 cm/s for the bubble columns with and without vertical internals (arranged in circular and hexagonal configurations)

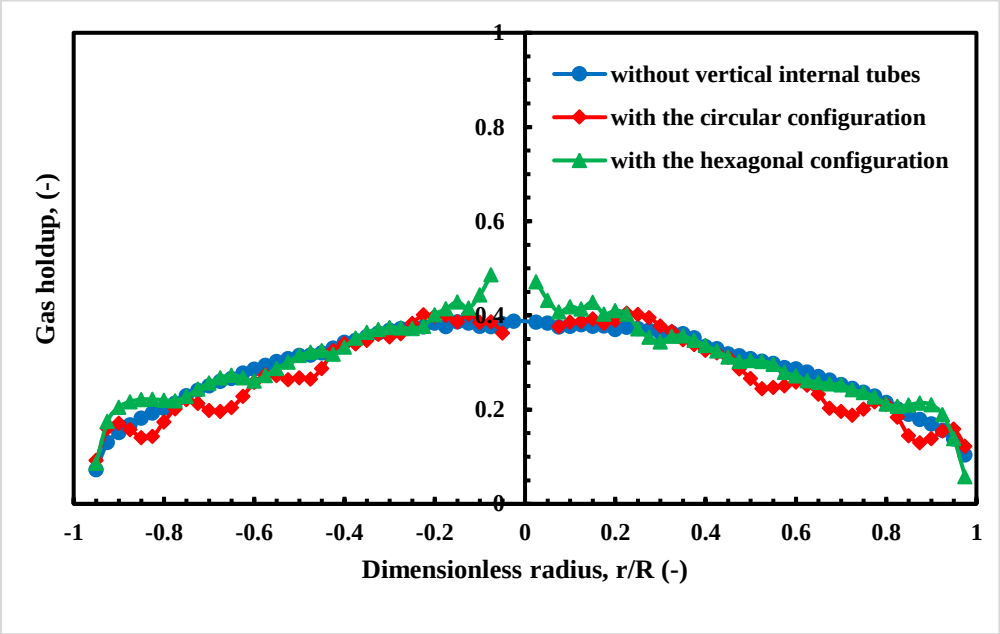

Figure 10: Comparison between the azimuthal average of the gas holdup profiles measured at a superficial gas velocity of 30 cm/s for the bubble columns with and without vertical internals (arranged in circular and hexagonal configurations)

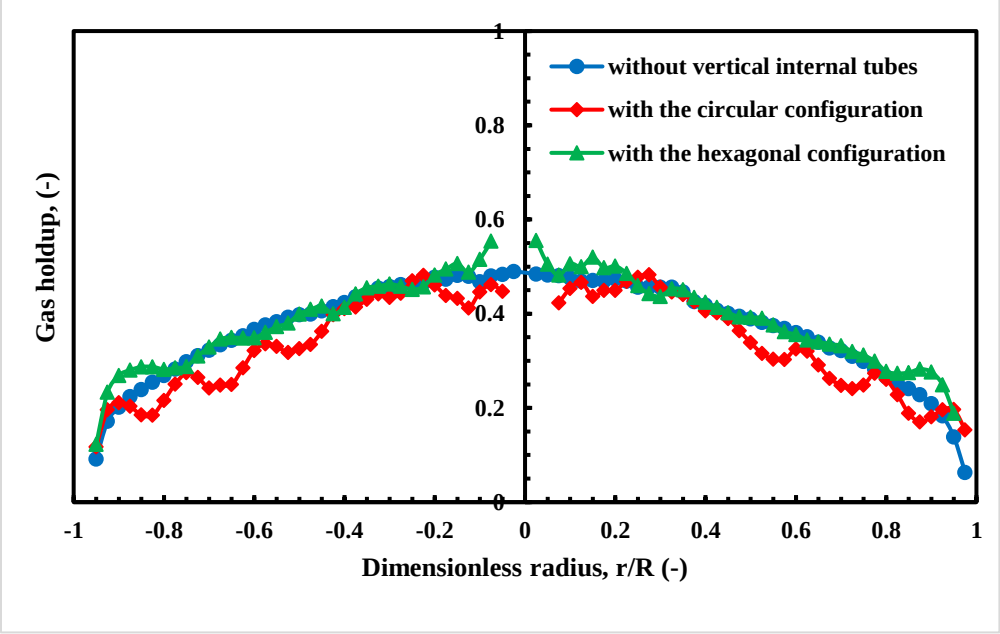

Figure 11: Comparison between the azimuthal average of the gas holdup profiles measured at a superficial gas velocity of 45 cm/s for the bubble columns with and without vertical internals (arranged in circular and hexagonal configurations)

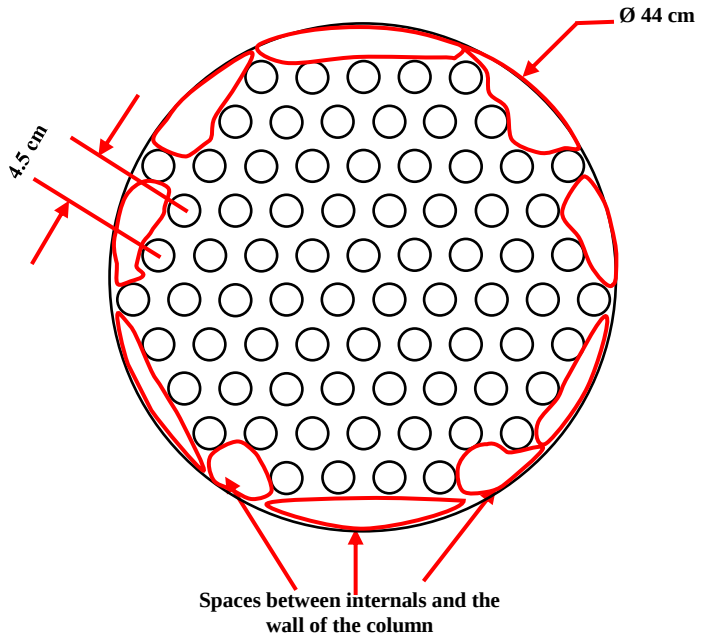

Figure 12: Schematic illustration showing the spaces between the bundle of vertical internals and the wall of the column

3.4. IMPACT OF THE SIZE OF THE BUBBLE COLUMNS ON THE GAS HOLDUP DISTRIBUTION AND THEIR PROFILES

The scale-up process of the bubble/slurry bubble columns in the absence of heat-exchanging tubes is a challenging task that becomes more difficult in the presence of vertical tubes due to the absence of a reliable phenomenological model that can predict the hydrodynamic parameters of these rectors and also due to the lack of experimental investigations of these columns with heat-exchanging tubes. Therefore, in the current study, the effect of the bubble column size on the gas holdup in the bubble columns with and without vertical internals at different superficial gas velocities was addressed to support the scale-up process because there is a lack of benchmark data to evaluate and verify the prediction of any scale-up methods for these kinds of reactors.

The subsequently presented figures represent the gas holdup distributions and their profiles for 18-inch bubble columns with and without vertical internals as well as results of gas holdup distributions and their profiles for 6-inch bubble columns with and without vertical internals, which were recently published [70].

Figure 13 shows the comparison of gas holdup distributions over the entire CSA and their diametrical profiles of two sizes (6- and 18-inch in the diameter) of bubble columns without vertical internals, operated under two superficial gas velocities (i.e., 5 and 45 cm/s). It is clear from the gas holdup distribution figures (Figure 13a, b, c, and d) that the gas phase was symmetrically and uniformly distributed over the CSA for both diameters of the columns. However, the larger bubble column (i.e., 18-inch diameter) was found to significantly enhance the gas phase distribution over the CSA of the column.

For example, the uniformity factor decreased by 39.361% and 44.18% when an 18-inch bubble column was used under the superficial gas velocities of 5 and 45 cm/ s, respectively. Additionally, the impact of the size of the column on the magnitude of the gas holdup was found to be significant at a low superficial gas velocity (5 cm/s), while it was insignificant at a high superficial gas velocity (45 cm/s), as displayed in Figure 13e. For instance, the average absolute relative differences between the two profiles were 40.12% at a superficial gas velocity of 5 cm/s, but 10.08% at a superficial gas velocity of 45 cm/s.

Contrary to the impacts of the size of the bubble column without vertical internals on the cross-sectional gas holdup distribution at a low superficial gas velocity (i.e., 5 cm/s), the larger bubble column equipped densely with vertical internals arranged in a circular configuration notably increased the non-uniformity of the gas phase distribution. For

example, the uniformity factor increased by 25.36% compared to the 6-inch bubble column with vertical internals arranged circularly.

However, the 18-inch bubble column with vertical internals arranged in a circular configuration was found to improve the gas phase distribution over the entire CSA of the column under a high superficial gas velocity, as shown in Figure 14. For instance, the uniformity factor was reduced by 38.67% when the larger bubble column with vertical internals was used compared to the 6-inch bubble column with vertical internals arranged in a circular configuration.

Moreover, the magnitude of the gas holdup profiles was significantly influenced by the size of the bubble column with vertical internal tubes (i.e., vertical internal tubes arranged in a circular configuration) under a low superficial gas velocity (i.e., 5 cm/s), while less effect was observed at a high superficial gas velocity (i.e., 45 cm/s), as presented in Figure 14e.

For example, the average absolute relative difference between the profiles of different sizes of the bubble column with vertical internals was 191.03% and 19.49% for low and high superficial gas velocities, respectively. Interestingly, the gas holdup profiles for the 6-inch and 18-inch bubble columns with vertical internals were very similar at a high superficial gas velocity, except in the core region of the column, due to the presence or absence of the central tube for both sizes of bubble columns.

Similar to the impact of the size of the bubble columns in the absence of vertical internals on the gas holdup distribution, the impact of the size of the bubble columns with vertical internals arranged in a hexagonal configuration significantly enhanced the gas holdup distribution over the entire CSA of the columns; this occurred under both low and

high superficial gas velocities, as shown in Figure 15. For example, the uniformity factor decreased by 29.42% and 44.93% at superficial gas velocities of 5 and 45 cm/s, respectively.

Additionally, for the hexagonal configuration, the effect of the size of the bubble column on the magnitude of the gas holdup profiles was significant at a low superficial gas velocity, while it was insignificant at a high superficial gas velocity, as displayed in Figure 15e. For example, the average absolute relative difference between the gas holdups profiles for different sizes of the bubble columns with a hexagonal configuration were 81.8% and 10.9% at superficial gas velocities of 5 and 45 cm/s, respectively.

In summary, increasing the size of the bubble column without vertical internals enhances the gas holdup distribution significantly over the entire CSA of the columns. Additionally, the gas phase distributions are further improved when a larger bubble column with vertical internals (arranged either circularly or hexagonally over the CSA of the column) was used, except in the larger bubble column with the circular configuration at a low superficial gas velocity. However, the 18-inch bubble column with vertical internals arranged in a hexagonal shape provided the best gas holdup distribution in comparison with the bubble column with and without vertical internals arranged in a circular configuration.

Furthermore, the impact of the size of the bubble columns with and without vertical internals on the gas holdup magnitude was remarkable at a low superficial gas velocity, while it was insignificant at high superficial gas velocities, which agrees with the findings of Youssef et al. [32], and Forret et al. [71].

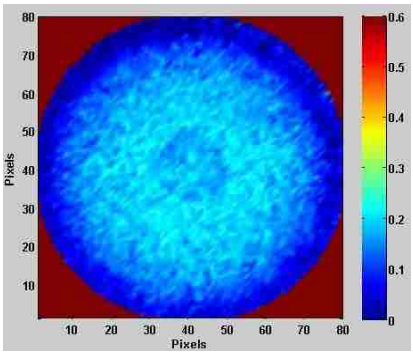

a) Gas holdup distribution in a 6-inch bubble column without vertical internal tubes at a superficial gas velocity of 5 cm/s

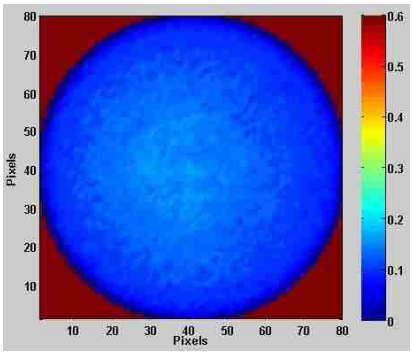

b) Gas holdup distribution in an 18-inch bubble column without vertical internal tubes at a superficial gas velocity of 5 cm/s

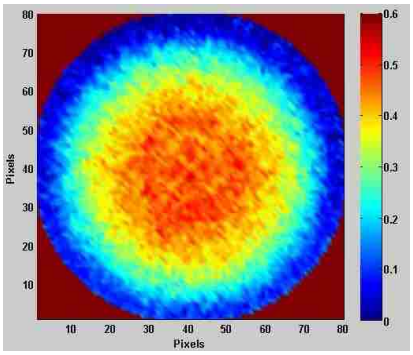

c) Gas holdup distribution in a 6-inch bubble column without vertical internal tubes at a superficial gas velocity of 45 cm/s

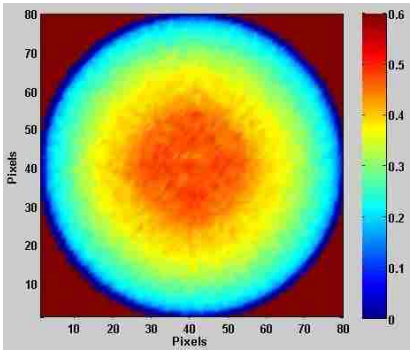

d) Gas holdup distribution in an 18-inch bubble column without vertical internal tubes at a superficial gas velocity of 45 cm/s

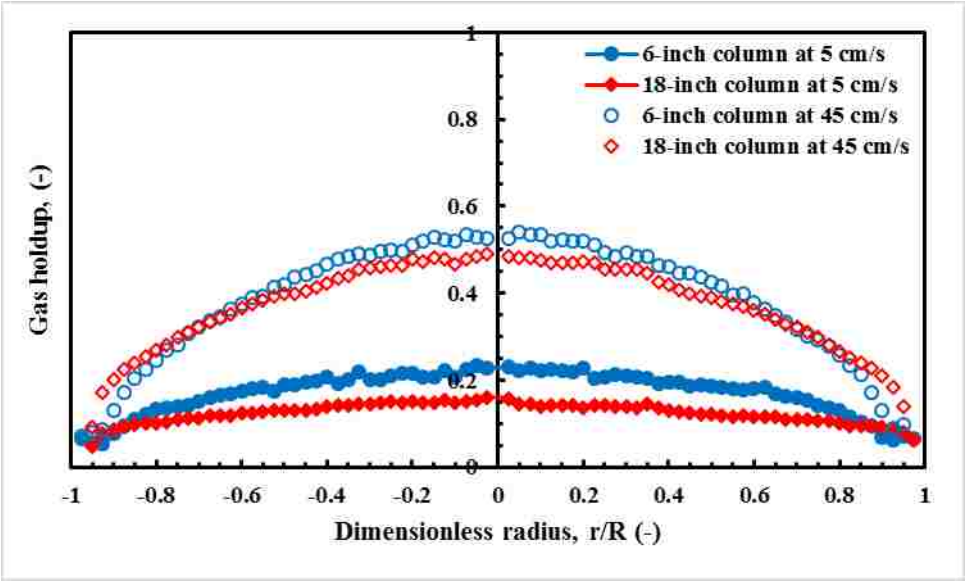

e) Gas holdup profiles obtained in 6- and 18-inch bubble columns without vertical internals at different superficial gas velocities (5 and 45 cm/s)

Figure 13: Comparison between gas holdup distributions and their profiles obtained in 6- and 18-inch bubble columns without vertical internals at different superficial gas velocities (5 and 45 cm/s)

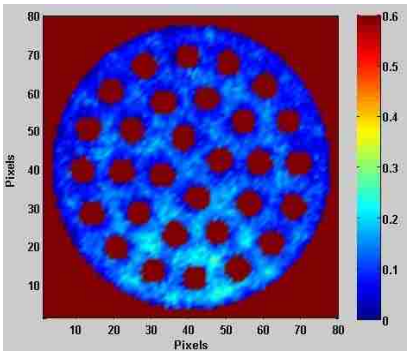

a) Gas holdup distribution in a 6-inch bubble column with a circular configuration at a superficial gas velocity of 5 cm/s

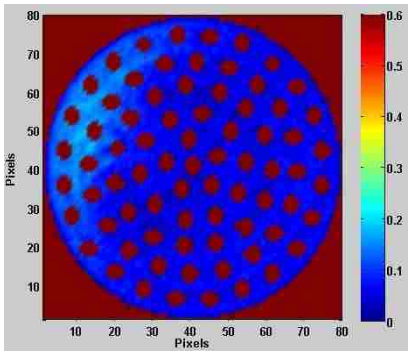

b) Gas holdup distribution in an 18-inch bubble column with a circular configuration at a superficial gas velocity of 5 cm/s

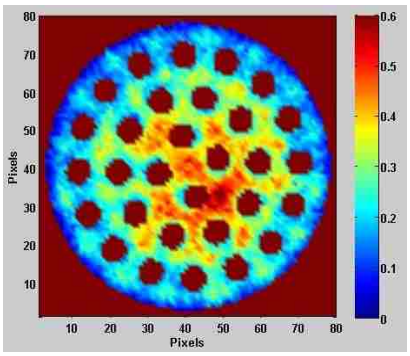

c) Gas holdup distribution in a 6-inch bubble column with a circular configuration at a superficial gas velocity of 45 cm/s

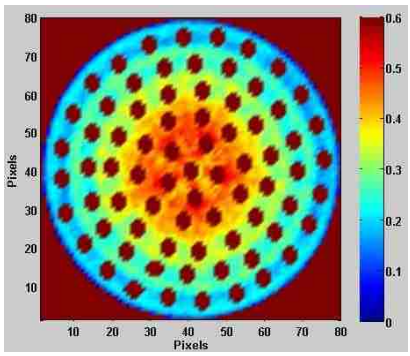

d) Gas holdup distribution in an 18-inch bubble column with a circular configuration at a superficial gas velocity of 45 cm/s

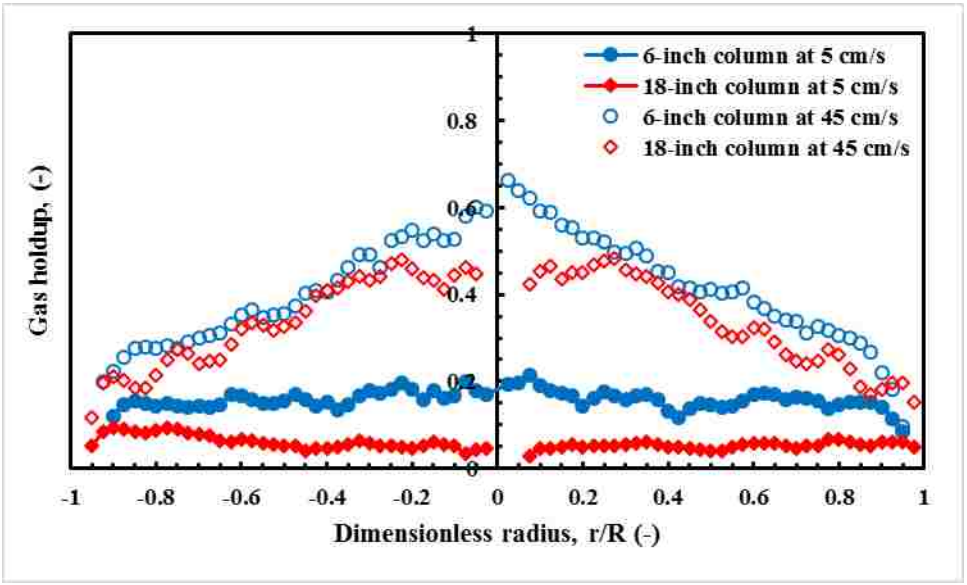

e) Gas holdup profiles obtained in 6- and 18-inch bubble columns with circular configuration at different superficial gas velocities (5 and 45 cm/s)

Figure 14: Comparison between gas holdup distributions and their profiles obtained in 6- and 18-inch bubble columns with a circular configuration at different superficial gas velocities (5 and 45 cm/s)

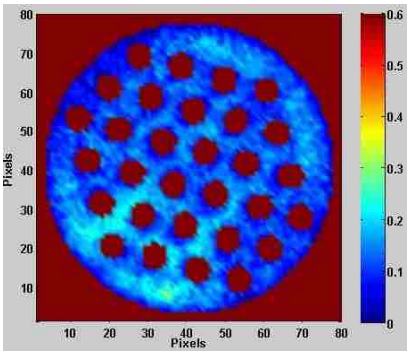

a) Gas holdup distribution in a 6-inch bubble column with a hexagonal configuration at a superficial gas velocity of 5 cm/s

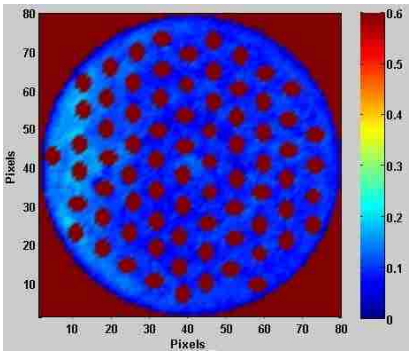

b) Gas holdup distribution in an 18-inch bubble column with a hexagonal configuration at a superficial gas velocity of 5 cm/s

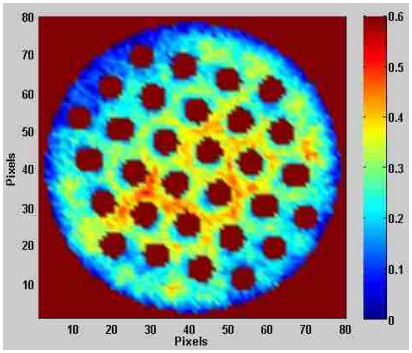

c) Gas holdup distribution in a 6-inch bubble column with a hexagonal configuration at a superficial gas velocity of 45 cm/s

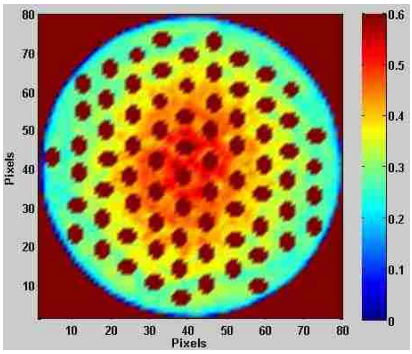

d) Gas holdup distribution in a 18-inch bubble column with a hexagonal configuration at a superficial gas velocity of 45 cm/s

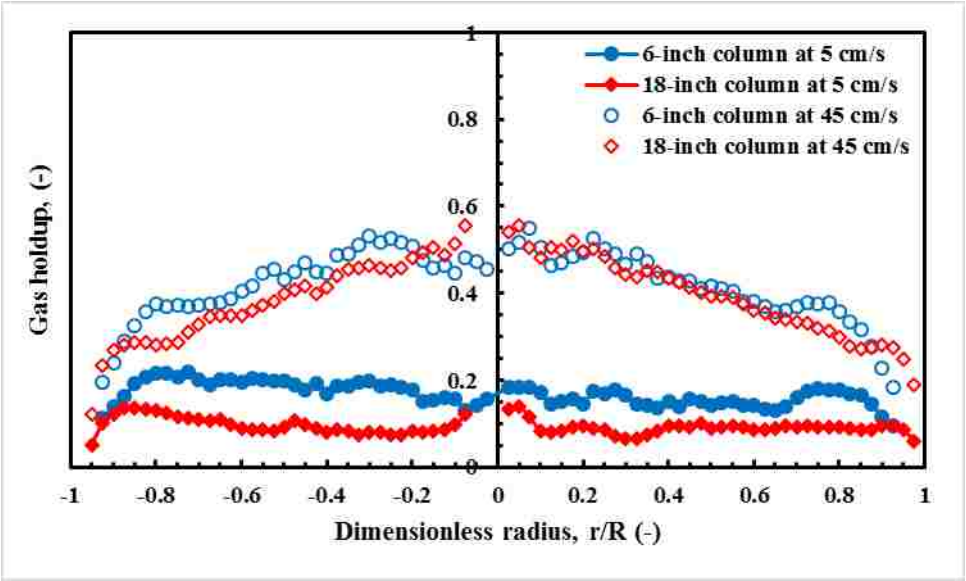

e) Gas holdup profiles obtained in 6- and 18-inch bubble columns with hexagonal configuration at different superficial gas velocities (5 and 45 cm/s)

Figure 15: Comparison between gas holdup distributions and their profiles obtained in 6- and 18-inch bubble columns with a hexagonal configuration at different superficial gas velocity (5 and 45 cm/s)

4. REMARKS

This investigation marks the first time that advanced gamma-ray computed tomography was used to investigate the influence of a configuration design of vertical internals on the gas holdup distribution over the entire cross-sectional area of a large-scale bubble column under different superficial gas velocities, covering the homogenous and heterogeneous flow regimes. This study examined two configurations (i.e., circular and hexagonal arrangements of vertical internals) where the vertical internals occupied the same amount of CSA (approximately 25% of the total CSA of the column, targeting the Fischer-Tropsch synthesis), with the same number and size of the vertical internal tubes. In addition, the obtained results in the 18-inch bubble column with and without vertical internals were compared with results achieved in the 6-inch bubble column with and without vertical internals to understand and assess the effect of the size of the reactor on the gas holdup distribution for bubble columns with and without vertical internals. The key results and findings of the current investigation can be summarized as follows:

- Symmetrical gas holdup distributions over the entire CSA of the bubble columns with and without vertical internal tubes were obtained for all studied superficial gas velocities, except that the bubble column with the circular configuration displayed a nonsymmetrical distribution at a low superficial gas velocity (5 cm/s).
- The well-known phenomenon in bubble columns without vertical internal tubes, where more gas resides at the center region and less gas at the wall region, persisted in the large-scale bubble column equipped densely with vertical internals for both configurations.

- For all studied superficial gas velocities, the presence of vertical internals arranged circularly or hexagonally inside the bubble columns enhanced the gas holdup distribution over the entire CSA of the bubble column compared with the column without vertical internals.
- For all investigated operating conditions, better gas holdup distributions were obtained in the bubble column with a hexagonal configuration (i.e., the gas phase was more homogeneously distributed over the CSA of the bubble column) compared to other bubble columns.
- Interestingly, the averages of the cross-sectional gas holdups and their profiles for the bubble columns with and without vertical internals were similar to one other when the bubble column with the vertical internals operated at a high superficial gas velocity that was calculated based on the free CSA for the flow.
- At a superficial gas velocity of 5 cm/s, there was a significant decrease in the gas holdup values for the circular and hexagonal configuration as compared to the column without vertical internals.
- A significant increase in the gas holdup values was obtained in the bubble column with the hexagonal arrangement of internals at the center and the wall regions and under a churn turbulent flow regime due to an absence of vertical internals in these areas.
- The shapes of the gas holdup profiles for the bubble column in the presence and absence of vertical internals differed. For example, the bubble column without vertical internals produced a parabolic profile, while the columns with vertical internals provided wavy profiles. However, the circular configuration offered more wavy profiles than the hexagonal arrangement.

- The effect of the configuration design on the gas holdup values was significant at a low superficial gas velocity, while it was insignificant at high superficial gas velocities that were calculated based on the free CSA for the flow.
- Increasing the size of the bubble column in the absence of vertical internals improved the gas holdup distribution significantly over the entire CSA of the columns. In addition, the gas holdup distributions were further enhanced when a larger bubble column with vertical internals (arranged either circularly or hexagonally over the column's CSA) was used, except in the case of the larger bubble column with the circular configuration under a low superficial gas velocity.
- The 18-inch bubble column with internals arranged in a hexagonal configuration produced better gas holdup distribution over the entire CSA of the column than the column with and without vertical internals organized in a circular shape.
- The influence of the diameter of the bubble columns in the presence and absence of the vertical internals on the gas holdup magnitude was notable at a low superficial gas velocity but insignificant at high superficial gas velocities.
- The obtained results in terms of the gas holdup distributions and their diametrical profiles for different configuration designs can serve as benchmark data to evaluate and validate CFD simulation toward better prediction of hydrodynamic parameters in bubble columns equipped with vertical internals. Once the CFD simulation is validated against the benchmark data, it can be used as a dependable tool to advance the fundamental understanding of these reactors without conducting expensive experiments. Additionally, it can be employed to design, scale-up, and evaluate the performance of these reactors.

ACKNOWLEDGMENTS

The authors would like to acknowledge the financial support in the form of scholarships awarded by the Higher Committee for Education Development in Iraq (HCED) and Ministry of Higher Education and Scientific Research (Iraq).

REFERENCES

(1) Larson, E. D.; Tingjin, R. Synthetic Fuel Production by Indirect Coal Liquefaction. *Energy Sustain. Dev.* **2003**, *7* (4), 79.

(2) Laborde-Boutet, Cédric and Larachi, F. CFD Simulations of Hydrodynamic/Thermal Coupling Phenomena in a Bubble Column with Internals. *AIChE J.* **2010**, *56*, 2397.

(3) Youssef, A. a.; Hamed, M. E.; Al-Dahhan, M. H.; Duduković, M. P. A New Approach for Scale-up of Bubble Column Reactors. *Chem. Eng. Res. Des.* **2013**, *2* (June 2013), 1.

(4) Boyer, C.; Gazarian, J.; Lecocq, V.; Maury, S.; Forret, A.; Schweitzer, J. M.; Souchon, V. Development of the Fischer-Tropsch Process: From the Reaction Concept to the Process Book. *Oil Gas Sci. Technol. – Rev. d'IFP Energies Nouv.* **2016**, *71* (3), 44.

(5) Al Mesfer, M. K.; Sultan, A. J.; Al-Dahhan, M. H. Study the Effect of Dense Internals on the Liquid Velocity Field and Turbulent Parameters in Bubble Column for Fischer–Tropsch (FT) Synthesis by Using Radioactive Particle Tracking (RPT) Technique. *Chem. Eng. Sci.* **2017**, *161*, 228.

(6) Kölbel,H ;Ralek, M. The Fischer-Tropsch Synthesis in Liquid Phase. *Catal. Rev. Eng.* **1980**, *21* (2), 225.

(7) Krishna, R.; Sie, S. T. Design and Scale-up of the Fischer – Tropsch Bubble Column Slurry Reactor. *Fuel Process. Technol.* **2000**.

(8) Guettel, R.; Kunz, U.; Turek, T. Reactors for Fischer-Tropsch Synthesis. *Chem. Eng. Technol.* **2008**, *31* (5), 746.

(9) Youssef, A. A.; Al-Dahhan, M. H.; Dudukovic, M. P. Bubble Columns with Internals: A Review. *Int. J. Chem. React. Eng.* **2013**, *11* (1), 169.

(10) Jhawar, A. K.; Prakash, A. Bubble Column with Internals: Effects on Hydrodynamics and Local Heat Transfer. *Chem. Eng. Res. Des.* **2014**, *92* (1), 25.

(11) Gidaspow, D.; He, Y.; Chandra, V. A New Slurry Bubble Column Reactor for Diesel Fuel. *Chem. Eng. Sci.* **2015**, *134*, 784.

(12) Basha, O. M.; Sehabiague, L.; Abdel-Wahab, A.; Morsi, B. I. Fischer-Tropsch Synthesis in Slurry Bubble Column Reactors: Experimental Investigations and Modeling - A Review. *Int. J. Chem. React. Eng.* **2015**, *13* (3), 201.

(13) Nedeltchev, S.; Nigam, K. D. P.; Schumpe, A. Prediction of Mass Transfer Coefficients in a Slurry Bubble Column Based on the Geometrical Characteristics of Bubbles. *Chem. Eng. Sci.* **2014**, *106*, 119.

(14) Saeidi, S.; Nikoo, M. K.; Mirvakili, A.; Bahrani, S.; Saidina Amin, N. A.; Rahimpour, M. R. Recent Advances in Reactors for Low-Temperature Fischer-Tropsch Synthesis: Process Intensification Perspective. *Rev. Chem. Eng.* **2015**, *31* (3), 19.

(15) Gheni, Saba;Abdulaziz, I.;Al-Dahhan, M. Effect of L / D Ratio on Phase Holdup and Bubble Dynamics in Slurry Bubble Column Using Optical Fiber Probe Measurements. *Int. J. Chem. React. Eng.* **2016**.

(16) Lee, B. W. Optical Probes in Multiphase Reactors, Washington University in St. Louis, 2016.

(17) Davis, B. H. Fischer-Tropsch Synthesis: Overview of Reactor Development and Future Potentialities. *Top. Catal.* **2005**, *32* (3–4), 143.

(18) Larachi, F.; Desvigne, D.; Donnat, L.; Schweich, D. Simulating the Effects of Liquid Circulation in Bubble Columns with Internals. *Chem. Eng. Sci.* **2006**, *61* (13), 4195.

(19) Abdulmohsin, R. S.; Al-Dahhan, M. H. Impact of Internals on the Heat-Transfer Coefficient in a Bubble Column. *Ind. Eng. Chem. Res.* **2012**, *51* (7), 2874.

(20) George, K. J. H.; Jhawar, A. K.; Prakash, A. Investigations of Flow Structure and Liquid Mixing in Bubble Column Equipped with Selected Internals. *Chem. Eng. Sci.* **2016**, *170*, 297.

(21) Kalaga, D. V.; Yadav, A.; Goswami, S.; Bhusare, V.; Pant, H. J.; Dalvi, S. V.; Joshi, J. B.; Roy, S. Comparative Analysis of Liquid Hydrodynamics in a Co-Current Flow-through Bubble Column with Densely Packed Internals via Radiotracing and Radioactive Particle Tracking (RPT). *Chem. Eng. Sci.* **2017**, *170*, 332.

(22) Kumar, S. B.; Moslemian, D.; Duduković, M. P. Gas-Holdup Measurements in Bubble Columns Using Computed Tomography. *AIChE J.* **1997**, *43* (6), 1414.

(23) Degaleesan, S.; Duduković, M. P. Liquid Backmixing in Bubble Columns and the Axial Dispersion Coefficient. *AIChE J.* **1998**, *44* (11), 2369.

(24) Rados, N.; Shaikh, A.; Al-dahhan, M. H. Phase Distribution in a High Pressure Slurry Bubble Column via a Single Source Computed Tomography. *Can. J. Chem. Eng.* **2005**, *83* (February).

(25) Youssef, A. A.; Al-Dahhan, M. H. Impact of Internals on the Gas Holdup and Bubble Properties of a Bubble Column. *Ind. Eng. Chem. Res.* **2009**, *48* (17), 8007.

(26) Yadav, A.; Kushwaha, A.; Roy, S. An Algorithm for Estimating Radial Gas Holdup Profiles in Bubble Columns from Chordal Densitometry Measurements. *Can. J. Chem. Eng.* **2016**, *94* (3), 524.

(27) Chen, J.; Gupta, P.; Degaleesan, S.; Al-Dahhan, M. H.; Dudukovic, M. P.; Toseland, B. A. Gas Holdup Distributions in Large-Diameter Bubble Columns Measured by Computed Tomography. *Flow Meas. Instrum.* **1998**, *9* (2), 91.

(28) Kulkarni, a. V. Design of a Pipe/Ring Type of Sparger for a Bubble Column Reactor. *Chem. Eng. Technol.* **2010**, *33* (6), 1015.

(29) Rabha, S.; Schubert, M.; Wagner, M.; Lucas, D.; Hampel, U. Bubble Size and Radial Gas Hold-up Distributions in a Slurry Bubble Column Using Ultrafast Electron Beam X-Ray Tomography. *AIChE J.* **2013**, *59* (5), 1709.

(30) Forret, A.; Schweitzer, J. M.; Gauthier, T.; Krishna, R.; Schweich, D. Liquid Dispersion in Large Diameter Bubble Columns, with and without Internals. *Can. J. Chem. Eng.* **2003**, *81* (3–4), 360.

(31) Hamed, M. Hydrodynamics, Mixing, and Mass Transfer in Bubble Columns with Internals, Washington University in St. Louis, 2012.

(32) Youssef, A. A.; Hamed, M. E.; Grimes, J. T.; Al-Dahhan, M. H.; Duduković, M. P. Hydrodynamics of Pilot-Scale Bubble Columns: Effect of Internals. *Ind. Eng. Chem. Res.* **2013**, *52* (1), 43.

(33) Kagumba, M.; Al-Dahhan, M. H. Impact of Internals Size and Configuration on Bubble Dynamics in Bubble Columns for Alternative Clean Fuels Production. *Ind. Eng. Chem. Res.* **2015**, *54* (4), 1359.

(34) Guan, X.; Gao, Y.; Tian, Z.; Wang, L.; Cheng, Y.; Li, X. Hydrodynamics in Bubble Columns with Pin-Fin Tube Internals. *Chem. Eng. Res. Des.* **2015**, *102*, 196.

(35) Chen, J.; Li, F.; Degaleesan, S.; Gupta, P.; Al-Dahhan, M. H.; Dudukovic, M. P.; Toseland, B. A. Fluid Dynamic Parameters in Bubble Columns with Internals. *Chem. Eng. Sci.* **1999**, *54* (13–14), 2187.

(36) Al Mesfer, M.; Sultan, A.; Al-Dahhan, M. Impacts of Dense Heat Exchanging Internals on Gas Holdup Cross-Sectional Distributions and Profiles of Bubble Column Using Gamma Ray Computed Tomography (CT) for FT Synthesis. *Chem. Eng. J.* **2016**, *300*, 317.

(37) Youssef, A. Fluid Dynamics and Scale-up of Bubble Columns with Internals, Washington University, Saint Louis, Missouri, 2010.

(38) Al-Mesfer, M. Effect of Dense Heat Exchanging Internals on the Hydrodynamics of Bubble Column Reactors Using Non-Invasive Measurement Techniques, Missouri University of Science and Technology, Rolla, MO, 2013.

(39) Kagumba, M. Heat Transfer and Bubble Dynamics in Bubble and Slurry, Missouri university of science and technology, 2013.

(40) Jasim, A. The Impact of Heat Exchanging Internals on Hydrodynamics of Bubble Column Reactor, Missouri University of Science and Technology, 2016.

(41) Chen, P.; Sanyal, J.; Duduković, M. P. P. Numerical Simulation of Bubble Columns Flows: Effect of Different Breakup and Coalescence Closures. *Chem. Eng. Sci.* **2005**, *60* (4), 1085.

(42) Al-Dahhan, M. Radioisotopes Applications in Industry: An Overview. *Atoms Peace – An Int. J.* **2009**, *2* (4), 324.

(43) Xue, J.;Al-Dahhan, M.;Dudukovic, M. P.;Mudde, R. F. Four-Point Optical Probe for Measurement of Bubble Dynamics: Validation of the Technique. *Flow Meas. Instrum.* **2008**, *19* (5), 293.

(44) Ong, B. C.; Gupta, P.; Youssef, A.; Al-Dahhan, M.; Duduković, M. P. Computed Tomographic Investigation of the Influence of Gas Sparger Design on Gas Holdup Distribution in a Bubble Column. *Ind. Eng. Chem. Res.* **2009**, *48* (1), 58.

(45) Ellenberger, J.; Van Baten, J. M.; Krishna, R. Intensification of Bubble Columns by Vibration Excitement. *Catal. Today* **2003**, *79–80*, 181.

(46) Krishna, R.; Ellenberger, J. Influence of Low-Frequency Vibrations on Bubble and Drop Sizes Formed at a Single Orifice. *Chem. Eng. Process.* **2003**, *42* (1), 15.

(47) Balamurugan, V.; Subbarao, D.; Roy, S. Enhancement in Gas Holdup in Bubble Columns through Use of Vibrating Internals. *Can. J. Chem. Eng.* **2010**, *88* (6), 1010.

(48) Elbing, B. R.; Still, A. L.; Ghajar, A. J. Review of Bubble Column Reactors with Vibration. *Ind. Eng. Chem. Res.* **2016**, *55* (2), 385.

(49) Al Falahi, F.; Al-Dahhan, M. Experimental Investigation of the Pebble Bed Structure by Using Gamma Ray Tomography. *Nucl. Eng. Des.* **2016**, *310*, 231.

(50) Al Falahi, F. S. Experimental Investigation of the Pebble Bed Structure by Using Gamma Ray Tomography, Missouri University of Science and Technology, 2014.

(51) Efhaima, A.; Al-Dahhan, M. Local Time-Averaged Gas Holdup in Fluidized Bed Reactor Using Gamma Ray Computed Tomography Technique (CT). *Int. J. Ind. Chem.* **2015**, *6* (3), 143.

(52) Efhaima, A. Scale-up Investigation and Hydrodynamics Study of Gas-Solid Fluidized Bed Reactor Using Advanced Non- Invasive Measurement Techniques. **2016**.

(53) Efhaima, A.; Al-Dahhan, M. Bed Diameter Effect on the Hydrodynamics of Gas-Solid Fluidized Beds via Radioactive Particle Tracking (RPT) Technique. *Can. J. Chem. Eng.* **2016**, *94* (12).

(54) Ali, N. Y. Evaluating of Scale-up Methodologies of Gas-Solid Spouted Beds for Coating Triso Nuclear Fuel Particles Using Advanced Measurement Techniques. **2016**.

(55) Ali, N.; Al-Juwaya, T.; Al-Dahhan, M. Demonstrating the Non-Similarity in Local Holdups of Spouted Beds Obtained by CT with Scale-up Methodology Based on Dimensionless Groups. *Chem. Eng. Res. Des.* **2016**, *114*, 129.

(56) Al-Juwaya, T.; Ali, N.; Al-Dahhan, M. Investigation of Cross-Sectional Gas-Solid Distributions in Spouted Beds Using Advanced Non-Invasive Gamma-Ray Computed Tomography (CT). *Exp. Therm. Fluid Sci.* **2017**, *86*, 37.

(57) Varma, R. Characterization of Anaerobic Bioreactors for Bioenergy Generation Using a Novel Tomography Technique, Washington University, 2008.

(58) Roy, S.; Kemoun, A.; Al-Dahhan, M. H.; Dudukovic, M. P.; Skourlis, T. B.; Dautzenberg, F. M. Countercurrent Flow Distribution in Structured Packing via Computed Tomography. *Chem. Eng. Process. Process Intensif.* **2005**, *44* (1), 59.

(59) Veera, U. P.; Kataria, K. L.; Joshi, J. . Gas Hold-up Profiles in Foaming Liquids in Bubble Columns. *Chem. Eng. J.* **2001**, *84* (3), 247.

(60) Hubers, J. L.; Striegel, A. C.; Heindel, T. J.; Gray, J. N.; Jensen, T. C. X-Ray Computed Tomography in Large Bubble Columns. *Chem. Eng. Sci.* **2005**, *60* (22), 6124.

(61) Narain, R.; Melo, S. B.; Santos, V. A. Collimator Design for Single Beam Gamma Ray Industrial Tomography and Fan Beam Geometry. **2011**.

(62) O'Sullivan, J. A.; Benac, J. Alternating Minimization Algorithms for Transmission Tomography. *IEEE Trans. Med. Imaging* **2007**, *26* (3), 283.

(63) Varma, R.; Bhusarapu, S.; Sullivan, J. A. O. A Comparison of Alternating Minimization and Expectation Maximization Algorithms for Single Source Gamma Ray Tomography. *Imaging* **2007**, *18*, 1.

(64) Sultan, A. J.; Sabri, L. S.; Al-Dahhan, M. H. Overcoming the Gamma-Ray Computed Tomography Data Processing Pitfalls for Bubble Column Equipped with Vertical Internals. submitted to *Can. J. Chem. Eng.* **2017**.

(65) Sultan, A. J.; Sabri, L. S.; Al-Dahhan, M. H. Influence of the Size of Heat Exchanging Tubes (Internals) on the Gas Holdup Distribution in a Bubble Column Using Gamma-Ray Computed Tomography. submitted to *Chem. Eng. Sci.* **2017**.

(66) Shaikh, A.; Al-Dahhan, M. Characterization of the Hydrodynamic Flow Regime in Bubble Columns via Computed Tomography. *Flow Meas. Instrum.* **2005**, *16* (2–3), 91.

(67) Shaikh, A.; Al-Dahhan, M. A New Method for Online Flow Regime Monitoring in Bubble Column Reactors via Nuclear Gauge Densitometry. *Chem. Eng. Sci.* **2013**, *89*, 120.

(68) Al-Dahhan, M. Radioisotope Applications in the Petrochemical Industry : An Overview. *Int. Symp. Peac. Appl. Nucl. Technol. GCC Ctries.* **2008**, No. 1, 10.

(69) Al-Dahhan, M. H. Trends in Minimizing and Treating Industrial Wastes for Sustainable Environment. *Procedia Eng.* **2016**, *138*, 347.

(70) Sultan, A. J.; Sabri, L. S.; Al-Dahhan, M. H. Impact of the Heat Exchanging Tube Configurations on Gas Holdup Distribution in Bubble Column via Gamma-Ray Computed Tomography. *Int. J. Multiph. Flow* **2017**.

(71) Forret, A.; Schweitzer, J. M.; Gauthier, T.; Krishna, R.; Schweich, D. Scale up of Slurry Bubble Reactors. *Oil Gas Sci. Technol.* **2006**, *61* (3), 443.

SECTION

2. RECOMMENDATIONS

This work has generated for the first time benchmarking data and enhanced the fundamental understanding of the hydrodynamics of bubble columns in the presence of vertical internal tubes. However, despite all of this investigation, many things remain unaddressed and unexamined. These unaddressed areas would make great research topics that will contribute to further improving the fundamental understanding and knowledge of this research area. Below are some suggestions that have been made for future work to be performed.

1. Investigating the impacts of the presence of vertical internal tubes and their configurations on the 3D liquid velocity and turbulence parameters (Reynolds stresses, turbulent kinetic energy, and turbulent eddy diffusivities) in small and large-scale bubble columns (18-inch and 24-inch diameter column) by using radioactive particle tracking (RPT) technique. Where the new structure and calibration device for RPT has been manufactured and tested in our laboratory that can handle these sizes.
2. Visualizing and quantifying the cross-sectional gas and solid holdup distributions and their profiles in slurry bubble columns with and without vertical internals by using our dual-source gamma-ray computed tomography technique.
3. Identifying flow regimes in a bubble column equipped densely with a bundle of heat-exchanging tubes, particularly for large size bubble columns (18 and 24-inch in diameter) and how they are compared to the small size columns.

4. Building and developing a 3D CFD simulation for a bubble column with vertical internals and validating this simulation against the benchmarking data of the current study.
5. Examining the influence of the clearance height between vertical internal tubes and the gas distributor on the cross-sectional gas phase distribution, bubble dynamics, and heat transfer coefficient.
6. Evaluating the effects of the bottom-end shape of vertical internal tubes (i.e., U shape, flat shape, and tapered shape) on the gas holdup distribution and their profiles, bubble properties, mass transfer coefficient, and heat transfer coefficient in bubble and slurry bubble columns.
7. Studying the impact of vertical internal tubes on the hydrodynamics of the bubble columns under relevant industrial conditions (i.e., Fischer-Tropsch conditions), using mimicked liquid of similar physical properties, operating under high temperature, pressure, and loading of the fine catalyst.
8. Investigating the hydrodynamics of the bubble/slurry bubble columns with and without vertical internal tubes operating under a low aspect ratio (L/D) by using non-invasive techniques (i.e., CT and RPT).

APPENDIX

STUDY THE IMPACT OF SIZE OF HEAT EXCHANGING TUBES (INTERNALS) ON THE LIQUID VELOCITY FIELD AND TURBULENT PARAMETERS IN BUBBLE COLUMN WITH INTERNALS BY USING RADIOACTIVE PARTICLE TRACKING (RPT) TECHNIQUE

The focus of this study is to investigate and quantify, for the first time, the effects of the dense vertical internals and their sizes on the liquid velocity field and turbulence parameter profiles (Reynolds stress and kinetic energy profiles) in a bubble column with and without internals using advanced measurement technique (RPT).

Radioactive Particle Tracking (RPT) Technique

RPT is a powerful technique for mapping the Lagrangian trajectory of a particular phase in a given system by tracking a single radioactive particle, which should match the density of the studied phase, with the aid of an array of scintillation detectors located strategically around the system.

From the Lagrangian trajectory, vital information can be extracted in the form of the velocity field, turbulence parameters, residence time distribution, stagnant zones, and many others. This technique includes a fully automatic calibration device (r, z, and θ), a signal processing, and data acquisition system, as seen in Figure 1.

Arrangement of detectors in RPT experiments

Twenty-eight of NaI scintillation detectors were strategically arranged around the 6-inch bubble column in this investigation as shown in Table 1. It is important to mention that all these detectors were located in the fully developed flow regime as displayed in Figure *2*.

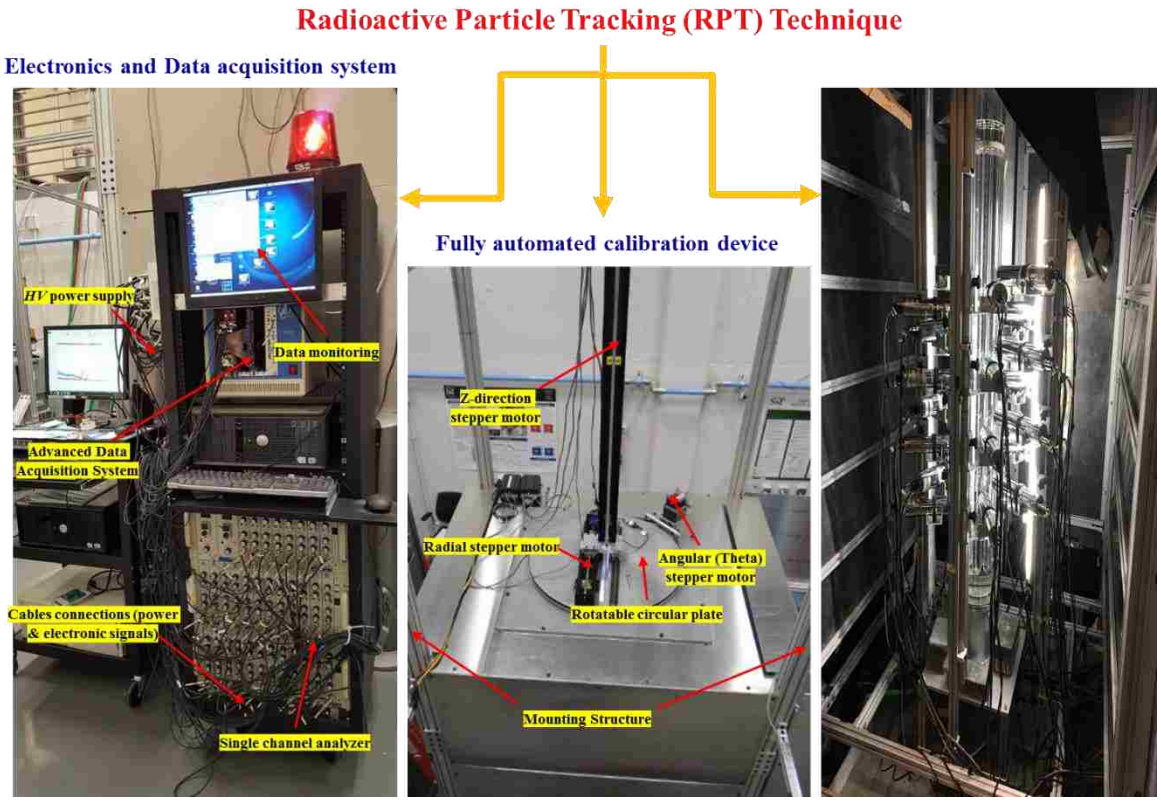

Figure 1: photo of the Radioactive Particle Tracking (RPT) Technique

Table 1: Coordinates of the twenty-eight detectors in three directions

No.	Radius, r (cm)	Angle, θ (°)	Height, z (cm)	No.	Radius, r (cm)	Angle, θ (o)	Height, z (cm)
1	10.16	118	65	**15**	10.16	298	65
2	10.16	62	71	**16**	10.16	242	71
3	10.16	118	77	**17**	10.16	298	77
4	10.16	62	83	**18**	10.16	242	83
5	10.16	118	89	**19**	10.16	298	89
6	10.16	62	95	**20**	10.16	242	95
7	10.16	118	101	**21**	10.16	298	101
8	10.16	28	65	**22**	10.16	208	65
9	10.16	332	71	**23**	10.16	152	71
10	10.16	28	77	**24**	10.16	208	77
11	10.16	332	83	**25**	10.16	152	83
12	10.16	28	89	**26**	10.16	208	89
13	10.16	332	95	**27**	10.16	152	95
14	10.16	28	101	**28**	10.16	208	101

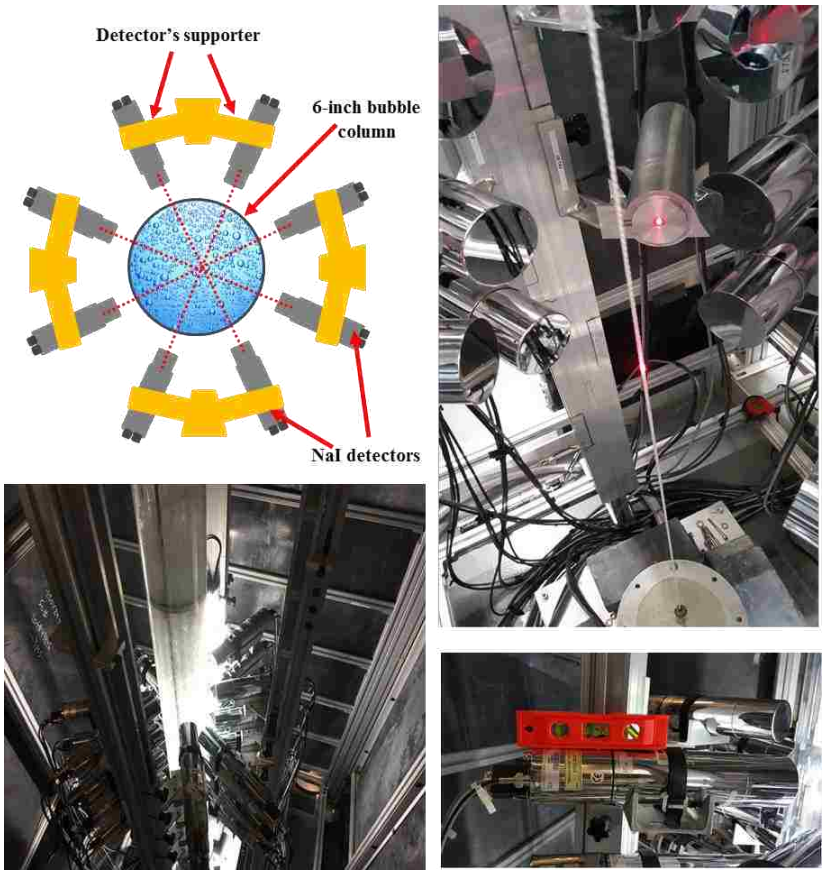

Figure 2: Cross-sectional view of the arrangement of detectors in RPT experiments

Capsulation of the radioactive particle

In this study, Cobalt-60 with an activity of about 200 µCi and a 600-µm diameter was used in all RPT experiments. Cobalt has a half-life of 5.28 years and presents two photopeaks, one at 1.18 MeV and one at 1.34 MeV. Since the Cobalt has a high density (i.e., 8.9 g/cm3), therefore, it was encapsulated with air in a polypropylene ball with a 2-mm outer diameter to obtain a composite particle density similar to the water density, as shown in Figure 3. It is important to mention that the process of the encapsulation of the radioactive particle was supervised by the Environmental Health and Safety Department at Missouri University of Science and Technology (Missouri S&T).

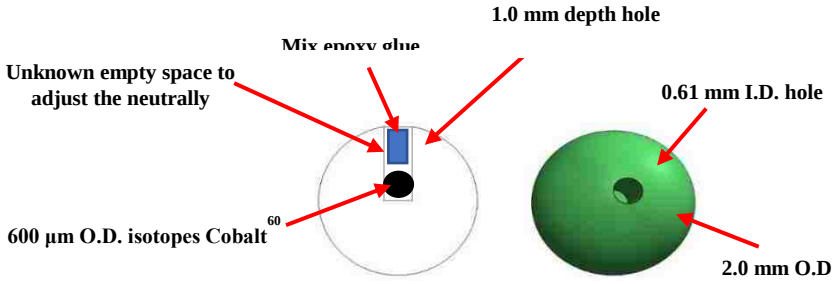

Figure 3: Capsulation of the radioactive particle (CO-60)

Experimental procedure for conducting RPT experiments

RPT experiments typically consist of two steps as follow:

1. RPT calibration (static experiment under the experimental conditions),

2. RPT experiment (dynamic experiment).

During the calibration step, a single radioactive particle is placed inside a Teflon vial (Figure 4a) and then attached to the rod (Figure 4b) which connects to the automatic calibration device (Figure 4c). The radioactive particle was moved to several known locations (Figure 4e) by using the automatic calibration device. During the residence of the radioactive particle in these known positions, the detectors receive intensity counts, which depend on the distance between the radioactive particle and each detector. From the calibration step, a count-distance map (Figure 4f) can be obtained, which will be used in the subsequent step to obtain the instantaneous locations of the particle. During the experimental run (i.e., dynamic experiment), the radioactive particle moves freely inside the bubble column to track the liquid phase motion. The experiments were conducted for 24 hours, and during this time, the radiation emitted by the radioactive particle was recorded by the detectors at a frequency of 50 Hz for each sampling instance.

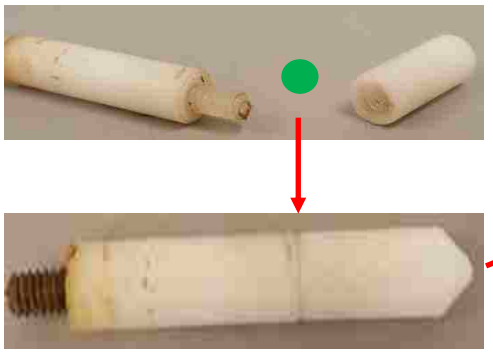

a) Teflon vial

b) Rod and attached Teflon vial

c) Automatic calibration device

d) the calibration rod inside the bubble column

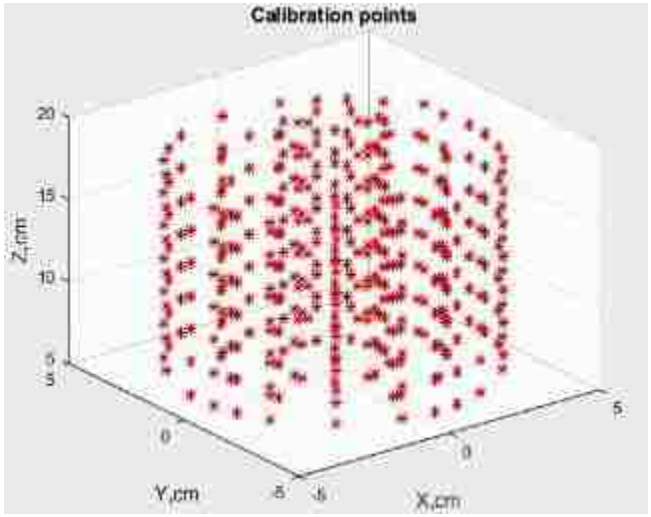

e) selected calibration points inside the bubble column

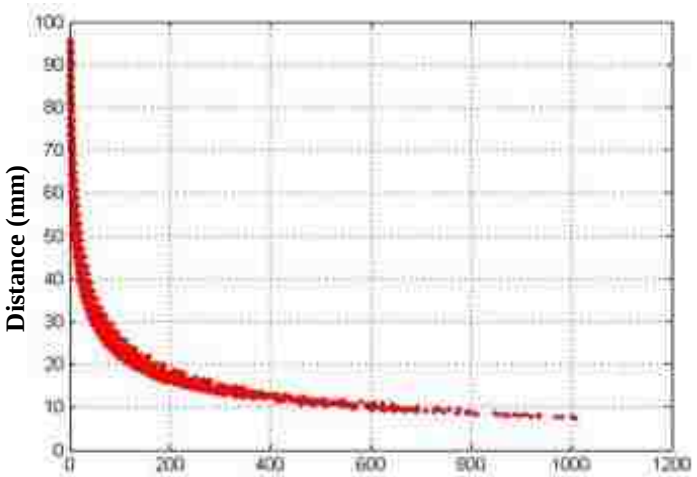

f) Count-distance map

Figure 4: RPT calibration step under the studied superficial gas velocity

Subsequently, the instantaneous velocity is calculated by time differentiation of two successive positions of the particle. From the Instantaneous velocity time series, a rich database (liquid velocity field and turbulent parameters) is calculated by applying suitable post-processing (see Figure 5).

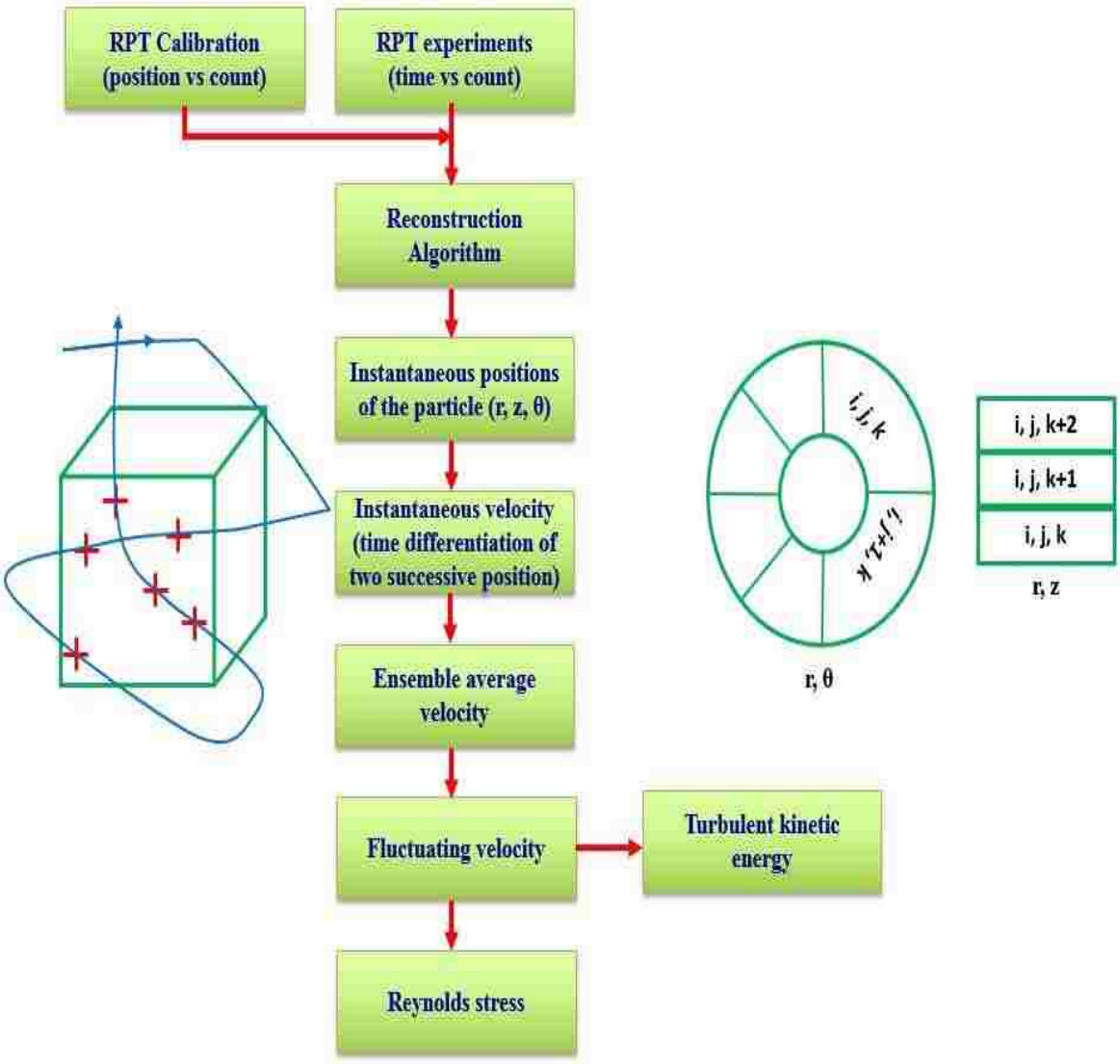

Figure 5: Illustration of the RPT steps to obtain liquid velocity field and turbulent parameters

3D liquid velocity field for bubble column without vertical internal tubes

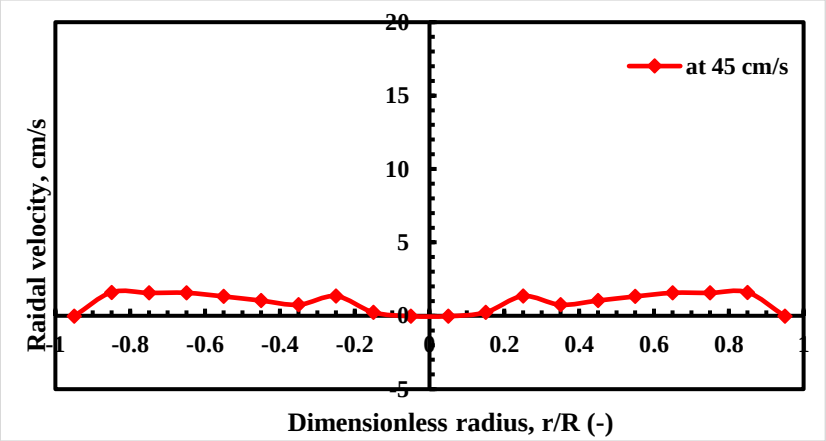

Figure 6: Radial liquid velocity under a superficial gas velocity of 45 cm/s

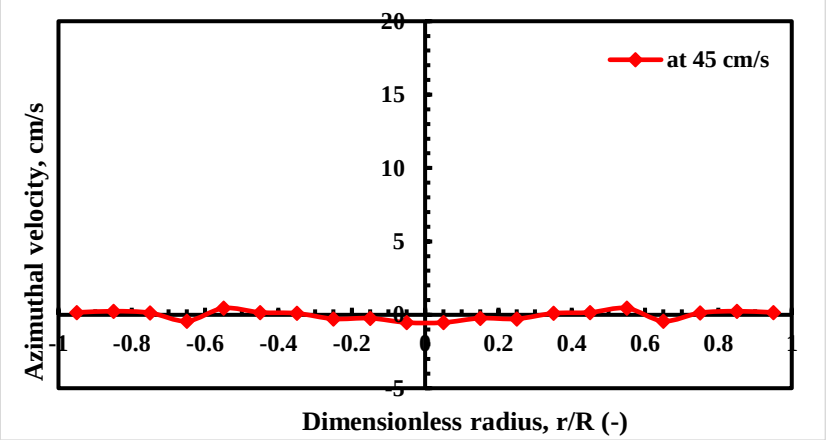

Figure 7: Azimuthal liquid velocity under a superficial gas velocity of 45 cm/s

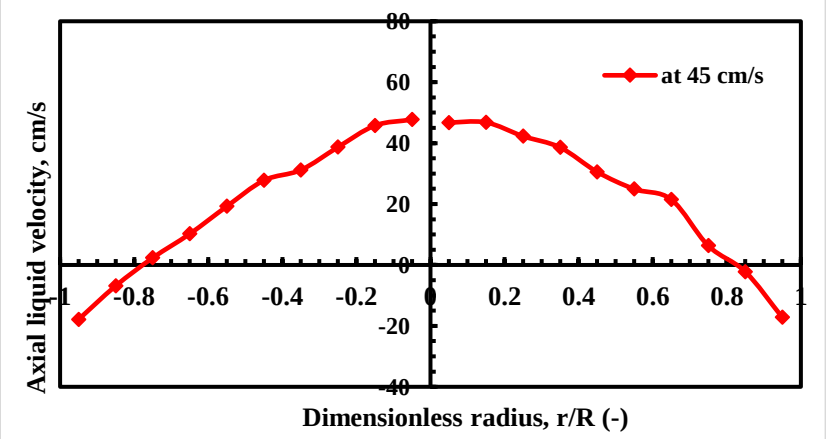

Figure 8: Axial liquid velocity under a superficial gas velocity of 45 cm/s

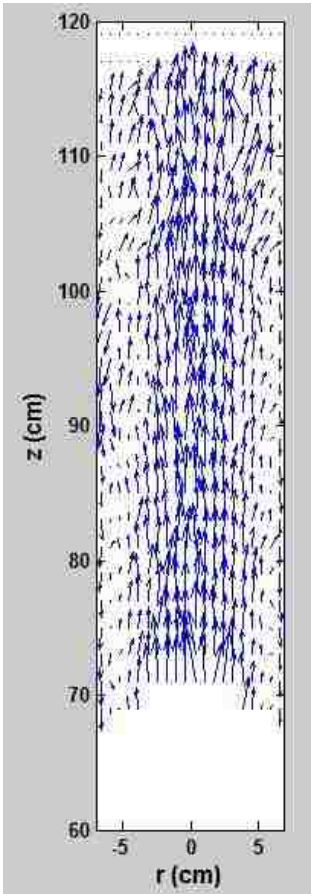

Velocity vector plots in r-z plane for bubble column without internals at 20 cm/s

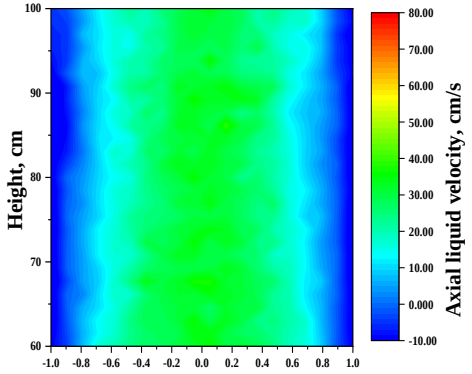

Contour plots in r-z plane for bubble column without internals at 20 cm/s

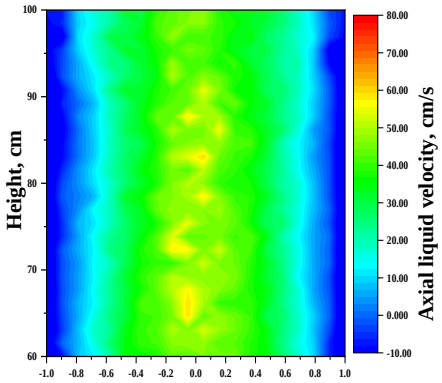

Contour plots in r-z plane for bubble column without internals at 45 cm/s

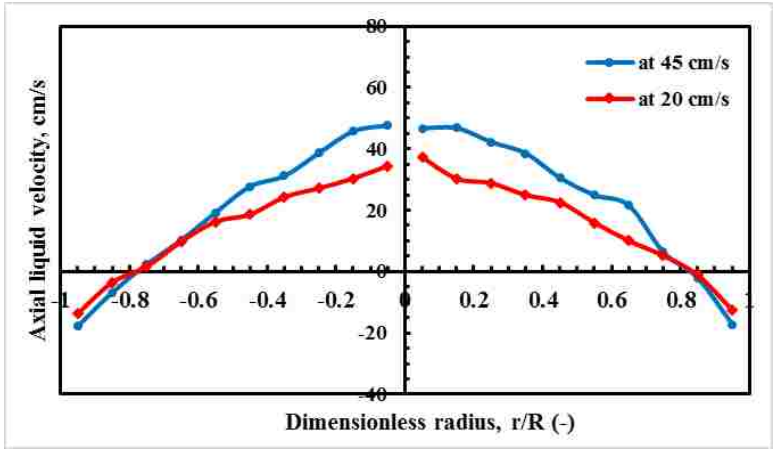

Azimuthally and axially averaged of liquid velocity under different superficial gas velocities of 20 and 45 cm/s

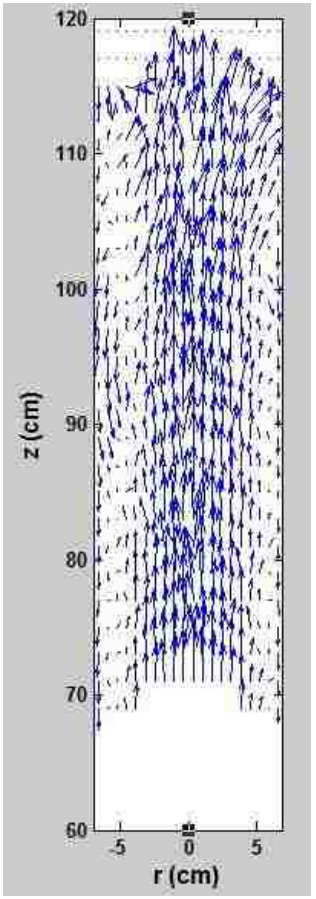

Velocity vector plots in r-z plane for bubble column without internals at 45 cm/s

Figure 9: Effect of superficial gas velocity on the axial liquid velocity for bubble column without vertical internals

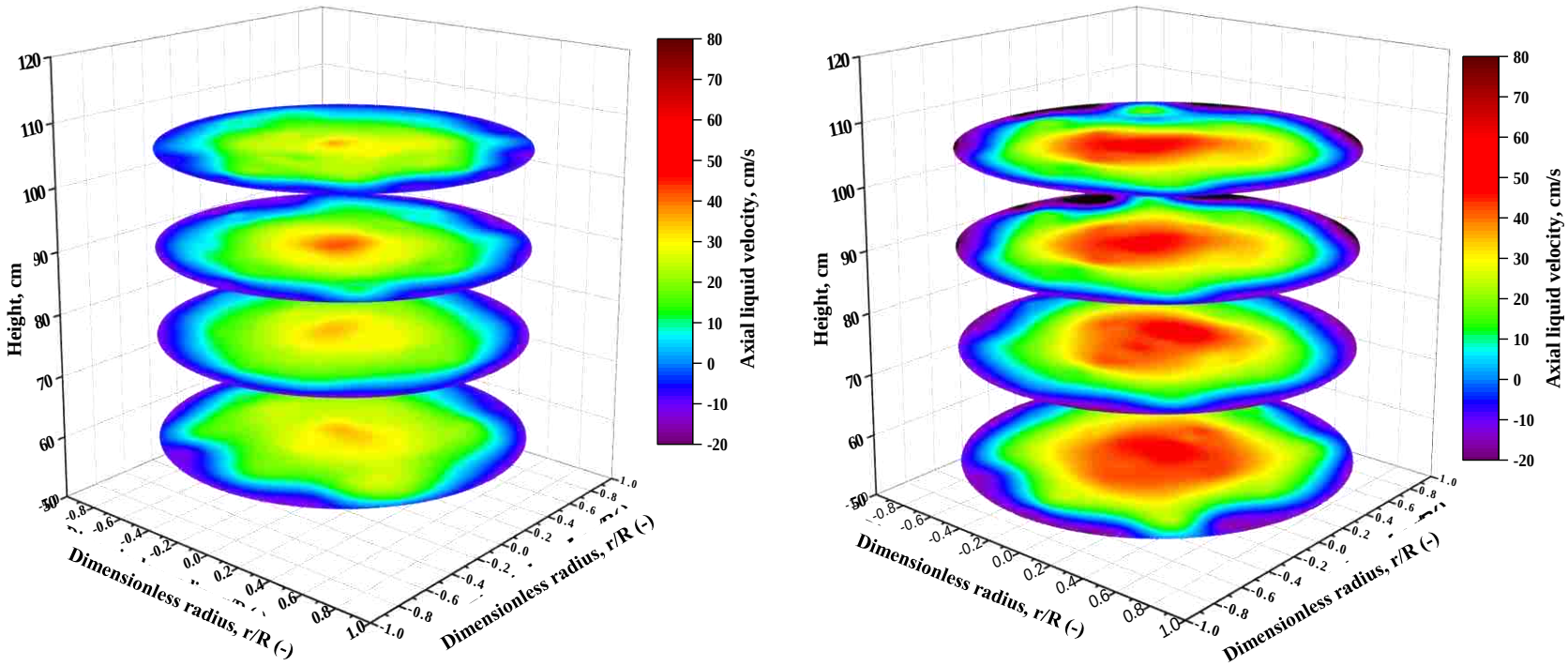

bubble column without vertical internals operated at superficial gas velocity 20 cm/s

bubble column without vertical internals operated at superficial gas velocity 45 cm/s

Figure 10: Liquid velocity at different axial levels of the bubble column without vertical internals operating under different superficial gas velocities of 20 and 45 cm/s

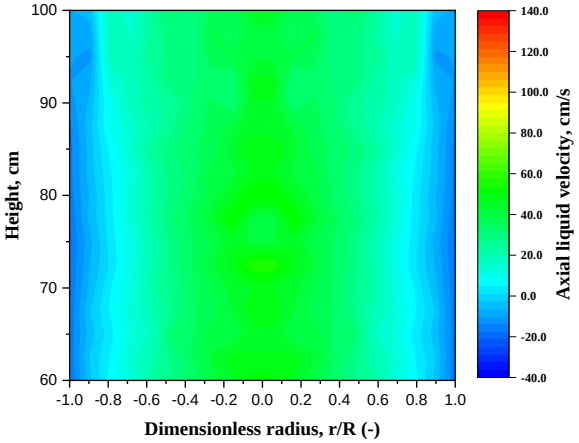

Contour plot of the axial liquid velocity for bubble column without vertical internals at 45 cm/s

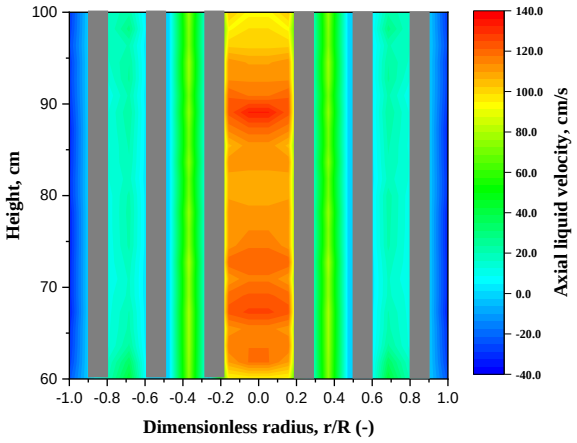

Contour plot of the axial liquid velocity for bubble column with 0.5-inch vertical internals at 45 cm/s

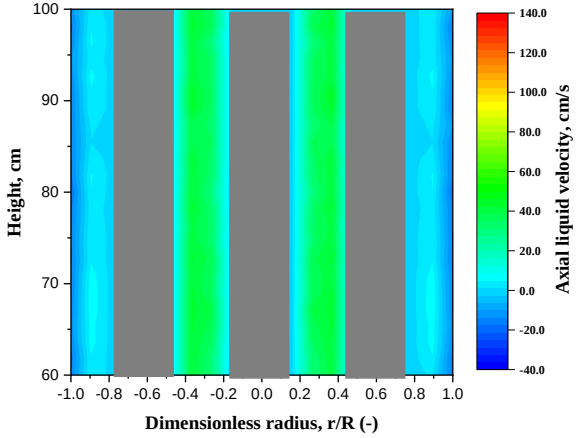

Contour plot of the axial liquid velocity for bubble column with 1-inch vertical internals at 45 cm/s

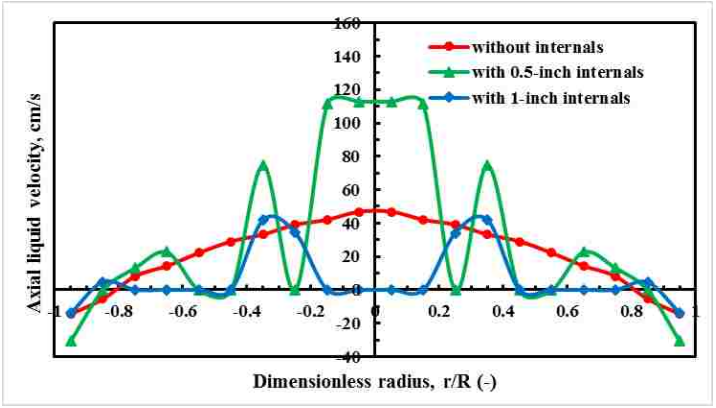

Comparison of the axial and azimuthal of liquid velocities for bubble columns with and without vertical internal at 45 cm/s

Figure 11: Impact of the size of vertical internals on the axial liquid velocity

VITA

Abbas Jawad Sultan was born in Baghdad, Iraq. He received his B.S. and the first M.S. in chemical engineering from the University of Technology Baghdad, Iraq in 2003 and 2006, respectively. In addition, he ranked the first out of 128 graduates in his specialization for his B.S. degree. Before joining Missouri University of Science and Technology (Missouri S&T), Abbas was a faculty member in the Chemical Engineering Department at the University of Technology Baghdad, Iraq from 2005 until 2012, where he was awarded a scholarship by The Higher Committee for Education Development in Iraq to study for his Ph.D. in Chemical Engineering. He started at Missouri S&T during the spring semester of 2013 to work under the supervision of Dr. Muthanna Al-Dahhan. He obtained his second M.S. in Chemical Engineering from Missouri S&T in May 2015. He has received several awards and recognitions for his research, including the Travel Award for the 24th and 25th International Symposium on Chemical Reaction Engineering (ISCRE 24, 2016, and ISCRE 25, 2018), won the 3rd place prize in the poster competition for ISCRE 24, the Best Poster Award for Graduate Research Showcase Spring, Missouri S&T (2017), and the Top Three Posters in Young Researcher Competition, Algae Biomass Summit (2017). Abbas is a member of AIChE and Society of Chemical Industry (SCI). He is a fellow of Tau Beta Pi engineering honor society. His research activities included six publications in peer-reviewed journals and over 20 national and international conference presentations. Additionally, four journal papers have been submitted and currently are under review. Abbas received his Ph.D. in Chemical Engineering from Missouri S&T in May 2018.